BHP COPPER'S RESPONSES TO COMMENTS OF THE ARIZONA DEPARTMENT OF ENVIRONMENTAL QUALITY DATED MAY 1, 1996 REGARDING THE FLORENCE PROJECT AQUIFER PROTECTION PERMIT APPLICATION

September 26, 1996

BROWN AND CALDWEI

BHP COPPER'S RESPONSES TO COMMENTS OF THE ARIZONA DEPARTMENT OF ENVIRONMENTAL QUALITY DATED MAY 1, 1996 REGARDING THE FLORENCE PROJECT AQUIFER PROTECTION PERMIT APPLICATION

September 26, 1996

Prepared for: **John Kline**
Project Manager
BHP Copper - Florence Project
14605 East Hunt Highway
Florence, Arizona 85232

Prepared by: **Brown and Caldwell**
3636 North Central Avenue
Suite 300
Phoenix, Arizona 85012

Table 1: Response to ADEQ Comments Issued May 1, 1996	
ADEQ Comments	**BHP Response**
II. HYDROGEOLOGIC STUDY REVIEW	
As required by A.R.S. § 49-243.A.4 and A.A.C. R18-9-108.C.1, BHP Copper Co. has included the results of a hydrogeologic study in the Florence Project application. An initial review of the hydrogeologic study was conducted by Gary Burchard of the Mining Unit. Mr. Burchard's comments are based on his review of the following document: 1. Magma Florence *In-Situ* Project Aquifer Protection Permit Application, Volume IV of V, Modeling Report, January 1996. Mr. Burchard has not yet reviewed the other volumes of the application. These will be reviewed during his ongoing hydrologic review. The comments below are identified by the section numbers in Volume IV. If a portion of the application is quoted, it will be presented here in italics.	
GENERAL COMMENTS	
The overall purpose of this review is to evaluate the demonstration required by the Arizona Revised Statutes (A.R.S.) §49-243.B.2 and B.3 that the discharge from a facility will not cause or contribute to a violation of aquifer water quality standards (AWQS) at the applicable point of compliance (POC). For the *in-situ* portion of this mining project, both the demonstrations of compliance with aquifer water quality standards and BADCT (A.R.S. §49-243.B.1) depend upon the maintenance of hydraulic control of the mining solutions. For the *in-situ* portion of this mining project, these two demonstrations are intertwined if not the same.	
SPECIFIC COMMENTS	
2.2.2 Conceptual Hydrogeology	
The conceptual and numeric models will likely be further refined as future investigations and observations are made before and during in-situ mining activities. Mr. Burchard recommends that, if a permit is issued for this project, that the permit contain a requirement for a post audit of the modeling efforts. Because most of the demonstrations required by A.R.S. §49-243.B.1, 2, and 3 rely heavily upon computer modeling, the Department should be shown that the *in-situ* mining process is behaving as predicted. BHP should conduct this post audit between five and ten years into the operational life of the project and will probably lead to a model redesign. This post audit will also aid a better prediction of post-closure conditions.	Please refer to Attachment 1 to Table 1.
2.6.3 Vertical Model Layers	
An individual model layer may contain various geologic materials. For example, model layer seven (Figure 2.6-1 (IV)) in the western portion of the *in-situ* mine area comprises the lower basin fill unit (LBFU) and the oxide zone. In the south-central portion of the *in-situ* mine area, model layer seven comprises the oxide zone and the sulfide zone. BHP should present the method by which a single hydrogeologic parameter is assigned to a cell that contains materials from multiple hydrostratigraphic units. Figures 2.7-1 (IV) through 2.7-4 (IV) show hydraulic conductivity distributions for the oxide and sulfide zones within model layers 2 through 5 respectively. BHP should also depict the hydraulic conductivity's for the LBFU that exists within model layers 2 through 5.	Please refer to Attachment 2 to Table 1.
2.6.5 Initial Conditions	
The different contouring algorithms available in SURFER can sometimes produce markedly different results. BHP should present the method used and the rationale for its use.	Please refer to Attachment 3 to Table 1.

Table 1: Response to ADEQ Comments Issued May 1, 1996	
ADEQ Comments	**BHP Response**
2.7.2 Calibrated Model Hydraulic Conductivities	
The hydraulic conductivity for the UBFU was set at 60 ft/day in regional domain and 40 ft/day in the vicinity of the in-situ mine area. BHP should provide the rationale for assigning a lower hydraulic conductivity in the vicinity of the *in-situ* mine area.	The value of 60 feet/day for hydraulic conductivity of the domain was based on the results of a literature review and a previously conducted hydraulic test at Well P8-GU. The 40 feet/day conductivity for the mine area was selected based on calibration results.
2.7.5 Vertical Conductance	
BHP references the method by which they calculated vertical conductance, but the values themselves were not presented. BHP should present the vertical conductance values used to construct the model.	The vertical conductance arrays in hard copy format would take 400 pages of paper. The vertical conductance arrays for the eight model layers are presented on floppy disk in the file called VCONT under electronic Attachment ADEQ-2.7.5-Vertical Conductances.
2.10 SENSITIVITY ANALYSIS	
Variations performed in the sensitivity analysis included increasing the hydraulic conductivity in Model Layer 5 by one order of magnitude. BHP should provide the rationale for selecting Layer 5 as the layer of interest. Also Figures 2.10-1 (IV) through 2.10-6 (IV) do not show residual head values as stated in the text.	Please refer to Attachment 4 to Table 1.
2.10.4 Sensitivity to River Conductance	
BHP has stated that the modeling efforts are apparently sensitive to river bed conductance. This sensitivity seems important in light of the fact that conductance is not a directly measured parameter. BHP stated that with an increased conductance value, "Over the mine area the groundwater elevations rose up to 6 feet in the UBFU and LBFU." BHP should elaborate on the consequences if the recharge rate along the Gila River is greater than anticipated.	Please refer to Attachment 5 to Table 1.
3.3 Method	
BHP used the geochemical computer program CHILLER "to evaluate the process of fluid/rock interactions and fluid/fluid mixing." However, very little information is given about the program itself. BHP should provide the Department more specific information about CHILLER. For example, is CHILLER an equilibrium, kinetic, or reaction path modeling program? What assumptions were included in the exercise? What are the reliability and accuracy of the database SOLTHERM?	CHILLER is a program for computing complex chemical processes that involve states of equilibrium or partial equilibrium in gas-solid-aqueous systems. CHILLER is an equilibrium reaction path model applicable to heterogeneous systems with an aqueous phase. The program solves a series of mass balance and mass action equations by a Newton-Raphson numerical solution to the algebraic form of the governing equations. CHILLER computes the heterogeneous equilibrium conditions (aqueous speciation and amounts of minerals precipitated) as reaction progress variables (e.g. composition, temperature, or pressure is changed incrementally). (Reed, M.H. Calculation of Multicomponent Chemical Equilibria and Reaction Processes in systems Involving Minerals, Gases, and an Aqueous Phase. *Geochim. Et Cosmochim. Acta,* Vol. 46, 1982. The principal assumptions included in the exercise were (1) the hypothesized geologic process being simulated is valid, (2) there is a chemical equilibrium condition, and (3) the thermodynamic data are valid. Soltherm is a reliable and accurate database, the data of which are obtained from accepted scientific publications. Soltherm was developed at the University of Oregon by N.E. Spycher and M.H. Reed and became available in 1989. It contains thermodynamic data for aqueous, gas, and mineral species, and equilibrium constants for aqueous-mineral-gas equilibria. Soltherm is external to CHILLER and consists of activity coefficients data, component species data, derived species data (aqueous), and gas and mineral data. The database includes species with equilibrium constants at temperatures from 25 to 300 degrees C.

Table 1: Response to ADEQ Comments Issued May 1, 1996	
ADEQ Comments	**BHP Response**
3.4.2 Attenuation	
BHP should clarify whether the attenuation estimates included competition for sites. *The only elements concentrated in aqueous form at the end of the calculation are sodium, potassium, calcium, and magnesium.* The Department does not understand how only cations can be concentrated in aqueous form. To maintain an electrically neutral charge, should not some anionic species also be concentrated?	Site competition was not taken into consideration because it is not relevant to the type of calculations being employed. Anions were not mentioned because the paragraph was focusing on metals. Nevertheless, the quoted sentence will be revised by substituting "cations" for "elements". Also the following sentence will be added. "The dominant anions concentrated in aqueous form are the sulfate and chloride ions.
3.7.3.2 Results	
The initial concentrations of ... continuously decreased as the reaction between the solution and the alluvial material progressed (Table 3.7-2). How Table 3.7-2 shows a progression is not clear. BHP should clarify the rationale for introducing a "partly attenuated solution" into a second column to determine attenuation. Also the meaning of the term "fluid/rock ratio" is not clear.	The purpose of introducing a partly attenuated solution to a second column is to simulate the continued interactions that will occur as a metal-rich solution moves through a geologic unit and is continuously exposed to "fresh" material within the unit. The additional attenuation that comes from the continued exposure of a solution to the geologic material can be seen by comparing concentrations reported under Columns ALUO-GL3 and ALUO-GL3(2) of Table 3.7-2. Note that the concentrations reported under Column ALUO-GL3 are the result of a column test where a known volume of the feed solution (see column on far left of Table 3.7-2) was passed through and allowed to equilibrate with a known mass of a particular sample (ALUO-3GL) of alluvial material. The partially attenuated solution was then passed through and allowed to equilibrate with a second sample of the same alluvial material. The additional attenuation that resulted from the exposure of the partially attenuated feed solution to the "fresh sample" is shown under Column ALUO-3GL(2). For example, the concentration of aluminum in the feed solution, 5,100 mg/l, was reduced to 3,610 mg/l after the feed solution was passed through, and equilibrated with Column ALUO-3GL. The 3,610 mg/l was then reduced to 3 mg/l after the partially attenuated feed solution was passed through and equilibrated with the second column (ALUO-3GL[2]). Only two tests were reported that involved the introduction of a partially attenuated solution into a second column. The first was the test involving ALUO-3GL as described above. The second was reported under Table 3.7-3 and involved the sample identified as "Basin-Fill Calcareous." All of the other tests reported in Tables 3.7-2 and 3.7-3 involved exposure of unattenuated feed solution to single columns prepared from the indicated samples. The liquid/rock ratio (the mass of solution exposed to a given material divided by the mass of the material) is used to "standardize" tests and thereby facilitate the comparison of the attenuation potential of different materials. Note that all tests shown in Table 3.7-2 except ALUO-3GL(2) were run at a liquid rock ratio of 5 to 1. A 2.5 to 1 ratio was used for test ALUO-3GL(2).
By the time the test was completed, aluminum, antimony, barium, chromium, lead, mercury, and nickel <u>were removed</u> from the solution (Table 3.7-3). [emphasis added] BHP cannot make this claim because the analytical detection levels were greater than the respective aquifer water quality standards.	The sentence will be changed to; "The concentrations of aluminum, antimony, barium, chromium, lead, mercury and nickel were removed from the solution to levels below the reported detection limits." As explained below, the purpose of the attenuation tests was not to demonstrate compliance with AWQS. Rather , it was to show the natural attenuation potential of the geologic units at the site.

Table 1: Response to ADEQ Comments Issued May 1, 1996	
ADEQ Comments	**BHP Response**
3.7.3.3 Summary	
The attenuation tests as presented have illustrated the potential of the geologic media present at the Florence Project site to attenuate pollutants in the groundwater. However, these tests have not determined the capacity of the geologic materials to attenuate pollutants. For a test to determine attenuation capacity, the test should continue until the capacity consumed, thus indicating the total amount of pollutants that a material can attenuate. For attenuation-capacity tests to be meaningful, they should determine an end point or the maximum attenuation capacity.	The summary given in Section 3.7.3.3 was not intended to mean that BHP would be relying on the attenuation capacity of the geologic media to protect groundwater water. Rather, it was intended to convey that column tests and numerical simulations indicate a potential for the geologic materials to attenuate the effects of inadvertent releases. It should be noted that the attenuation tests were conducted with carefully prepared and epoxyed columns using minimally disturbed core samples. As a consequence, the attenuation interactions did not involve the total rock mass but the fracture networks within the rock. Thus, the tests are more indicative of the condition of the rock than the total capacity of the rock to attenuate pollutants.
3.7.4.2 Results	
The pH of the initial solution was 1.64, and as the first overflow discharged from the column, the pH of the overflow solution was 3.34. The change in pH of the solution was caused by the consumption of hydrogen ions from the solution by the ore-bearing rock. This change in pH indicates the natural attenuation capacity of the rock. and later *The pH of the initial solution was 1.61, and as the first overflow discharged from the column, the pH of the overflow solution was 2.43. The change in pH of the solution was caused by consumption of hydrogen ions from the solution by the ore-bearing rock. This change in pH indicates the natural attenuation capacity of the rock.* Both the quartz monzonite and granodiorite porphyry do not appear to possess much attenuation capacity if they can only raise the pH to between 2.5 and 3.5.	The change in pH does not represent the total attenuation capacity of the rock because the pH was measured after the first pass through the rock, not after the solution equilibrated with the rock. The change in pH does illustrate the existence of acid neutralization potential in both quartz monzonite and granodiorite rocks. Also, it should be remembered that pH is measured on a logarithmic scale. Thus, a change from 2.5 to 3.5 represents a 10-fold reduction in acid strength. Furthermore, the pH will approach 7 as the solution contacts fresh alluvial material.
3.7.5 Solvent Extraction	
Because the injected raffinate stream will contain entrained organic reagents, BHP should determine both the amounts of organics that will both build up in the aquifer and move in the groundwater.	Please refer to Attachment 6 to Table 1.
3.7.6.2 Method	
The amount of water used for sweeping was calculated as "pore volume" which is the volume obtained by subtracting the volume of the column occupied by the core material from the total volume of the column. The number of pore volumes of water given in the figures (Appendix A, Metcon Laboratory Results) are much higher when compared to what it might be if the true pore volume of the rock materials were used in the calculation. BHP should clarify how the "pore volume" relates to the porosity of the geologic medium. BHP should also explain the consequences of the number of pore volumes being much higher when compared to the true pore volume of the rock materials in the column wash testing.	Despite careful efforts to duplicate natural conditions in column tests, the pore volume of undisturbed rock or compacted alluvial material will be less than the pore volume measured in the column. First, the material is disturbed by the coring required to obtain samples. Second, the material expands as it experiences reduced pressure. Third, the pore volume in the column includes the pore volume of the core material plus the volume of space between the core material and the column wall. The number of "pore volumes" of water used in column washing, therefore, is greater than if the test considered only the porosity of the geologic material in the column. As a result, the number of pore volumes of water actually needed to adequately clean a block will be less than the number indicated by the column tests.
3.8 ACID GENERATION POTENTIAL	
BHP differentiates basin fill deposits as "calcareous" and "non-calcareous." BHP should clarify how they define each type of fill deposit and their location.	The differentiation between "calcareous" and "non-calcareous" materials was based on sample responses to dilute hydrochloric acid, a technique that is routinely used by geologists during the logging of cores to determine the location and relative quantities of calcareous material. The material that was labeled "calcareous" reacted vigorously when dilute hydrochloric acid was applied to it, whereas the material labeled "non-calcareous" showed a milder reaction to the acid. The distribution of the "calcareous" and "non-calcareous" materials varies throughout the Lower Basin-Fill Unit.

Table 1: Response to ADEQ Comments Issued May 1, 1996	
ADEQ Comments	**BHP Response**
3.8.1 Method	
The Department is not familiar with EPA Method 3.2.3. BHP should provide more information about this method.	The correct EPA Method used is EPA 600 3.2.3.
4.3 Simulation of Mine Block Operation	
Several of the figures show stagnation points either very close to the simulated mine block (Figure 4.3-52 (IV)) or within the simulated mine block (Figures 4.3-10 and 4.3-44 (IV)). These figures indicate a potential for fluids to escape containment. BHP should demonstrate that in these scenarios they will still be able to maintain hydraulic control. What is actually capturing the particles from the north side of the example mining block in Figure 4.3-44 (IV) is not apparent. The Department suggests that the small number of particles placed within the "injection" cells is not sufficient to demonstrate capture through the various flow paths. BHP should re-run the particle tracking illustrations with an increased number of particles (say at least 10). BHP should also clarify in what layers particles are placed and in what layers they are captured. The Department suggests that the little boxes signifying captured particles be omitted from the illustrations. Instead the illustrations should show the injection wells, recovery wells, and the flow paths.	Please refer to Attachment 7 to Table 1.
4.2.1 Injection-Recovery Process	
BHP proposes to leach in 100 to 400 foot vertical sections, "beginning from the top of the bedrock and ending at the base of the oxide ore zone." The Department insists that, because the hydraulic conductivity in the overlying sediments is greater than within the bedrock, fluids must not be injected at the bedrock/sediment interface. The Department is concerned that some injected fluids may preferentially flow into the sediments and not the recovery well. Some non-leached thickness of bedrock must remain at the top of the oxide zone. The Department requests that BHP conduct another modeling exercise with particle tracking. This new model should be focused on, say, one injection well or one injection and one recovery well. The cell size, vertically as wells as horizontally, should be sufficiently fine to illustrate the hydrodynamics near the well bore and the bedrock/sediment interface. The purpose of this exercise is to determine the thickness of the oxide "buffer zone" that must exist above the leaching activities. The Department should then write this "buffer zone" thickness into the permit.	Please refer to Attachment 8 to Table 1.
4.3.1.3 Regional Pumping	
BHP's proposal to decommission the SCIDD wells that extend into the ore body is excellent. The Department should include this proposal in the compliance schedule for the project.	The decommissioning of the SCIDD wells will be included in the compliance schedule for the project.
4.3.1.4 Results of Base Simulation	
For clarification, BHP should depict the referenced capture zones for the Town of Florence municipal wells.	Please refer to Attachment 9 to Table 1.

Table 1: Response to ADEQ Comments Issued May 1, 1996	
ADEQ Comments	**BHP Response**
4.3.3.1 Rationale	
BHP should clarify whether they also consider recharge from the Arizona Sierra Utility Company WWTP to be "insignificant and unlikely to change with time."	The Arizona Sierra Utility Company has changed its name to Florence Gardens Wastewater Treatment Plant. On May 17, 1996, Ms. Tekla King of Brown and Caldwell conducted a telephone conversation with Ms. Linda Taunt of ADEQ. Ms. Taunt stated that Florence Gardens does not have a National Pollutant Discharge Elimination System (NPDES) permit and has applied for an APP that would allow it to use the water to maintain the golf course. The APP has been approved. The reuse permit has a limit of 11,314 gallons per day (gpd). This information indicates that the amount of possible recharge to date has been less than 11,314 gpd and the potential maximum amount is 11,314 gpd. This corresponds to 12.67 acre-feet/year which applied to an area of 13 acres, results in 0.97 ft/yr or 0.0027 ft/day of recharge. This small amount of recharge will not impact the modeling results.
4.4.1 Rationale	
BHP should clarify from which model layers the extraction wells were pumping.	Please refer to Attachment 10 to Table 1.
4.5.3 Geochemical Transport Parameters	
Distribution coefficient (K_d) values for sulfate and other parameters were calculated and compared with published results. BHP should provide these calculations, with all terms defined, to the Department.	Please refer to Attachment 11 to Table 1.
4.5.4 Initial Conditions for Post-Closure	
As discussed in Section 4.5.3, geochemical modeling established a range of the K_d sulfate at the expected pH. Section 3.0 of Volume IV ("Geochemical Evaluation") did not contain a discussion of the derivation of K_d values. BHP should provide this discussion of the derivation of K_d values. BHP should also indicate the source of the bulk density parameters listed in Table 4.5-1.	Please refer to Attachment 11 to Table 1.
The Department is not familiar with the cited methods of estimating dispersivity. BHP should provide the pertinent parts of Gelhar and others (1992) and Zheng and Bennett (1995) that describe these methods.	The pertinent sections of Gelhar and others (1992) and Zheng and Bennett (1995) that describe the methods of estimating dispersivity were previously submitted. They are also attached to Attachment 11-A to Table 1.
4.5.5 Results of Post Closure Simulations	
BHP should provide the rationale for the 30-year duration of the post-closure transport simulation and the rationale for not using a longer duration. BHP should also clarify whether the maximum extent of sulfate concentration is 0.5 ppm above background, the background value used and its determination.	Please refer to Attachment 12 to Table 1.
4.5.6 Chemical Transport Sensitivity Analysis	
As stated in section 2.7.4 of Volume IV, BHP did not determine site-specific porosity values. Because assumed values were used in the modeling efforts, BHP should determine the sensitivity of the calculations to porosity to assess whether site-specific porosity measurements should be conducted.	Please refer to Attachment 13 to Table 1.
5.0 References	
The reference section did not include the following citations: 1. Halpenny and Greene (1976); 2. Gorelick and others (1993); 3. Gelhar and others (1992); and 4. Montgomery and Assoc. (1992)	The APP will be amended to include these references.

Attachment 1 to Table 1

Attachment 1 to Table 1

Response to ADEQ Comment-2.2.2-Post Audit Plan

ADEQ-2.2.2-Conceptual Hydrogeology-The conceptual and numeric models will likely be further refined as future investigations and observations are made before and during in-situ mining activities. Mr. Burchard recommends that if a permit is issues for this project, that the permit contain a requirement for a post audit of the modeling efforts. Because most of the demonstrations required by A.R.S. 49-243.B.1, 2 and 3 rely heavily upon computer modeling, the department should be shown that the in-situ mining process is behaving as predicted. BHP should conduct this post audit between 5 and 10 years into the operational life of the project and will probably lead to a model redesign. This post audit will also aid a better prediction of post-closure conditions.

Post Audit Plan

BHP proposes to conduct a post audit 3 and 5 years after production of the first copper cathode. The post audits will consider both groundwater quality data collected from POC monitoring wells and head data collected from the mine site and regional wells and piezometers. Three and 5 years were selected as appropriate time periods because after 3 years the first set of injection and recovery wells will be nearly ready to begin closure, and after 5 years this first set of wells will be nearly ready to begin post closure. These data will be compared to the simulated values in order to assess the predictive accuracy of the model. Any major differences between observed and simulated values will be reported, and the model will be appropriately recalibrated. A letter report will be submitted to ADEQ following BHP's analysis. This report will summarize the post audit and present pertinent information on the recalibrated model, if necessary.

Attachment 2 to Table 1

Attachment 2 to Table 1

Response to ADEQ Comment-2.6.3-Vertical Model Layers

ADEQ-2.6-3-Vertical Model Layers-An individual model layer may contain various geologic materials. BHP should present the method by which a single hydrogeologic parameter is assigned to a cell that contains material from multiple hydrostratrigraphic units.

Figures 2.7-1 (IV) through 2.7-4 (IV) show hydraulic conductivity distribution for the oxide and sulfide zones within model layers 2 through 5 respectively. BHP should also depict the hydraulic conductivity's for the LBFU that exists within model layers 2 through 5.

Vertical Model Layers and Cross Sections

Presented on Figures 1 through 3 are west-east-oriented cross sections through the mine area. These figures show how the model layers correspond to different geologic units across the site. For example, model layer 7 contains LBFU material in the northwestern portion of the site, but oxide zone material in the north-central portion.

The hydraulic conductivity distribution within the oxide and sulfide zones and the LBFU for model layers 2 through 8 are shown in Figures 4 through 10. Also shown is the conductivity distribution within the fault zones found in the mine area.

In cells with more than one geologic unit present, the cell was assigned the geologic properties of the unit that occupies the majority of the cell.

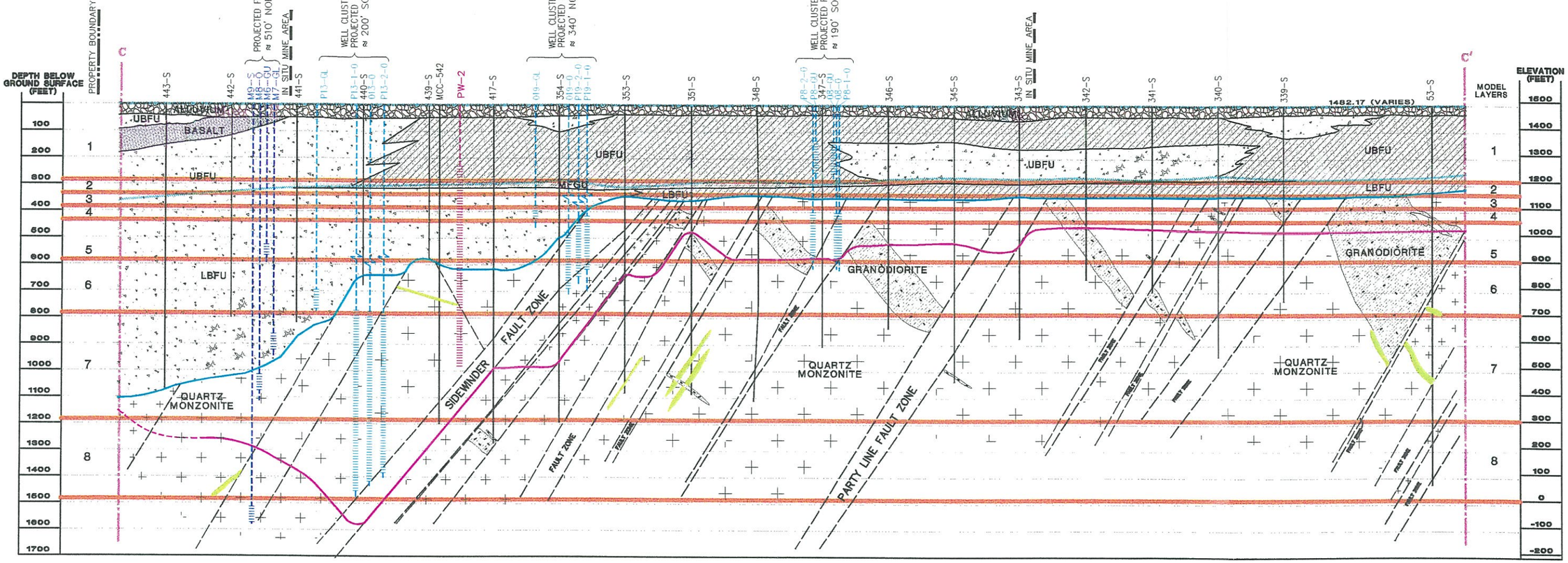

GEOLOGIC CROSS-SECTION 747,030 N
LOOKING NORTH

VERT SCALE IN FEET: 0 100 200

HORIZ SCALE IN FEET: 0 100 200

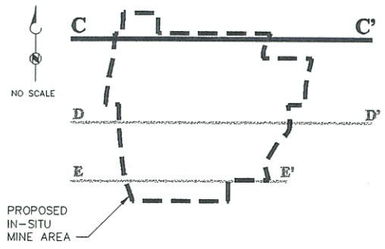

LOCATION MAP

EXPLANATION

- ALLUVIUM
- SAND, SILT AND CLAY
- SAND, BOULDERS AND CLAY
- SAND, GRAVEL AND BOULDERS
- SAND & GRAVEL
- SAND, GRAVEL AND CLAY
- SILT AND CLAY
- BASALT
- UBFU UPPER BASIN FILL UNIT
- MFGU MIDDLE FINE-GRAINED UNIT
- LBFU LOWER BASIN FILL UNIT
- GRANODIORITE PORPHYRY
- QUARTZ MONZONITE PORPHYRY
- DIABASE/DIORITE
- TERTIARY VOLCANIC UNITS
- MODEL LAYER CONTACT
- 5 MODEL LAYER
- INTERPRETED UNCONFORMITY
- LBFU/OXIDE CONTACT
- OXIDE/SULFIDE CONTACT
- EXISTING COREHOLES
- WELLS (DASHED WHERE PROJECTED)
- MONITORING
- EXISTING
- AQUIFER TESTING
- SCREEN DISTORTION DUE TO PROJECTION

NOTE:
DEPICTIONS OF WELL PROJECTED ONTO SECTION ARE ADJUSTED TO PLACE SCREENS IN PROPER GEOLOGIC VIEW

Figure 1 - Attachment 2 to Table 1

HYDROGEOLOGIC CROSS-SECTION C-C' SHOWING MODEL LAYERS

BHP

BHP Copper *Florence Project*

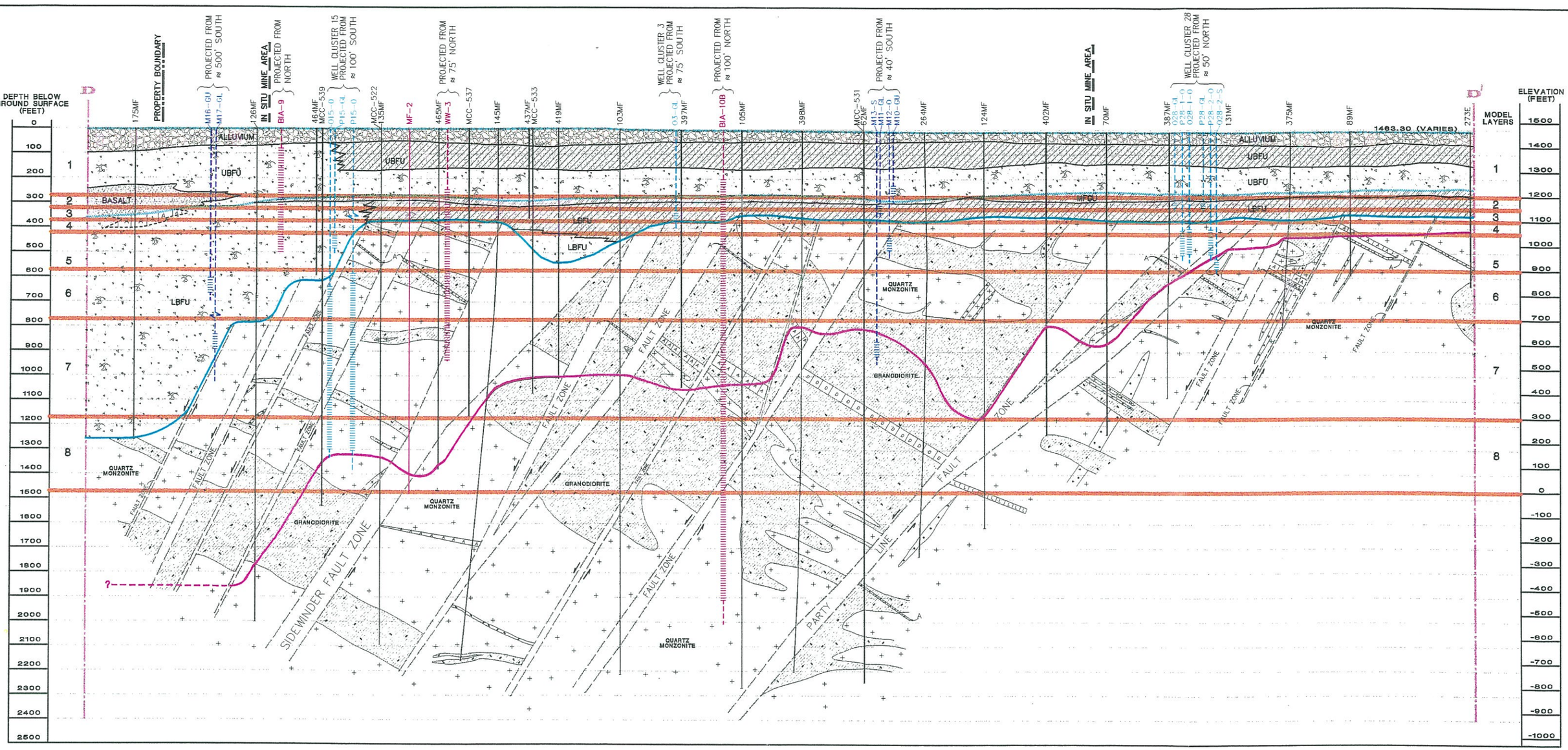

GENERALIZED GEOLOGIC CROSS-SECTION D-D'
VIEW LOOKING TO THE NORTH

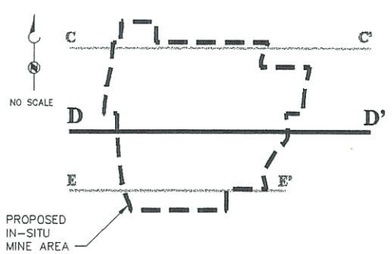

KEY MAP

EXPLANATION

- ALLUVIUM
- SAND, SILT AND CLAY
- SAND, BOULDERS AND CLAY
- SAND, GRAVEL AND BOULDERS
- SAND & GRAVEL
- SAND, GRAVEL AND CLAY
- SILT AND CLAY
- BASALT
- UBFU UPPER BASIN FILL UNIT
- MFGU MIDDLE FINE-GRAINED UNIT
- LBFU LOWER BASIN FILL UNIT
- GRANODIORITE PORPHYRY
- QUARTZ MONZONITE PORPHYRY
- DIABASE/DIORITE
- A ANDESITE
- D DACITE
- L QUARTZ LATITE
- MODEL LAYER CONTACT
- 5 MODEL LAYER
- INTERPRETED UNCONFORMITY
- LBFU/OXIDE CONTACT
- OXIDE/SULFIDE CONTACT
- EXISTING COREHOLES
- WELLS (DASHED WHERE PROJECTED)
- MONITORING
- EXISTING
- AQUIFER TESTING
- SCREEN DISTORTION DUE TO PROJECTION

NOTE: DEPICTIONS OF WELL PROJECTED ONTO SECTION ARE ADJUSTED TO PLACE SCREENS IN PROPER GEOLOGIC VIEW

0 200 400
VERT SCALE IN FEET

0 200 400
HORIZ SCALE IN FEET

Figure 2 - Attachment 2 to Table 1
HYDROGEOLOGIC CROSS-SECTION D-D' SHOWING MODEL LAYERS

BROWN AND CALDWELL

BHP
BHP Copper *Florence Project*

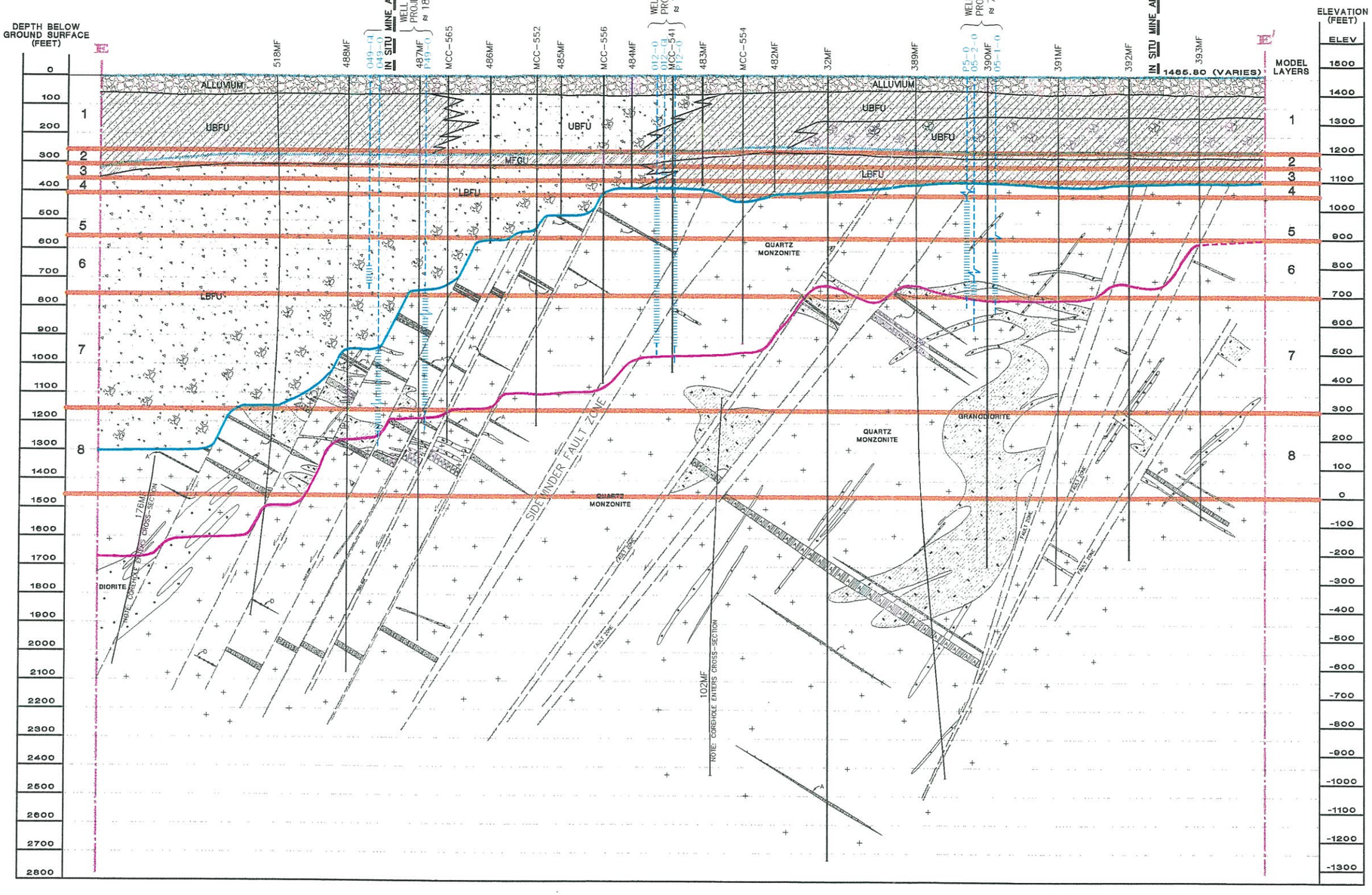

EXPLANATION

- ALLUVIUM
- SAND, SILT AND CLAY
- SAND, BOULDERS AND CLAY
- SAND, GRAVEL AND BOULDERS
- SAND & GRAVEL
- SAND, GRAVEL AND CLAY
- SILT AND CLAY
- BASALT
- UBFU UPPER BASIN FILL UNIT
- MPGU MIDDLE FINE-GRAINED UNIT
- LBFU LOWER BASIN FILL UNIT
- GRANODIORITE PORPHYRY
- QUARTZ MONZONITE PORPHYRY
- DIABASE/DIORITE
- A ANDESITE
- D DACITE
- L QUARTZ LATITE
- MODEL LAYER CONTACT
- 5 MODEL LAYER
- INTERPRETED UNCONFORMITY
- LBFU/OXIDE CONTACT
- OXIDE/SULFIDE CONTACT
- EXISTING COREHOLES

WELLS (DASHED WHERE PROJECTED)

MONITORING | EXISTING | AQUIFER TESTING | SCREEN DISTORTION DUE TO PROJECTION

NOTE: DEPICTIONS OF WELL PROJECTED ONTO SECTION ARE ADJUSTED TO PLACE SCREENS IN PROPER GEOLOGIC VIEW

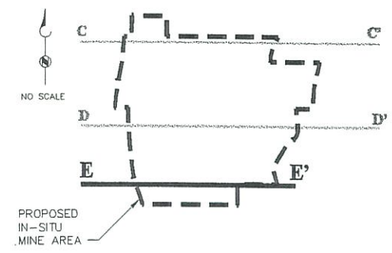

KEY MAP

0 200 400
VERT SCALE IN FEET

0 200 400
HORIZ SCALE IN FEET

GENERALIZED GEOLOGIC CROSS-SECTION E-E'
VIEW LOOKING TO THE NORTH

BROWN AND CALDWELL

Figure 3- Attachment 2 to Table 1

HYDROGEOLOGIC CROSS-SECTION E-E'
SHOWING MODEL LAYERS

BHP Copper *Florence Project*

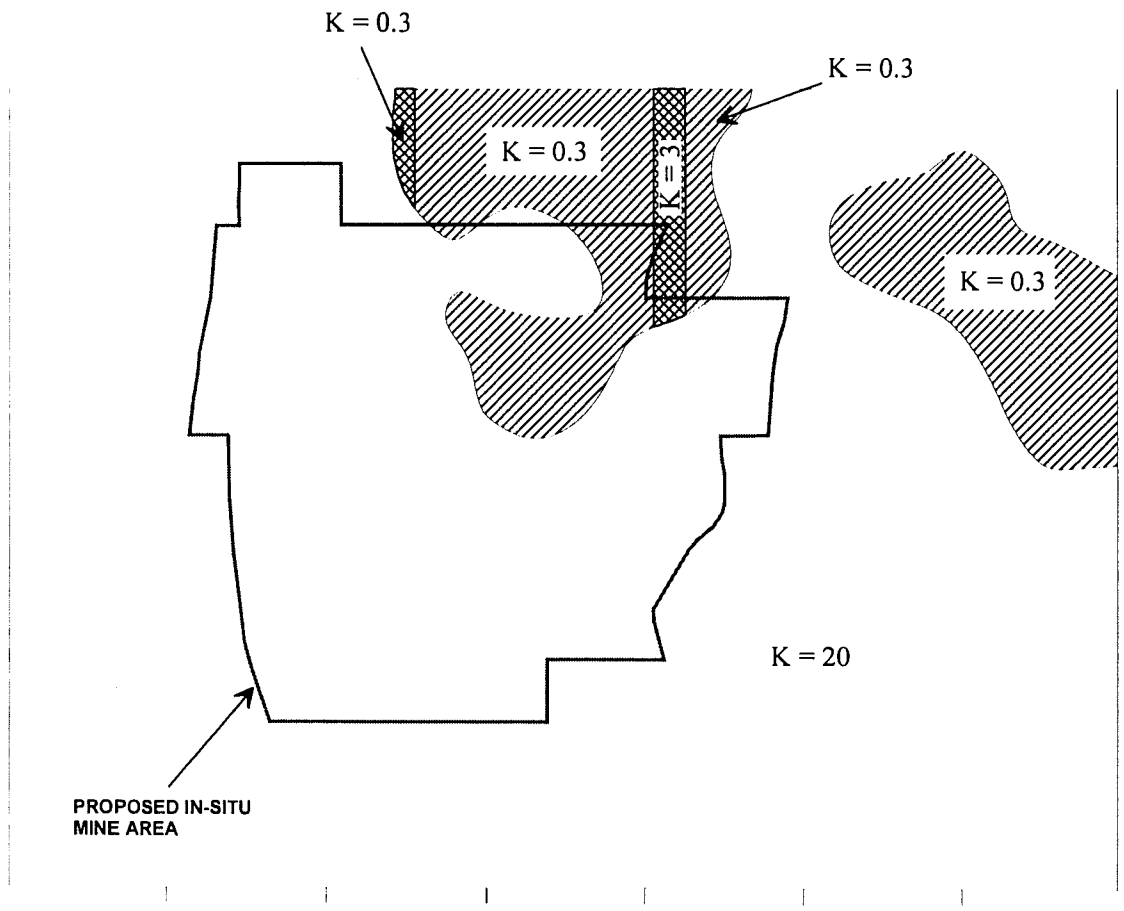

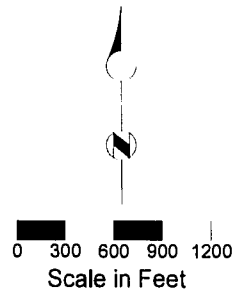

K = HYDRAULIC CONDUCTIVITY
IN FEET/DAY

LBFU

Oxide

Sulfide

Fault Zone

Figure 4 - Attachment 2 to Table 1
MODEL LAYER 2
HYDRAULIC CONDUCTIVITY
DISTRIBUTION FOR OXIDE AND
SULFIDE ZONES

BHP

BHP COPPER
Florence, Arizona

BROWN AND CALDWELL

SFIG053 09/23/96 MikeS

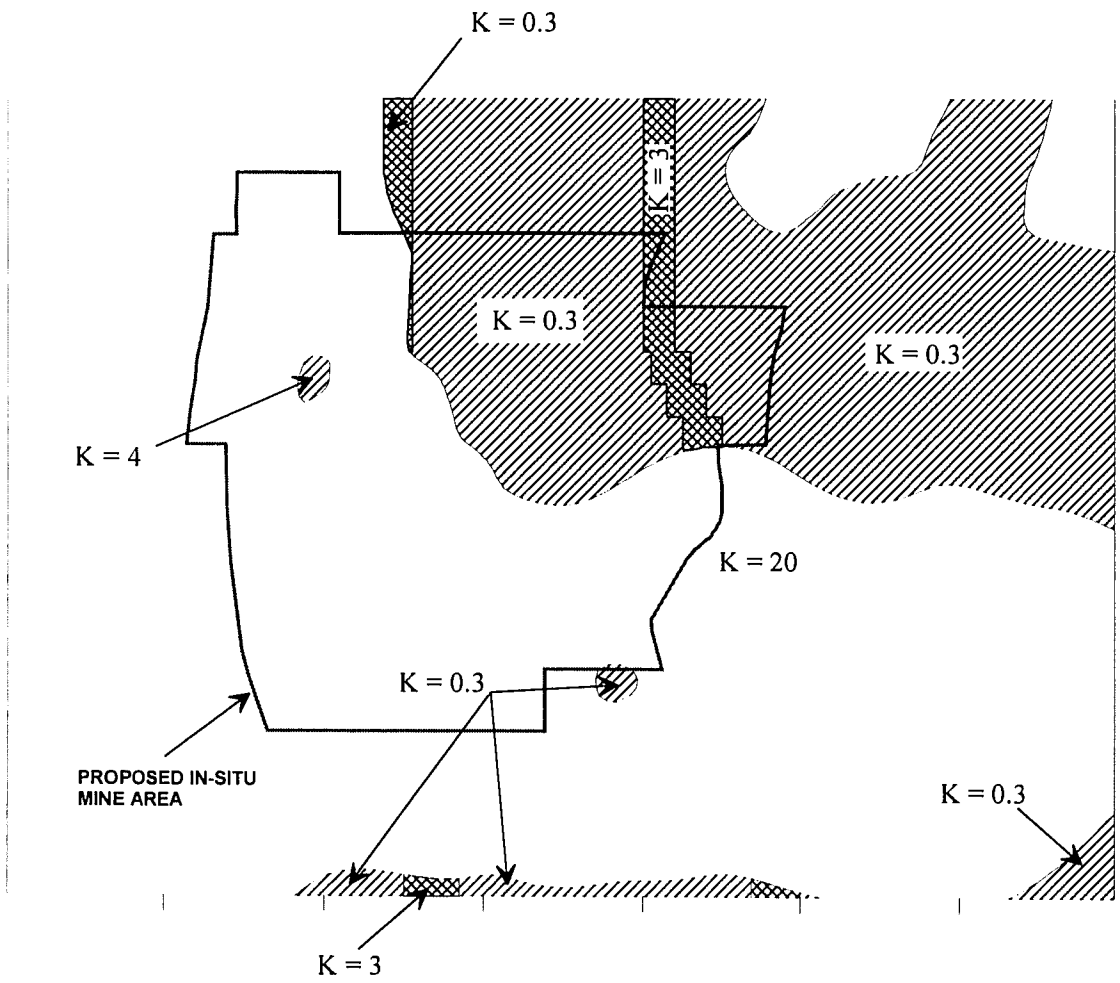

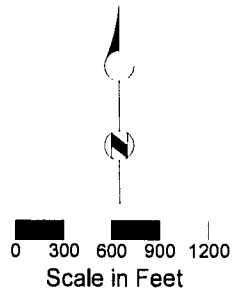

K = HYDRAULIC CONDUCTIVITY
IN FEET/DAY

LBFU

Oxide

Sulfide

Fault Zone

Figure 5 - Attachment 2 to Table 1
MODEL LAYER 3
HYDRAULIC CONDUCTIVITY
DISTRIBUTION FOR OXIDE AND
SULFIDE ZONES

BHP

BHP COPPER
Florence, Arizona

BROWN AND CALDWELL

SFIG054 09/23/96 MikeS

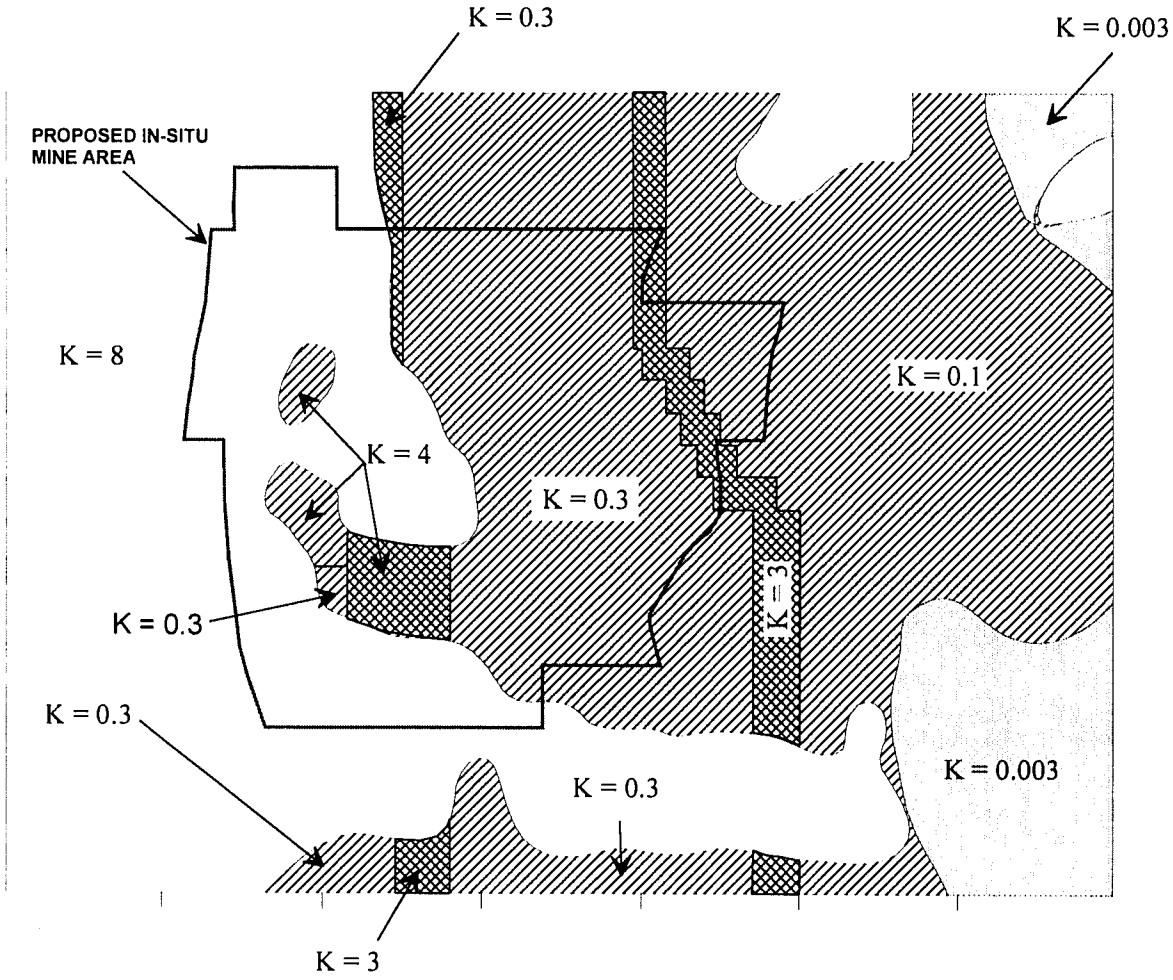

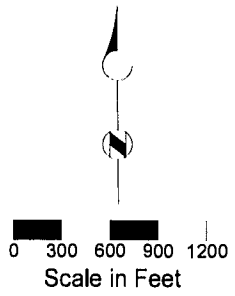

K = HYDRAULIC CONDUCTIVITY IN FEET/DAY

LBFU

Oxide

Sulfide

Fault Zone

Figure 6 - Attachment 2 to Table 1
MODEL LAYER 4
HYDRAULIC CONDUCTIVITY DISTRIBUTION FOR OXIDE AND SULFIDE ZONES

BHP

BHP COPPER
Florence, Arizona

BROWN AND CALDWELL

SFIG055 09/23/96 MikeS

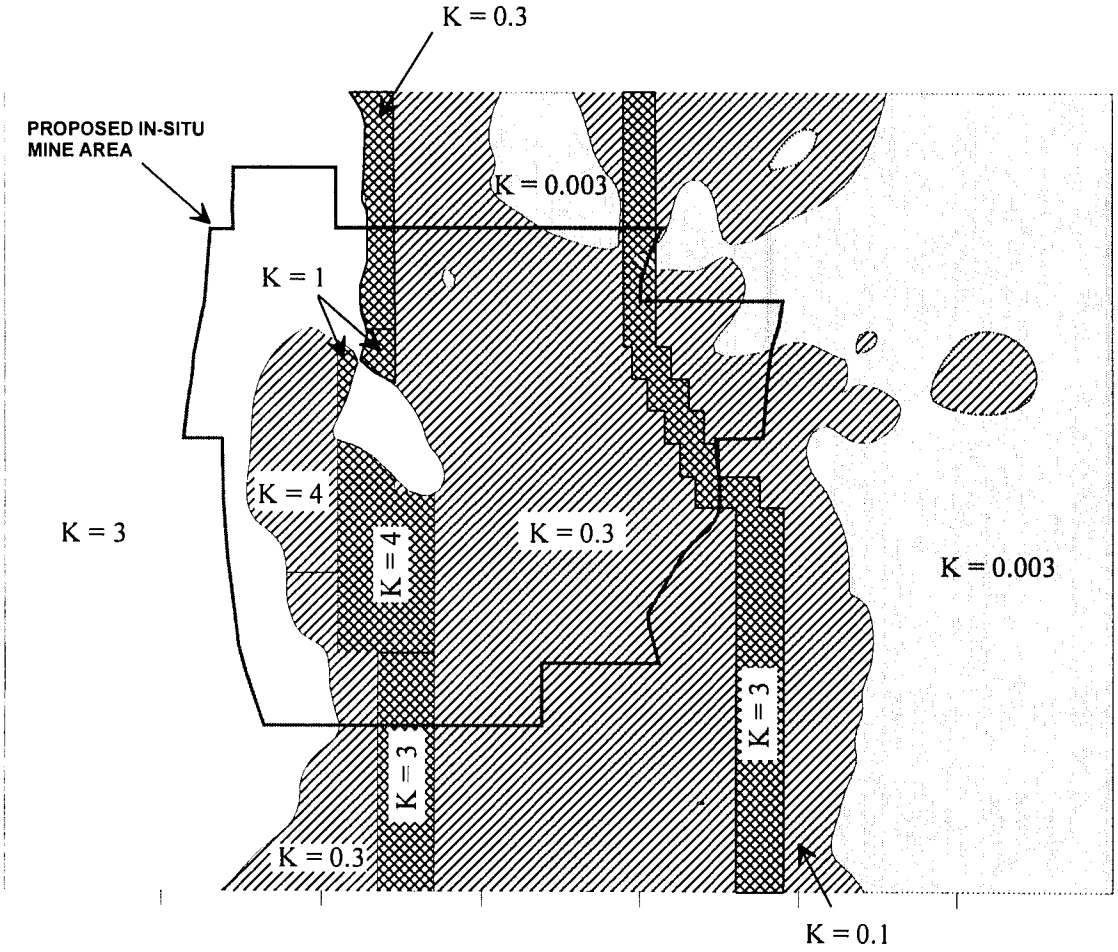

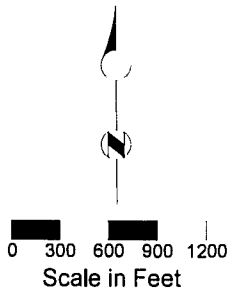

K = HYDRAULIC CONDUCTIVITY IN FEET/DAY

LBFU

Oxide

Sulfide

Fault Zone

Figure 7 - Attachment 2 to Table 1
MODEL LAYER 5
HYDRAULIC CONDUCTIVITY DISTRIBUTION FOR OXIDE AND SULFIDE ZONES

BHP

BHP COPPER
Florence, Arizona

BROWN AND CALDWELL

SFIG056 09/23/96 MikeS

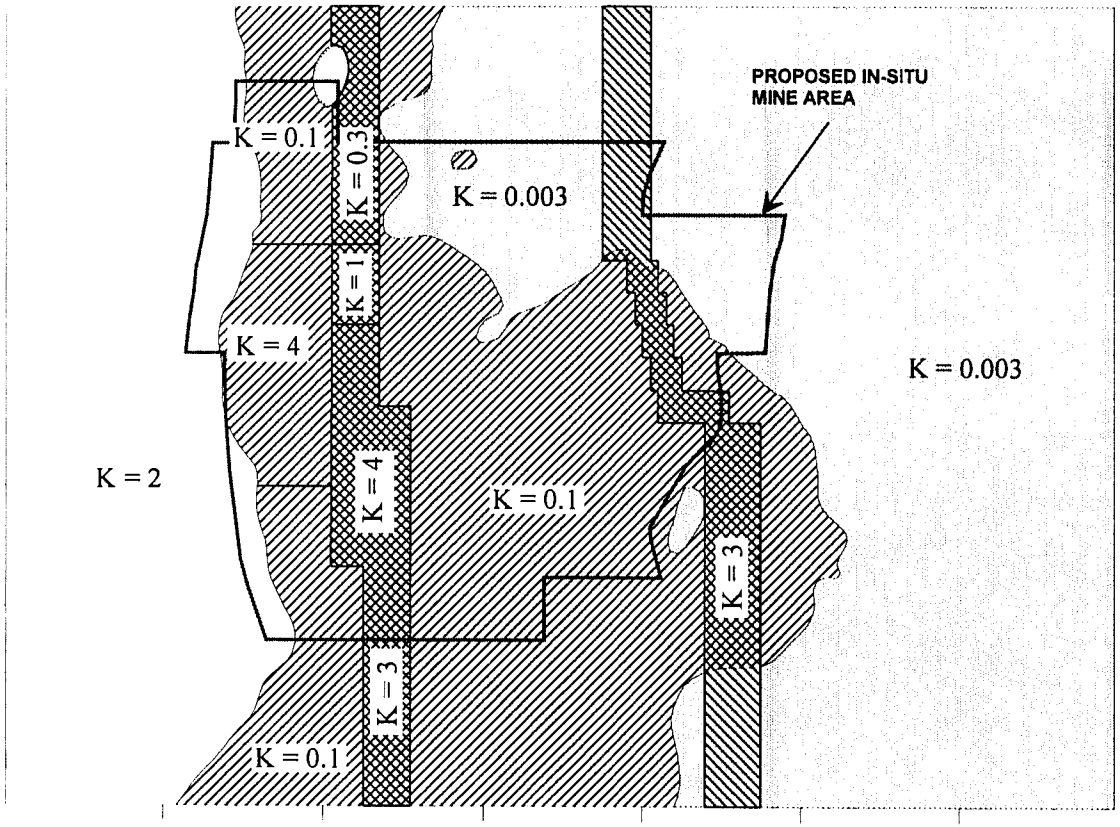

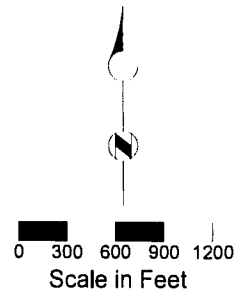

K = HYDRAULIC CONDUCTIVITY
IN FEET/DAY

LBFU

Oxide

Sulfide

Fault Zone

Figure 8 - Attachment 2 to Table 1
MODEL LAYER 6
HYDRAULIC CONDUCTIVITY
DISTRIBUTION FOR OXIDE AND
SULFIDE ZONES

BHP

BHP COPPER
Florence, Arizona

BROWN AND CALDWELL

SFIG057 09/23/96 MikeS

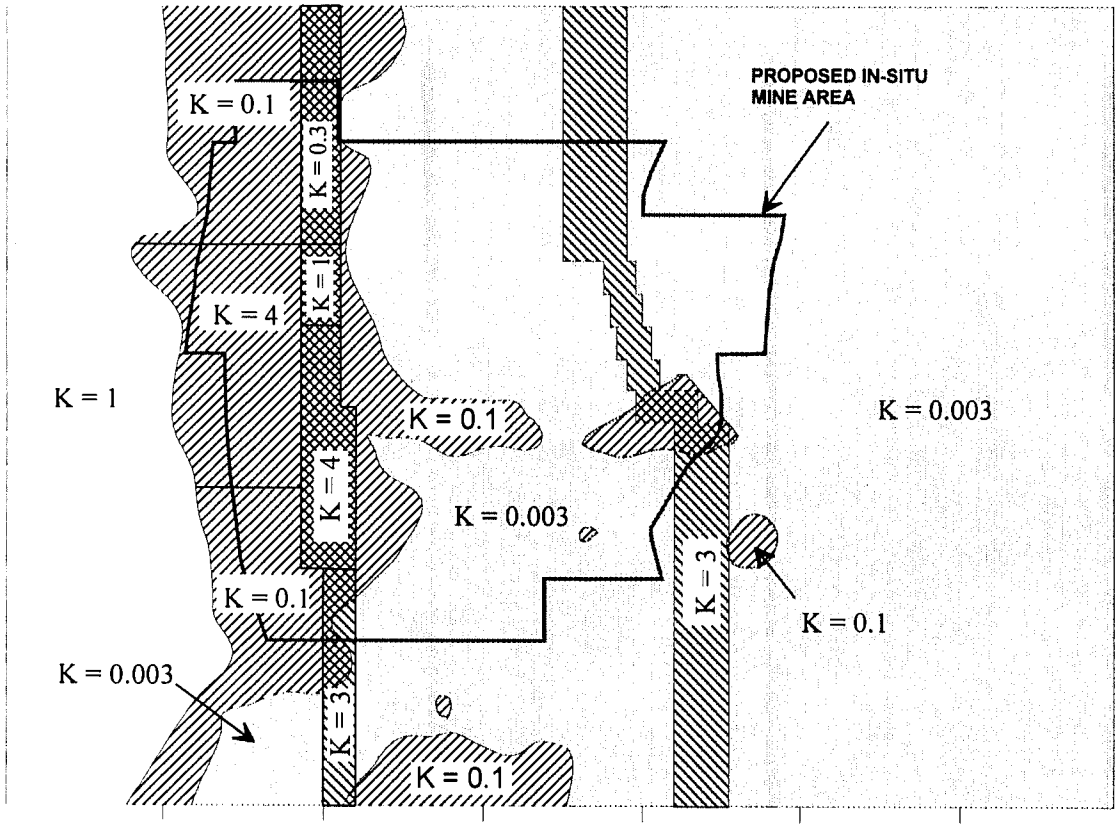

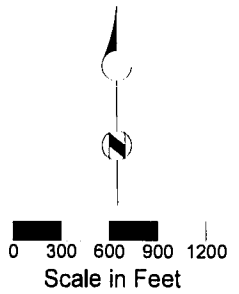

K = HYDRAULIC CONDUCTIVITY
IN FEET/DAY

LBFU

Oxide

Sulfide

Fault Zone

Figure 9 - Attachment 2 to Table 1
MODEL LAYER 7
HYDRAULIC CONDUCTIVITY
DISTRIBUTION FOR OXIDE AND
SULFIDE ZONES

BHP

BHP COPPER
Florence, Arizona

BROWN AND CALDWELL

SFIG058 09/23/96 MikeS

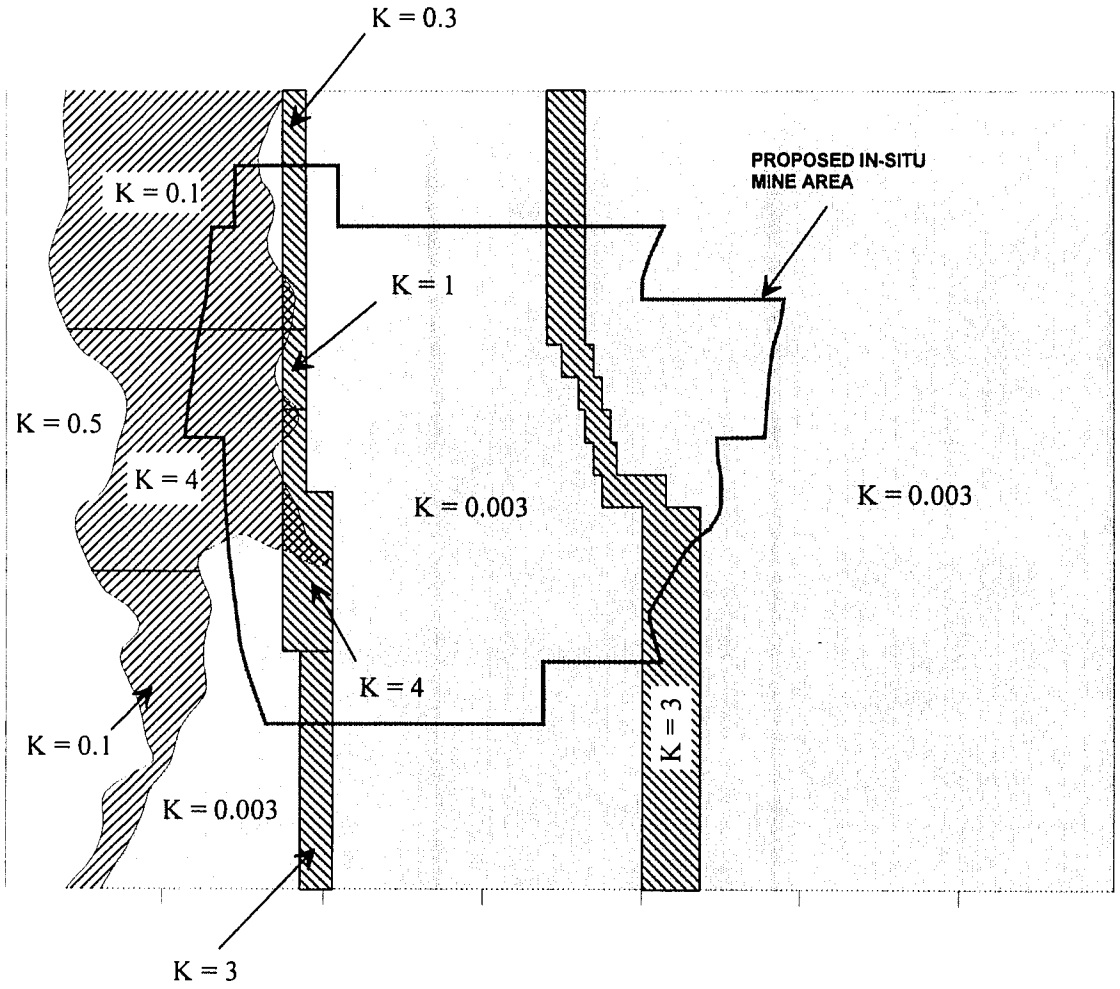

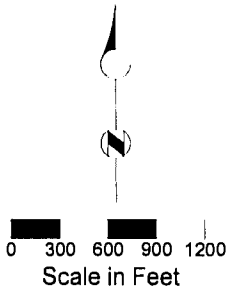

K = HYDRAULIC CONDUCTIVITY IN FEET/DAY

LBFU

Oxide

Sulfide

Fault Zone

Figure 10 - Attachment 2 to Table 1
MODEL LAYER 8
HYDRAULIC CONDUCTIVITY DISTRIBUTION FOR OXIDE AND SULFIDE ZONES

BHP

BHP COPPER
Florence, Arizona

BROWN AND CALDWELL

SFIG059 09/25/96 MikeS

Attachment 3 to Table 1

Attachment 3 to Table 1

Response to ADEQ Comment-2.6.5-Surfer Contouring Algorithms

ADEQ-2.6.5-Initial Conditions-The different contouring algorithms available in SURFER can sometimes produce markedly different results. BHP should present the method used and the rationale for its use.

SURFER Contouring Algorithms

The Kriging contouring algorithm was used for developing the water-level contours that were used as initial conditions in the model. All of the SURFER contouring algorithms produce similar groundwater flow patterns. Below, available contouring algorithms in SURFER are discussed and compared, and the rationale for selecting the Kriging algorithm is presented in more detail.

SURFER provides a variety of gridding algorithms to create contour maps. Each method produces different results depending on the nature, density and distribution of the data being gridded. The water-level elevation data for the Florence Project area from November, 1995 was chosen to demonstrate differences in gridding algorithms. The following algorithms were used for comparison:

- Triangulation with Linear Interpolation
- Inverse Distance to a Power
- Minimum Curvature
- Kriging:
  - All Data Search Method
  - Quadrant Search Method, Radius = 20000
  - Quadrant Search Method, Radius = 35600

Triangulation with Linear Interpolation

Triangulation interpolates by creating a network of triangular planes between data points. Every data point in triangulation is honored exactly. Triangulation is an effective interpolation algorithm with is a dense or regularly spaced set of data. Where this is not the case, distinctly sharp contours result between data points. In general, the accuracy of triangulation is similar to Kriging; however, Kriging creates much smoother contour lines.

Figure 1 shows an example of interpolation with triangulation. The sharp facets between data points are characteristic of triangulation with few data points. In addition, there is no extrapolation beyond exterior data points.

Inverse Distance to a Power

The inverse distance to a power method weighs each data point based on its distance from a grid node. This method typically creates numerous concentric contour lines around data points, depending on the power used. Selecting an appropriate parameter for the power is very difficult.

As shown on Figure 2, Inverse Distance to a Power is inappropriate for this data set since inverse distance does not represent the trends in the regional groundwater data.

Minimum Curvature

Minimum curvature performs an interpolation with an effect similar to bending an "elastic rod" around the data points, where smooth contour lines are created with a minimum amount of bending. The resulting contours are smooth, but minimum curvature may not honor all data points exactly due to smoothing which occurs on each pass through the data set.

Figure 3 shows how minimum curvature produces a slightly different map than triangulation or Kriging. This method was not selected because it was not representative of the regional groundwater system.

Kriging

The Kriging method interpolates using a weighting factor for data points, but unlike inverse distance or minimum curvature, it identifies general trends in the data. Unlike triangulation, Kriging can perform well with smaller data sets. Larger data sets take more time to grid than other methods, but this method generally consistently produces the most accurate and the smoothest contour lines.

Kriging has many different options included for flexibility. One option is the search method. This determines the number of sectors SURFER uses to search for data points and the radius of the ellipse it searches in. The "All Data" option uses all data points to perform the interpolation. This produces the smoothest contours. The quadrant and octant search methods only search four or eight sectors, respectively, within the given radius, causing data points outside the ellipse to be excluded form interpolation. This may create irregular contour lines, but disregards data which is not within a required distance of the node being gridded.

Figures 4, 5 and 6 show Kriging with different options. The quadrant search method shown in Figures 4 and 5 with radii of 20000 and 32600, respectively, produces somewhat jagged contour lines. The smoothest contours are created with the "All Data" search options as shown in Figure 6. Based on a comparison to "hand drawn" interpretations, Figure 6 is believed to be the most representative of the regional groundwater system.

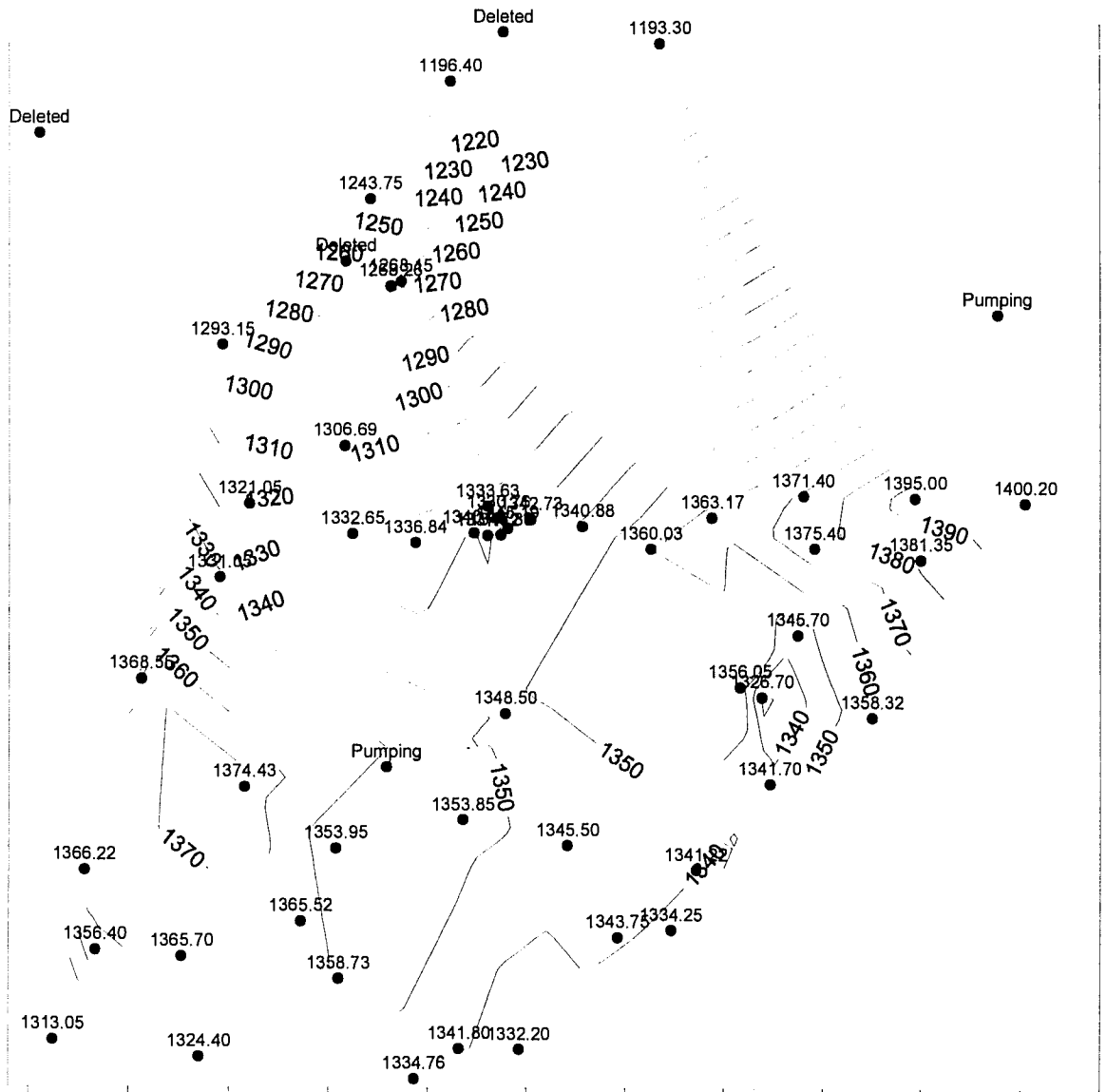

0 2500 5000 7500 10000
Scale in Feet

Grid Cell Size: 500 x 500
Data Points: 50

Figure 1 - Attachment 3 to Table 1
NOVEMBER 1995 WATER-LEVEL ELEVATIONS GRIDDED WITH THE TRIANGULATION METHOD

BHP COPPER *Florence Project*

BROWN AND CALDWELL

SFIG061 08/28/96 MikeS

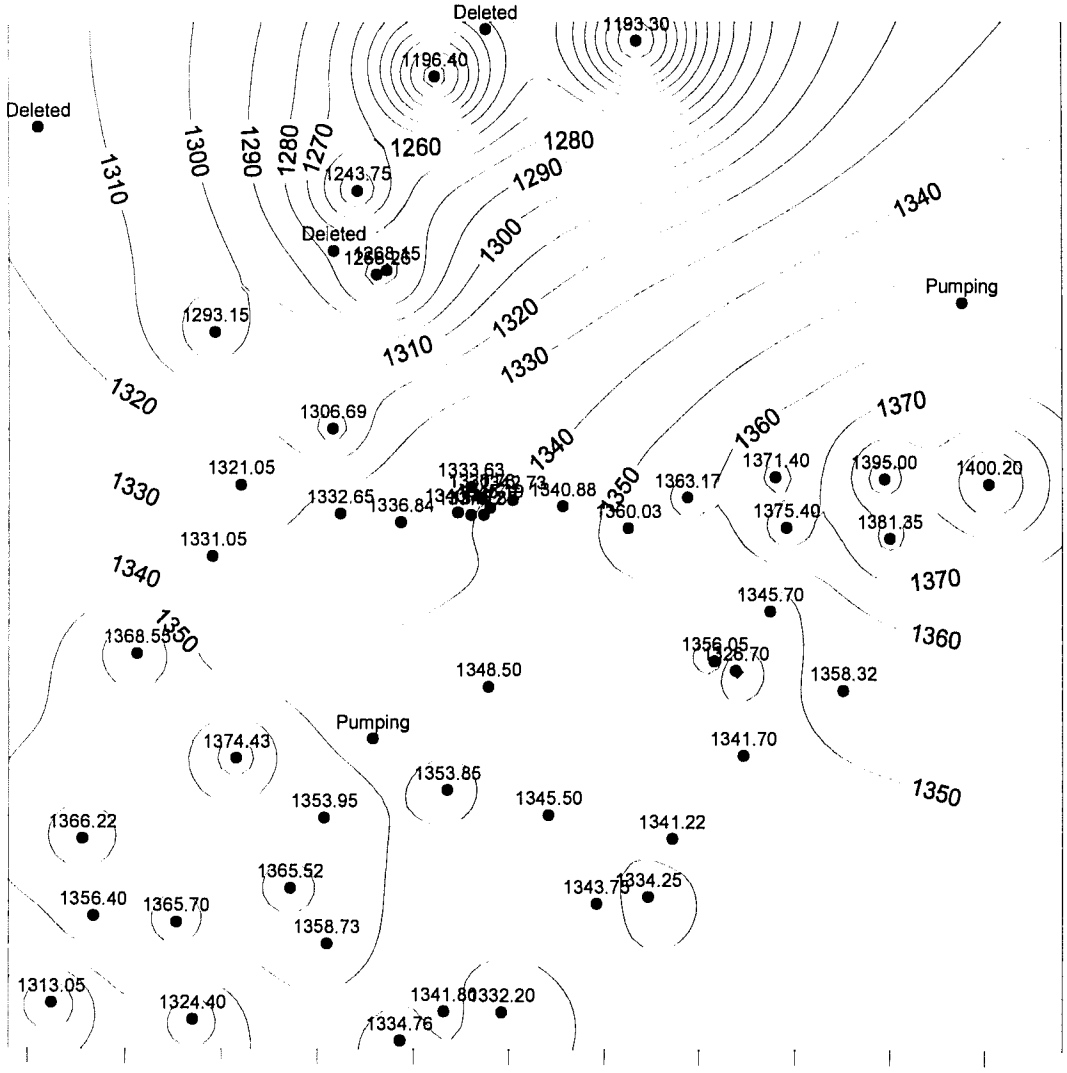

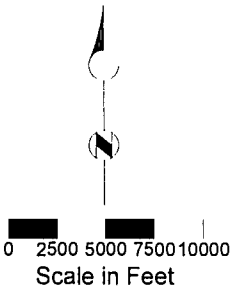

Grid Cell Size: 500 x 500
Data Points: 50

Figure 2 - Attachment 3 to Table 1
NOVEMBER 1995 WATER-LEVEL ELEVATIONS GRIDDED WITH THE INVERSE DISTANCE METHOD

BHP
BHP COPPER *Florence Project*

BROWN AND CALDWELL

SFIG060 08/28/96 MikeS

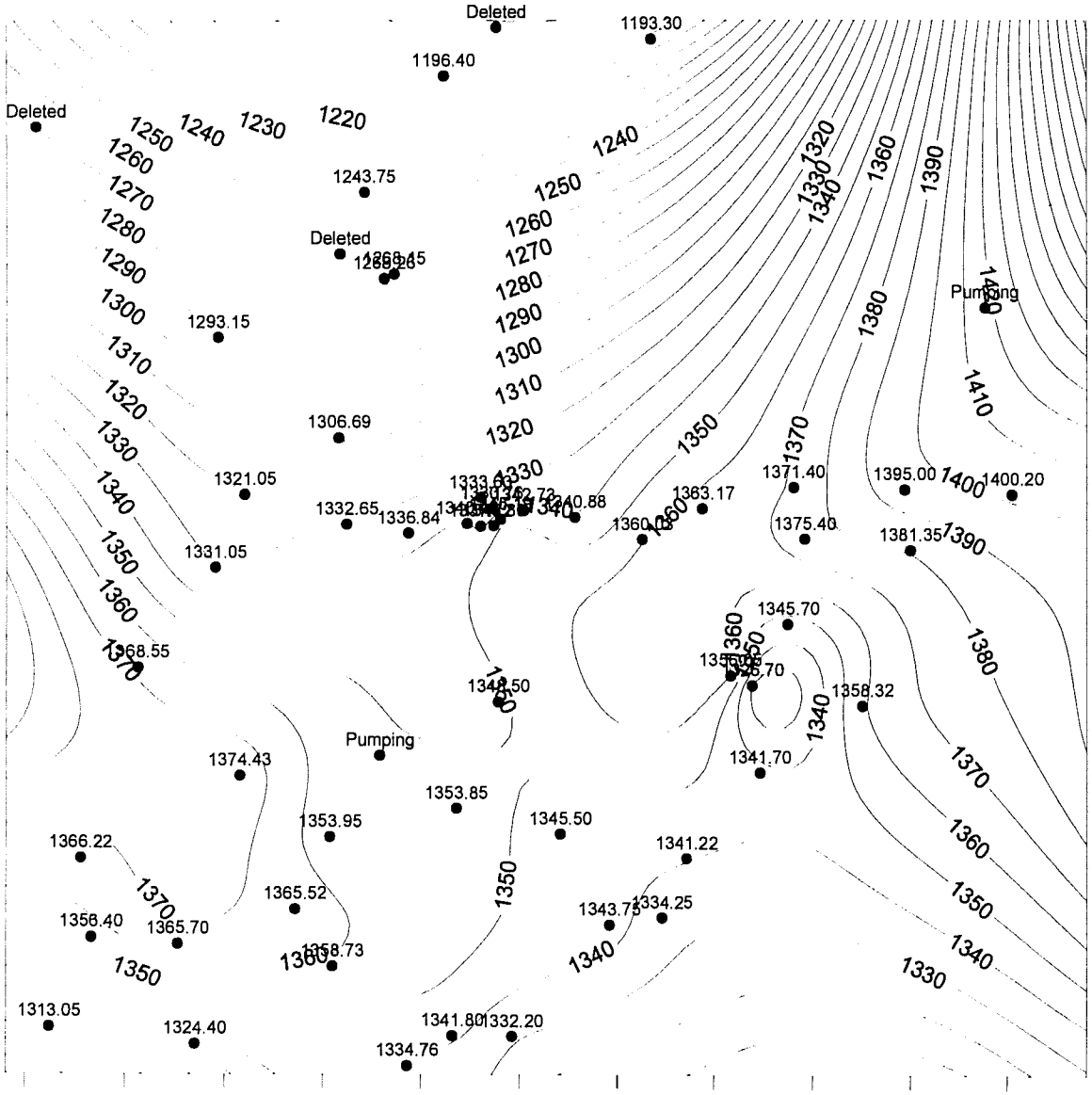

Figure 3 - Attachment 3 to Table 1
NOVEMBER 1995 WATER-LEVEL ELEVATIONS GRIDDED WITH THE MINIMUM CURVATURE METHOD

BHP COPPER *Florence Project*

BROWN AND CALDWELL

SFIG062 08/28/96 MikeS

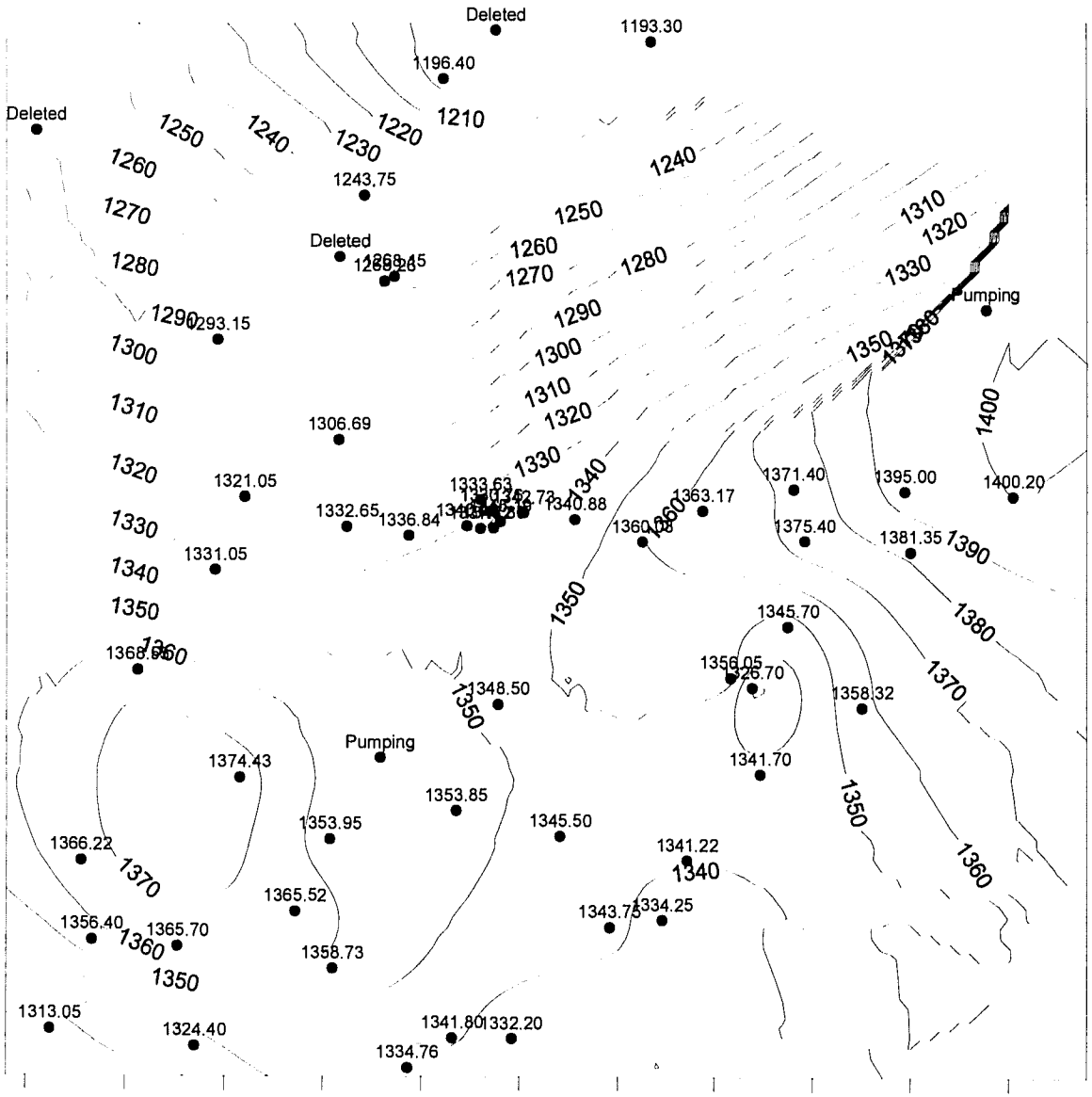

Grid Cell Size: 500 x 500
Search Type: Quadrant
Data Points: 50
Search Radius: 20000

Figure 4 - Attachment 3 to Table 1
NOVEMBER 1995 WATER-LEVEL ELEVATIONS GRIDDED WITH THE KRIGING METHOD

BHP
BHP COPPER *Florence Project*

BROWN AND CALDWELL

SFIG063 09/04/96 MikeS

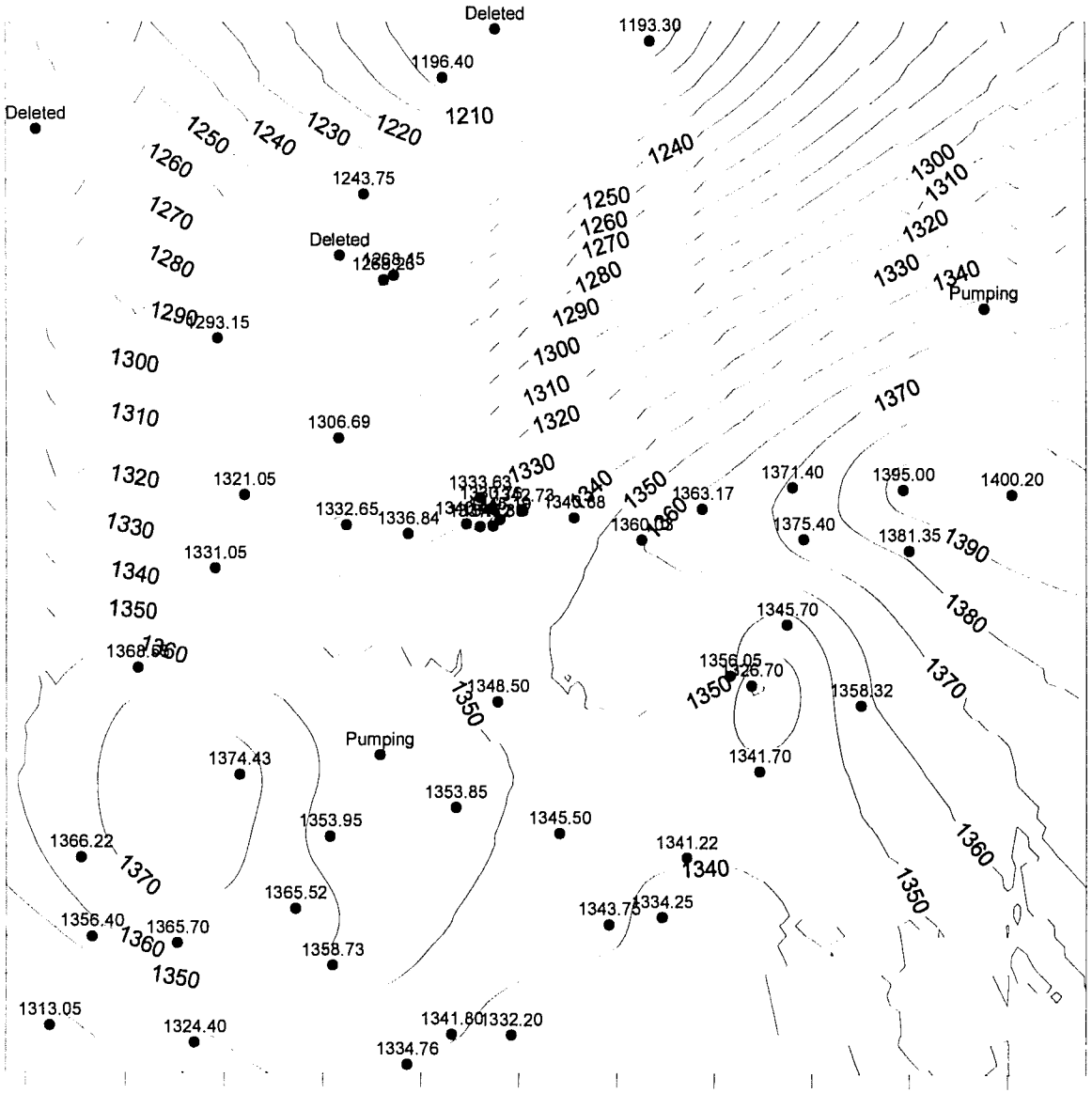

Grid Cell Size: 500 x 500
Search Type: Quadrant
Data Points: 50
Search Radius: 35600

Figure 5 - Attachment 3 to Table 1
NOVEMBER 1995 WATER-LEVEL ELEVATIONS
KRIGING METHOD

BHP
BHP COPPER *Florence Project*

BROWN AND CALDWELL

SFIG065 09/04/96 MikeS

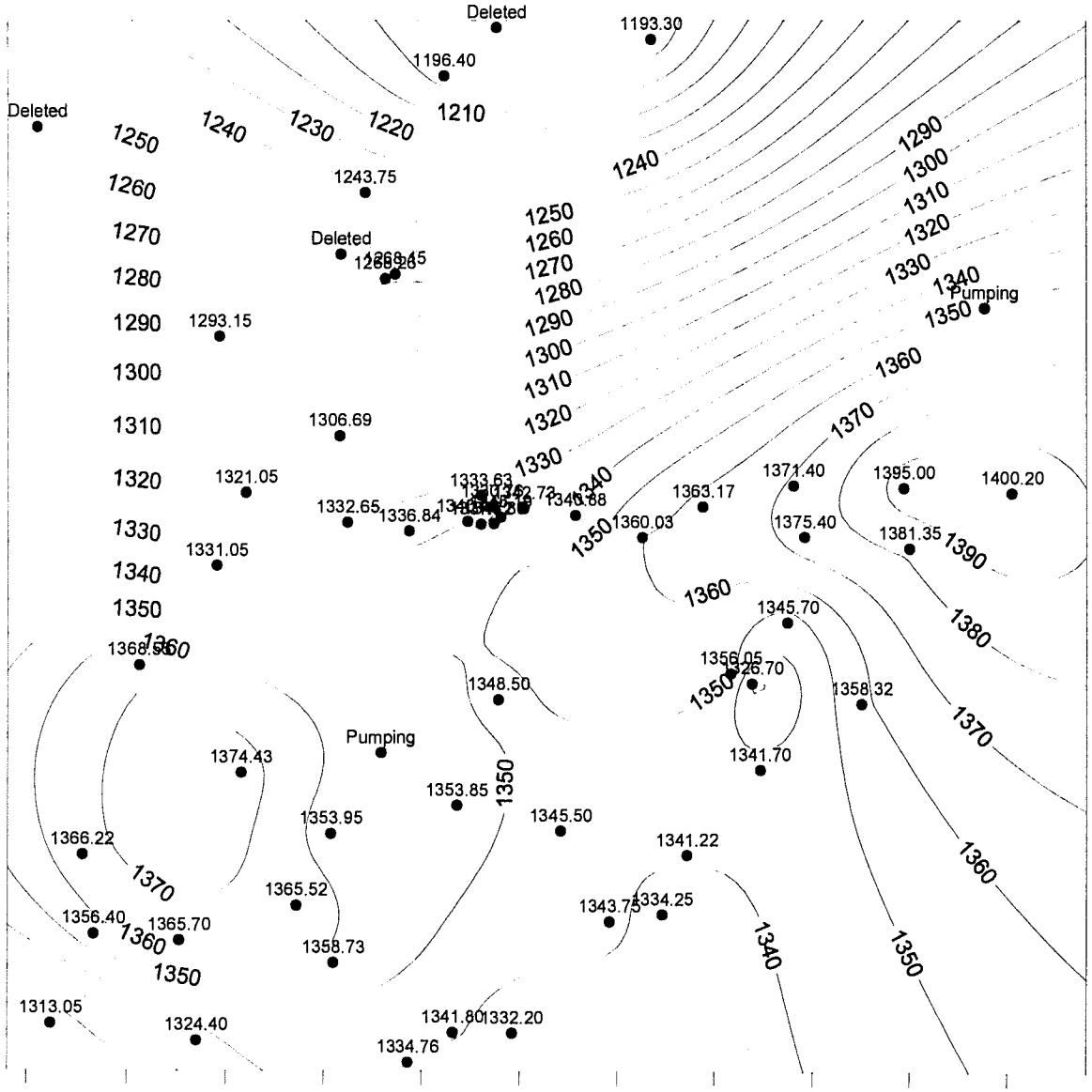

Grid Cell Size: 500 x 500
Search Type: All Data
Data Points: 50
Search Radius: N/A

Figure 6 - Attachment 3 to Table 1
NOVEMBER 1995 WATER-LEVEL ELEVATIONS GRIDDED WITH THE KRIGING METHOD

BHP
BHP COPPER *Florence Project*

BROWN AND CALDWELL

SFIG064 09/04/96 MikeS

Attachment 4 to Table 1

Attachment 4 to Table 1

Response to ADEQ Comment-2.10-Sensitivity Analysis Residuals

ADEQ-2.10-Sensitivity Analysis-Variations performed in the sensitivity analysis included increasing the hydraulic conductivity in Model Layer 5 by one order of magnitude. BHP should provide the rationale for selecting Layer 5 as the layer of interest. Also Figures 2.10-1 (IV) through 2.10-6 (IV) do not show residual head values as stated in the text.

Sensitivity Analysis Residuals

Layer 5 was shown as the layer of interest because it is the first layer with considerable thickness of the oxide zone (150 feet) that also includes the LBFU/oxide zone contact. Section 4.3.4.1 of Volume IV of the APP, page 4-10, last paragraph, states: "In the vicinity of Block 10, Model Layer 5 was selected to represent the variations in geologic conditions because hydraulic control would be sensitive to these changes. The oxide ore present within model layer 5 of Block 10 is overlain by oxide bedrock and surrounded by LBFU to the west, north and east. Therefore, if lateral excursions of mine solutions were to occur in this layer, the LBFU would be affected." These conditions represent the potential worst case for excursion of mining fluids (Figure 4.3-4 [IV]).

Figures 1 through 6 of this attachment present residual head contours for the following sensitivity analysis scenarios: Increased Storage, Decreased Storage, Increase in all General Head boundaries, Increase in Eastern General Head Boundaries, Increase in Hydraulic Conductivity, and Increase in Gila River Bed Conductance.

The model exhibits sensitivity Type III relative to the river bed conductance. This is discussed in Attachment 5 to Table 1. As shown in Figures 1 through 5, the model shows sensitivity Type I relative to all other input parameters tested. According to the ASTM document referenced in the comment (ASTM D 5611-94, Standard Guide for Conducting a Sensitivity Analysis for a Ground-Water Flow Model Application), Type I sensitivity occurs when variation of an input causes insignificant changes in the calibration residuals as well as in the model's conclusions. Type I sensitivity is of little concern because regardless of the value of the input, the conclusion will remain the same. As seen in residual maps 1 through 5, the change in head due to the change in parameter reaches a maximum of 2.5 feet over the mine area which is the area of interest. The largest change in head, 7 feet, occurs at the increase in all General Head Boundaries scenario (Figure 3). Neither the calibration nor the results vary significantly as a result of these changes.

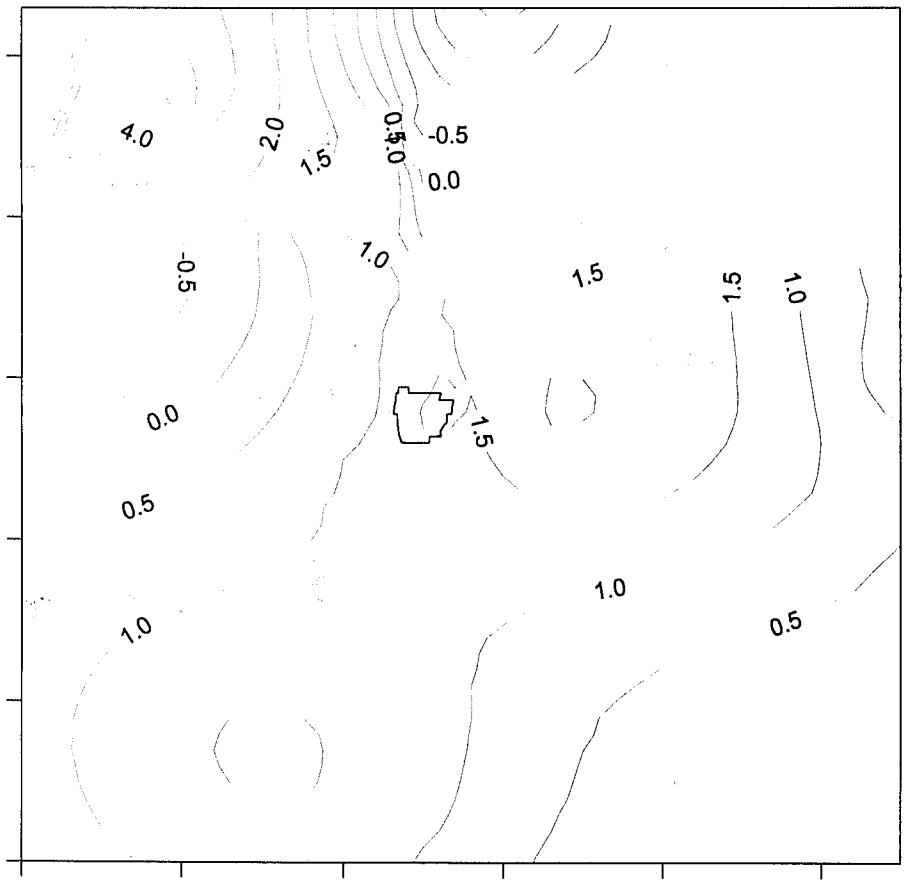

Model Layer 1

0 6000 12000

Scale in Feet

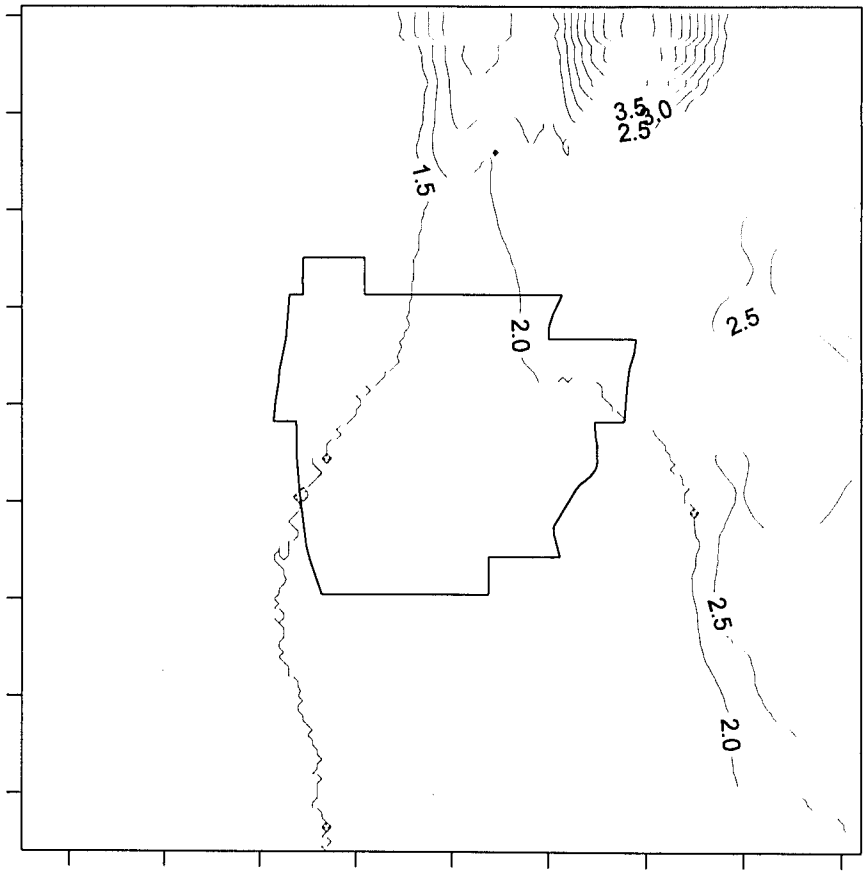

Model Layer 5

0 1000 2000

Scale in Feet

Figure 1 - Attachment 4 to Table 1
RESIDUAL MAP
SENSITIVITY ANALYSIS
INCREASED STORAGE

BROWN AND CALDWELL

Residual = Sensitivity Simulation - Base Simulation
Contours Reflect Residual Head in Feet

BHP

BHP COPPER *Florence Project*

SFIG068 08/13/96 MikeS

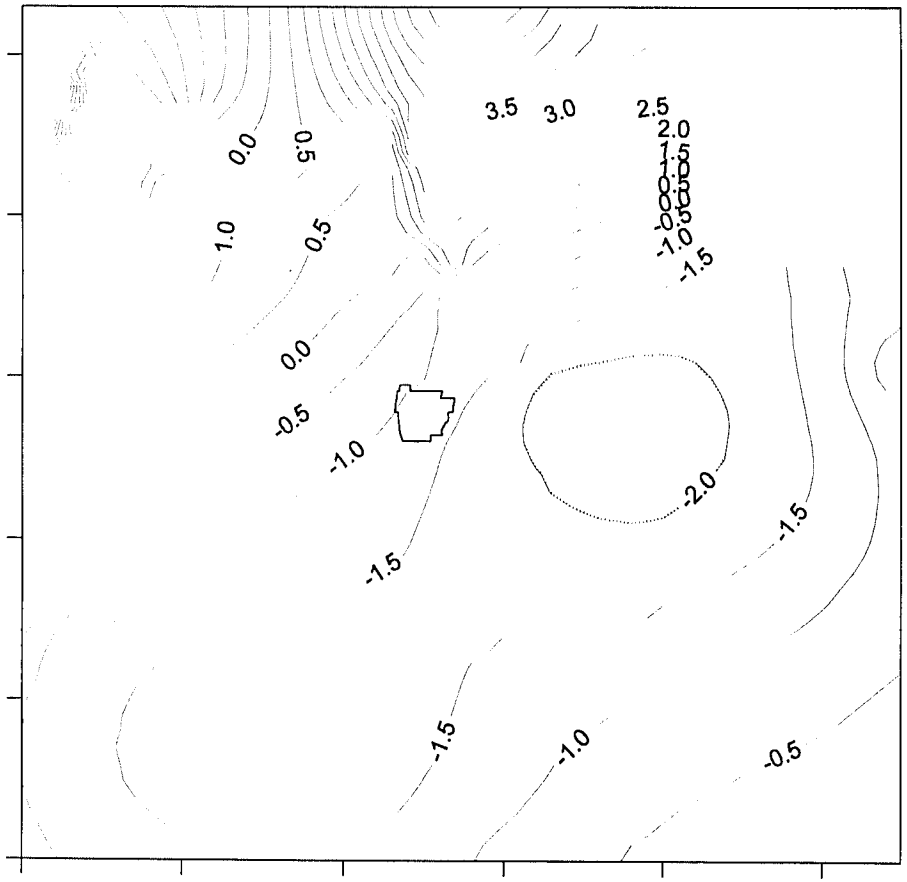

Model Layer 1

0 6000 12000

Scale in Feet

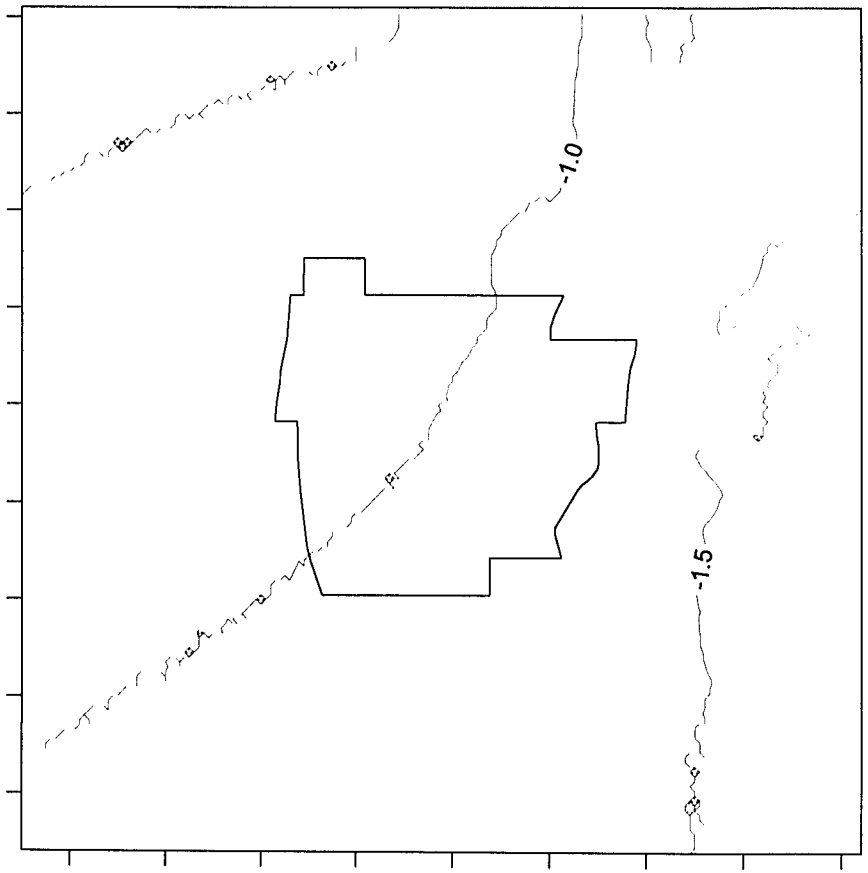

Model Layer 5

0 1000 2000

Scale in Feet

Figure 2 - Attachment4 to Table 1
RESIDUAL MAP
SENSITIVITY ANALYSIS
DECREASED STORAGE

BHP

BHP COPPER *Florence Project*

BROWN AND CALDWELL

Residual = Sensitivity Simulation - Base Simulation
Contours Reflect Residual Head in Feet

SFIG069 08/13/96 MikeS

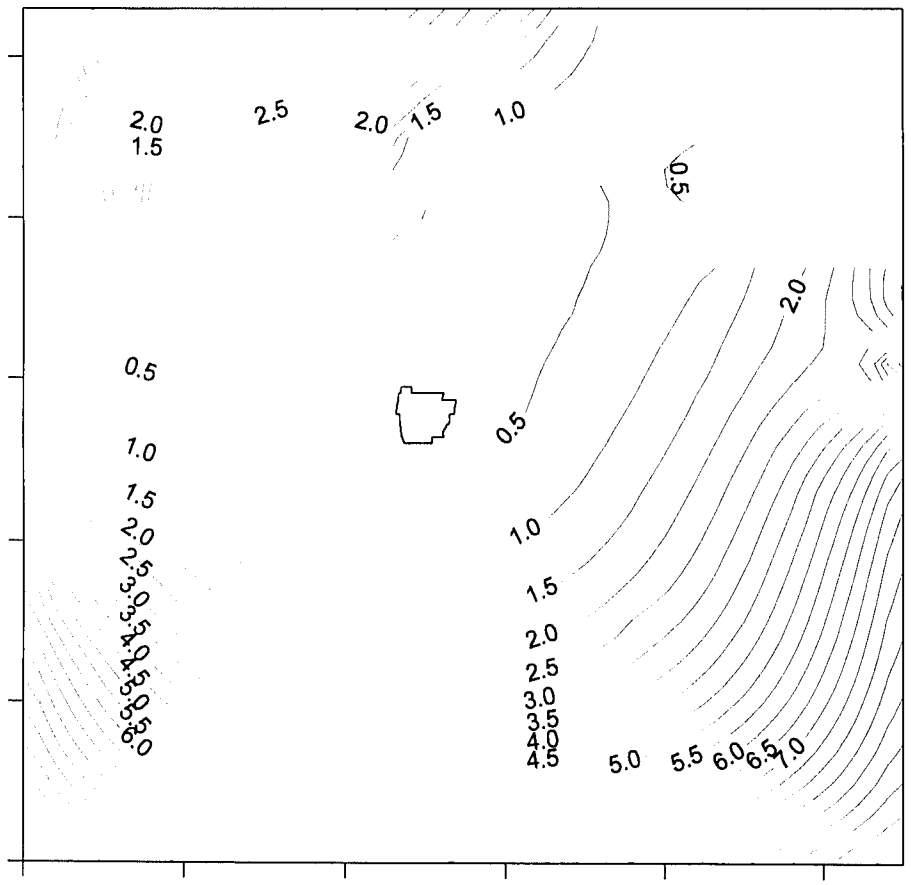

Model Layer 1

0 6000 12000

Scale in Feet

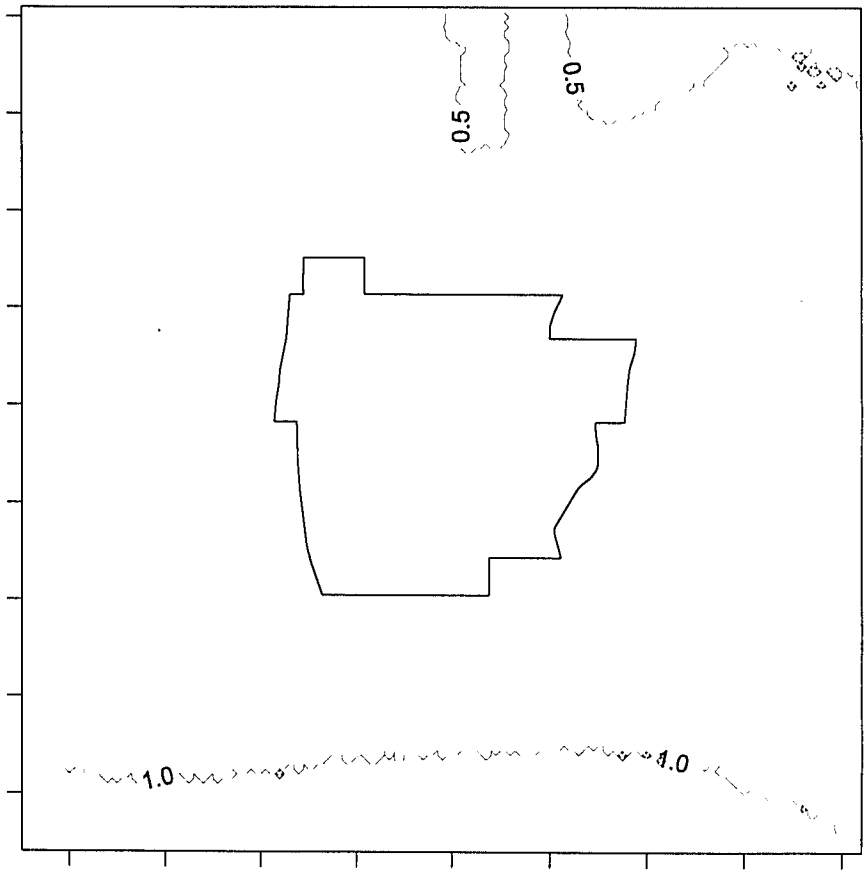

Model Layer 5

0 1000 2000

Scale in Feet

Figure 3 - Attachment 4 to Table 1
RESIDUAL MAP
SENSITIVITY ANALYSIS
INCREASE IN ALL
GENERAL HEAD
BOUNDARIES

Residual = Sensitivity Simulation - Base Simulation
Contours Reflect Residual Head in Feet

BROWN AND CALDWELL

BHP

BHP COPPER *Florence Project*

SFIG070 08/13/96 MikeS

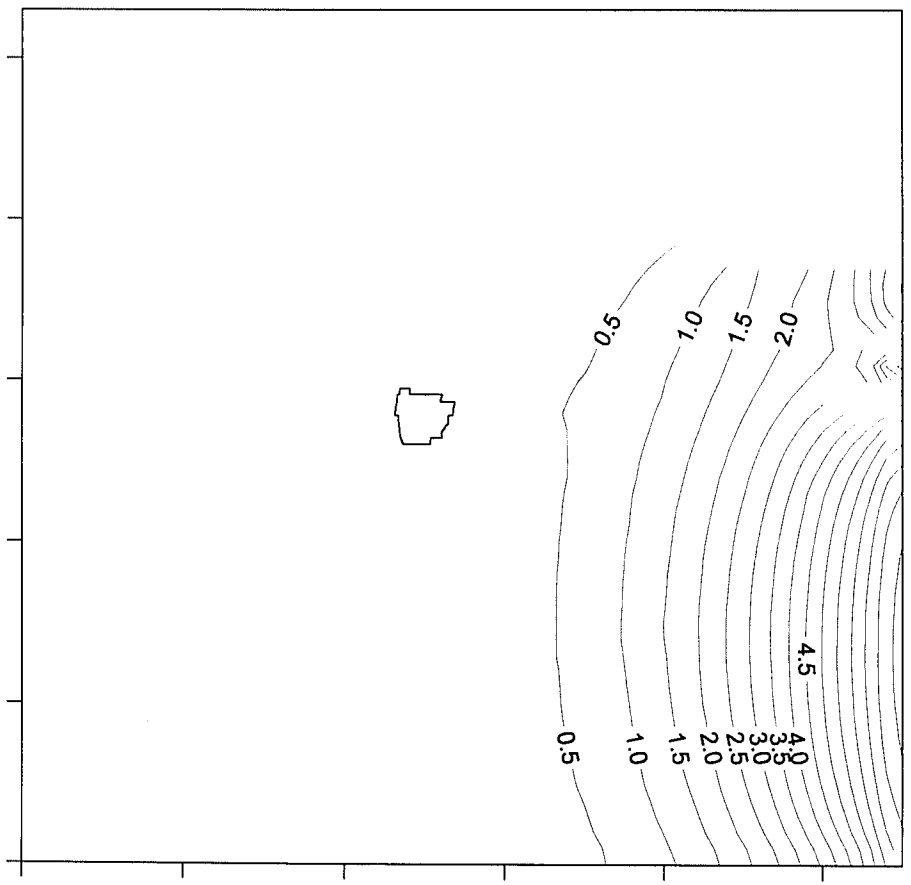

Model Layer 1

0 6000 12000

Scale in Feet

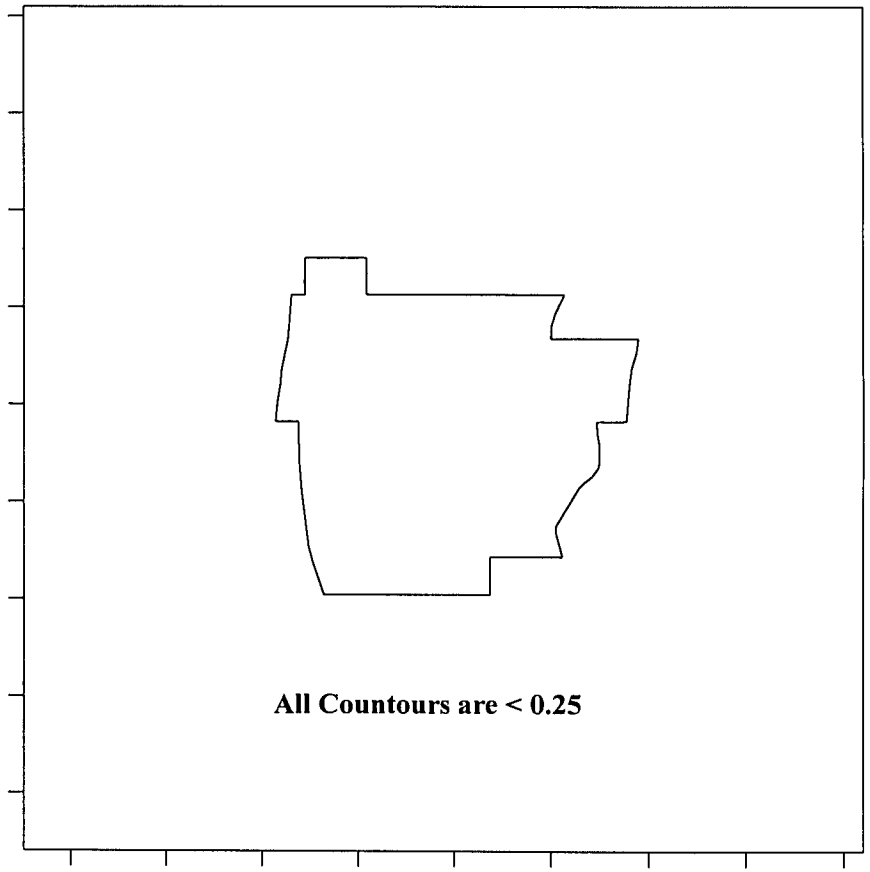

Model Layer 5

0 1000 2000

Scale in Feet

Figure 4 - Attachment 4 to Table 1
RESIDUAL MAP
SENSITIVITY ANALYSIS
INCREASE IN EASTERN
GENERAL HEAD
BOUNDARIES

BHP

BHP COPPER *Florence Project*

BROWN AND CALDWELL

Residual = Sensitivity Simulation - Base Simulation
Contours Reflect Residual Head in Feet

SFIG071 08/13/96 MikeS

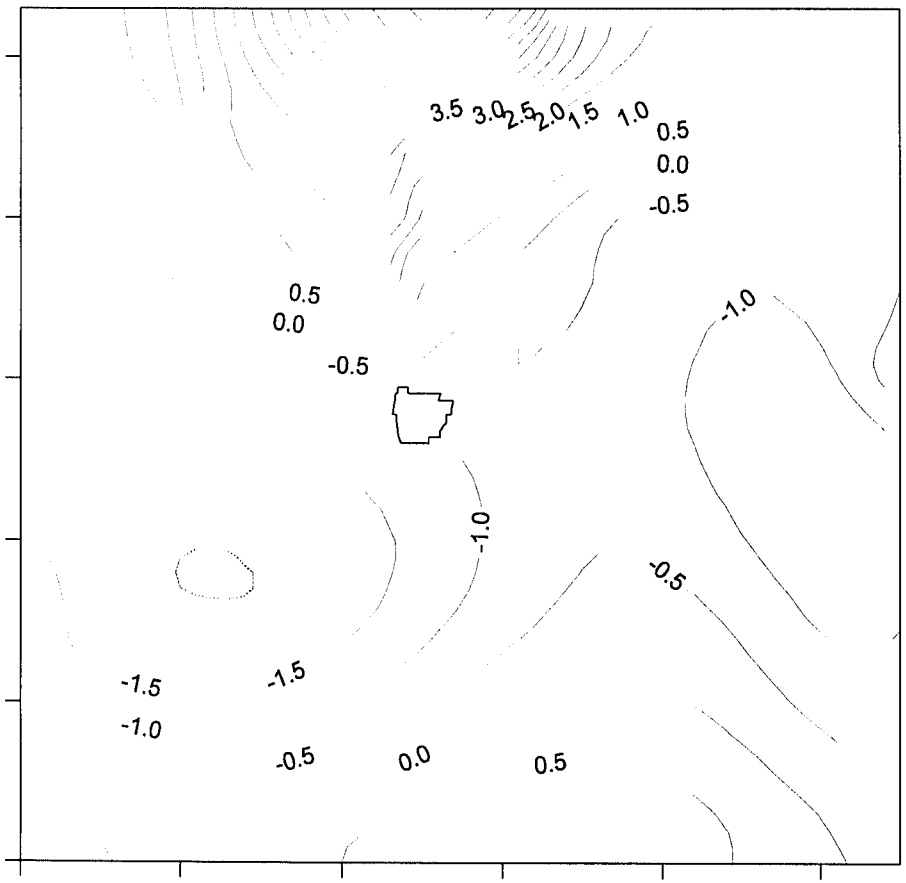

Model Layer 1

0 6000 12000

Scale in Feet

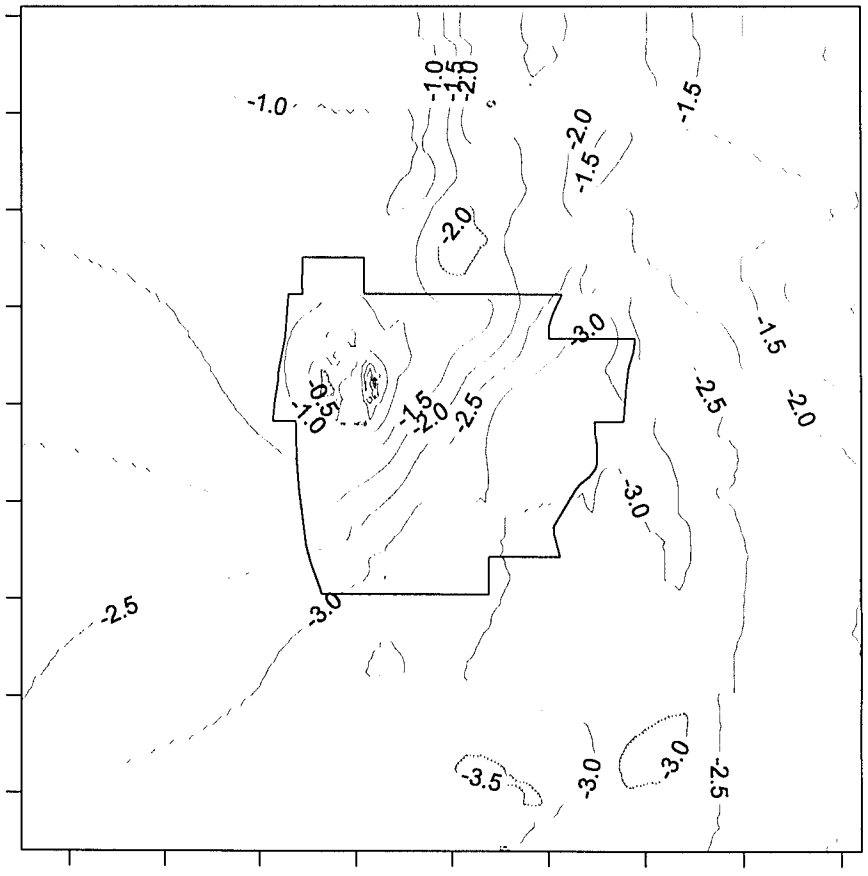

Model Layer 5

0 1000 2000

Scale in Feet

Figure 5 - Attachment 4 to Table 1
RESIDUAL MAP
SENSITIVITY ANALYSIS
INCREASE IN
HYDRAULIC
CONDUCTIVITY

BHP

BHP COPPER *Florence Project*

BROWN AND CALDWELL

Residual = Sensitivity Simulation - Base Simulation
Contours Reflect Residual Head in Feet

SFIG072 08/13/96 MikeS

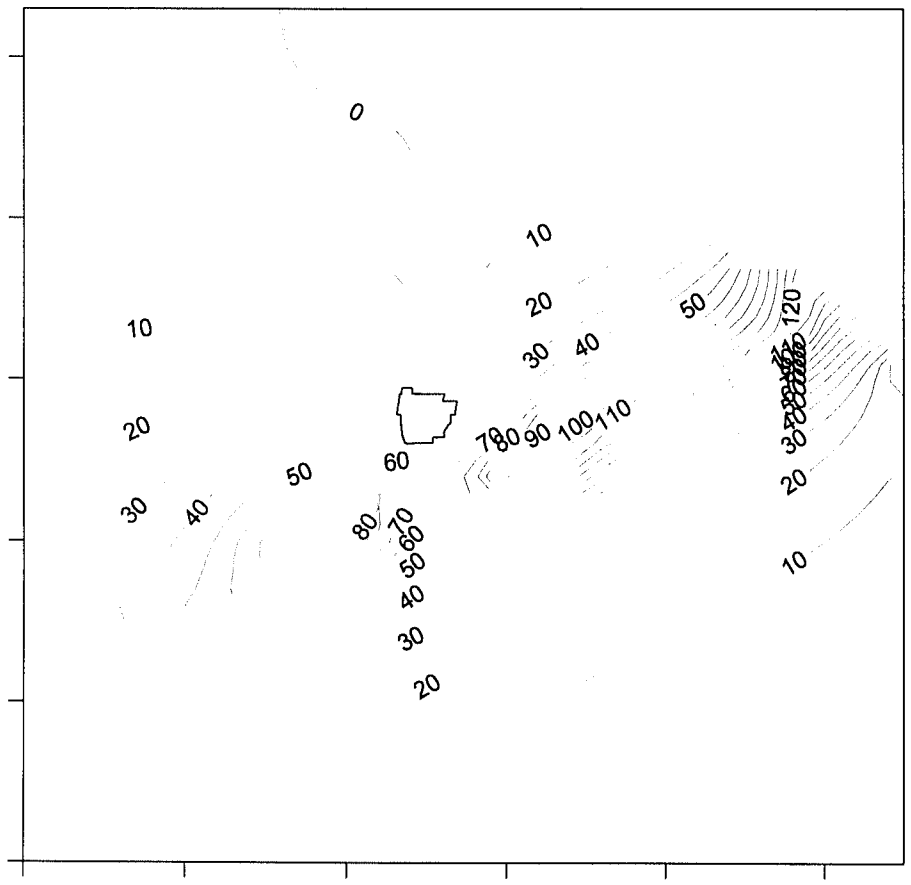

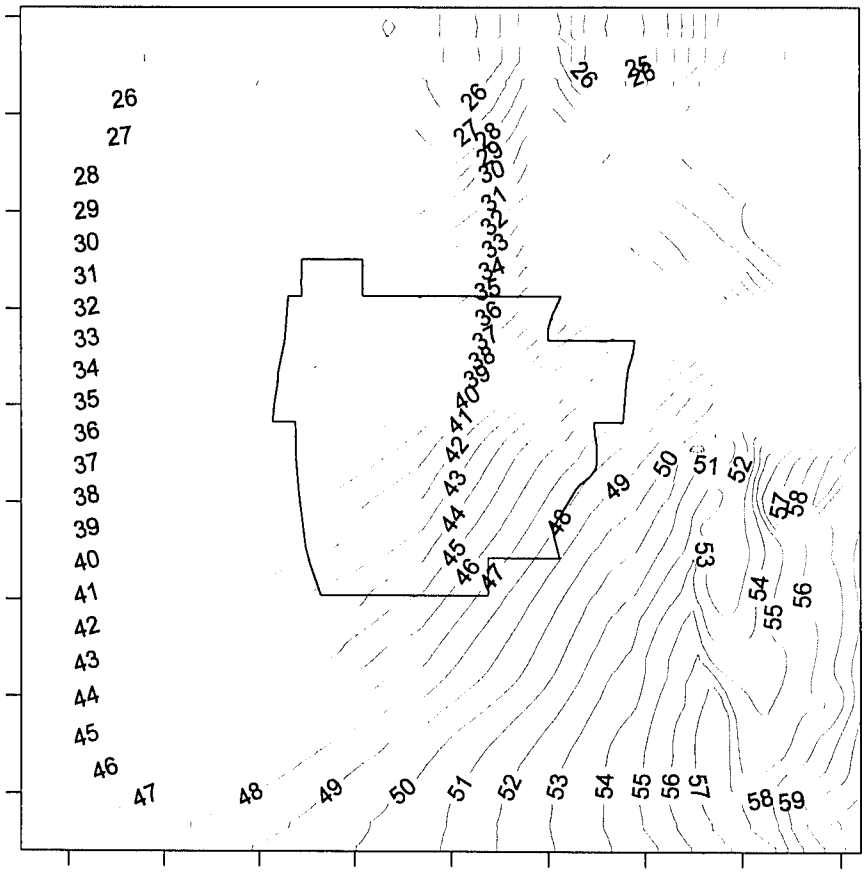

Figure 6 - Attachment 4 to Table 1
RESIDUAL MAP
SENSITIVITY ANALYSIS
INCREASE IN
GILA RIVER BED
CONDUCTANCE

BROWN AND CALDWELL

Residual = Sensitivity Simulation - Base Simulation
Contours Reflect Residual Head in Feet

BHP COPPER *Florence Project*

SFIG073 08/13/96 MikeS

Attachment 5 to Table 1

Attachment 5 to Table 1

Response to ADEQ Comment-2.10.4--The River

ADEQ-2.10.4: Sensitivity to River Conductance- BHP has stated that the modeling efforts are apparently sensitive to river bed conductance. This sensitivity seems important in light of the fact that conductance is not a directly measured parameter. BHP stated that with an increased conductance value, "Over the mine area the groundwater elevations rose up to 6 feet in the UBFU and LBFU." BHP should elaborate on the consequences if the recharge rate along the Gila River is greater than anticipated.

The River

Based on further review of Gila River parameters, the modeling scenario, Increased Recharge, was revised. The revised input parameters and conditions and the results are presented below:

Figures 4.3-24(IV) through 4.3-31(IV) of the report will be replaced with the new figures (Figures 4.3-24- (IV) through 4.3-31(IV)) enclosed. Table 2.8-3(IV), Stream Package Input Parameters, will be replaced with the new Table 2.8-3-modified (IV) enclosed. In this table, the thickness of the river bed between columns 1 through 36 and columns 177 through 216 is set to 0.2 feet. Between columns 37 through 176 the thickness is set to 2 feet. The conductivity of the river bed material is set to 0.003 ft/day throughout.

The simulation was performed with four stress periods of duration of 365 days, 365 days, 365 days and 90 days, respectively. The first three stress periods are identical to the base case scenario, starting with 1 year of no pumping followed by 2 years of "Regular" pumping as described in the scenarios table. During the fourth stress period of 90 days, the flow introduced in the river is increased from 250 cubic feet per second (cfs) to 120,000 cfs while pumping remained "Regular." The base flow rate of 250 cfs was derived from a hydrograph of the "Mean Monthly Discharge - Gila River at Florence" between 1950 and 1990. The 100-year 24-hour peak discharge rate of 120,000 cfs was based on the Flood Insurance Study developed for Florence, Arizona and Pinal County, Arizona used in a previous simulation of a 100-year flood using HEC-2 surface flow model (Magma Copper Company, Florence, Arizona, Gila River Bank Stabilization Project, 1-26-95, Cella Barr Associates, Tucson, Arizona). The use of a 24-hour peak flow for a duration of 90-days is conservative because the average 90-day flow would be considerably less. A FEMA Letter of Map Revision dated April 4, 1995 provides another element of conservatism. It indicates that the 100-year peak discharge at Florence has been revised downward to 66,300 cfs, or approximately one-half of the value used in the model.

Particle tracking using 10 particles per injection well was conducted for the revised Increased Recharge Scenario indicating that increased recharge along the river causes a 11 percent increase in gradient across the mine area. Results, however, indicate that all particles (10 per injection well) are captured under the base case pumping scenario of 25-percent excess extraction.

The sensitivity to river bed conductance during the Flood simulation was investigated by increasing the river bed conductance by one order of magnitude. This increase is large considering that the values already in the model provide a rate of loss from the river comparable to values estimated by the United States Geologic Survey (USGS)[1]. The flow introduced in the river during the flood simulation is already excessive and an increase in the recharge rate along the Gila River is not likely to occur. Under the currently simulated recharge the injected material is hydraulically controlled using the 25 percent overpumping.

The increased bed conductance exhibited Type III Sensitivity as categorized by ASTM D5611-94 (Standard Guide for Conducting a Sensitivity Analysis for a Ground-Water Flow Model Application). Type III Sensitivity occurs "when variation of an input causes significant changes to both the calibration residuals and the model's conclusions... Type III sensitivity is of low concern because even though the model's conclusions change as a result of variation of the input, the parameters used in those simulations cause the model to become uncalibrated. Therefore, the calibration process eliminates those values from being considered to be realistic."

Because the results of Scenario 3 approximate the observed conditions during the 1983 flooding event, it is unlikely that the stream bed conductance values would be much beyond those represented in this scenario.

[1] (Evaluation of Ground-Water Recharge Along the Gila River as a Result of the Flood of October 1983, in and Near the Gila River Indian Reservation, Maricopa and Pinal Counties, Arizona, USGS Water-Resources Investigations Report 89-4148, June 1990)

Table 2.8-3. Stream Package Input Parameters

Segment Number (-)	Reach Number (-)	Reach Layer (-)	Reach Row (-)	Reach Column (-)	Segment Initial Flow (ft^3/day)	Bottom Elevation (ft)	Top Elevation (ft)	River Bed Thickness (ft)	Bottom Conductivity (ft/day)	Cell Length (ft)	River Width (ft)	River Bed Conductance (ft^2/day)	River Stage (ft)	Bottom Slope (ft)	Manning's n (-)
1	1	1	17	216	1.04E+10	1505	1,506.00	0.2	0.003	1,000	500	7,500	1,515	0.002775	0.035
1	2	1	17	215	-	1504	1,504.61	0.2	0.003	1,000	500	7,500	1,514	0.002775	0.035
1	3	1	17	214	-	1502	1,503.23	0.2	0.003	1,000	500	7,500	1,512	0.002775	0.035
1	4	1	17	213	-	1500	1,501.00	0.2	0.003	1,000	500	7,500	1,510	0.002505	0.035
1	5	1	17	212	-	1499	1,499.75	0.2	0.003	1,000	500	7,500	1,509	0.002505	0.035
1	6	1	17	211	-	1497	1,498.50	0.2	0.003	1,000	500	7,500	1,507	0.002505	0.035
1	7	1	17	210	-	1495	1,496.00	0.2	0.003	1,000	500	7,500	1,505	0.007050	0.035
1	8	1	18	210	-	1490	1,491.00	0.2	0.003	1,000	500	7,500	1,500	0.002145	0.035
1	9	1	19	210	-	1489	1,489.93	0.2	0.003	1,000	500	7,500	1,499	0.002145	0.035
1	10	1	20	210	-	1488	1,488.86	0.2	0.003	1,000	500	7,500	1,498	0.002145	0.035
1	11	1	21	210	-	1487	1,487.78	0.2	0.003	1,000	500	7,500	1,497	0.002145	0.035
1	12	1	22	210	-	1485	1,486.00	0.2	0.003	1,000	500	7,500	1,495	0.004050	0.035
1	13	1	23	209	-	1483	1,483.98	0.2	0.003	1,000	500	7,500	1,493	0.004050	0.035
1	14	1	25	208	-	1481	1,481.95	0.2	0.003	1,000	500	7,500	1,491	0.004050	0.035
1	15	1	25	207	-	1480	1,481.00	0.2	0.003	1,000	500	7,500	1,490	0.004995	0.035
1	16	1	29	206	-	1475	1,476.00	0.2	0.003	1,000	500	7,500	1,485	0.004995	0.035
1	17	1	34	205	-	1473	1,474.37	0.2	0.003	1,000	500	7,500	1,483	0.003255	0.035
1	18	1	38	204	-	1470	1,471.00	0.2	0.003	1,000	500	7,500	1,480	0.003255	0.035
1	19	1	45	203	-	1469	1,469.61	0.2	0.003	1,000	500	7,500	1,479	0.002775	0.035
1	20	1	50	202	-	1467	1,468.23	0.2	0.003	1,000	1,400	21,000	1,479	0.002775	0.035
1	21	1	60	201	-	1465	1,466.00	0.2	0.003	1,000	1,200	18,000	1,475	0.003000	0.035
1	22	1	70	200	-	1464	1,464.50	0.2	0.003	1,000	1,200	18,000	1,474	0.003000	0.035
1	23	1	80	199	-	1462	1,463.00	0.2	0.003	1,000	800	12,000	1,472	0.003000	0.035
1	24	1	90	198	-	1460	1,461.00	0.2	0.003	1,000	400	6,000	1,470	0.003945	0.035
1	25	1	107	197	-	1455	1,456.00	0.2	0.003	1,000	400	6,000	1,465	0.003945	0.035
1	26	1	122	196	-	1454	1,455.30	0.2	0.003	900	500	6,750	1,464	0.001560	0.035
1	27	1	143	195	-	1454	1,454.67	0.2	0.003	800	1,300	15,600	1,464	0.001560	0.035
1	28	1	143	194	-	1453	1,454.13	0.2	0.003	700	1,100	11,550	1,463	0.001560	0.035
1	29	1	143	193	-	1453	1,453.66	0.2	0.003	600	800	7,200	1,463	0.001560	0.035
1	30	1	146	192	-	1452	1,453.27	0.2	0.003	500	800	6,000	1,462	0.001560	0.035
1	31	1	146	191	-	1452	1,452.94	0.2	0.003	420	800	5,040	1,462	0.001560	0.035
1	32	1	146	190	-	1452	1,452.67	0.2	0.003	350	900	4,725	1,462	0.001560	0.035
1	33	1	146	189	-	1451	1,452.44	0.2	0.003	290	900	3,915	1,461	0.001560	0.035
1	34	1	146	188	-	1450	1,451.00	0.2	0.003	240	1,100	3,960	1,460	0.002340	0.035
1	35	1	146	187	-	1450	1,450.77	0.2	0.003	200	1,200	3,600	1,460	0.002340	0.035
1	36	1	146	186	-	1450	1,450.57	0.2	0.003	170	1,400	3,570	1,460	0.002340	0.035
1	37	1	146	185	-	1449	1,450.40	0.2	0.003	145	1,500	3,263	1,459	0.002340	0.035
1	38	1	146	184	-	1449	1,450.25	0.2	0.003	125	1,600	3,000	1,459	0.002340	0.035
1	39	1	146	183	-	1449	1,450.12	0.2	0.003	110	1,600	2,640	1,459	0.002340	0.035

Table 2.8-3. Stream Package Input Parameters															
Segment Number (-)	Reach Number (-)	Reach Layer (-)	Reach Row (-)	Reach Column (-)	Segment Initial Flow (ft^3/day)	Bottom Elevation (ft)	Top Elevation (ft)	River Bed Thickness (ft)	Bottom Conductivity (ft/day)	Cell Length (ft)	River Width (ft)	River Bed Conductance (ft^2/day)	River Stage (ft)	Bottom Slope (ft)	Manning's n (-)
1	40	1	146	182	-	1449	1,450.01	0.2	0.003	95	1,700	2,423	1,459	0.002340	0.035
1	41	1	146	181	-	1449	1,449.91	0.2	0.003	85	1,800	2,295	1,459	0.002340	0.035
1	42	1	146	180	-	1449	1,449.82	0.2	0.003	75	2,000	2,250	1,459	0.002340	0.035
1	43	1	146	179	-	1449	1,449.74	0.2	0.003	70	2,000	2,100	1,459	0.002340	0.035
1	44	1	146	178	-	1449	1,449.67	0.2	0.003	65	2,000	1,950	1,459	0.002340	0.035
1	45	1	147	177	-	1449	1,449.60	0.2	0.003	60	666	599	1,459	0.002340	0.035
1	46	1	148	177	-	1449	1,449.53	0.2	0.003	60	666	599	1,459	0.002340	0.035
1	47	1	149	177	-	1448	1,449.46	0.2	0.003	60	666	599	1,458	0.002340	0.035
1	48	1	150	176	-	1448	1,449.40	2	0.003	50	2,000	1,500	1,458	0.002340	0.035
1	49	1	150	175	-	1448	1,449.34	2	0.003	50	2,000	1,500	1,458	0.002340	0.035
1	50	1	150	174	-	1448	1,449.28	2	0.003	50	2,000	1,500	1,458	0.002340	0.035
1	51	1	150	173	-	1448	1,449.22	2	0.003	50	2,000	1,500	1,458	0.002340	0.035
1	52	1	150	172	-	1448	1,449.16	2	0.003	50	2,000	1,500	1,458	0.002340	0.035
1	53	1	150	171	-	1448	1,449.10	2	0.003	50	2,000	1,500	1,458	0.002340	0.035
1	54	1	150	170	-	1448	1,449.05	2	0.003	50	2,000	1,500	1,458	0.002340	0.035
1	55	1	150	169	-	1448	1,448.99	2	0.003	50	2,000	1,500	1,458	0.002340	0.035
1	56	1	150	168	-	1448	1,448.93	2	0.003	50	2,000	1,500	1,458	0.002340	0.035
1	57	1	150	167	-	1448	1,448.87	2	0.003	50	2,000	1,500	1,458	0.002340	0.035
1	58	1	150	166	-	1448	1,448.81	2	0.003	50	2,000	1,500	1,458	0.002340	0.035
1	59	1	150	165	-	1448	1,448.75	2	0.003	50	2,000	1,500	1,458	0.002340	0.035
1	60	1	150	164	-	1448	1,448.70	2	0.003	50	2,000	1,500	1,458	0.002340	0.035
1	61	1	150	163	-	1448	1,448.64	2	0.003	50	2,000	1,500	1,458	0.002340	0.035
1	62	1	150	162	-	1448	1,448.58	2	0.003	50	2,000	1,500	1,458	0.002340	0.035
1	63	1	150	161	-	1448	1,448.52	2	0.003	50	2,000	1,500	1,458	0.002340	0.035
1	64	1	150	160	-	1447	1,448.46	2	0.003	50	2,000	1,500	1,457	0.002340	0.035
1	65	1	150	159	-	1447	1,448.40	2	0.003	50	2,000	1,500	1,457	0.002340	0.035
1	66	1	150	158	-	1447	1,448.34	2	0.003	50	2,000	1,500	1,457	0.002340	0.035
1	67	1	150	157	-	1447	1,448.29	2	0.003	50	2,000	1,500	1,457	0.002340	0.035
1	68	1	150	156	-	1447	1,448.23	2	0.003	50	2,000	1,500	1,457	0.002340	0.035
1	69	1	150	155	-	1447	1,448.17	2	0.003	50	2,000	1,500	1,457	0.002340	0.035
1	70	1	150	154	-	1447	1,448.11	2	0.003	50	2,000	1,500	1,457	0.002340	0.035
1	71	1	150	153	-	1447	1,448.05	2	0.003	50	2,000	1,500	1,457	0.002340	0.035
1	72	1	150	152	-	1447	1,447.99	2	0.003	50	2,000	1,500	1,457	0.002340	0.035
1	73	1	150	151	-	1447	1,447.93	2	0.003	50	2,000	1,500	1,457	0.002340	0.035
1	74	1	150	150	-	1447	1,447.88	2	0.003	50	2,000	1,500	1,457	0.002340	0.035
1	75	1	150	149	-	1447	1,447.82	2	0.003	50	2,000	1,500	1,457	0.002340	0.035
1	76	1	150	148	-	1447	1,447.76	2	0.003	50	2,000	1,500	1,457	0.002340	0.035
1	77	1	150	147	-	1447	1,447.70	2	0.003	50	2,000	1,500	1,457	0.002340	0.035
1	78	1	150	146	-	1447	1,447.64	2	0.003	50	2,000	1,500	1,457	0.002340	0.035

Table 2.8-3. Stream Package Input Parameters

Segment Number (-)	Reach Number (-)	Reach Layer (-)	Reach Row (-)	Reach Column (-)	Segment Initial Flow (ft^3/day)	Bottom Elevation (ft)	Top Elevation (ft)	River Bed Thickness (ft)	Bottom Conductivity (ft/day)	Cell Length (ft)	River Width (ft)	River Bed Conductance (ft^2/day)	River Stage (ft)	Bottom Slope (ft)	Manning's n (-)
1	79	1	150	145	-	1447	1,447.58	2	0.003	50	2,000	1,500	1,457	0.002340	0.035
1	80	1	150	144	-	1447	1,447.53	2	0.003	50	2,000	1,500	1,457	0.002340	0.035
1	81	1	150	143	-	1446	1,447.47	2	0.003	50	2,000	1,500	1,456	0.002340	0.035
1	82	1	150	142	-	1446	1,447.41	2	0.003	50	2,000	1,500	1,456	0.002340	0.035
1	83	1	150	141	-	1446	1,447.35	2	0.003	50	2,000	1,500	1,456	0.002340	0.035
1	84	1	150	140	-	1445	1,446.00	2	0.003	50	2,000	1,500	1,455	0.004695	0.035
1	85	1	150	139	-	1445	1,445.88	2	0.003	50	2,000	1,500	1,455	0.004695	0.035
1	86	1	150	138	-	1445	1,445.77	2	0.003	50	2,000	1,500	1,455	0.004695	0.035
1	87	1	150	137	-	1445	1,445.65	2	0.003	50	2,000	1,500	1,455	0.004695	0.035
1	88	1	150	136	-	1445	1,445.53	2	0.003	50	2,000	1,500	1,455	0.004695	0.035
1	89	1	150	135	-	1444	1,445.41	2	0.003	50	2,000	1,500	1,454	0.004695	0.035
1	90	1	150	134	-	1444	1,445.30	2	0.003	50	2,000	1,500	1,454	0.004695	0.035
1	91	1	150	133	-	1444	1,445.18	2	0.003	50	2,000	1,500	1,454	0.004695	0.035
1	92	1	150	132	-	1444	1,445.06	2	0.003	50	2,000	1,500	1,454	0.004695	0.035
1	93	1	150	131	-	1444	1,444.94	2	0.003	50	2,000	1,500	1,454	0.004695	0.035
1	94	1	150	130	-	1444	1,444.83	2	0.003	50	2,000	1,500	1,454	0.004695	0.035
1	95	1	150	129	-	1444	1,444.71	2	0.003	50	2,000	1,500	1,454	0.004695	0.035
1	96	1	150	128	-	1444	1,444.59	2	0.003	50	2,000	1,500	1,454	0.004695	0.035
1	97	1	150	127	-	1443	1,444.47	2	0.003	50	2,000	1,500	1,453	0.004695	0.035
1	98	1	150	126	-	1443	1,444.36	2	0.003	50	2,000	1,500	1,453	0.004695	0.035
1	99	1	150	125	-	1443	1,444.24	2	0.003	50	2,000	1,500	1,453	0.004695	0.035
1	100	1	150	124	-	1443	1,444.12	2	0.003	50	2,000	1,500	1,453	0.004695	0.035
1	101	1	150	123	-	1443	1,444.00	2	0.003	50	2,000	1,500	1,453	0.004695	0.035
1	102	1	150	122	-	1443	1,443.89	2	0.003	50	2,000	1,500	1,453	0.004695	0.035
1	103	1	150	121	-	1443	1,443.77	2	0.003	50	2,000	1,500	1,453	0.004695	0.035
1	104	1	150	120	-	1443	1,443.65	2	0.003	50	2,000	1,500	1,453	0.004695	0.035
1	105	1	150	119	-	1443	1,443.54	2	0.003	50	2,000	1,500	1,453	0.004695	0.035
1	106	1	150	118	-	1442	1,443.42	2	0.003	50	2,000	1,500	1,452	0.004695	0.035
1	107	1	150	117	-	1442	1,443.30	2	0.003	50	2,000	1,500	1,452	0.004695	0.035
1	108	1	150	116	-	1442	1,443.18	2	0.003	50	2,000	1,500	1,452	0.004695	0.035
1	109	1	150	115	-	1442	1,443.07	2	0.003	50	2,000	1,500	1,452	0.004695	0.035
1	110	1	150	114	-	1442	1,442.95	2	0.003	50	2,000	1,500	1,452	0.004695	0.035
1	111	1	150	113	-	1442	1,442.83	2	0.003	50	2,000	1,500	1,452	0.004695	0.035
1	112	1	150	112	-	1442	1,442.71	2	0.003	50	2,000	1,500	1,452	0.004695	0.035
1	113	1	150	111	-	1442	1,442.60	2	0.003	50	2,000	1,500	1,452	0.004695	0.035
1	114	1	150	110	-	1440	1,441.00	2	0.003	50	2,000	1,500	1,450	0.003750	0.035
1	115	1	150	109	-	1440	1,440.91	2	0.003	50	2,000	1,500	1,450	0.003750	0.035
1	116	1	150	108	-	1440	1,440.81	2	0.003	50	2,000	1,500	1,450	0.003750	0.035
1	117	1	150	107	-	1440	1,440.72	2	0.003	50	2,000	1,500	1,450	0.003750	0.035

Table 2.8-3. Stream Package Input Parameters															
Segment Number (-)	Reach Number (-)	Reach Layer (-)	Reach Row (-)	Reach Column (-)	Segment Initial Flow (ft^3/day)	Bottom Elevation (ft)	Top Elevation (ft)	River Bed Thickness (ft)	Bottom Conductivity (ft/day)	Cell Length (ft)	River Width (ft)	River Bed Conductance (ft^2/day)	River Stage (ft)	Bottom Slope (ft)	Manning's n (-)
1	118	1	150	106	-	1440	1,440.63	2	0.003	50	2,000	1,500	1,450	0.003750	0.035
1	119	1	150	105	-	1440	1,440.53	2	0.003	50	2,000	1,500	1,450	0.003750	0.035
1	120	1	150	104	-	1439	1,440.44	2	0.003	50	2,000	1,500	1,449	0.003750	0.035
1	121	1	150	103	-	1439	1,440.34	2	0.003	50	2,000	1,500	1,449	0.003750	0.035
1	122	1	150	102	-	1439	1,440.25	2	0.003	50	2,000	1,500	1,449	0.003750	0.035
1	123	1	150	101	-	1439	1,440.16	2	0.003	50	2,000	1,500	1,449	0.003750	0.035
1	124	1	150	100	-	1439	1,440.06	2	0.003	50	2,000	1,500	1,449	0.003750	0.035
1	125	1	150	99	-	1439	1,439.97	2	0.003	50	2,000	1,500	1,449	0.003750	0.035
1	126	1	150	98	-	1439	1,439.88	2	0.003	50	2,000	1,500	1,449	0.003750	0.035
1	127	1	150	97	-	1439	1,439.78	2	0.003	50	2,000	1,500	1,449	0.003750	0.035
1	128	1	150	96	-	1439	1,439.69	2	0.003	50	2,000	1,500	1,449	0.003750	0.035
1	129	1	150	95	-	1439	1,439.59	2	0.003	50	2,000	1,500	1,449	0.003750	0.035
1	130	1	150	94	-	1439	1,439.50	2	0.003	50	2,000	1,500	1,449	0.003750	0.035
1	131	1	150	93	-	1438	1,439.41	2	0.003	50	2,000	1,500	1,448	0.003750	0.035
1	132	1	150	92	-	1438	1,439.31	2	0.003	50	2,000	1,500	1,448	0.003750	0.035
1	133	1	150	91	-	1438	1,439.22	2	0.003	50	2,000	1,500	1,448	0.003750	0.035
1	134	1	150	90	-	1438	1,439.13	2	0.003	50	2,000	1,500	1,448	0.003750	0.035
1	135	1	150	89	-	1438	1,439.03	2	0.003	50	2,000	1,500	1,448	0.003750	0.035
1	136	1	150	88	-	1438	1,438.94	2	0.003	50	2,000	1,500	1,448	0.003750	0.035
1	137	1	150	87	-	1438	1,438.84	2	0.003	50	3,000	2,250	1,448	0.003750	0.035
1	138	1	150	86	-	1438	1,438.75	2	0.003	50	3,000	2,250	1,448	0.003750	0.035
1	139	1	150	85	-	1438	1,438.66	2	0.003	50	3,000	2,250	1,448	0.003750	0.035
1	140	1	150	84	-	1438	1,438.56	2	0.003	50	3,000	2,250	1,448	0.003750	0.035
1	141	1	150	83	-	1437	1,438.47	2	0.003	50	3,000	2,250	1,447	0.003750	0.035
1	142	1	150	82	-	1437	1,438.38	2	0.003	50	3,000	2,250	1,447	0.003750	0.035
1	143	1	150	81	-	1437	1,438.28	2	0.003	50	3,000	2,250	1,447	0.003750	0.035
1	144	1	150	80	-	1437	1,438.19	2	0.003	50	3,000	2,250	1,447	0.003750	0.035
1	145	1	150	79	-	1437	1,438.09	2	0.003	50	3,000	2,250	1,447	0.003750	0.035
1	146	1	150	78	-	1437	1,438.00	2	0.003	50	3,000	2,250	1,447	0.003750	0.035
1	147	1	150	77	-	1437	1,437.91	2	0.003	50	3,000	2,250	1,447	0.003750	0.035
1	148	1	150	76	-	1437	1,437.81	2	0.003	50	3,000	2,250	1,447	0.003750	0.035
1	149	1	150	75	-	1437	1,437.72	2	0.003	50	3,000	2,250	1,447	0.003750	0.035
1	150	1	150	74	-	1437	1,437.63	2	0.003	50	3,000	2,250	1,447	0.003750	0.035
1	151	1	150	73	-	1437	1,437.53	2	0.003	50	3,000	2,250	1,447	0.003750	0.035
1	152	1	150	72	-	1436	1,437.44	2	0.003	50	3,000	2,250	1,446	0.003750	0.035
1	153	1	150	71	-	1436	1,437.34	2	0.003	50	3,000	2,250	1,446	0.003750	0.035
1	154	1	150	70	-	1435	1,436.00	2	0.003	50	3,000	2,250	1,445	0.010710	0.035
1	155	1	150	69	-	1435	1,435.73	2	0.003	50	3,000	2,250	1,445	0.010710	0.035
1	156	1	150	68	-	1434	1,435.46	2	0.003	50	3,000	2,250	1,444	0.010710	0.035

Table 2.8-3. Stream Package Input Parameters

Segment Number (-)	Reach Number (-)	Reach Layer (-)	Reach Row (-)	Reach Column (-)	Segment Initial Flow (ft^3/day)	Bottom Elevation (ft)	Top Elevation (ft)	River Bed Thickness (ft)	Bottom Conductivity (ft/day)	Cell Length (ft)	River Width (ft)	River Bed Conductance (ft^2/day)	River Stage (ft)	Bottom Slope (ft)	Manning's n (-)
1	157	1	150	67	-	1434	1,435.20	2	0.003	50	3,000	2,250	1,444	0.010710	0.035
1	158	1	150	66	-	1434	1,434.93	2	0.003	50	3,000	2,250	1,444	0.010710	0.035
1	159	1	150	65	-	1434	1,434.66	2	0.003	50	3,000	2,250	1,444	0.010710	0.035
1	160	1	150	64	-	1433	1,434.39	2	0.003	50	3,000	2,250	1,443	0.010710	0.035
1	161	1	150	63	-	1433	1,434.13	2	0.003	50	3,000	2,250	1,443	0.010710	0.035
1	162	1	150	62	-	1433	1,433.86	2	0.003	50	3,000	2,250	1,443	0.010710	0.035
1	163	1	150	61	-	1433	1,433.59	2	0.003	50	3,000	2,250	1,443	0.010710	0.035
1	164	1	150	60	-	1432	1,433.32	2	0.003	50	3,000	2,250	1,442	0.010710	0.035
1	165	1	150	59	-	1432	1,433.05	2	0.003	50	3,000	2,250	1,442	0.010710	0.035
1	166	1	150	58	-	1430	1,431.00	2	0.003	50	3,000	2,250	1,440	0.001440	0.035
1	167	1	150	57	-	1430	1,430.96	2	0.003	50	3,000	2,250	1,440	0.001440	0.035
1	168	1	150	56	-	1430	1,430.93	2	0.003	50	3,000	2,250	1,440	0.001440	0.035
1	169	1	150	55	-	1430	1,430.89	2	0.003	50	3,000	2,250	1,440	0.001440	0.035
1	170	1	150	54	-	1430	1,430.86	2	0.003	50	3,000	2,250	1,440	0.001440	0.035
1	171	1	150	53	-	1430	1,430.82	2	0.003	50	3,000	2,250	1,440	0.001440	0.035
1	172	1	150	52	-	1430	1,430.78	2	0.003	50	3,000	2,250	1,440	0.001440	0.035
1	173	1	150	51	-	1430	1,430.75	2	0.003	50	3,000	2,250	1,440	0.001440	0.035
1	174	1	150	50	-	1430	1,430.71	2	0.003	50	3,000	2,250	1,440	0.001440	0.035
1	175	1	150	49	-	1430	1,430.68	2	0.003	50	3,000	2,250	1,440	0.001440	0.035
1	176	1	150	48	-	1430	1,430.64	2	0.003	50	3,000	2,250	1,440	0.001440	0.035
1	177	1	150	47	-	1430	1,430.60	2	0.003	50	3,000	2,250	1,440	0.001440	0.035
1	178	1	150	46	-	1430	1,430.57	2	0.003	50	3,000	2,250	1,440	0.001440	0.035
1	179	1	150	45	-	1430	1,430.53	2	0.003	50	3,000	2,250	1,440	0.001440	0.035
1	180	1	150	44	-	1429	1,430.50	2	0.003	50	3,000	2,250	1,439	0.001440	0.035
1	181	1	150	43	-	1429	1,430.46	2	0.003	50	3,000	2,250	1,439	0.001440	0.035
1	182	1	150	42	-	1429	1,430.42	2	0.003	50	3,000	2,250	1,439	0.001440	0.035
1	183	1	150	41	-	1429	1,430.39	2	0.003	50	3,000	2,250	1,439	0.001440	0.035
1	184	1	150	40	-	1429	1,430.35	2	0.003	50	3,000	2,250	1,439	0.001440	0.035
1	185	1	150	39	-	1429	1,430.32	2	0.003	50	3,000	2,250	1,439	0.001440	0.035
1	186	1	150	38	-	1429	1,430.28	2	0.003	50	3,000	2,250	1,439	0.001440	0.035
1	187	1	150	37	-	1429	1,430.24	2	0.003	50	3,000	2,250	1,439	0.001440	0.035
1	188	1	151	36	-	1429	1,430.20	0.2	0.003	60	600	540	1,439	0.001440	0.035
1	189	1	152	36	-	1429	1,430.16	0.2	0.003	60	600	540	1,439	0.001440	0.035
1	190	1	153	36	-	1429	1,430.11	0.2	0.003	60	600	540	1,439	0.001440	0.035
1	191	1	154	36	-	1429	1,430.07	0.2	0.003	60	600	540	1,439	0.001440	0.035
1	192	1	155	36	-	1429	1,430.03	0.2	0.003	60	600	540	1,439	0.001440	0.035
1	193	1	156	36	-	1429	1,429.98	0.2	0.003	60	600	540	1,439	0.001440	0.035
1	194	1	156	35	-	1429	1,429.94	0.2	0.003	65	3,000	2,925	1,439	0.001440	0.035
1	195	1	156	34	-	1429	1,429.89	0.2	0.003	70	3,000	3,150	1,439	0.001440	0.035

Table 2.8-3. Stream Package Input Parameters															
Segment Number (-)	Reach Number (-)	Reach Layer (-)	Reach Row (-)	Reach Column (-)	Segment Initial Flow (ft^3/day)	Bottom Elevation (ft)	Top Elevation (ft)	River Bed Thickness (ft)	Bottom Conductivity (ft/day)	Cell Length (ft)	River Width (ft)	River Bed Conductance (ft^2/day)	River Stage (ft)	Bottom Slope (ft)	Manning's n (-)
1	196	1	156	33	-	1429	1,429.83	0.2	0.003	75	3,000	3,375	1,439	0.001440	0.035
1	197	1	156	32	-	1429	1,429.77	0.2	0.003	85	3,000	3,825	1,439	0.001440	0.035
1	198	1	156	31	-	1429	1,429.70	0.2	0.003	95	3,000	4,275	1,439	0.001440	0.035
1	199	1	156	30	-	1429	1,429.62	0.2	0.003	110	3,000	4,950	1,439	0.001440	0.035
1	200	1	156	29	-	1429	1,429.53	0.2	0.003	125	3,000	5,625	1,439	0.001440	0.035
1	201	1	156	28	-	1428	1,429.43	0.2	0.003	145	3,000	6,525	1,438	0.001440	0.035
1	202	1	156	27	-	1428	1,429.31	0.2	0.003	170	3,000	7,650	1,438	0.001440	0.035
1	203	1	156	26	-	1428	1,429.16	0.2	0.003	200	3,000	9,000	1,434	0.001440	0.035
1	204	1	156	25	-	1428	1,428.99	0.2	0.003	240	3,000	10,800	1,438	0.001440	0.035
1	205	1	156	24	-	1428	1,428.78	0.2	0.003	290	3,000	13,050	1,438	0.001440	0.035
1	206	1	156	23	-	1428	1,428.53	0.2	0.003	350	3,000	15,750	1,438	0.001440	0.035
1	207	1	156	22	-	1427	1,428.23	0.2	0.003	420	3,000	18,900	1,437	0.001440	0.035
1	208	1	156	21	-	1427	1,427.87	0.2	0.003	500	3,000	22,500	1,437	0.001440	0.035
1	209	1	156	20	-	1426	1,427.44	0.2	0.003	600	3,000	27,000	1,436	0.001440	0.035
1	210	1	156	19	-	1425	1,426.00	0.2	0.003	700	3,000	31,500	1,435	0.001440	0.035
1	211	1	156	18	-	1424	1,425.25	0.2	0.003	800	3,000	36,000	1,434	0.001875	0.035
1	212	1	156	17	-	1423	1,424.41	0.2	0.003	900	3,000	40,500	1,433	0.001875	0.035
1	213	1	156	16	-	1422	1,423.47	0.2	0.003	1,000	3,000	45,000	1,432	0.001875	0.035
1	214	1	157	15	-	1422	1,422.53	0.2	0.003	1,000	1,500	22,500	1,432	0.001875	0.035
1	215	1	158	15	-	1420	1,421.00	0.2	0.003	1,000	1,500	22,500	1,430	0.009990	0.035
1	216	1	159	14	-	1415	1,416.01	0.2	0.003	1,000	1,500	22,500	1,425	0.009990	0.035
1	217	1	160	14	-	1414	1,414.93	0.2	0.003	1,000	1,500	22,500	1,424	0.002145	0.035
1	218	1	161	13	-	1410	1,411.00	0.2	0.003	1,000	3,000	45,000	1,420	0.002145	0.035
1	219	1	161	12	-	1409	1,409.93	0.2	0.003	1,000	3,000	45,000	1,419	0.002145	0.035
1	220	1	161	11	-	1408	1,408.86	0.2	0.003	1,000	3,000	45,000	1,418	0.002145	0.035
1	221	1	161	10	-	1407	1,407.78	0.2	0.003	1,000	3,000	45,000	1,417	0.002145	0.035
1	222	1	161	9	-	1406	1,406.53	0.2	0.003	1,000	3,000	45,000	1,416	0.002505	0.035
1	223	1	161	8	-	1404	1,405.28	0.2	0.003	1,000	3,000	45,000	1,414	0.002505	0.035
1	224	1	161	7	-	1400	1,401.00	0.2	0.003	1,000	3,000	45,000	1,410	0.002505	0.035
1	225	1	161	6	-	1399	1,399.75	0.2	0.003	1,000	3,000	45,000	1,409	0.002505	0.035
1	226	1	161	5	-	1397	1,398.50	0.2	0.003	1,000	3,000	45,000	1,407	0.002505	0.035
1	227	1	161	4	-	1396	1,397.24	0.2	0.003	1,000	3,000	45,000	1,406	0.002505	0.035
1	228	1	161	3	-	1395	1,396.00	0.2	0.003	1,000	3,000	45,000	1,405	0.002505	0.035
1	229	1	161	2	-	1394	1,394.75	0.2	0.003	1,000	3,000	45,000	1,404	0.002505	0.035
1	230	1	161	1	-	1392	1,393.50	0.2	0.003	1,000	3,000	45,000	1,402	0.002505	0.035

Simulation Scenario 3: Increased Groundwater Recharge
90 Days of 100-Year Gila River Flood Event

Model Layer 1: Elevation of Layer Base = 1200 Feet
Above Mean Sea Level

Contour Interval = 10 Feet

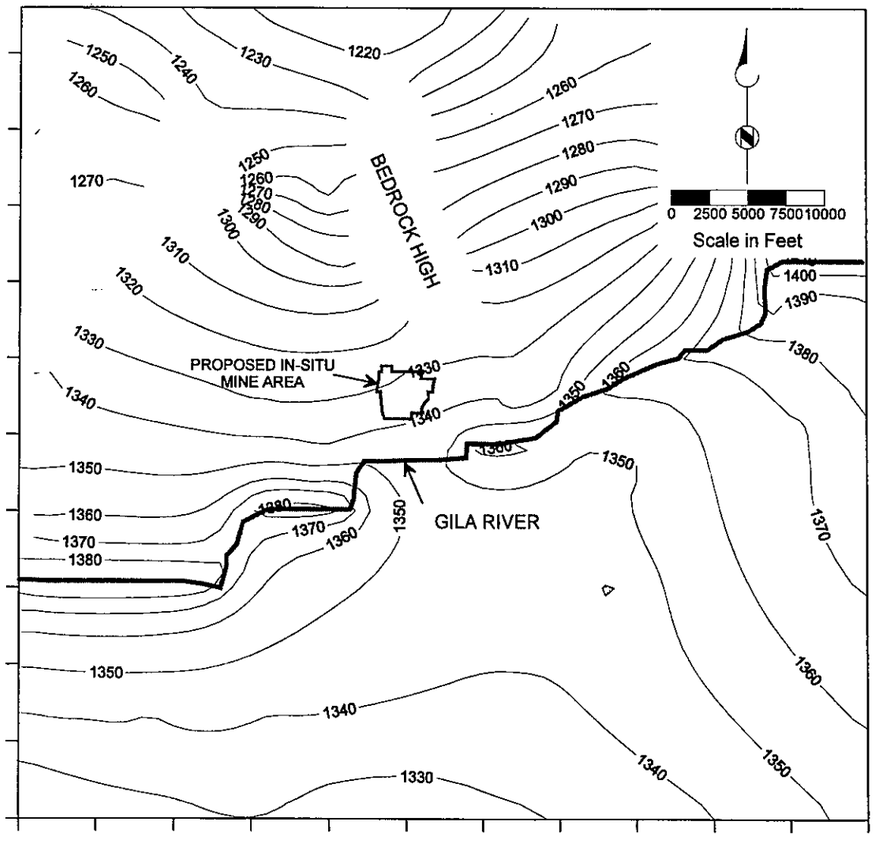

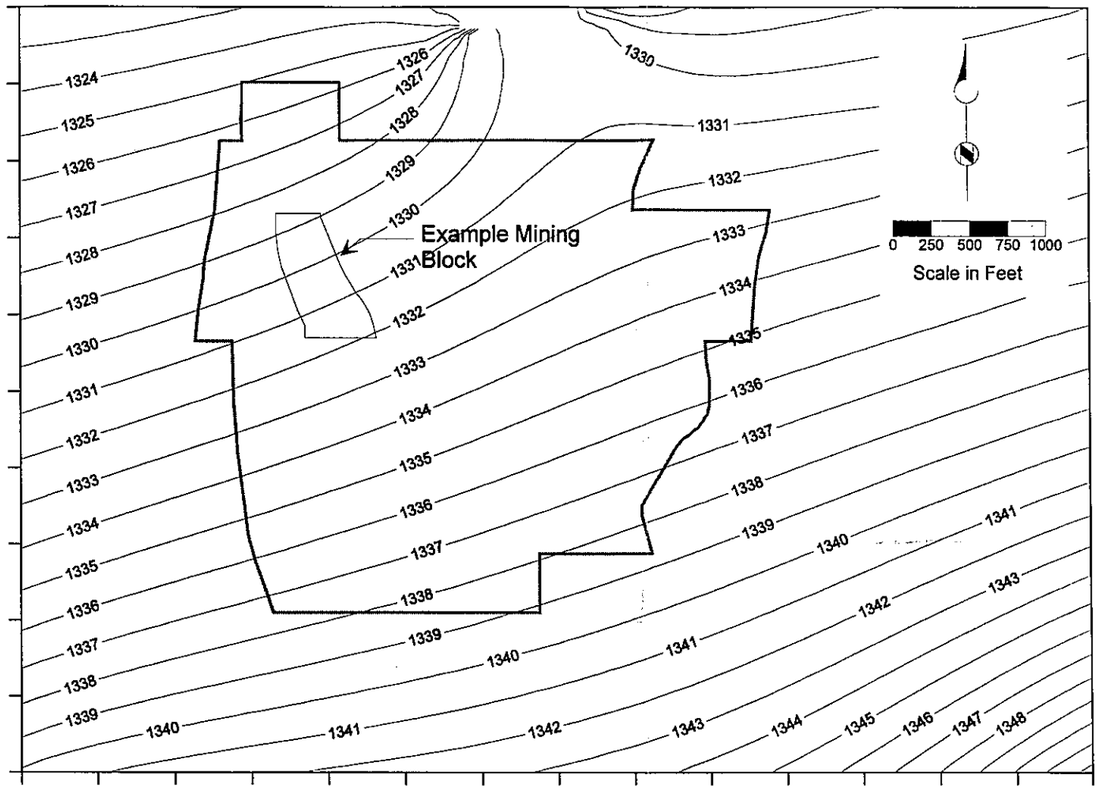

Contour Interval = 1 Foot

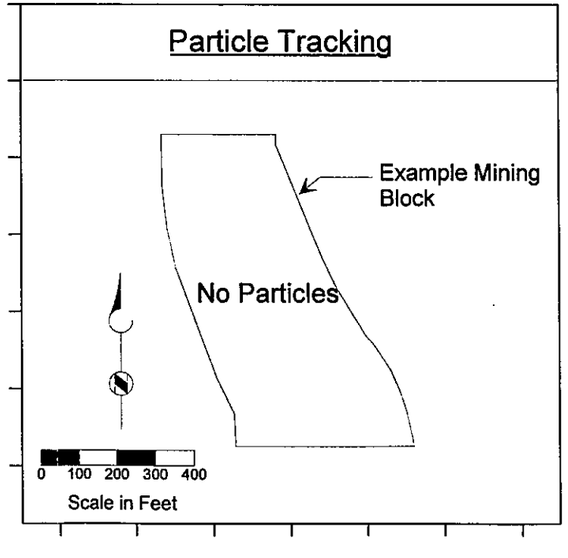

Explanation

1300 — Potentiometric Surface Contour (feet above mean sea level)

Figure 4.3-24 (IV)
SIMULATION SCENARIO 3
INCREASED RECHARGE
MODEL LAYER 1

BHP
BHP COPPER *Florence Project*

BROWN AND CALDWELL

SFIG074 08/13/96 MikeS

REVISED 7/19/96

Simulation Scenario 3: Increased Groundwater Recharge
90 Days of 100-Year Gila River Flood Event

Model Layer 2: Elevation = 1150 - 1200 Feet
Above Mean Sea Level

Contour Interval = 10 Feet

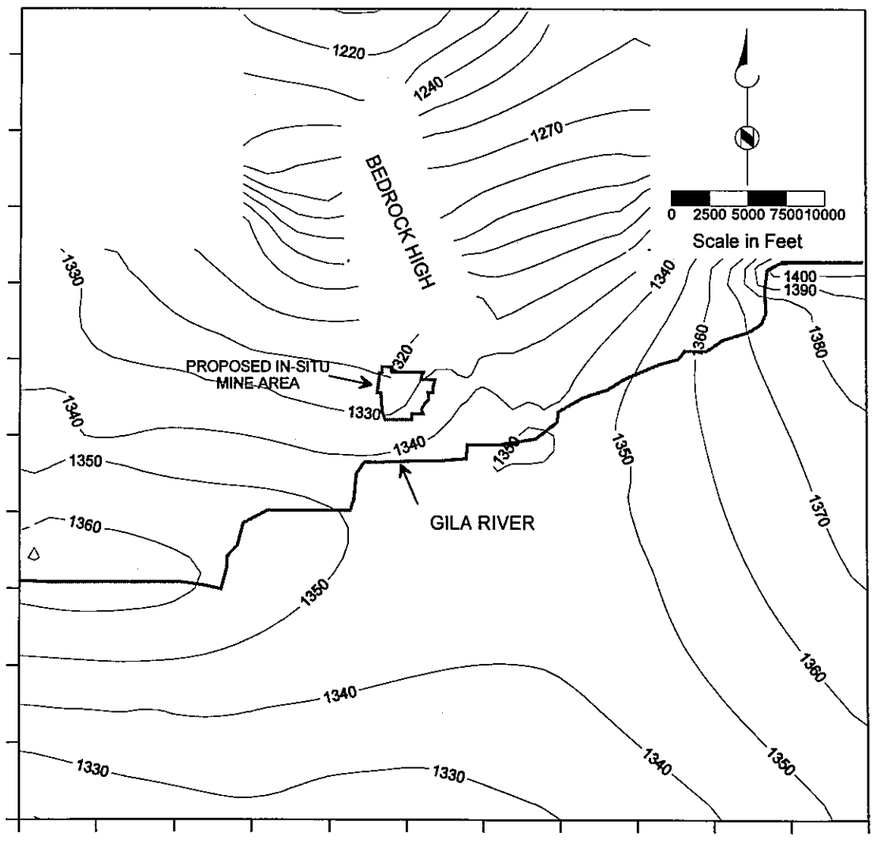

BROWN AND CALDWELL

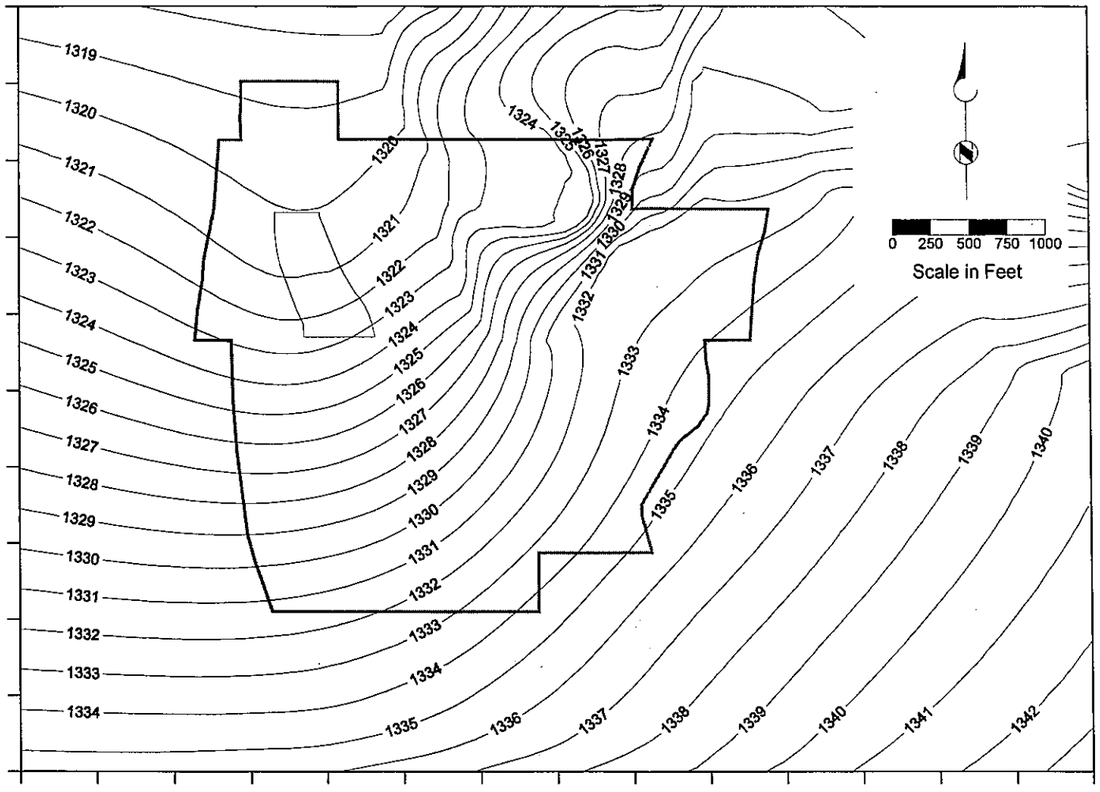

Contour Interval = 1 Foot

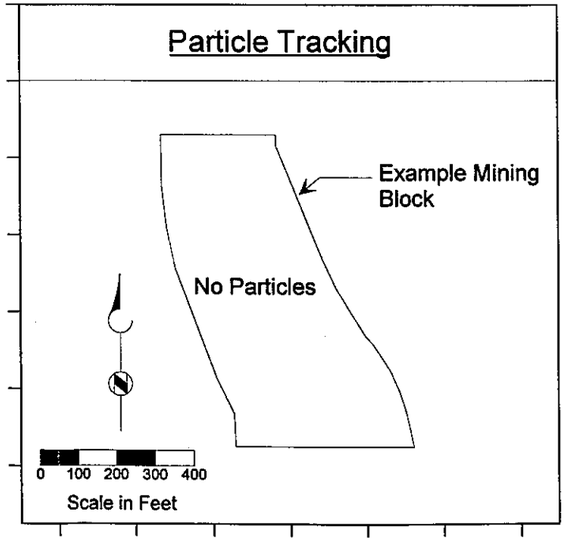

Explanation

1300 — Potentiometric Surface Contour (feet above mean sea level)

Figure 4.3-25 (IV)
SIMULATION SCENARIO 3
INCREASED RECHARGE
MODEL LAYER 2

BHP
BHP COPPER *Florence Project*

SFIG075 08/13/96 MikeS

REVISED 7/19/96

Simulation Scenario 3: Increased Groundwater Recharge
90 Days of 100-Year Gila River Flood Event

Model Layer 3: Elevation = 1100 - 1150 Feet
Above Mean Sea Level

Contour Interval = 10 Feet

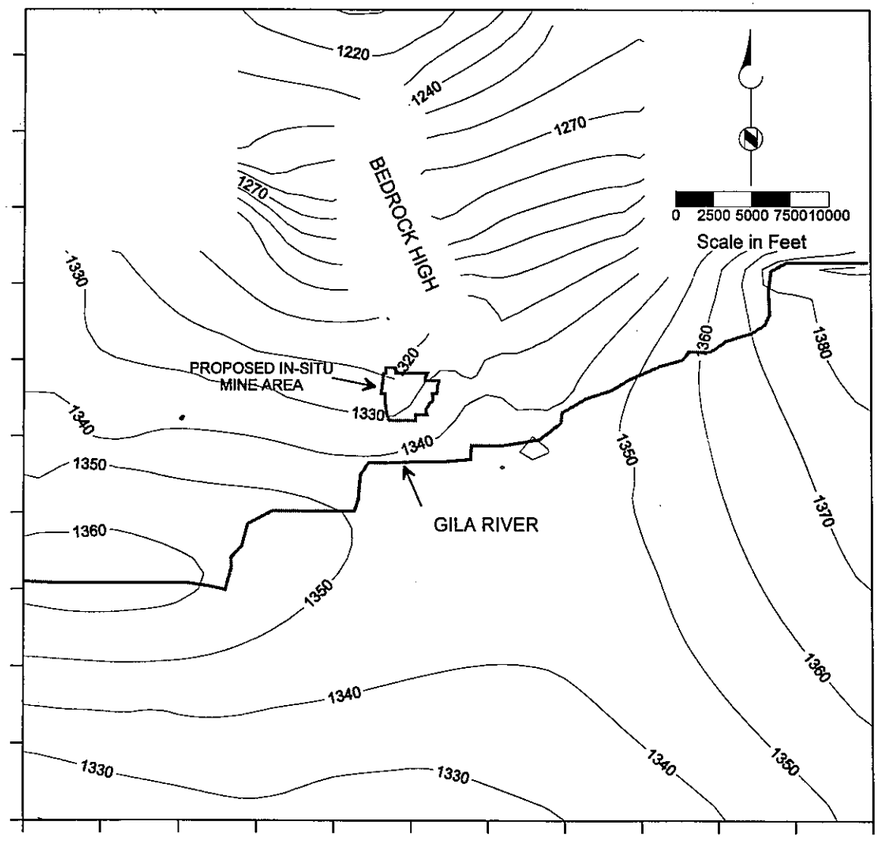

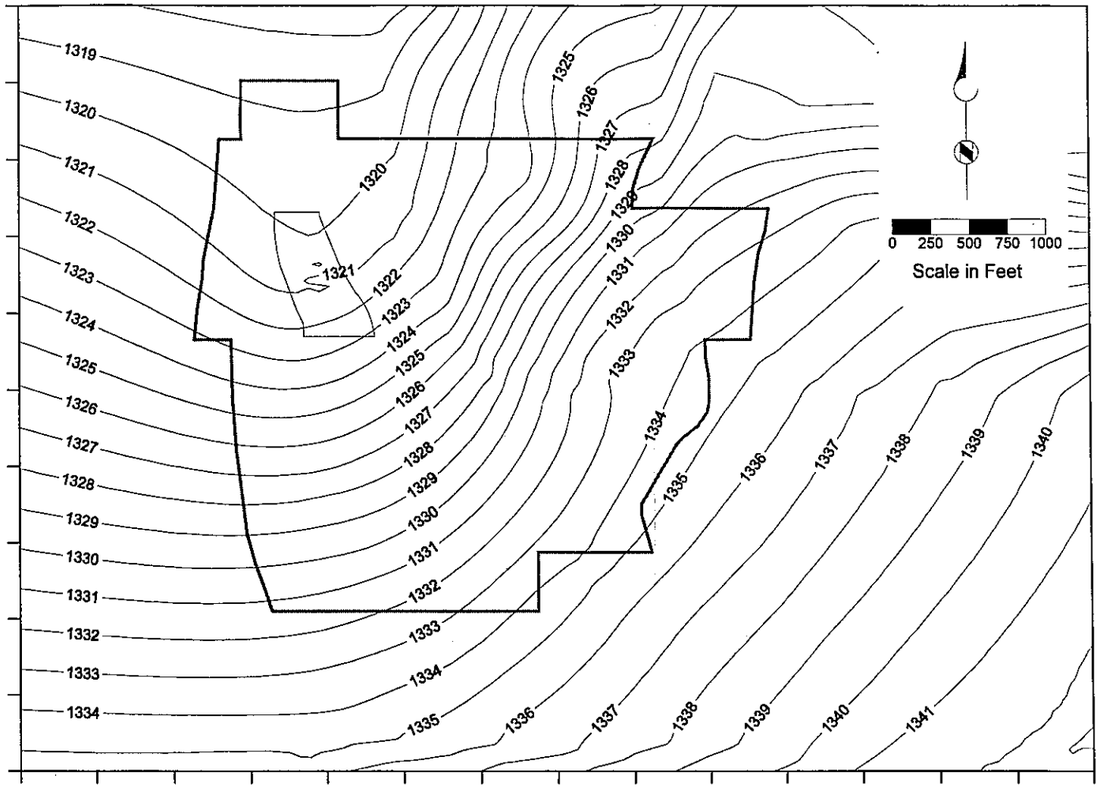

Contour Interval = 1 Foot

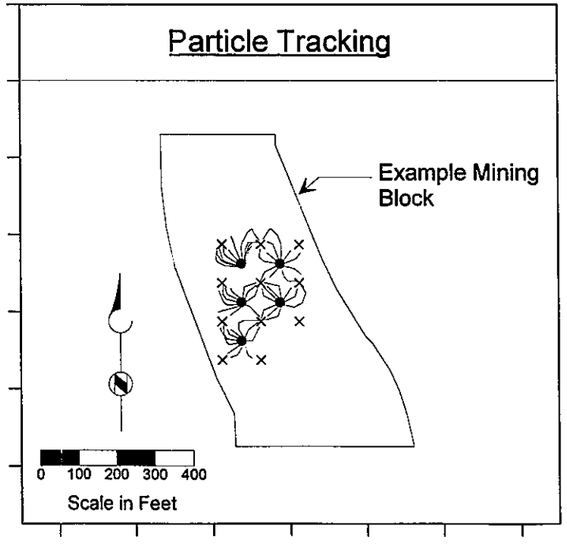

Explanation

- 1300 — Potentiometric Surface Contour (feet above mean sea level)
- ● Injection Well
- × Recovery Well
- Simulated Path Lines of Particles Released from Injection Wells

Figure 4.3-26 (IV)
SIMULATION SCENARIO 3
INCREASED RECHARGE
MODEL LAYER 3

BHP
BHP COPPER *Florence Project*

BROWN AND CALDWELL

SFIG076 08/13/96 MikeS

REVISED 7/19/96

Simulation Scenario 3: Increased Groundwater Recharge
90 Days of 100-Year Gila River Flood Event

Model Layer 4: Elevation = 1050 - 1100 Feet
Above Mean Sea Level

Contour Interval = 10 Feet

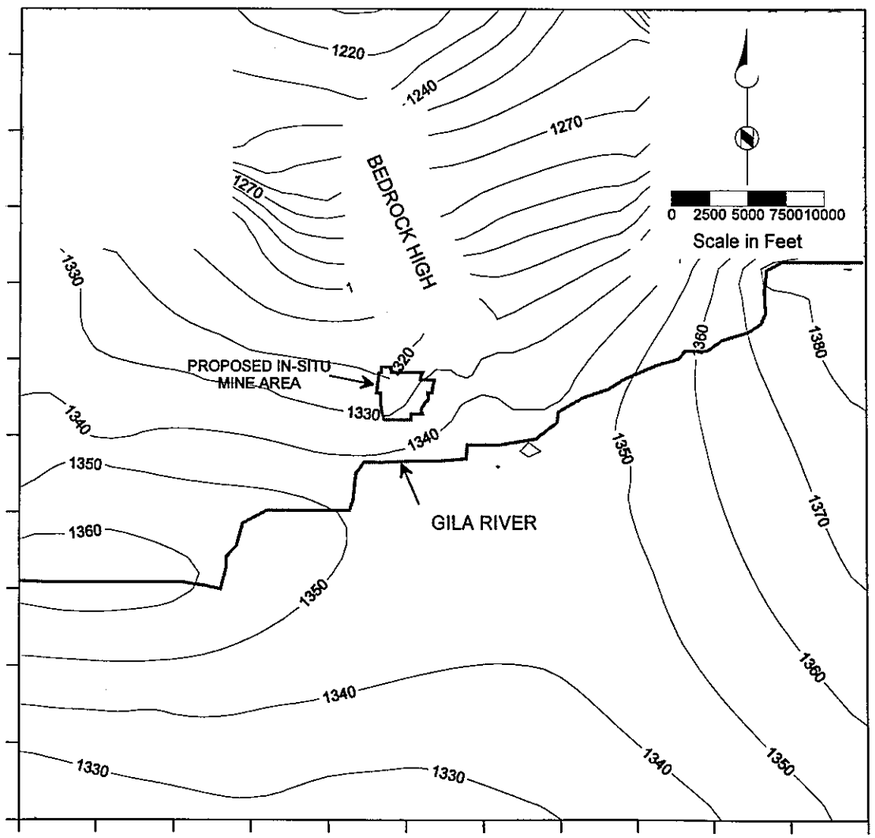

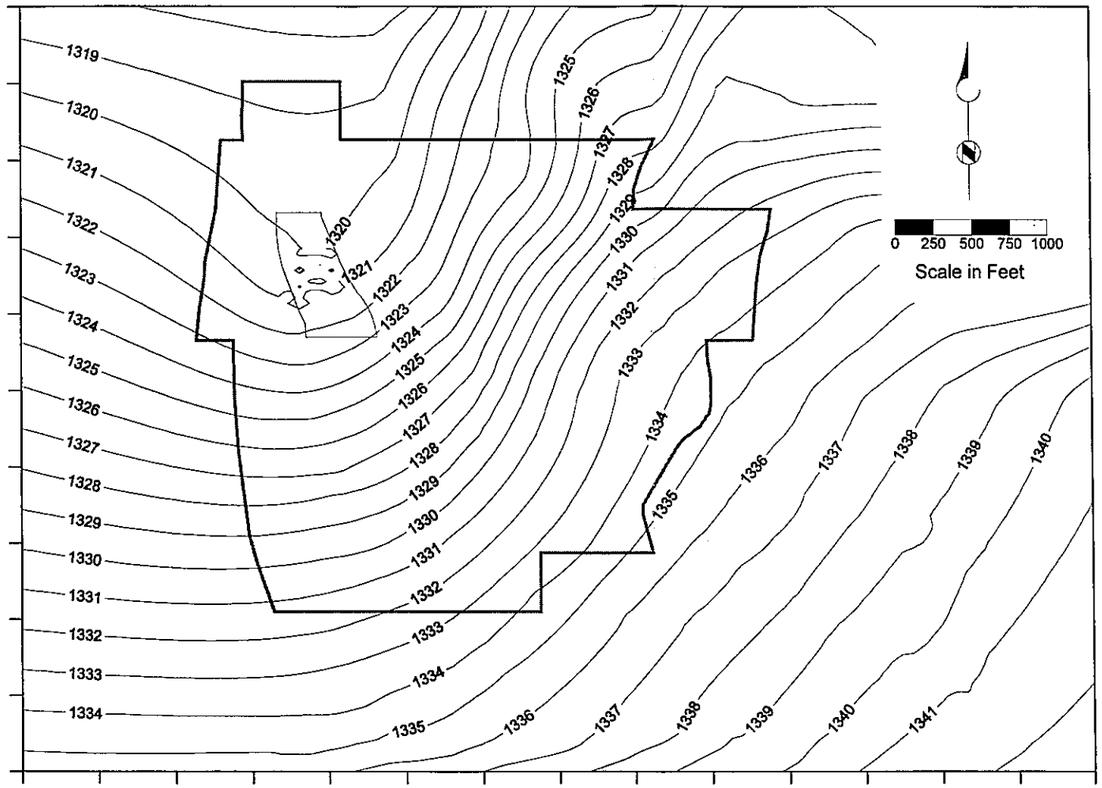

Contour Interval = 1 Foot

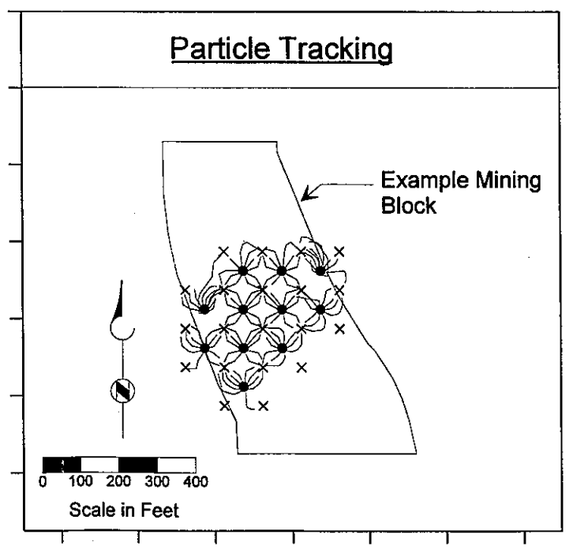

Explanation

- 1300 — Potentiometric Surface Contour (feet above mean sea level)
- ● Injection Well
- × Recovery Well
- Simulated Path Lines of Particles Released from Injection Wells

Figure 4.3-27 (IV)
SIMULATION SCENARIO 3
INCREASED RECHARGE
MODEL LAYER 4

BHP
BHP COPPER *Florence Project*

BROWN AND CALDWELL

SFIG077 08/13/96 MikeS

REVISED 7/19/96

Simulation Scenario 3: Increased Groundwater Recharge
90 Days of 100-Year Gila River Flood Event

Model Layer 5: Elevation = 900 - 1050 Feet
Above Mean Sea Level

Contour Interval = 10 Feet

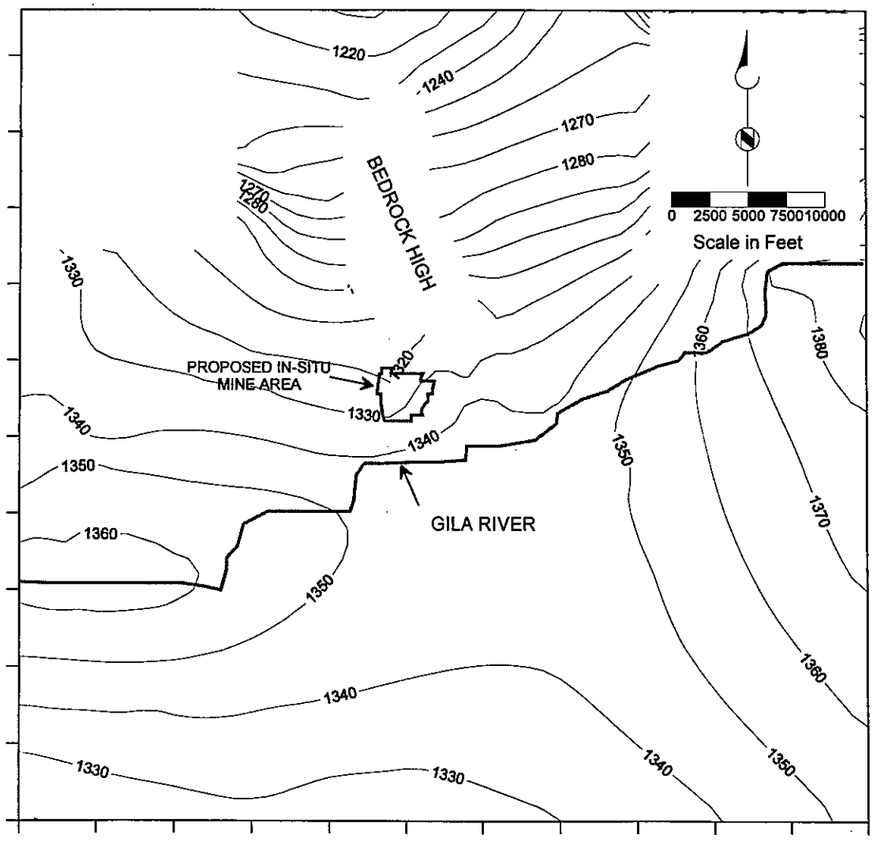

BROWN AND CALDWELL

SFIG078 08/13/96 MikeS

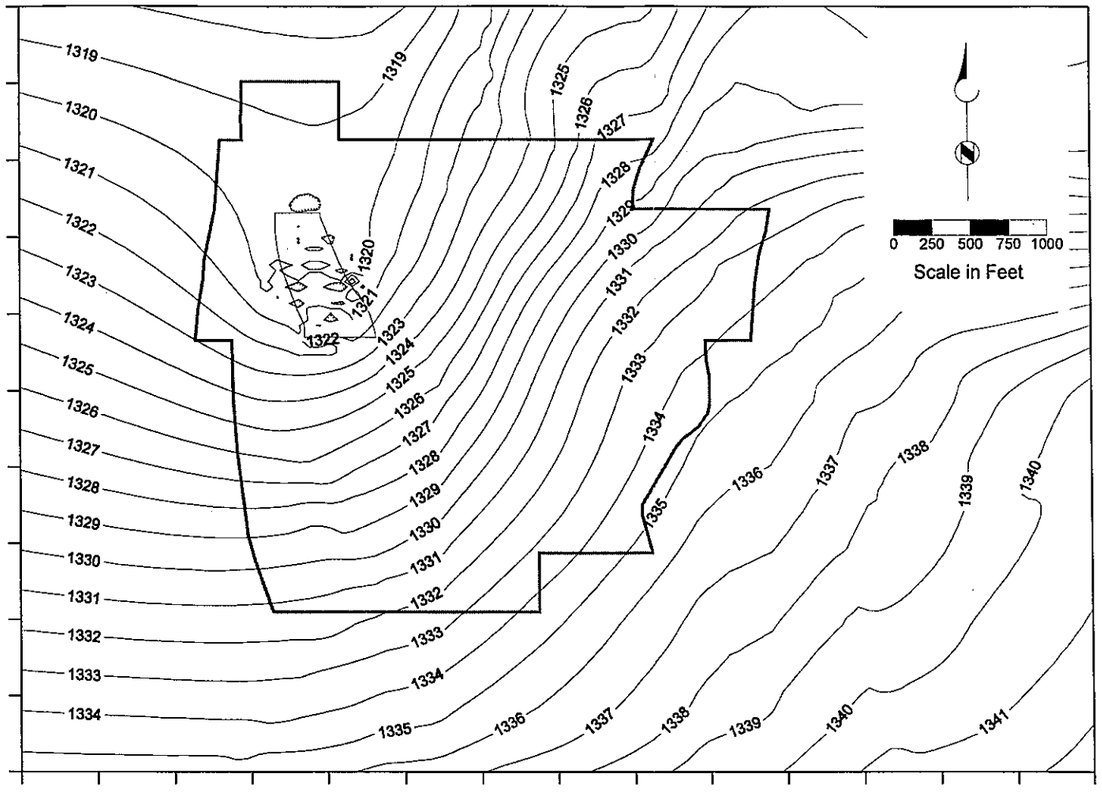

Contour Interval = 1 Foot

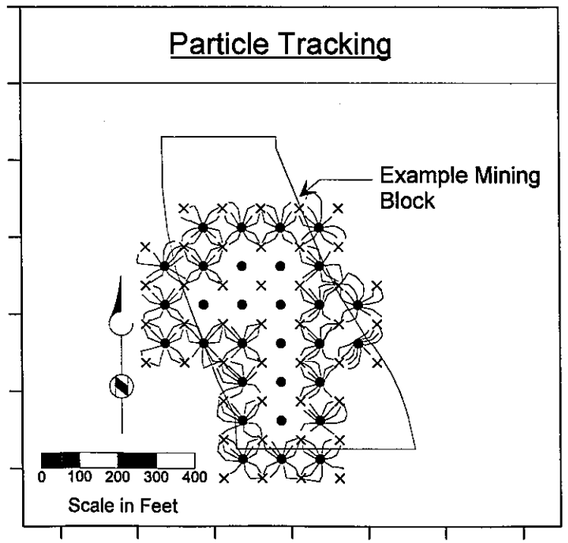

Explanation

- 1300 — Potentiometric Surface Contour (feet above mean sea level)
- Injection Well
- Recovery Well
- Simulated Path Lines of Particles Released from Injection Wells

Figure 4.3-28 (IV)
SIMULATION SCENARIO 3
INCREASED RECHARGE
MODEL LAYER 5

BHP
BHP COPPER *Florence Project*

REVISED 7/19/96

Simulation Scenario 3: Increased Groundwater Recharge
90 Days of 100-Year Gila River Flood Event

Model Layer 6: Elevation = 700 - 900 Feet
Above Mean Sea Level

Contour Interval = 10 Feet

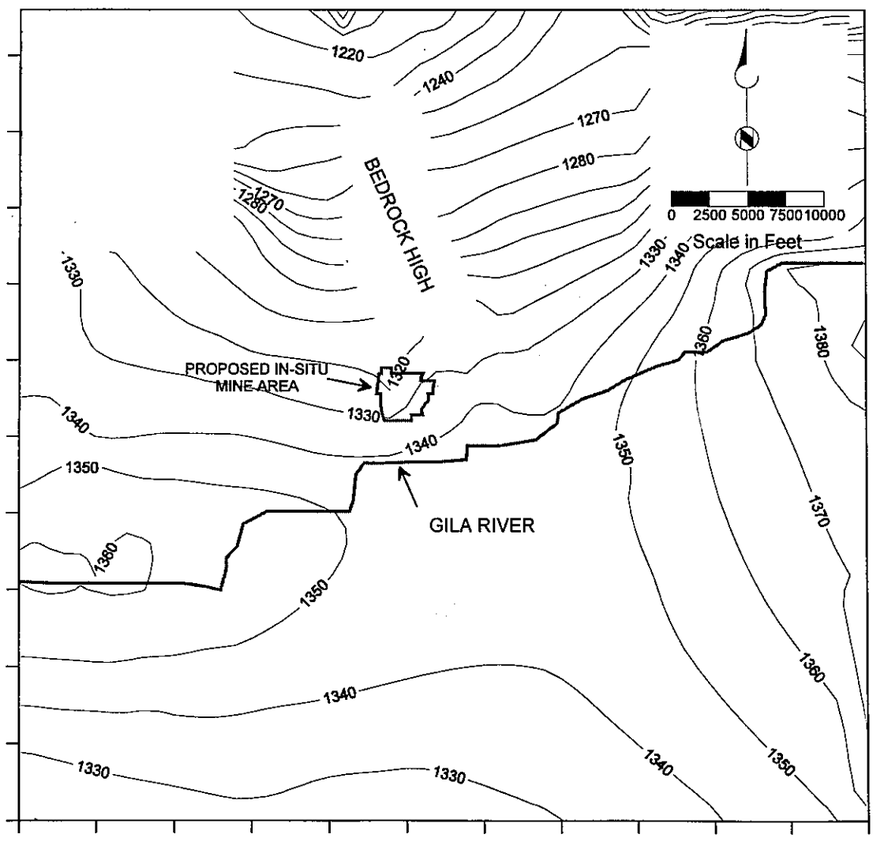

BROWN AND CALDWELL

SFIG079 08/13/96 MikeS

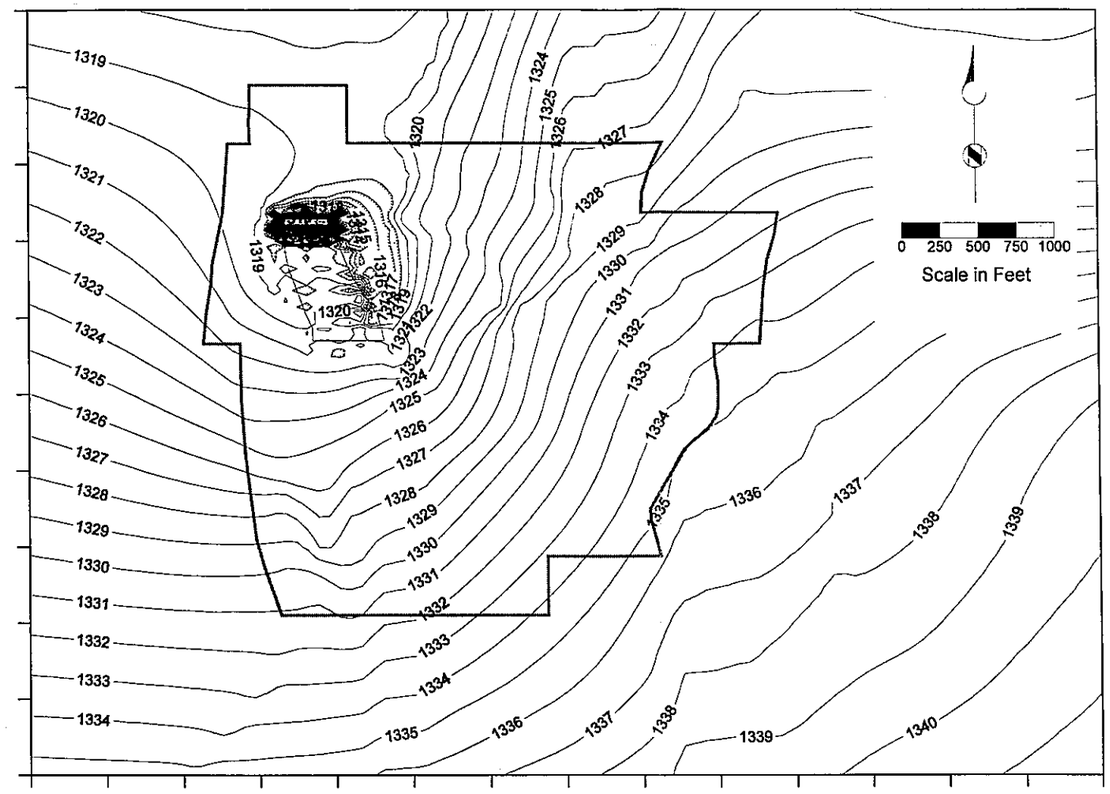

Contour Interval = 1 Foot

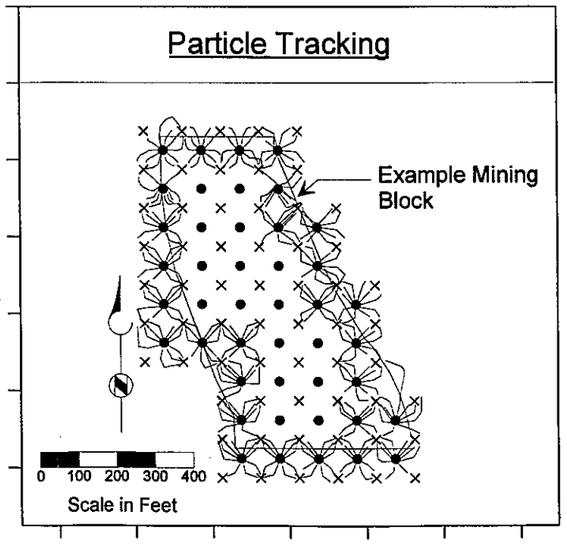

Explanation

- 1300 — Potentiometric Surface Contour (feet above mean sea level)
- ● Injection Well
- × Recovery Well
- Simulated Path Lines of Particles Released from Injection Wells

Figure 4.3-29 (IV)
SIMULATION SCENARIO 3
INCREASED RECHARGE
MODEL LAYER 6

BHP
BHP COPPER *Florence Project*

REVISED 7/19/96

Simulation Scenario 3: Increased Groundwater Recharge
90 Days of 100-Year Gila River Flood Event

Model Layer 7: Elevation = 300 - 700 Feet
Above Mean Sea Level

Contour Interval = 10 Feet

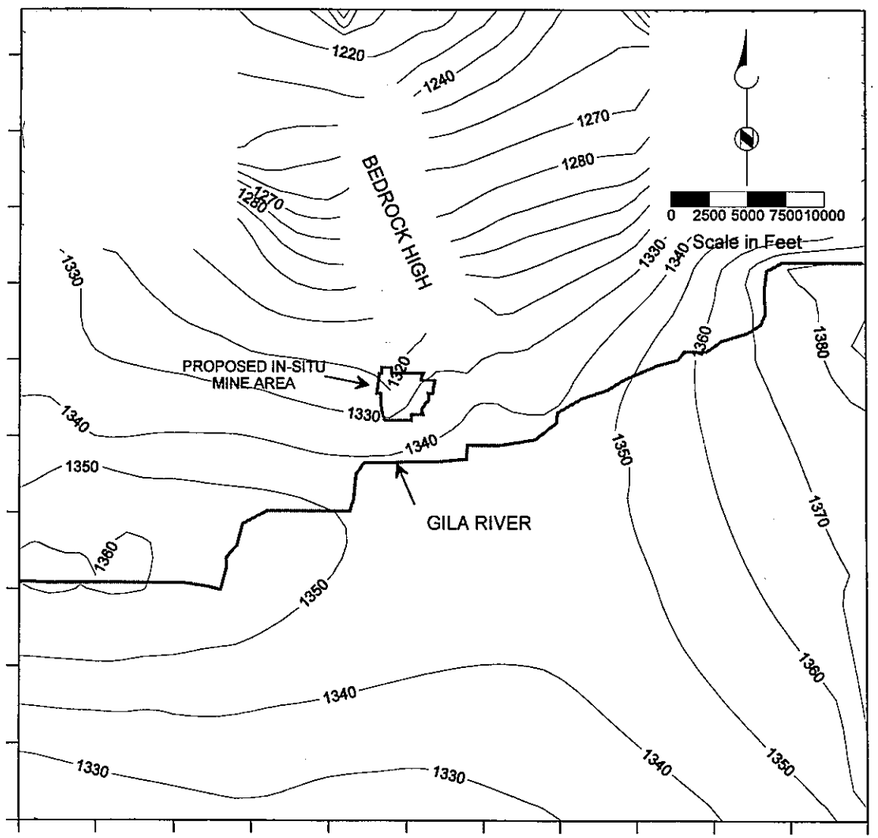

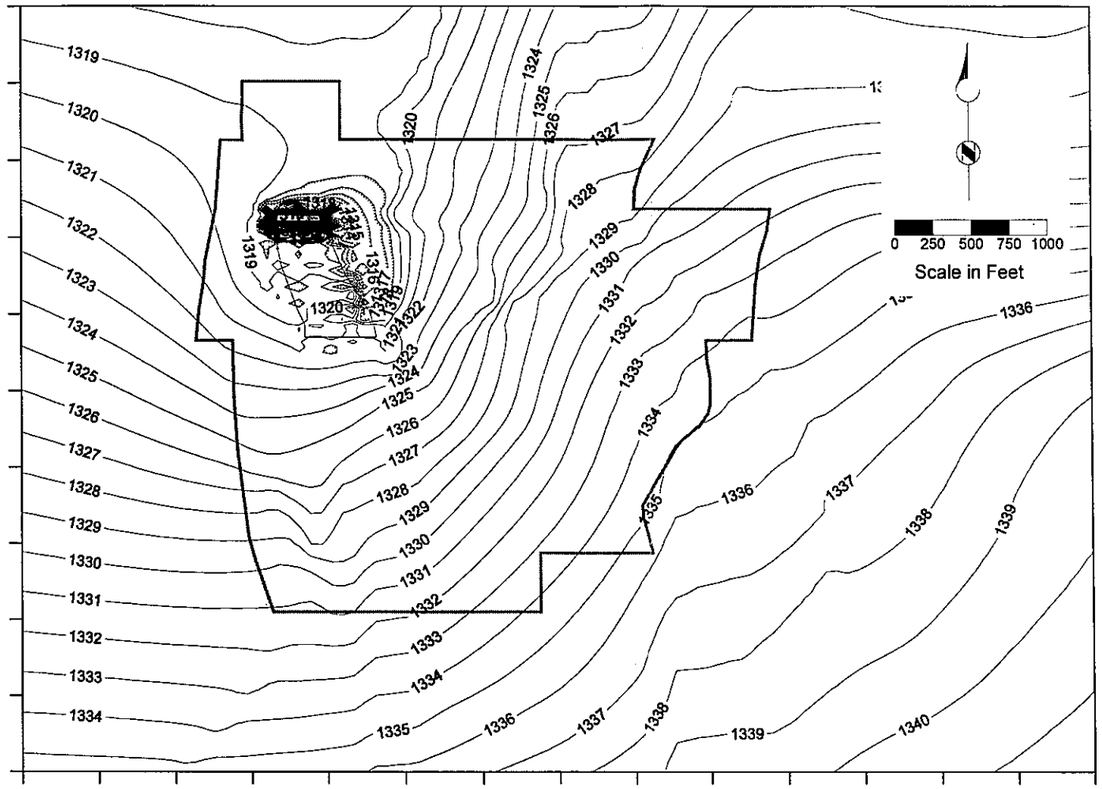

Contour Interval = 1 Foot

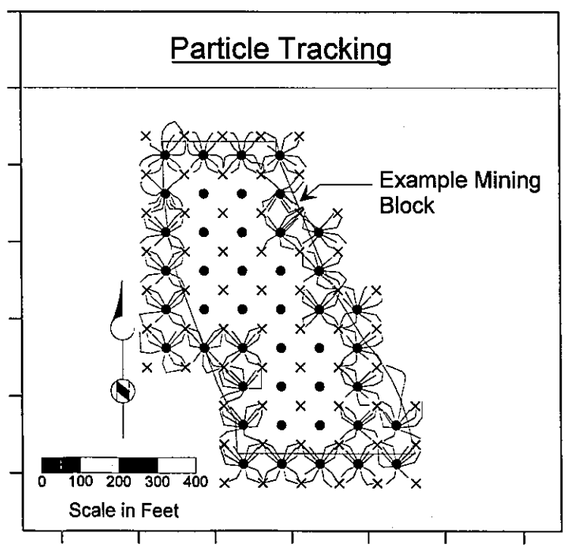

Explanation

- 1300 — Potentiometric Surface Contour (feet above mean sea level)
- ● Injection Well
- × Recovery Well
- Simulated Path Lines of Particles Released from Injection Wells

Figure 4.3-30 (IV)
SIMULATION SCENARIO 3
INCREASED RECHARGE
MODEL LAYER 7

BHP
BHP COPPER *Florence Project*

BROWN AND CALDWELL

SFIG080 08/13/96 MikeS

REVISED 7/19/96

Simulation Scenario 3: Increased Groundwater Recharge
90 Days of 100-Year Gila River Flood Event

Model Layer 8: Elevation = 0 - 300 Feet
Above Mean Sea Level

Contour Interval = 10 Feet

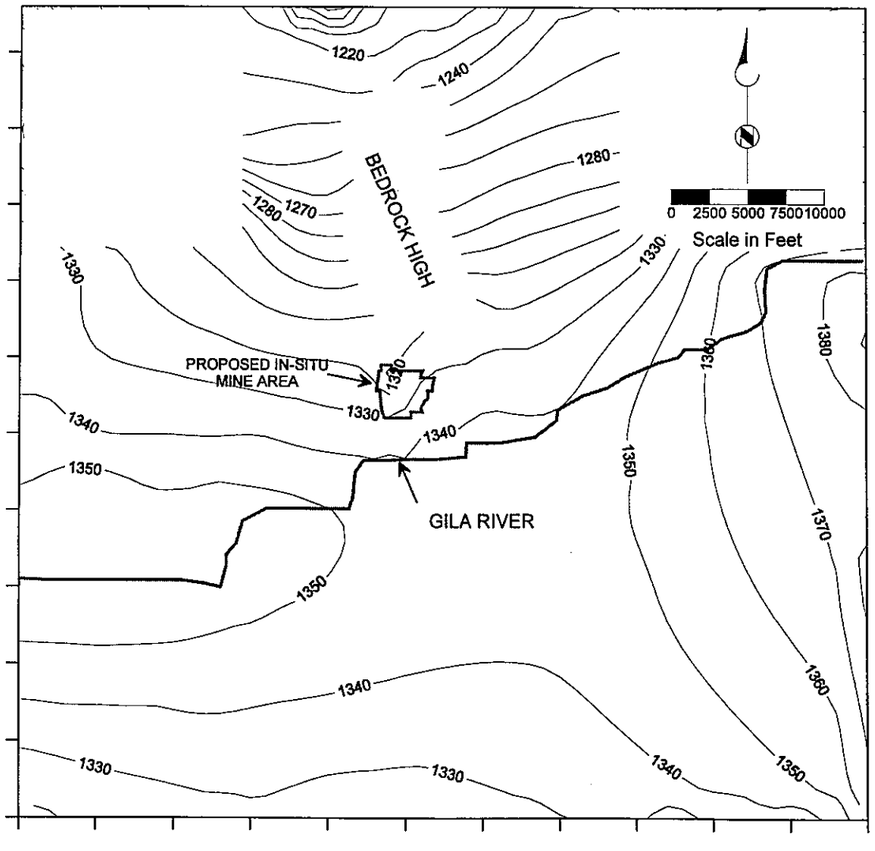

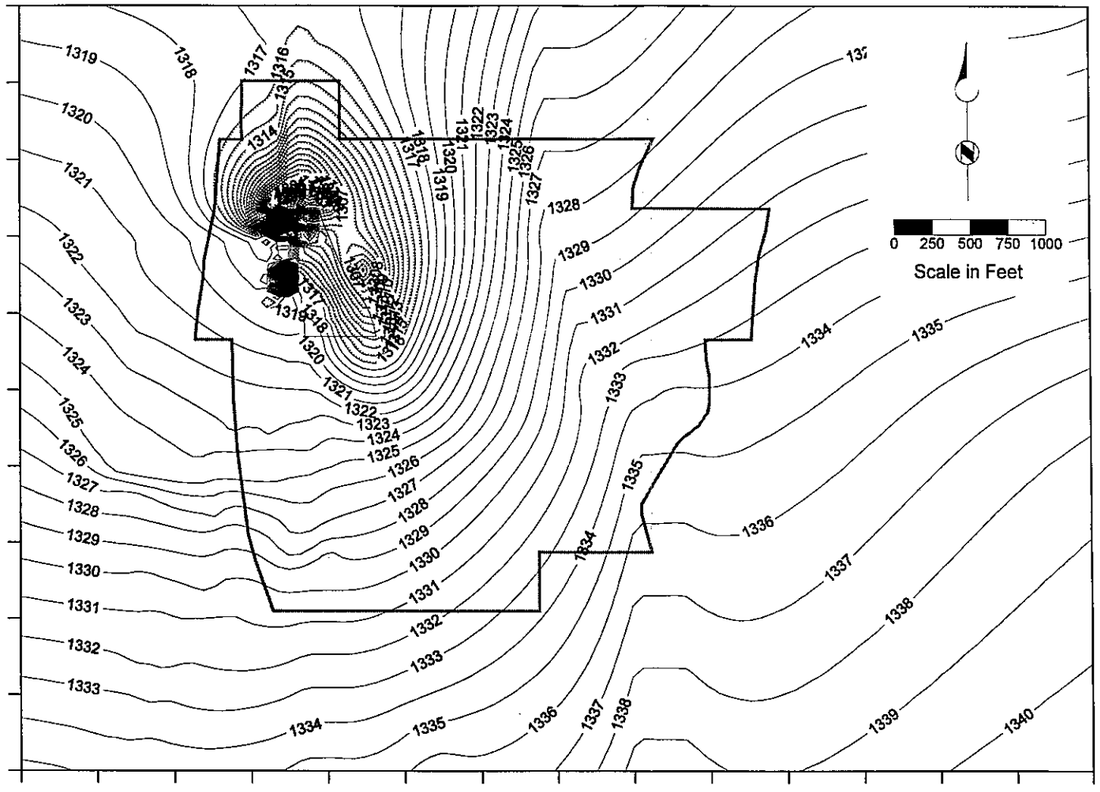

Contour Interval = 1 Foot

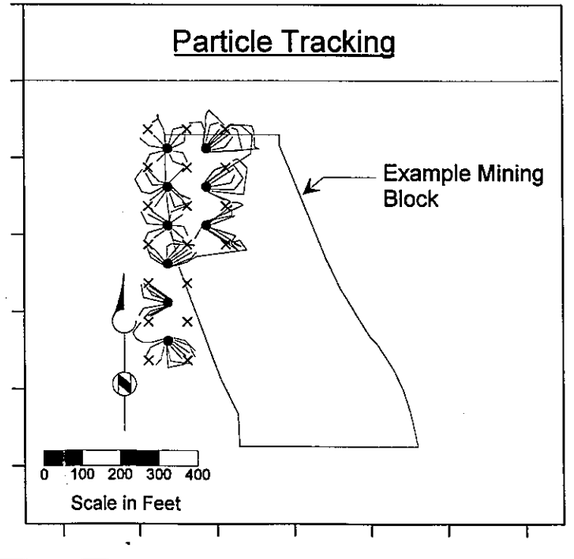

Explanation

- Potentiometric Surface Contour (feet above mean sea level)
- Injection Well
- Recovery Well
- Simulated Path Lines of Particles Released from Injection Wells

Figure 4.3-31 (IV)
SIMULATION SCENARIO 3
INCREASED RECHARGE
MODEL LAYER 8

BHP
BHP COPPER *Florence Project*

BROWN AND CALDWELL

SFIG081 08/13/96 MikeS

REVISED 7/19/96

Attachment 6 to Table 1

Attachment 6 to Table 1

Response to ADEQ Comment-3.7.5-Solvent Extraction

ADEQ-3.7.5-Solvent Extraction-Because the injection raffinate stream will contain entrained organic reagents, BHP should determine both the amounts of organics that will both build up in the aquifer and move in the groundwater.

As explained below, raffinate that is injected into the orebody is expected to have very low concentrations of organics (generally less than the detection limit for individual species). Measurable build-ups of organics are not expected because the organics should be in the dissolved phase and virtually all of the injected fluids will be returned to the surface.

Source of Organics

An organic solvent (7 percent reagent, 93 percent diluent) is used to remove copper from the pregnant leachate solutions (PLS). The solvent and the PLS are mixed to form a dispersion to facilitate contact between the reagent and the copper. After mixing, the two-phase mixture then flows through a settler system to separates the organic phase from the aqueous phase. The aqueous stream (raffinate) flows from the extraction units into a Jameson feed tank. The raffinate is then directed to two Jameson cells, operating in series. The Jameson cells use air to float organic particles out of the aqueous phase where they are then skimmed off and directed to the organic decant tank for recovery and re-use. The aqueous stream from the Jameson cells will then flow to the Raffinate Impoundment for eventual injection. A 50 gallon per minute (gpm) skimmer pump is located on the impoundment to collect organics collected on the impoundment raffinate. The collected organics are directed to the organic decant tank for recovery and re-use.

The facility's spill control system is designed to direct spills away from the raffinate area. Thus, the only material in the raffinate pond available for injection will be the raffinate from the extraction system that has passed through the Jameson cells. The Jameson cells are expected to operate at a 75 percent or greater efficiency. Assuming that raffinate from the extraction process contains 80 ppm organic, the raffinate in the impoundment will contain about 20 ppm, most of which will be collected by the skimmer in the impoundment. Available data indicate that the concentration of organics in the raffinate at San Manuel is less than 10 ppm.

Composition of Organics

A reagent now in use at BHP's SX/EW facilities is LIX®984. It is a 1:1 volume blend of LIX®860 (5-dodecylsalicylaldoxime) and LIX®84 (2-hydroxy-5-nonylacetophenone oxime).

A diluent now used at BHP's SX/EW facilities is Orfom®SX-7. The following table indicates concentrations of trace organics that have been reported in Orfom® SX-7 by the product's manufacturer, Phillips Mining Chemicals. The next column of the table indicates the estimated

concentration of individual organic constituents in the raffinate, assuming that the total organic concentrations in the raffinate is 10 ppm and that the concentration of organics in the raffinate is directly proportional to the initial concentrations reported by Phillips Mining Chemicals. The next column in the table indicates the maximum contaminant levels (MCLs) for the indicated contaminants.

Selected Constituents of Orfom®SX-7			
Constituent (Cn)	Constituent Concentrations (ppm)		Maximum Contaminant Level (ppm)
	Orfom®SX-7	Raffinate	
Benzene (C6)	20-30	0.0003	0.005
Ethylbenzene (C8)	1400	0.014	0.7
Toluene (C7)	350	.0035	1.0
Xylene Total (C8)	1912	0.019	10.0
Napthalene C10)	3100	0.031	NA
Octane (C8)	2300	0.23	NA

ppm - parts per million
NA - Not applicable, MCLs have not been established

Measured Constituent Concentrations

Samples of raffinate from BHP's San Manuel facility were collected by Brown and Caldwell earlier in 1996 for analysis using the EPA Test Method 418.1 procedures for total petroleum hydrocarbons (TPH). The reported concentration was less than detectable (less than 2 ppm).

In 1995 a sample of raffinate from San Manuel was sampled and analyzed. Less than detectable concentrations (<0.010 ppm) were reported for xylenes, toluene, napthalene, benzene and ethylbenzene using EPA Test Method 8260. The TPH (diesel range) concentration (EPA Test Method 8015M) was reported to be 1.2 ppm.

Proposed Monitoring

BHP proposes to base its organic monitoring of raffinate on diluents rather than reagents. Not only are the diluents present in greater concentration than the reagents (93 percent to 7 percent), the diluents are composed of smaller organic molecules which are more soluble in water than the reagents which are large organic molecules immiscibile in water. The large differences in miscibility and solubility make it much more likely that diluent rather than reagent will be entrained in the raffinate leaving the solvent extraction process.

Diluents that have been used in copper extraction processes include Orfom®SX-7, SX-10, SX-11, and SX-12. SX-10 and SX-11 generally do not function as well as Orfom®SX-7 and SX-12 in applications such as will be experienced at the Florence facility. SX-7 and SX-12 contain aromatics whereas SX-10 and SX-11 do not. The attached safety material data sheets indicate the

range of carbon atoms for the principal constituents in the Orfom® products. They are: C9-C16 for SX-7; C10-C14 for SX-10; C13-C17 for SX-11, and C9-C16 for SX-10.

The distribution of carbon numbers and the potential for trace amounts of benzene and other lower weight aromatics in the diluents dictate the analytical methods to be used in monitoring the raffinate stream for organics. The proposed methods are described below.

Modified EPA 5030/8015 will be used as a screening method for raffinate whenever SX-7, SX-10 or SX-12 are used as diluents at the Florence facility. That method has been selected because it covers C6-C10 and is very sensitive 0.5 µg/l (ppb). The range covered by the method ensures that benzene concentrations above the Arizona Water Quality Standard (5 ppb) will be seen in the raffinate. The range also captures one or more of the carbon numbers associated with all diluents except SX-11.

BHP proposes to collect a sample of the raffinate at a point at, or downstream, of the raffinate pond at least one time per month. If the total organic (TPH) concentration, using the aforementioned method, is greater than 10 ppm, BHP will collect a follow-up sample for analysis using Modified EPA 3510/8015. That method will enable heavier carbon molecules (C10-C25) to be detected and quantified. For that reason, Method 3510/8015 must be used if SX-11 is used as a diluent because its carbon numbers range from C13-C17. The method detection limit for 3510/8015 (generally less than 10 ppb) is not as sensitive as the first-mentioned method. However, the higher sensitivity is not needed except for benzene and benzene will be reported under Method 5030/8015.

Note that the principal difference between the two methods is the manner in which samples are prepared and introduced to the gas chromatograph. Method 5030 uses a purge and trap technique, which is good for light hydrocarbons in the C6-C10 range but not good for heavier molecules. Method 3510 uses liquid/liquid extraction. It is good for the heavier molecules but the lighter molecules, such as benzene, are often lost in the process.

If the total organic concentration reported under either method exceeds 20 ppm for any month or more than 10 ppm for any 2 consecutive months, BHP will institute a contingency sampling program for all wells in the POC network. Sampling will be continued thereafter semi-annually in each well in which organics are detected of the types found in the raffinate. If such organics are not detected during the first contingency testing, or are not detected in subsequent semi-annual samples, the sampling for organics will revert back to the biennual sampling frequency.

October 31, 1994

Material Safety Data Sheet

ORFOM® SX-7 (SOLVENT EXTRACTION DILUENT)

PHILLIPS CHEMICAL COMPANY
A Division of Phillips Petroleum Company
Bartlesville, Oklahoma 74004

PHONE NUMBERS
Emergency: (918) 661-8118
Technical Services: 1-800 221-1956
For Additional MSDSs: (918) 661-1764

A. Product Identification

Synonyms: Solvent Extraction Diluent
Chemical Name: Hydrotreated Distillate, Light C9-C16
Chemical Family: Paraffinic and Aromatic Hydrocarbon
Chemical Formula: Mixture
CAS Reg. No.: 64742-47-8
Product No.: Not Applicable

Product and/or Components Entered on EPA's TSCA Inventory: YES

This product is in U.S. commerce, and is listed in the Toxic Substances Control Act (TSCA) Inventory of Chemicals; hence, it is subject to all applicable provisions and restrictions of 40 CFR, section 721 and 723.250.

B. Components

Ingredients	CAS Number	% By Wt.	OSHA PEL	ACGIH TLV
Hydrotreated Distillate, Light C9-C16	64742-47-8	100	NE	NE

See Recommended Exposure Limits in Section F.

NA - Not Applicable NE - Not Established

C. Personal Protection Information

Ventilation:	Use adequate ventilation to control exposure below recommended exposure limit.
Respiratory Protection:	For concentration exceeding the recommended exposure limit, use NIOSH/MSHA approved air purifying respirator. In case of spill or leak resulting in unknown concentration or in confined spaces or other poorly ventilated areas, use NIOSH/MSHA approved supplied air respirator.
Eye Protection:	Use safety glasses with side shields. For splash protection, use chemical goggles and face shield.
Skin Protection:	Use protective garments to prevent skin contact. Use impervious gloves such as neoprene or nitrile rubber.

NOTE: Personal protection information shown in Section C is based upon general information as to normal uses and conditions. Where special or unusual uses or conditions exist, it is suggested that the expert assistance of an industrial hygienist or other qualified professional be sought.

D. Handling and Storage Precautions

Do not get in eyes, on skin or on clothing. Avoid breathing vapors. Wear protective equipment and/or garments described in Section C if exposure conditions warrant. Wash thoroughly after handling. Launder contaminated clothing before reuse. Use with adequate ventilation.

Store and use in well-ventilated area away from ignition sources. Bond and ground during liquid transfer. Store in a closed container.

E. Reactivity Data

Stability:	Stable
Conditions to Avoid:	Not Applicable
Incompatibility (Materials to Avoid):	Oxygen and strong oxidizing agents
Hazardous Polymerization:	Will Not Occur
Conditions to Avoid:	Not Applicable
Hazardous Decomposition Products:	Carbon oxides and various hydrocarbons are formed when burned.

F. Health Hazard Data

Recommended Exposure Limits:

The Company recommends a permissible exposure level (8-hr. TWA) of 100 ppm or 525 mg/m3.

Acute Effects of Overexposure:

Eye: May be mildly irritating to the eyes.

Skin: May cause severe skin irritation, especially upon repeated contact.

Inhalation: May cause headache and dizziness.

Ingestion: May be mildly irritating to intestines. May be aspirated into the lungs if swallowed resulting in pulmonary edema and chemical pneumonitis.

Subchronic and Chronic Effects of Overexposure:

No known applicable information.

Other Health Effects:

Long term exposure to high oil mist concentrations may cause non-debilitating lung changes.

Health Hazard Categories:

	Animal	Human		Animal	Human
Known Carcinogen	___	___	Toxic	___	___
Suspect Carcinogen	___	___	Corrosive	___	___
Mutagen	___	___	Irritant	_X_	_X_
Teratogen	___	___	Target Organ Toxin	_X_	_X_
Allergic Sensitizer	___	___	Specify - Lung-Aspiration Hazard		
Highly Toxic	___	___			

First Aid and Emergency Procedures:

Eye: Flush eyes with running water for at least fifteen minutes. If irritation develops, seek medical attention.

Skin: Immediately wash with soap and water for fifteen minutes. Seek medical attention.

Inhalation: Remove from exposure. If illness or adverse symptoms develop, seek medical attention.

Ingestion: Do not induce vomiting. Seek immediate medical attention.

Note to Physician: Gastric lavage using a cuffed endotracheal tube may be performed at your discretion.

G. Physical Data

Appearance:	Colorless Liquid
Odor:	Mild, Characteristic
Boiling Point:	370-525F (187-274C)
Vapor Pressure:	0.2 psia (Reid)
Vapor Density (Air = 1):	4.5
Solubility in Water:	Negligible
Specific Gravity (H2O = 1):	0.81-0.82 at 60/60F (16/16C)
Percent Volatile by Volume:	100
Evaporation Rate (Ethyl Ether = 1):	<1
Viscosity:	2.0-2.2 cSt at 25C (77F)

H. Fire and Explosion Data

Flash Point (Method Used):	155-165F (68-74C) (PMCC, ASTM D93)
Flammable Limits (% by Volume in Air):	LEL - 0.7 UEL - 5.0
Fire Extinguishing Media:	Dry chemical, foam, carbon dioxide (CO2)
Special Fire Fighting Procedures:	Evacuate area of all unnecessary personnel. Wear appropriate safety equipment for fire conditions including self-contained breathing apparatus (SCBA) and other equipment and/or garments described in Section C if exposure conditions warrant. Shut off source, if possible. Do not spray water directly on fire product will float and could be reignited on surface of water. Water fog or spray may be used to cool exposed equipment and containers.
Fire and Explosion Hazards:	Carbon oxides and various hydrocarbons are released when burned.

I. Spill, Leak and Disposal Procedures

Precautions Required if Material is Released or Spilled:
Evacuate area of all unnecessary personnel. Wear protective equipment and/or garments described in Section C if exposure conditions warrant. Shut off source, if possible and contain spill. Protect from ignition. Keep out of water sources and sewers. Absorb in dry, inert material. Transfer to disposal containers using non-sparking equipment.

Waste Disposal (Insure Conformity with all Applicable Disposal Regulations):
Incinerate or place in a permitted waste management facility.

J. DOT Transportation

Shipping Name:	Combustible liquid, n.o.s. (Paraffinic and aromatic hydrocarbons)
Hazard Class:	Combustible liquid
ID Number:	NA 1993
Packing Group:	III
Marking:	1993 on Bulk Containers
Label:	None
Placard:	Combustible/1993
Hazardous Substance/RQ:	None
Shipping Description:	Combustible liquid, n.o.s. (Paraffinic and aromatic hydrocarbons), Combustible liquid, NA 1993, PG III
Packaging References:	49 CFR 173.150, 173.203, 173.241

NOTE: The above information is applicable when the product is shipped in containers larger than 119 gallons. If shipped in 119 gallon or smaller containers it is not regulated by the DOT Hazardous Material Regulations.

K. RCRA Classification - Unadulterated Product as a Waste

Not Applicable

L. Protection Required for Work on Contaminated Equipment

Contact immediate supervisor for specific instructions before work is initiated. Wear protective equipment and/or garments described in Section C if exposure conditions warrant.

M. Hazard Classification

_X_ This product meets the following hazard definition(s) as defined by the Occupational Safety and Health Hazard Communication Standard (29 CFR Section 1910.1200):

_X_ Combustible Liquid	___ Flammable Aerosol	___ Oxidizer
___ Compressed Gas	___ Explosive	___ Pyrophoric
___ Flammable Gas	_X_ Health Hazard (Section F)	___ Unstable
___ Flammable Liquid	___ Organic Peroxide	___ Water Reactive
___ Flammable Solid		

___ Based on information presently available, this product does not meet any of the hazard definitions of 29 CFR Section 1910.1200.

N. Additional Comments

SARA 313

As of the preparation date, this product did not contain a chemical or chemicals subject to the reporting requirements of Section 313 of Title III of the Superfund Amendments and Reauthorization Act of 1986 and 40 CFR Part 372.

April 30, 1992

Material Safety Data Sheet

ORFOM® SX-10 (SOLVENT EXTRACTION DILUENT)

PHILLIPS 66 COMPANY
A Division of Phillips Petroleum Company
Bartlesville, Oklahoma 74004

PHONE NUMBERS
Emergency:
Business Hours (918) 661-3865
After Hours (918) 661-8118
General MSDS Information:
(918) 661-8327
For Additional MSDSs: (918) 661-5952

A. Product Identification

Synonyms: Solvent extraction diluent
Chemical Name: Mixture
Chemical Family: Hydrocarbon
Chemical Formula: Mixture
CAS Reg. No.: 68551-19-9
Product No.: Not Established

Product and/or Components Entered on EPA's TSCA Inventory: YES

This product is in U.S. commerce, and is listed in the Toxic Substances Control Act (TSCA) Inventory of Chemicals; hence, it may be subject to applicable TSCA provisions and restrictions.

B. Components

Ingredients	CAS Number	% By Wt.	OSHA PEL	ACGIH TLV
Mixture of C10-C14 Isoalkanes	68551-19-9	100	NE	NE

NA - Not Applicable NE - Not Established

C. Personal Protection Information

Ventilation:	Use adequate ventilation to control below recommended exposure levels.
Respiratory Protection:	Not generally required unless needed to prevent respiratory irritation.
Eye Protection:	Use safety glasses with side shields or face shield if splashes could occur.
Skin Protection:	Rubber, neoprene or vinyl alcohol gloves. Use protective garments to prevent skin contact.

NOTE: Personal protection information shown in Section C is based upon general information as to normal uses and conditions. Where special or unusual uses or conditions exist, it is suggested that the expert assistance of an industrial hygienist or other qualified professional be sought.

D. Handling and Storage Precautions

Avoid contact with eyes, skin or clothing. Avoid breathing vapors or mists. Do not swallow. May be aspirated into lungs. Wear protective equipment and/or garments described in Section C if exposure conditions warrant. Wash thoroughly after handling. Launder contaminated clothing before reuse. Use with adequate ventilation.

Store in closed container. Store in well-ventilated area. Keep away from heat, spark and flame. Bond and ground during transfer.

E. Reactivity Data

Stability:	Stable
Conditions to Avoid:	Not Applicable
Incompatibility (Materials to Avoid):	Oxygen or strong oxidizing materials
Hazardous Polymerization:	Will Not Occur
Conditions to Avoid:	Not Applicable
Hazardous Decomposition Products:	Carbon oxides formed when burned.

F. Health Hazard Data

Recommended Exposure Limits:

The Company recommends a permissible exposure level (8 hr. TWA) of 400 ppm for isoparaffins.

Acute Effects of Overexposure:

Eye: May be mildly irritating.

Skin: May be mildly irritating.

Inhalation: May cause headache, dizziness, nausea or unconsciousness.

Ingestion: May irritate stomach and intestines. If swallowed, may be aspirated resulting in inflammation and possible fluid accumulation in the lungs.

Subchronic and Chronic Effects of Overexposure:

Some isoparaffins have produced kidney damage in male rats only. No comparable kidney disease is known to occur in humans.

Other Health Effects:

No know applicable information.

Health Hazard Categories:

	Animal	Human		Animal	Human
Known Carcinogen	___	___	Toxic	___	___
Suspect Carcinogen	___	___	Corrosive	___	___
Mutagen	___	___	Irritant	___	___
Teratogen	___	___	Target Organ Toxin	_X_	_X_
Allergic Sensitizer	___	___	Specify - Lung-Aspiration Hazard		
Highly Toxic	___	___			

First Aid and Emergency Procedures:

Eye: Flush eyes with running water for at least fifteen minutes. If irritation or adverse symptoms develop, seek medical attention.

Skin: Wash skin with soap and water for at least fifteen minutes. If irritation or adverse symptoms develop, seek medical attention.

Inhalation: Remove from exposure. If breathing is difficult, give oxygen. If breathing ceases, administer artificial respiration followed by oxygen. Seek immediate medical attention.

Ingestion: Do not induce vomiting. Seek immediate medical attention.

Note to Physician: Gastric lavage using a cuffed endotracheal tube may be performed at your discretion.

G. Physical Data

Appearance:	Colorless liquid
Odor:	Mild
Boiling Point:	424-460F (218-238C)
Vapor Pressure:	0.012 psia (0.6 mm Hg) @ 77F (25C)
Vapor Density (Air = 1):	> 1
Solubility in Water:	Negligible
Specific Gravity (H2O = 1):	0.778 @ 60/60F (16/16C)
Percent Volatile by Volume:	100
Evaporation Rate (Butyl Acetate = 1):	< 1
Viscosity:	38.0 SUS @ 77F (25C)

H. Fire and Explosion Data

Flash Point (Method Used):	185F (85C) (TCC, ASTM D56)
Flammable Limits (% by Volume in Air):	LEL - Not Established UEL - Not Established
Fire Extinguishing Media:	Dry chemical, foam or carbon dioxide (CO2)
Special Fire Fighting Procedures:	Evacuate area of all unnecessary personnel. Shut off source. Use NIOSH/MSHA approved self-contained breathing apparatus and other protective equipment and/or garments described in Section C if conditions warrant. Water fog or spray to cool exposed equipment and containers. Do not spray water directly on fire - product will float and could be reignited on surface of water.
Fire and Explosion Hazards:	Carbon oxides formed when burned.

I. Spill, Leak and Disposal Procedures

Precautions Required if Material is Released or Spilled:
Evacuate area of all unnecessary personnel. Wear protective equipment and/or garments described in Section C if exposure conditions warrant. Shut off source, if possible and contain spill. Keep out of water sources and sewers. Absorb in dry, inert material (sand, clay, sawdust, etc.). Transfer to disposal containers using non-sparking equipment.

Waste Disposal (Insure Conformity with all Applicable Disposal Regulations):
Incinerate or place in RCRA permitted waste management facility.

J. DOT Transportation

Shipping Name:	Combustible liquid, n.o.s. (Isoparaffinic hydrocarbons)
Hazard Class:	Combustible liquid
ID Number:	NA 1993
Packing Group:	III
Marking:	1993 (bulk containers only)
Label:	None
Placard:	Combustible/1993
Hazardous Substance/RQ:	Not Applicable
Shipping Description:	Combustible liquid, n.o.s. (Isoparaffinic hydrocarbon), Combustible liquid, NA 1993, PG III
Packaging References:	49 CFR 173.150, 173.202, 173.241

NOTE: This product is regulated only when shipped in bulk quantities, domestically, by land.

K. RCRA Classification - Unadulterated Product as a Waste

Prior to disposal, consult your environmental contact to determine if TCLP (Toxicity Characteristic Leaching Procedure, EPA Test Method 1311) is required. Reference 40 CFR Part 261.

L. Protection Required for Work on Contaminated Equipment

Contact immediate supervisor for specific instructions before work is initiated. Wear protective equipment and/or garments described in Section C if exposure conditions warrant.

M. Hazard Classification

_X_ This product meets the following hazard definition(s) as defined by the Occupational Safety and Health Hazard Communication Standard (29 CFR Section 1910.1200):

_X_ Combustible Liquid	___ Flammable Aerosol	___ Oxidizer
___ Compressed Gas	___ Explosive	___ Pyrophoric
___ Flammable Gas	_X_ Health Hazard (Section F)	___ Unstable
___ Flammable Liquid	___ Organic Peroxide	___ Water Reactive
___ Flammable Solid		

___ Based on information presently available, this product does not meet any of the hazard definitions of 29 CFR Section 1910.1200.

N. Additional Comments

SARA 313

As of the preparation date, this product did not contain a chemical or chemicals subject to the reporting requirements of Section 313 of Title III of the Superfund Amendments and Reauthorization Act of 1986 and 40 CFR Part 372.

June 30, 1995

Material Safety Data Sheet

ORFOM® SX-11 (SOLVENT EXTRACTION DILUENT)

PHILLIPS CHEMICAL COMPANY
A Division of Phillips Petroleum Company
Bartlesville, Oklahoma 74004

PHONE NUMBERS
Emergency: (918) 661-8118
Technical Services: (800) 221-1956
For Additional MSDSs: (918) 661-1764

A. Product Identification

Synonyms: Solvent extraction diluent
Chemical Name: Mixture
Chemical Family: Hydrocarbon
Chemical Formula: Mixture
CAS Reg. No.: 68551-20-2
Product No.: Not Established

Product and/or Components Entered on EPA's TSCA Inventory: YES

This product is in U.S. commerce, and is listed in the Toxic Substances Control Act (TSCA) Inventory of Chemicals; hence, it may be subject to applicable TSCA provisions and restrictions.

B. Components

Ingredients	CAS Number	% By Wt.	OSHA PEL	ACGIH TLV
Mixture of C13-C17 Isoalkanes	68551-20-2	100	NE	NE

NA - Not Applicable NE - Not Established

C. Personal Protection Information

Ventilation: Use adequate ventilation to control below recommended exposure levels.

Respiratory Protection: Not generally required unless needed to prevent respiratory irritation.

Eye Protection: Use safety glasses with side shields or face shield if splashes could occur.

Skin Protection: Rubber, neoprene or vinyl alcohol gloves. Use protective garments to prevent skin contact.

NOTE: Personal protection information shown in Section C is based upon general information as to normal uses and conditions. Where special or unusual uses or conditions exist, it is suggested that the expert assistance of an industrial hygienist or other qualified professional be sought.

D. Handling and Storage Precautions

Avoid contact with eyes, skin or clothing. Avoid breathing vapors or mists. Do not swallow, may be aspirated into lungs. Wear protective equipment and/or garments described in Section C if exposure conditions warrant. Wash thoroughly after handling. Launder contaminated clothing before reuse. Use with adequate ventilation.

Store in closed container. Store in well-ventilated area.

E. Reactivity Data

Stability: Stable
Conditions to Avoid: Not Applicable
Incompatibility (Materials to Avoid): Oxygen or strong oxidizing materials

Hazardous Polymerization: Will Not Occur
Conditions to Avoid: Not Applicable
Hazardous Decomposition Products: Carbon oxides formed when burned.

F. Health Hazard Data

Recommended Exposure Limits:

The Company recommends a permissible exposure level (8 hr. TWA) of 400 ppm for isoparaffins.

Acute Effects of Overexposure:

Eye: May be mildly irritating.

Skin: May be mildly irritating.

Inhalation: May cause headache, dizziness, nausea or unconsciousness.

Ingestion: May irritate stomach and intestines. If swallowed, may be aspirated resulting in inflammation and possible fluid accumulation in the lungs.

Subchronic and Chronic Effects of Overexposure:

Some isoparaffins have produced kidney damage in male rats only. No comparable kidney disease is known to occur in humans.

Other Health Effects:

No known applicable information.

Health Hazard Categories:

	Animal	Human		Animal	Human
Known Carcinogen	___	___	Toxic	___	___
Suspect Carcinogen	___	___	Corrosive	___	___
Mutagen	___	___	Irritant	___	___
Teratogen	___	___	Target Organ Toxin	_X_	_X_
Allergic Sensitizer	___	___	Specify - Lung-Aspiration Hazard		
Highly Toxic	___	___			

First Aid and Emergency Procedures:

Eye: Flush eyes with running water for at least fifteen minutes. If irritation or adverse symptoms develop, seek medical attention.

Skin: Wash skin with soap and water for at least fifteen minutes. If irritation or adverse symptoms develop, seek medical attention.

Inhalation: Remove from exposure. If breathing is difficult, give oxygen. If breathing ceases, administer artificial respiration followed by oxygen. Seek immediate medical attention.

Ingestion: Do not induce vomiting. Seek immediate medical attention.

Note to Physician: Gastric lavage using a cuffed endotracheal tube may be performed at your discretion.

G. Physical Data

Appearance:	Colorless Liquid
Odor:	Mild
Boiling Point:	450-550F (232-288C)
Vapor Pressure:	0.004 psia (0.2 mm Hg) @ 77F (25C)
Vapor Density (Air = 1):	> 1
Solubility in Water:	Negligible
Specific Gravity (H2O = 1):	0.809 @ 60/60F (16/16C)
Percent Volatile by Volume:	100
Evaporation Rate (Butyl Acetate = 1):	< 1
Viscosity:	39.2 SUS @ 77F (25C)

H. Fire and Explosion Data

Flash Point (Method Used):	222F (106C) (COC, ASTM D92)
Flammable Limits (% by Volume in Air):	LEL - Not Established UEL - Not Established
Fire Extinguishing Media:	Dry chemical, foam or carbon dioxide (CO2)
Special Fire Fighting Procedures:	Evacuate area of all unnecessary personnel. Shut off source. Use NIOSH/MSHA approved self-contained breathing apparatus and other protective equipment and/or garments described in Section C if conditions warrant. Water fog or spray to cool exposed equipment and containers.
Fire and Explosion Hazards:	Carbon oxides formed when burned.

I. Spill, Leak and Disposal Procedures

Precautions Required if Material is Released or Spilled:
Evacuate area of all unnecessary personnel. Wear protective equipment and/or garments described in Section C if exposure conditions warrant. Shut off source, if possible and contain spill. Protect from ignition. Keep out of water sources and sewers. Absorb in a dry, inert material (sand, clay, etc). Transfer to disposal drums using non-sparking equipment.

Waste Disposal (Insure Conformity with all Applicable Disposal Regulations):
Incinerate or place in permitted waste management facility.

J. DOT Transportation

Shipping Name:	Not Applicable
Hazard Class:	Not Applicable
ID Number:	Not Applicable
Packing Group:	Not Applicable
Marking:	Not Applicable
Label:	Not Applicable
Placard:	Not Applicable
Hazardous Substance/RQ:	Not Applicable
Shipping Description:	Not Applicable
Packaging References:	Not Applicable

K. RCRA Classification - Unadulterated Product as a Waste

Prior to disposal, consult your environmental contact to determine if TCLP (Toxicity Characteristic Leaching Procedure, EPA Test Method 1311) is required. Reference 40 CFR Part 261.

L. Protection Required for Work on Contaminated Equipment

Contact immediate supervisor for specific instructions before work is initiated. Wear protective equipment and/or garments described in Section C if exposure conditions warrant.

M. Hazard Classification

_X_ This product meets the following hazard definition(s) as defined by the Occupational Safety and Health Hazard Communication Standard (29 CFR Section 1910.1200):

___ Combustible Liquid	___ Flammable Aerosol	___ Oxidizer
___ Compressed Gas	___ Explosive	___ Pyrophoric
___ Flammable Gas	_X_ Health Hazard (Section F)	___ Unstable
___ Flammable Liquid	___ Organic Peroxide	___ Water Reactive
___ Flammable Solid		

___ Based on information presently available, this product does not meet any of the hazard definitions of 29 CFR Section 1910.1200.

N. Additional Comments

SARA 313

As of the preparation date, this product did not contain a chemical or chemicals subject to the reporting requirements of Section 313 of Title III of the Superfund Amendments and Reauthorization Act of 1986 and 40 CFR Part 372.

NFPA 704 Hazard Codes - - - - - - - - Signals

Health : 2	Least - 0
Flammability: 1	Slight - 1
Reactivity : 0	Moderate - 2
Special Haz.: -	High - 3
	Extreme - 4

October 31, 1994

Material Safety Data Sheet

ORFOM® SX-12 (SOLVENT EXTRACTION DILUENT)

PHILLIPS CHEMICAL COMPANY
A Division of Phillips Petroleum Company
Bartlesville, Oklahoma 74004

PHONE NUMBERS
Emergency: (918) 661-8118
Technical Services: 1-800 221-1956
For Additional MSDSs: (918) 661-1764

A. Product Identification

Synonyms: Solvent Extraction Diluent
Chemical Name: Hydrotreated Distillate, Light C9-C16
Chemical Family: Paraffinic and Aromatic Hydrocarbon
Chemical Formula: Mixture
CAS Reg. No.: 64742-47-8
Product No.: Not Applicable

Product and/or Components Entered on EPA's TSCA Inventory: YES

This product is in U.S. commerce, and is listed in the Toxic Substances Control Act (TSCA) Inventory of Chemicals; hence, it is subject to all applicable provisions and restrictions of 40 CFR, section 721 and 723.250.

B. Components

Ingredients	CAS Number	% By Wt.	OSHA PEL	ACGIH TLV
Hydrotreated Distillate, Light C9-C16	64742-47-8	100	NE	NE

See Recommended Exposure Limits in Section F.

NA - Not Applicable NE - Not Established

C. Personal Protection Information

Ventilation:	Use adequate ventilation to control exposure below recommended exposure limit.
Respiratory Protection:	For concentration exceeding the recommended exposure limit, use NIOSH/MSHA approved air purifying respirator. In case of spill or leak resulting in unknown concentration or in confined spaces or other poorly ventilated areas, use NIOSH/MSHA approved supplied air respirator.
Eye Protection:	Use safety glasses with side shields. For splash protection, use chemical goggles and face shield.
Skin Protection:	Use protective garments to prevent skin contact. Use impervious gloves such as neoprene or nitrile rubber.

NOTE: Personal protection information shown in Section C is based upon general information as to normal uses and conditions. Where special or unusual uses or conditions exist, it is suggested that the expert assistance of an industrial hygienist or other qualified professional be sought.

D. Handling and Storage Precautions

Do not get in eyes, on skin or on clothing. Avoid breathing vapors. Wear protective equipment and/or garments described in Section C if exposure conditions warrant. Wash thoroughly after handling. Launder contaminated clothing before reuse. Use with adequate ventilation.

Store and use in well-ventilated area away from ignition sources. Bond and ground during liquid transfer. Store in a closed container.

E. Reactivity Data

Stability:	Stable
Conditions to Avoid:	Not Applicable
Incompatibility (Materials to Avoid):	Oxygen and strong oxidizing agents
Hazardous Polymerization:	Will Not Occur
Conditions to Avoid:	Not Applicable
Hazardous Decomposition Products:	Carbon oxides and various hydrocarbons are formed when burned.

F. Health Hazard Data

Recommended Exposure Limits:

The Company recommends a permissible exposure level (8-hr. TWA) of 100 ppm or 525 mg/m3.

Acute Effects of Overexposure:

Eye: May be mildly irritating to the eyes.

Skin: May cause severe skin irritation, especially upon repeated contact.

Inhalation: May cause headache and dizziness.

Ingestion: May be mildly irritating to intestines. May be aspirated into the lungs if swallowed resulting in pulmonary edema and chemical pneumonitis.

Subchronic and Chronic Effects of Overexposure:

No known applicable information.

Other Health Effects:

Long term exposure to high oil mist concentrations may cause non-debilitating lung changes.

Health Hazard Categories:

	Animal	Human		Animal	Human
Known Carcinogen	___	___	Toxic	___	___
Suspect Carcinogen	___	___	Corrosive	___	___
Mutagen	___	___	Irritant	_X_	_X_
Teratogen	___	___	Target Organ Toxin	_X_	_X_
Allergic Sensitizer	___	___	Specify - Lung-Aspiration Hazard		
Highly Toxic	___	___			

First Aid and Emergency Procedures:

Eye: Flush eyes with running water for at least fifteen minutes. If irritation develops, seek medical attention.

Skin: Immediately wash with soap and water for at least fifteen minutes. Seek medical attention.

Inhalation: Remove from exposure. If illness or adverse symptoms develop, seek medical attention.

Ingestion: Do not induce vomiting. Seek immediate medical attention.

Note to Physician: Gastric lavage using a cuffed endotracheal tube may be performed at your discretion.

G. Physical Data

Appearance:	Colorless Liquid
Odor:	Mild, Characteristic
Boiling Point:	370-525F (187-274C)
Vapor Pressure:	0.2 psia (Reid)
Vapor Density (Air = 1):	4.5
Solubility in Water:	Negligible
Specific Gravity (H2O = 1):	0.81-0.82 at 60/60F (16/16C)
Percent Volatile by Volume:	100
Evaporation Rate (Ethyl Ether = 1):	<1
Viscosity:	2.0-2.2 cSt at 25C (77F)

H. Fire and Explosion Data

Flash Point (Method Used):	155-165F (68-74C) (PMCC, ASTM D93)
Flammable Limits (% by Volume in Air):	LEL - 0.7 UEL - 5.0
Fire Extinguishing Media:	Dry chemical, foam, carbon dioxide (CO2)
Special Fire Fighting Procedures:	Evacuate area of all unnecessary personnel. Wear appropriate safety equipment for fire conditions including self-contained breathing apparatus (SCBA) and other equipment and/or garments described in Section C if exposure conditions warrant. Shut off source, if possible. Do not spray water directly on fire product will float and could be reignited on surface of water. Water fog or spray may be used to cool exposed equipment and containers.
Fire and Explosion Hazards:	Carbon oxides and various hydrocarbons are released when burned.

I. Spill, Leak and Disposal Procedures

Precautions Required if Material is Released or Spilled:
Evacuate area of all unnecessary personnel. Wear protective equipment and/or garments described in Section C if exposure conditions warrant. Shut off source, if possible and contain spill. Protect from ignition. Keep out of water sources and sewers. Absorb in dry, inert material. Transfer to disposal containers using non-sparking equipment.

Waste Disposal (Insure Conformity with all Applicable Disposal Regulations):
Incinerate or place in a permitted waste management facility.

J. DOT Transportation

Shipping Name:	Combustible liquid, n.o.s. (Paraffinic and aromatic hydrocarbons)
Hazard Class:	Combustible liquid
ID Number:	NA 1993
Packing Group:	III
Marking:	1993 on Bulk Containers
Label:	None
Placard:	Combustible/1993
Hazardous Substance/RQ:	None
Shipping Description:	Combustible liquid, n.o.s. (Paraffinic and aromatic hydrocarbons), Combustible liquid, NA 1993, PG III
Packaging References:	49 CFR 173.150, 173.203, 173.241

NOTE: The above information is applicable when the product is shipped in containers larger than 119 gallons. If shipped in 119 gallon or smaller containers it is not regulated by the DOT Hazardous Material Regulations.

K. RCRA Classification - Unadulterated Product as a Waste

Prior to disposal, consult your environmental contact to determine if the TCLP (Toxicity Characteristic Leaching Procedure, EPA Test Method 1311) is required. Reference 40 CFR Part 261.

L. Protection Required for Work on Contaminated Equipment

Contact immediate supervisor for specific instructions before work is initiated. Wear protective equipment and/or garments described in Section C if exposure conditions warrant.

M. Hazard Classification

_X_ This product meets the following hazard definition(s) as defined by the Occupational Safety and Health Hazard Communication Standard (29 CFR Section 1910.1200):

_X_ Combustible Liquid	___ Flammable Aerosol	___ Oxidizer
___ Compressed Gas	___ Explosive	___ Pyrophoric
___ Flammable Gas	_X_ Health Hazard (Section F)	___ Unstable
___ Flammable Liquid	___ Organic Peroxide	___ Water Reactive
___ Flammable Solid		

___ Based on information presently available, this product does not meet any of the hazard definitions of 29 CFR Section 1910.1200.

N. Additional Comments

SARA 313

As of the preparation date, this product did not contain a chemical or chemicals subject to the reporting requirements of Section 313 of Title III of the Superfund Amendments and Reauthorization Act of 1986 and 40 CFR Part 372.

Attachment 7 to Table 1

Attachment 7 to Table 1

Response to ADEQ Comment-4.3-Particle Tracking

ADEQ-4.3-Simulation of Mine Block Operations-Several of the figures show stagnation points either very close to the simulated mine block or within the simulated mine block. These figures indicate a potential for fluids to escape containment. BHP should demonstrate that in these scenarios they will still be able to maintain hydraulic control. The department suggests that the small number of particles placed within the injection cells is not sufficient to demonstrate capture throughout the various flow paths. BHP should re-run the particle tracking illustrations with an increased number of particles (say, at least 10).

Particle Tracking

The particle tracking simulations were performed on each of the original model scenarios (Figures 4.3-10 [IV] through 4.3-55 [IV]) using 10 particles. Particles are placed at the injection wells in each layer. Particle capture is attained in all simulations. The particles are either captured at the extraction wells in the same layer or one of the layers below. All scenarios were simulated with 25-percent overpumping at the perimeter wells, with the exception of simulation scenario 4a. In order to achieve capture of all particles in this scenario, the scenario was run with 35-percent overpumping at the perimeter wells. The revised figures showing 10 particles (Figures 1 through 36) and an abbreviated sample Path3D output file, showing progress of each particle through each layer during the last time step, are included. Table 1 shows a summary of the distribution of particles released in each layer and the layer captured for each scenario.

The results of the particle tracking show that hydraulic control of the mine solutions can be achieved by over pumping the perimeter recovery wells. Weak hydraulic gradients are observed on the downgradient (northwestern) boundary of the mine block that result in extended particle traces. In the proposed operation, hydraulic control will be based on the inward gradients between the mine block observation wells and the perimeter recovery wells. Therefore, the adjusted pumping rates may be higher in the northwestern section (downgradient) perimeter recovery wells to increase the hydraulic gradient where there is a greater potential for excursion.

Table 1 - Attachment 7 to Table 1. Particle Summary							
		Particles Captured					
Model Layer	Particles Released	Simulation Scenario 1	Simulation Scenario 2	Simulation Scenario 3	Simulation Scenario 4a	Simulation Scenario 4b	Simulation Scenario 4c
Layer 1	0	0	0	0	0	0	0
Layer 2	0	0	0	0	0	0	0
Layer 3	50	51	51	51	54	50	52
Layer 4	110	93	93	89	105	99	97
Layer 5	220	237	237	240	211	209	224
Layer 6	280	279	279	278	287	300	285
Layer 7	280	280	280	282	283	282	282
Layer 8	90	90	90	90	90	90	90
Total	1030	1030	1030	1030	1030	1030	1030
% Captured		100	100	100	100	100	100

NOTE:
Table generated from Path3D output files.

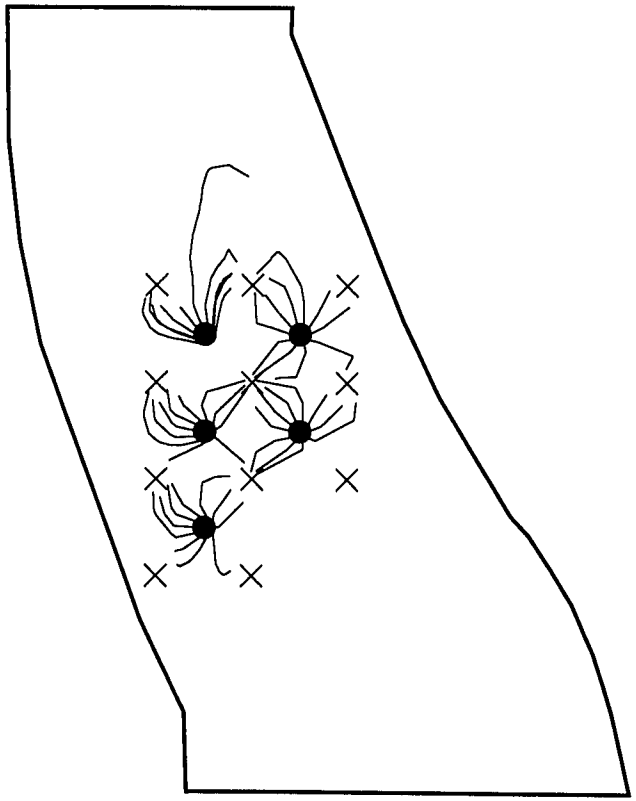

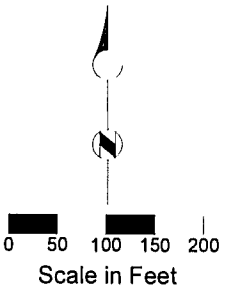

INJECTION WELL

RECOVERY WELL

PARTICLE TRACE FROM POINT OF INJECTION TO POINT OF CAPTURE

Particle trace output files show all particles not captured in this layer are captured in other layers

Figure 1 - Attachment 7 to Table 1
PARTICLE TRACKING
SIMULATION SCENARIO 1
BASE CONDITIONS
MODEL LAYER 3

BROWN AND CALDWELL

BHP COPPER *Florence Project*

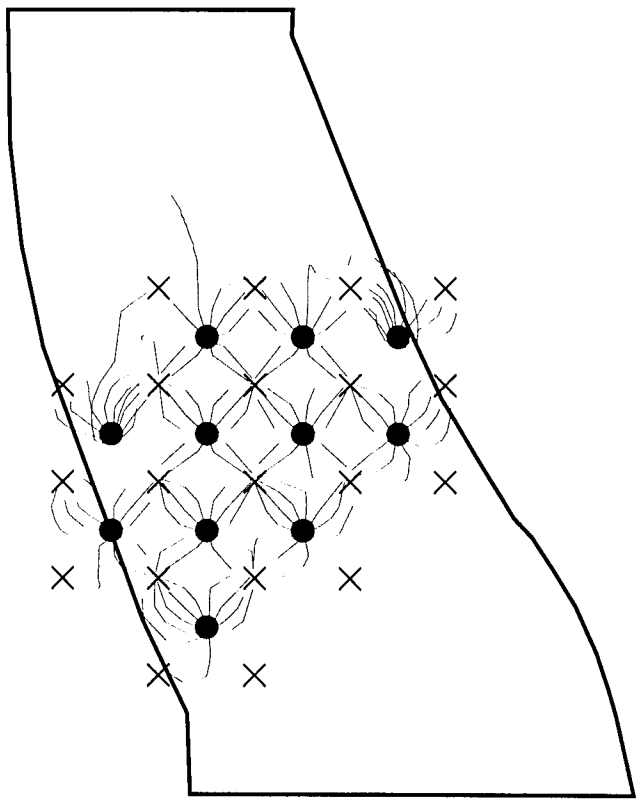

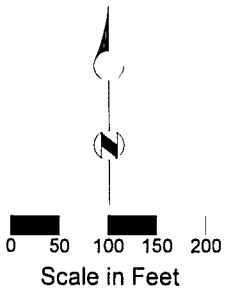

INJECTION WELL

RECOVERY WELL

PARTICLE TRACE FROM POINT OF INJECTION TO POINT OF CAPTURE

Particle trace output files show all particles not captured in this layer are captured in other layers

Figure 2 - Attachment 7 to Table 1
PARTICLE TRACKING
SIMULATION SCENARIO 1
BASE CONDITIONS
MODEL LAYER 4

BHP

BHP COPPER *Florence Project*

BROWN AND CALDWELL

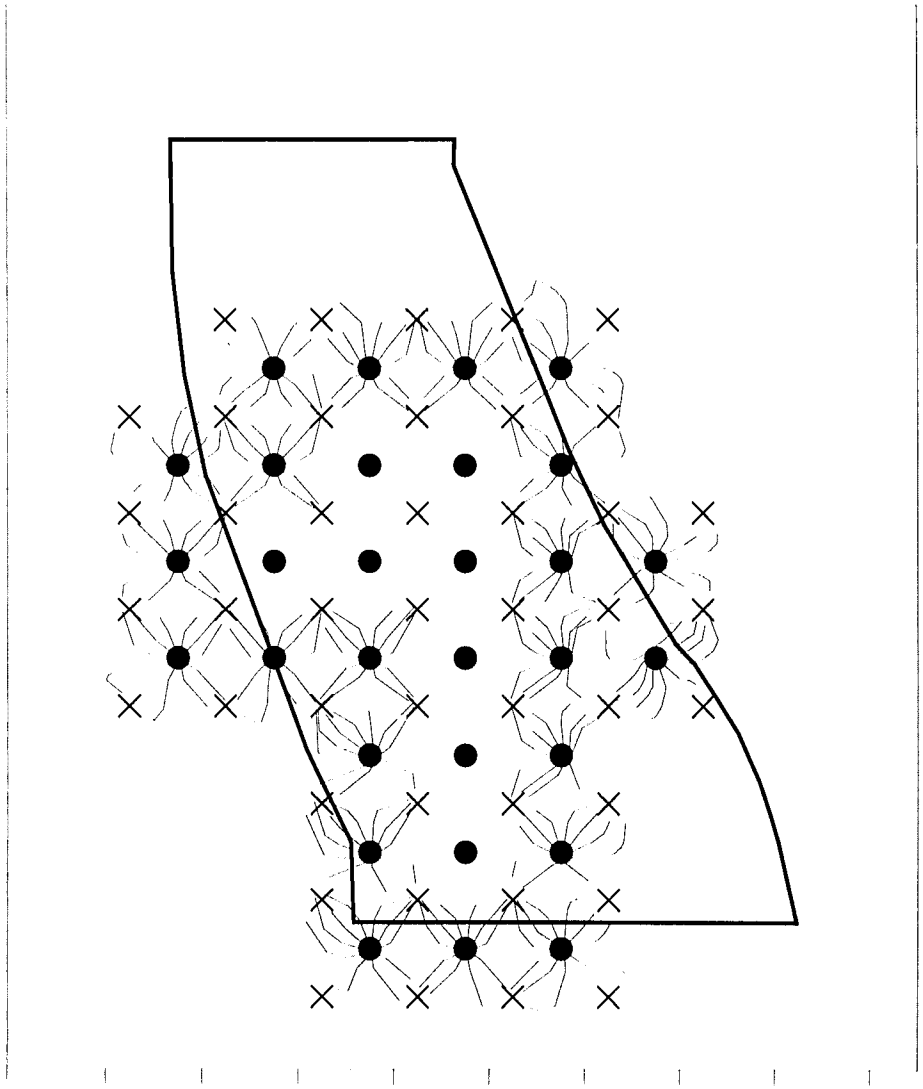

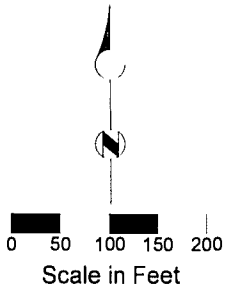

INJECTION WELL

RECOVERY WELL

PARTICLE TRACE FROM POINT OF INJECTION TO POINT OF CAPTURE

Particle trace output files show all particles not captured in this layer are captured in other layers

Figure 3 - Attachment 7 to Table 1
PARTICLE TRACKING
SIMULATION SCENARIO 1
BASE CONDITIONS
MODEL LAYER 5

BHP

BHP COPPER *Florence Project*

BROWN AND CALDWELL

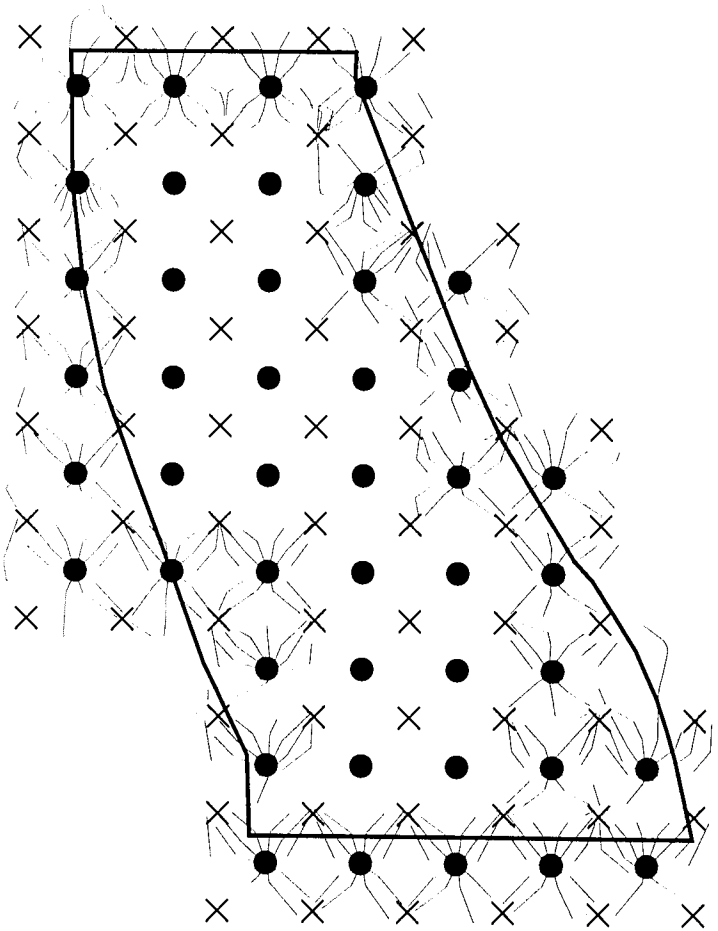

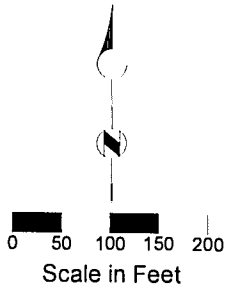

INJECTION WELL

RECOVERY WELL

PARTICLE TRACE FROM POINT OF INJECTION TO POINT OF CAPTURE

Particle trace output files show all particles not captured in this layer are captured in other layers

Figure 4 - Attachment 7 to Table 1
PARTICLE TRACKING
SIMULATION SCENARIO 1
BASE CONDITIONS
MODEL LAYER 6

BROWN AND CALDWELL

BHP

BHP COPPER *Florence Project*

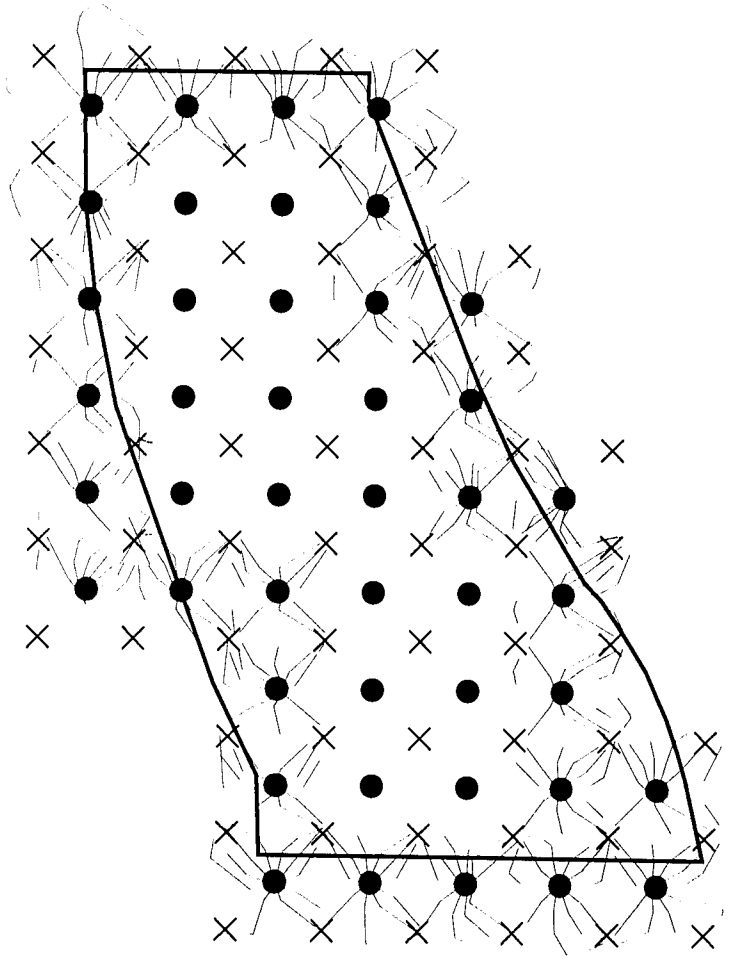

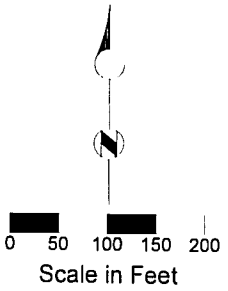

INJECTION WELL

RECOVERY WELL

PARTICLE TRACE FROM POINT OF INJECTION TO POINT OF CAPTURE

Particle trace output files show all particles not captured in this layer are captured in other layers

Figure 5 - Attachment 7 to Table 1
PARTICLE TRACKING
SIMULATION SCENARIO 1
BASE CONDITIONS
MODEL LAYER 7

BROWN AND CALDWELL

BHP

BHP COPPER *Florence Project*

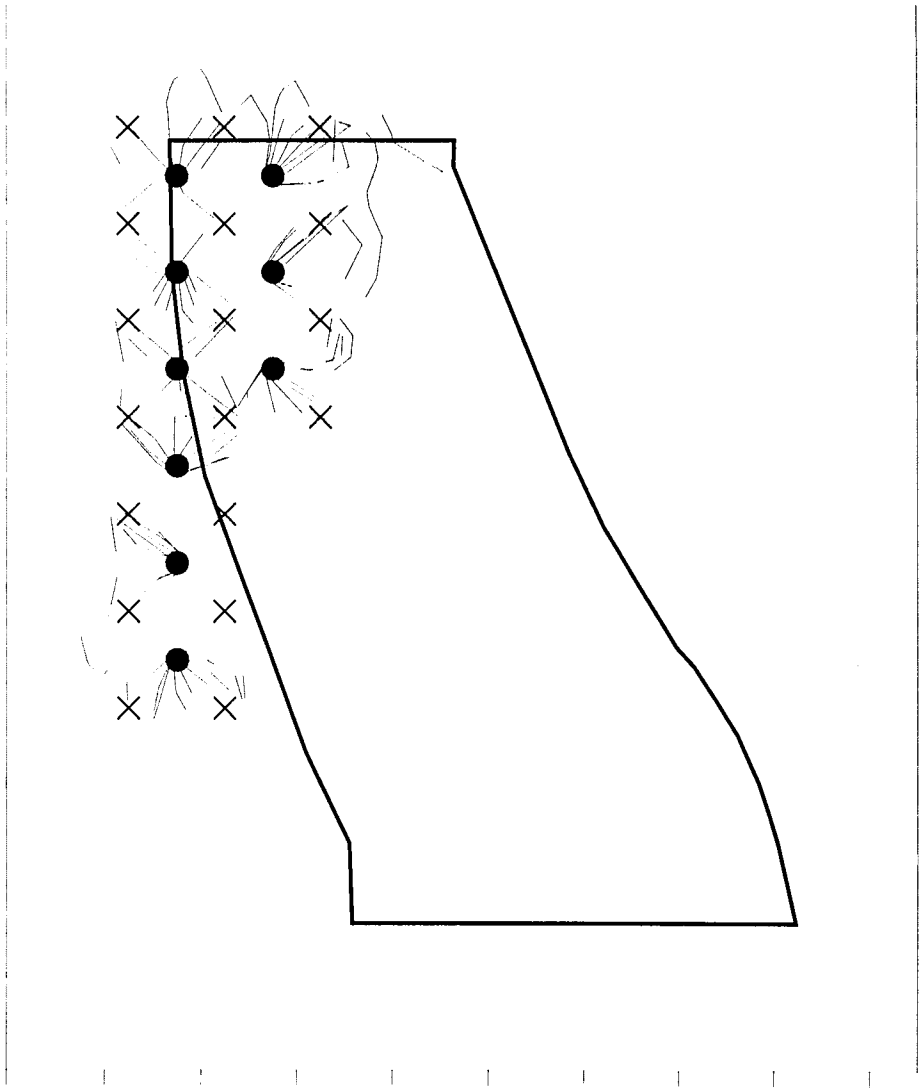

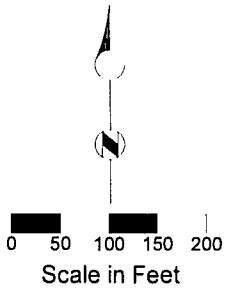

INJECTION WELL

RECOVERY WELL

PARTICLE TRACE FROM POINT OF INJECTION TO POINT OF CAPTURE

Particle trace output files show all particles not captured in this layer are captured in other layers

Figure 6 - Attachment 7 to Table 1
PARTICLE TRACKING SIMULATION SCENARIO 1
BASE CONDITIONS
MODEL LAYER 8

BHP

BHP COPPER *Florence Project*

BROWN AND CALDWELL

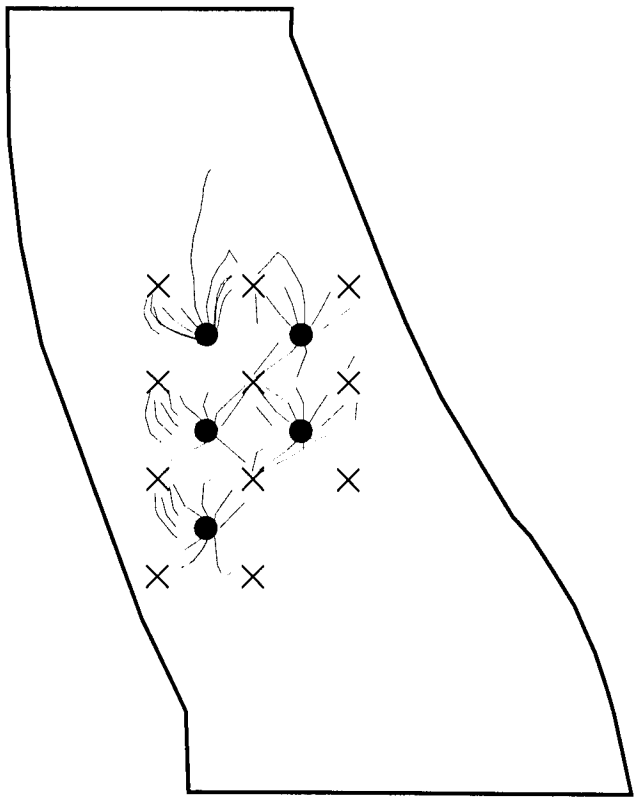

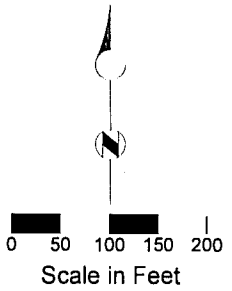

INJECTION WELL

RECOVERY WELL

PARTICLE TRACE FROM POINT OF INJECTION TO POINT OF CAPTURE

Particle trace output files show all particles not captured in this layer are captured in other layers

Figure 7 - Attachment 7 to Table 1
PARTICLE TRACKING SIMULATION SCENARIO 2 INCREASED WITHDRAWAL MODEL LAYER 3

BHP COPPER *Florence Project*

BROWN AND CALDWELL

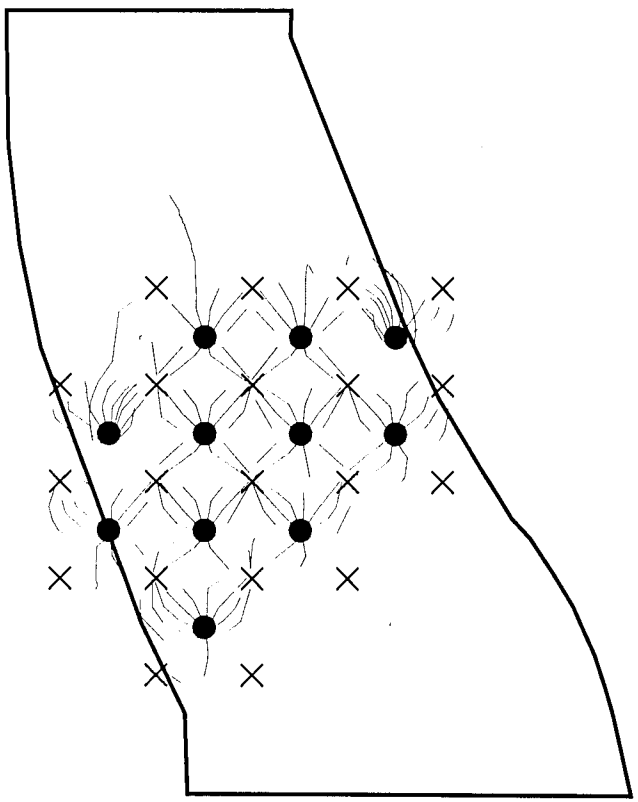

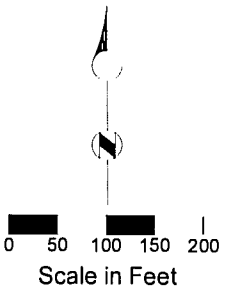

INJECTION WELL

RECOVERY WELL

PARTICLE TRACE FROM POINT OF INJECTION TO POINT OF CAPTURE

Particle trace output files show all particles not captured in this layer are captured in other layers

Figure 8 - Attachment 7 to Table 1
PARTICLE TRACKING
SIMULATION SCENARIO 2
INCREASED WITHDRAWAL
MODEL LAYER 4

BHP

BHP COPPER *Florence Project*

BROWN AND CALDWELL

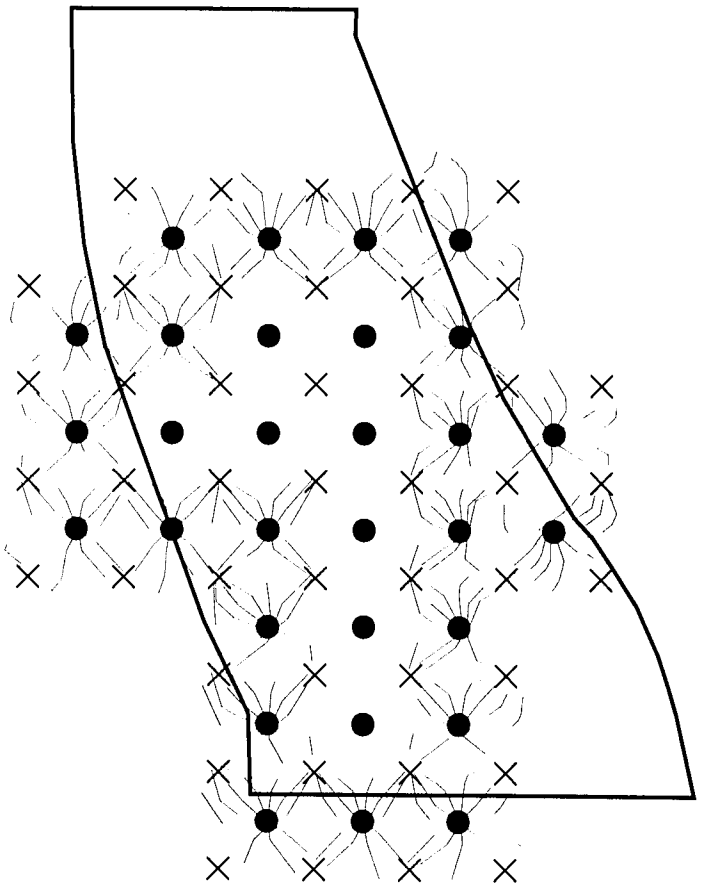

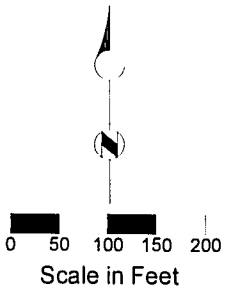

INJECTION WELL

RECOVERY WELL

PARTICLE TRACE FROM POINT OF INJECTION TO POINT OF CAPTURE

Particle trace output files show all particles not captured in this layer are captured in other layers

Figure 9 - Attachment 7 to Table 1
PARTICLE TRACKING SIMULATION SCENARIO 2 INCREASED WITHDRAWAL MODEL LAYER 5

BHP
BHP COPPER *Florence Project*

BROWN AND CALDWELL

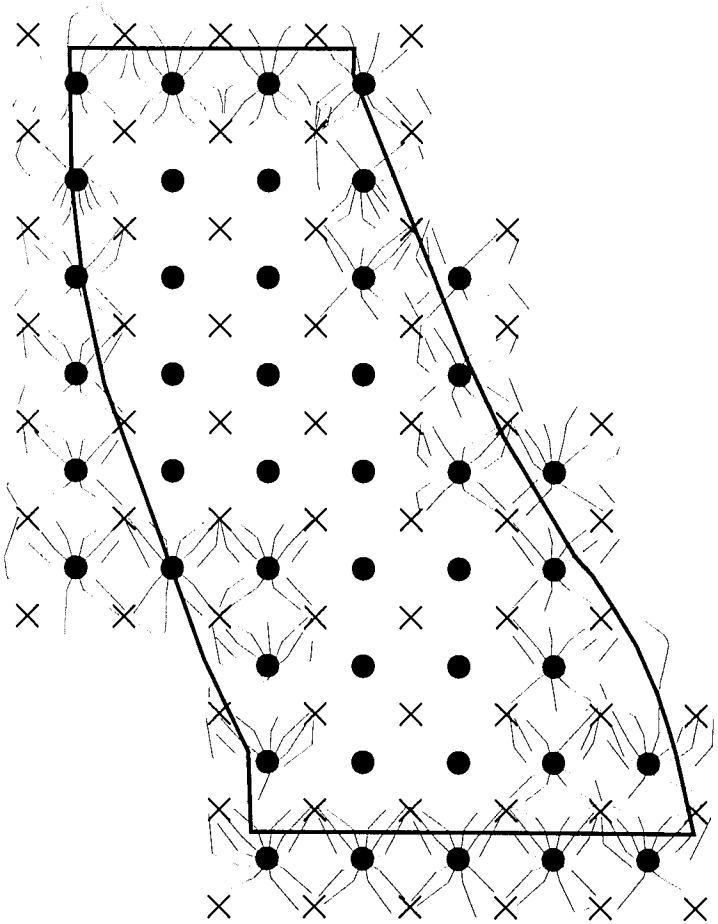

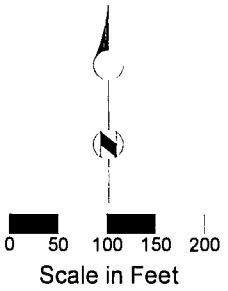

INJECTION WELL

RECOVERY WELL

PARTICLE TRACE FROM POINT OF INJECTION TO POINT OF CAPTURE

Particle trace output files show all particles not captured in this layer are captured in other layers

Figure 10 - Attachment 7 to Table 1
PARTICLE TRACKING SIMULATION SCENARIO 2
INCREASED WITHDRAWAL
MODEL LAYER 6

BHP
BHP COPPER *Florence Project*

BROWN AND CALDWELL

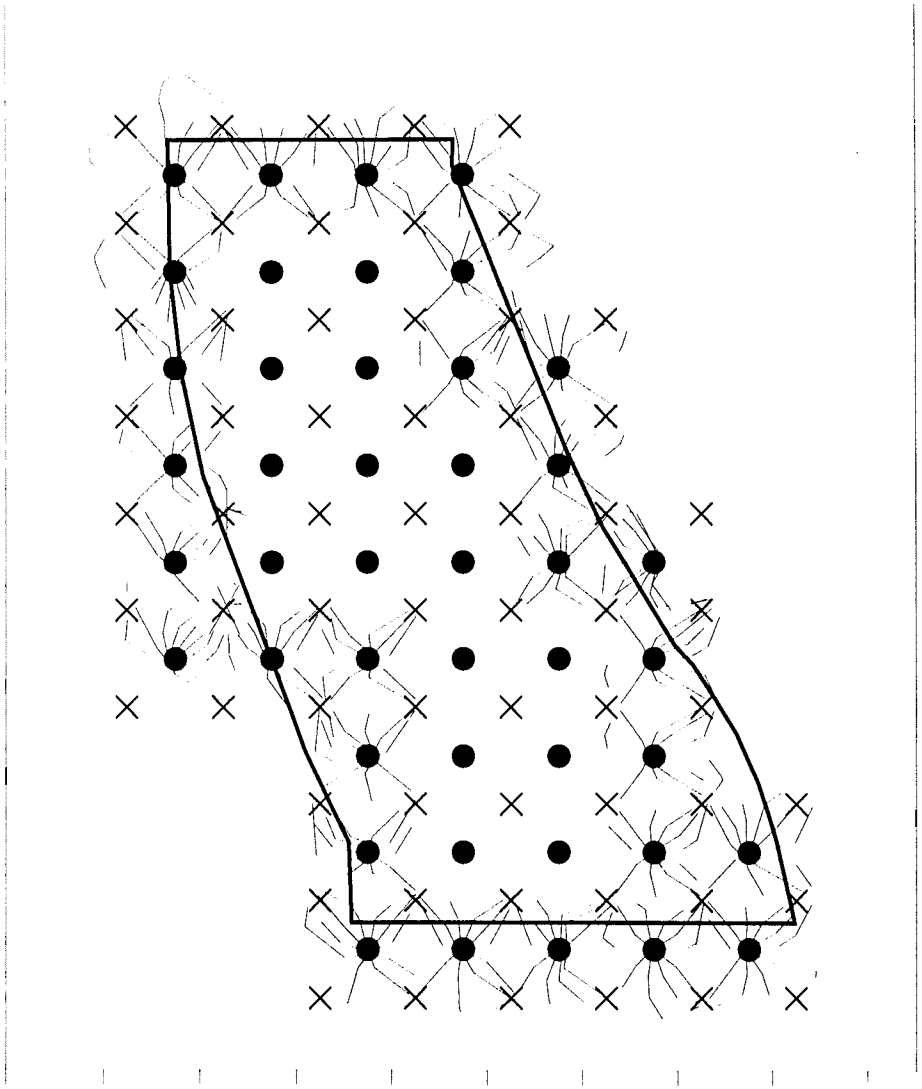

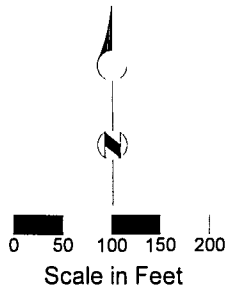

INJECTION WELL

RECOVERY WELL

PARTICLE TRACE FROM POINT OF INJECTION TO POINT OF CAPTURE

Particle trace output files show all particles not captured in this layer are captured in other layers

Figure 11 - Attachment 7 to Table 1
PARTICLE TRACKING SIMULATION SCENARIO 2 INCREASED WITHDRAWAL MODEL LAYER 7

BHP

BHP COPPER *Florence Project*

BROWN AND CALDWELL

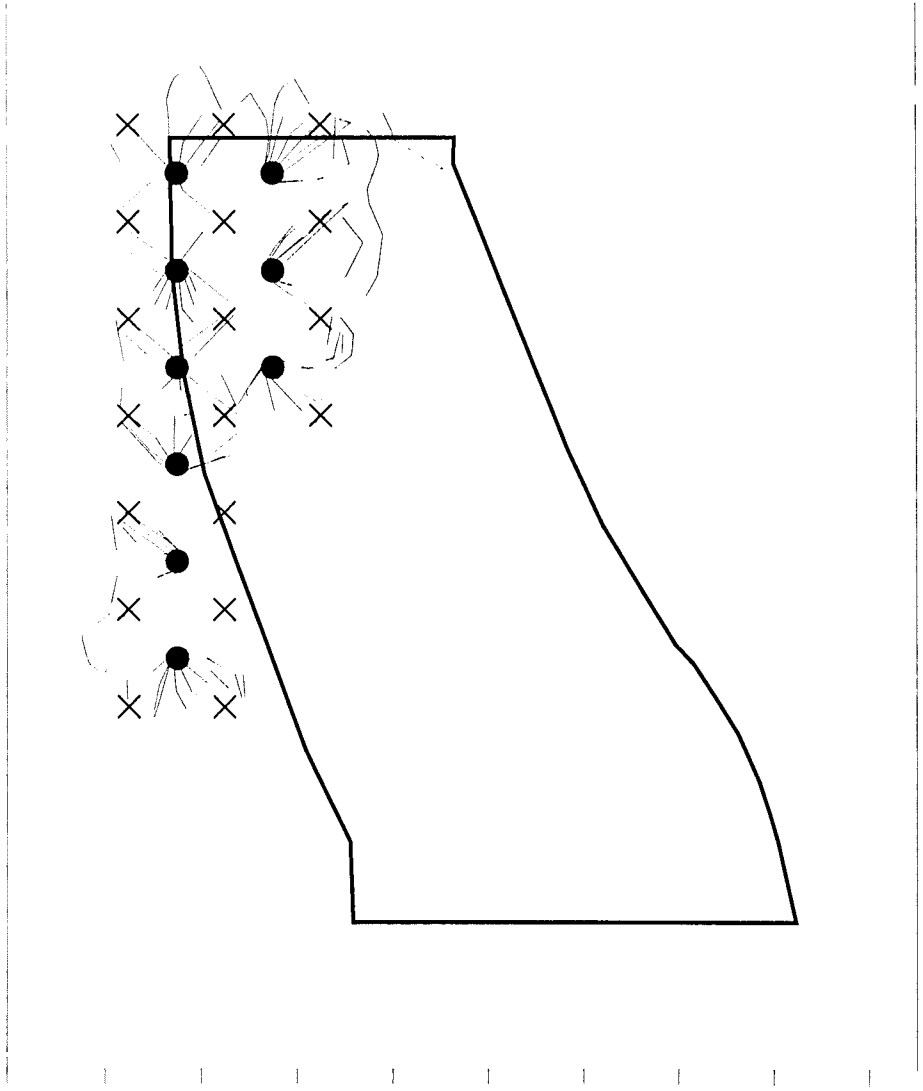

0 50 100 150 200
Scale in Feet

INJECTION WELL

RECOVERY WELL

PARTICLE TRACE FROM POINT OF INJECTION TO POINT OF CAPTURE

Particle trace output files show all particles not captured in this layer are captured in other layers

Figure 12 - Attachment 7 to Table 1
PARTICLE TRACKING
SIMULATION SCENARIO 2
INCREASED WITHDRAWAL
MODEL LAYER 8

BHP COPPER *Florence Project*

BROWN AND CALDWELL

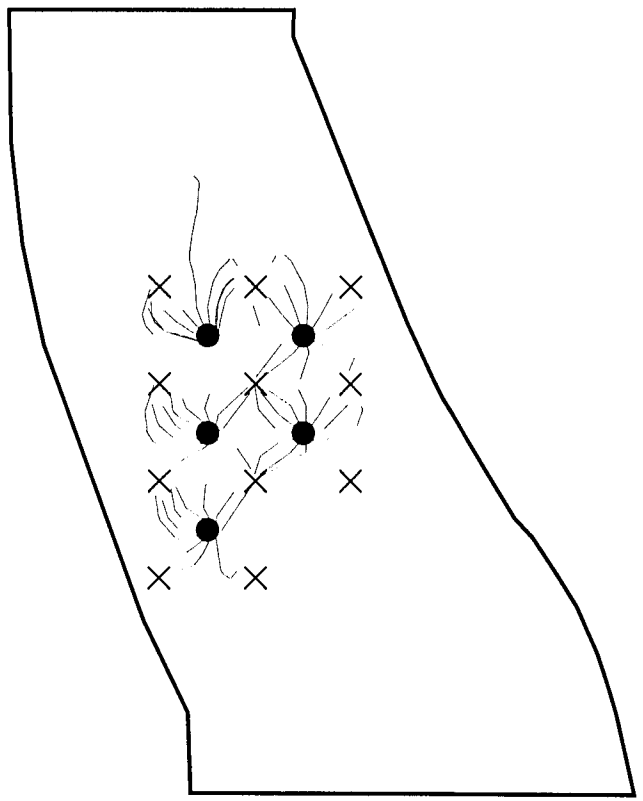

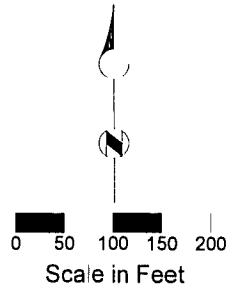

INJECTION WELL

RECOVERY WELL

PARTICLE TRACE FROM POINT OF INJECTION TO POINT OF CAPTURE

Particle trace output files show all particles not captured in this layer are captured in other layers

Figure 13 - Attachment 7 to Table 1
PARTICLE TRACKING SIMULATION SCENARIO 3
INCREASED RECHARGE
MODEL LAYER 3

BROWN AND CALDWELL

BHP COPPER *Florence Project*

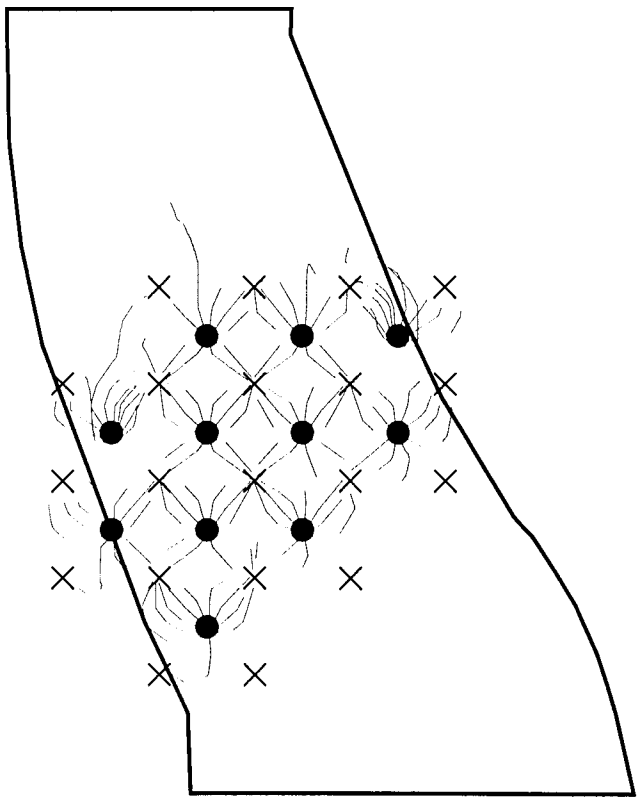

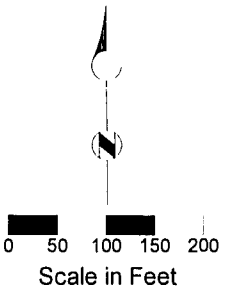

INJECTION WELL

RECOVERY WELL

PARTICLE TRACE FROM POINT OF INJECTION TO POINT OF CAPTURE

Particle trace output files show all particles not captured in this layer are captured in other layers

Figure 14 - Attachment 7 to Table 1
PARTICLE TRACKING
SIMULATION SCENARIO 3
INCREASED RECHARGE
MODEL LAYER 4

BHP

BHP COPPER *Florence Project*

BROWN AND CALDWELL

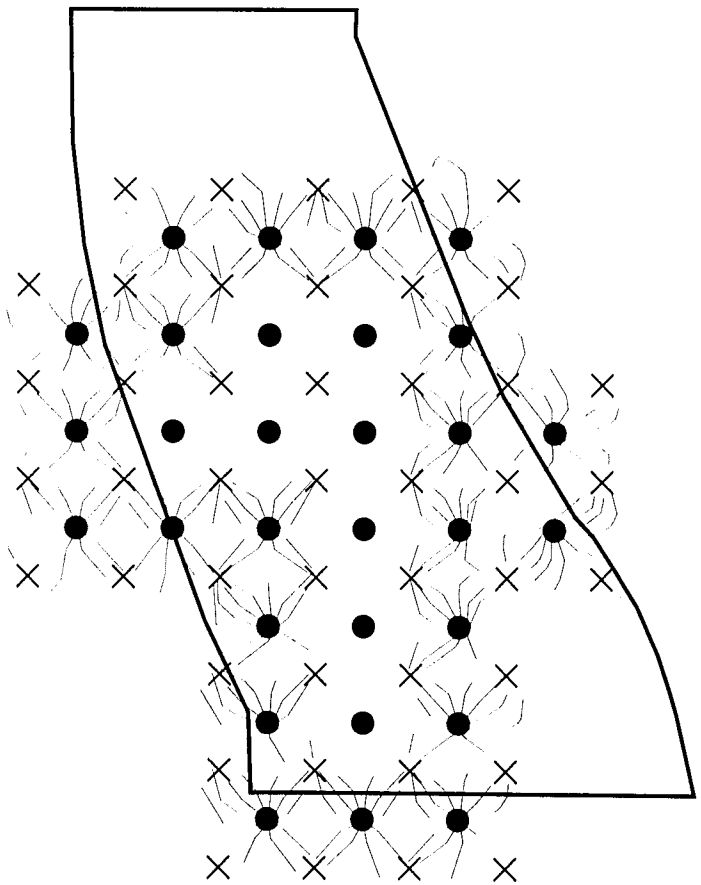

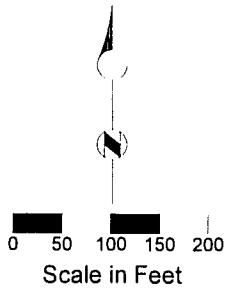

INJECTION WELL

RECOVERY WELL

PARTICLE TRACE FROM POINT OF INJECTION TO POINT OF CAPTURE

Particle trace output files show all particles not captured in this layer are captured in other layers

Figure 15 - Attachment 7 to Table 1
PARTICLE TRACKING
SIMULATION SCENARIO 3
INCREASED RECHARGE
MODEL LAYER 5

BROWN AND CALDWELL

BHP

BHP COPPER *Florence Project*

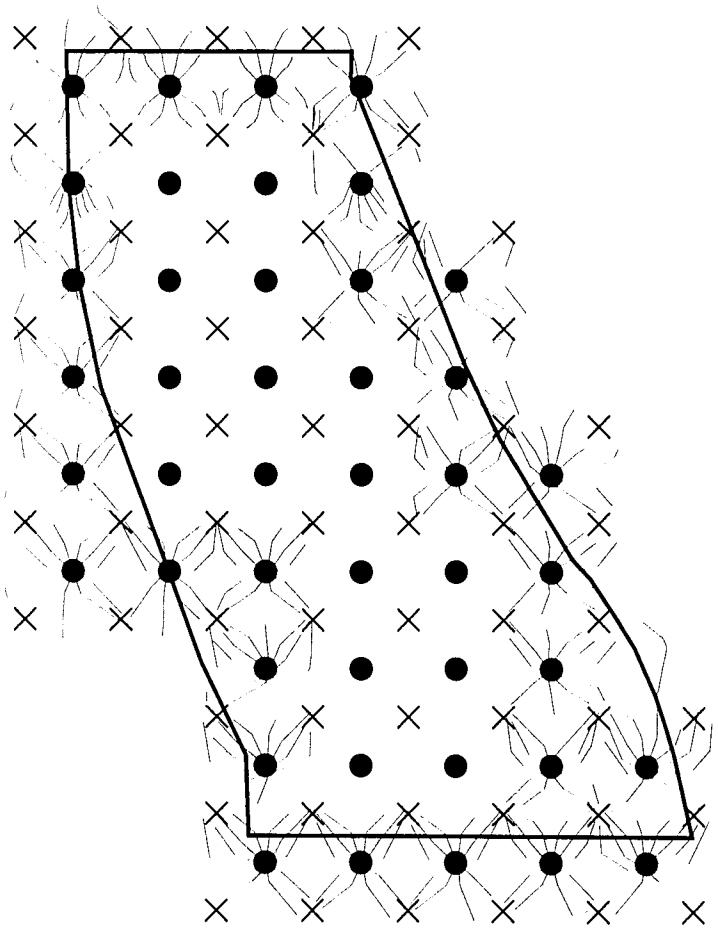

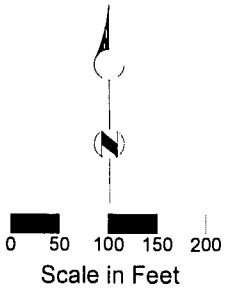

INJECTION WELL

RECOVERY WELL

PARTICLE TRACE FROM POINT OF INJECTION TO POINT OF CAPTURE

Particle trace output files show all particles not captured in this layer are captured in other layers

Figure 16 - Attachment 7 to Table 1
PARTICLE TRACKING SIMULATION SCENARIO 3
INCREASED RECHARGE
MODEL LAYER 6

BHP
BHP COPPER *Florence Project*

BROWN AND CALDWELL

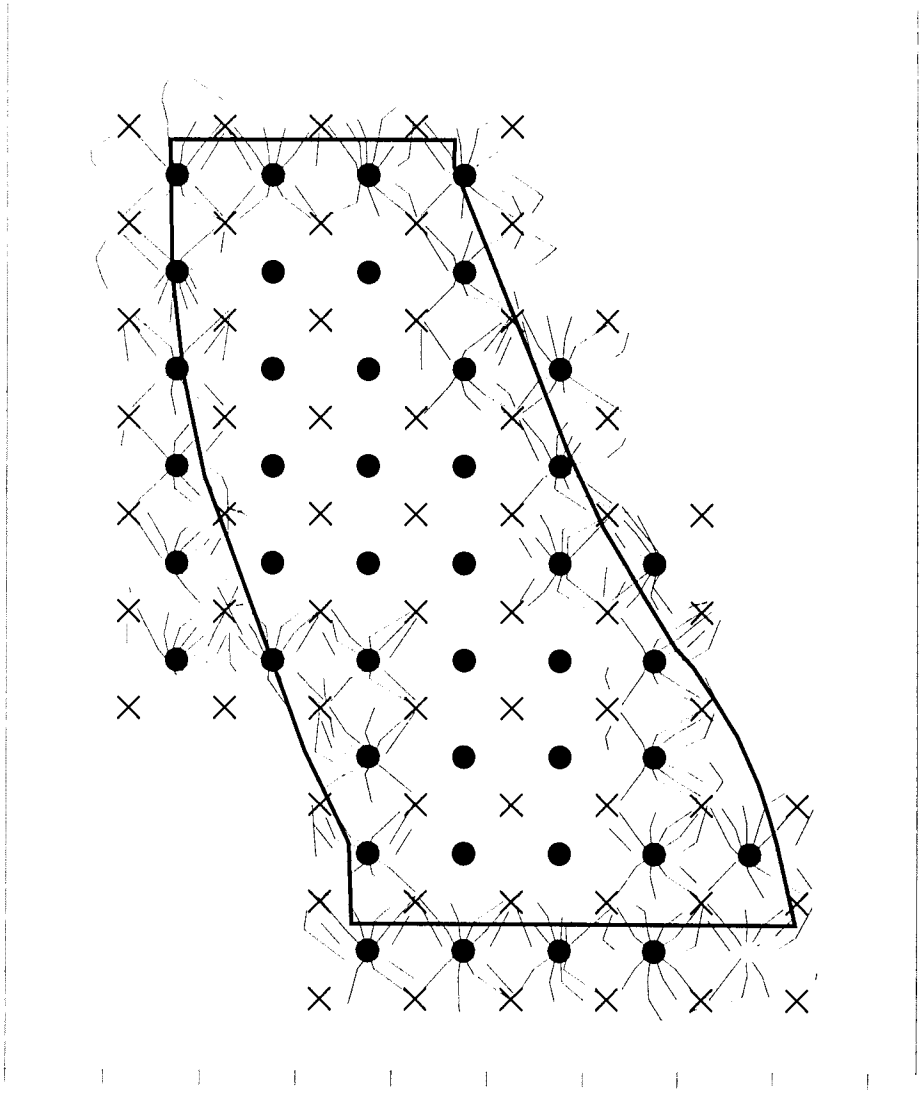

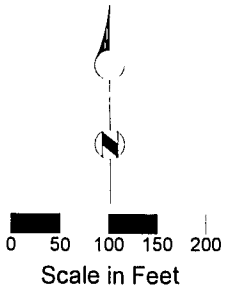

INJECTION WELL

RECOVERY WELL

PARTICLE TRACE FROM POINT OF INJECTION TO POINT OF CAPTURE

Particle trace output files show all particles not captured in this layer are captured in other layers

Figure 17 - Attachment 7 to Table 1
PARTICLE TRACKING
SIMULATION SCENARIO 3
INCREASED RECHARGE
MODEL LAYER 7

BROWN AND CALDWELL

BHP

BHP COPPER *Florence Project*

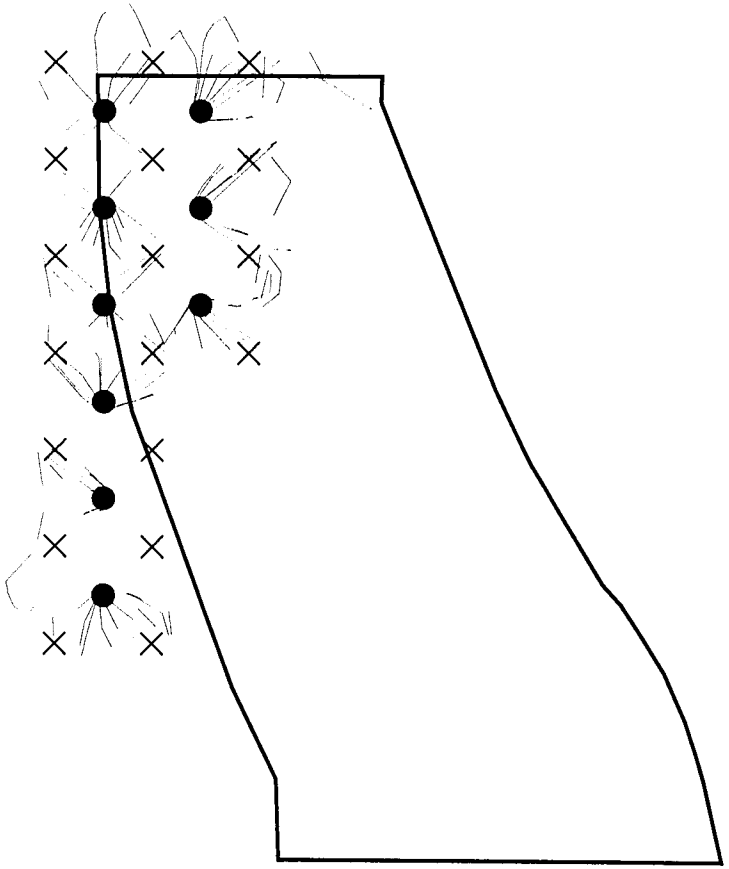

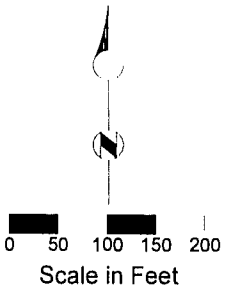

INJECTION WELL

RECOVERY WELL

PARTICLE TRACE FROM POINT OF INJECTION TO POINT OF CAPTURE

Particle trace output files show all particles not captured in this layer are captured in other layers

Figure 18 - Attachment 7 to Table 1
PARTICLE TRACKING
SIMULATION SCENARIO 3
INCREASED RECHARGE
MODEL LAYER 8

BHP

BHP COPPER *Florence Project*

BROWN AND CALDWELL

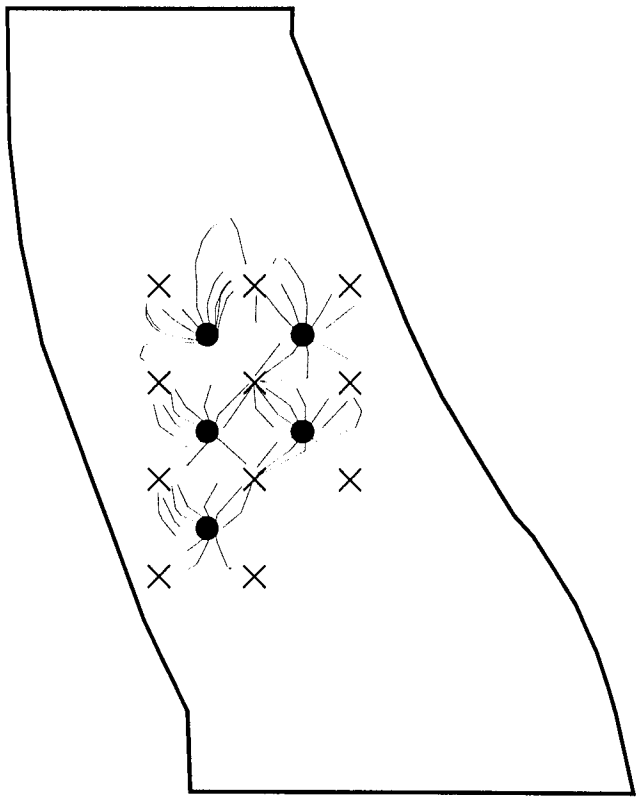

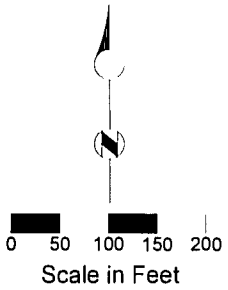

INJECTION WELL

RECOVERY WELL

PARTICLE TRACE FROM POINT OF INJECTION TO POINT OF CAPTURE

Particle trace output files show all particles not captured in this layer are captured in other layers

Figure 19 - Attachment 7 to Table 1
PARTICLE TRACKING SIMULATION SCENARIO 4a
PREFERENTIAL PATHWAY IN MODEL LAYER 5
MODEL LAYER 3

BHP

BHP COPPER *Florence Project*

BROWN AND CALDWELL

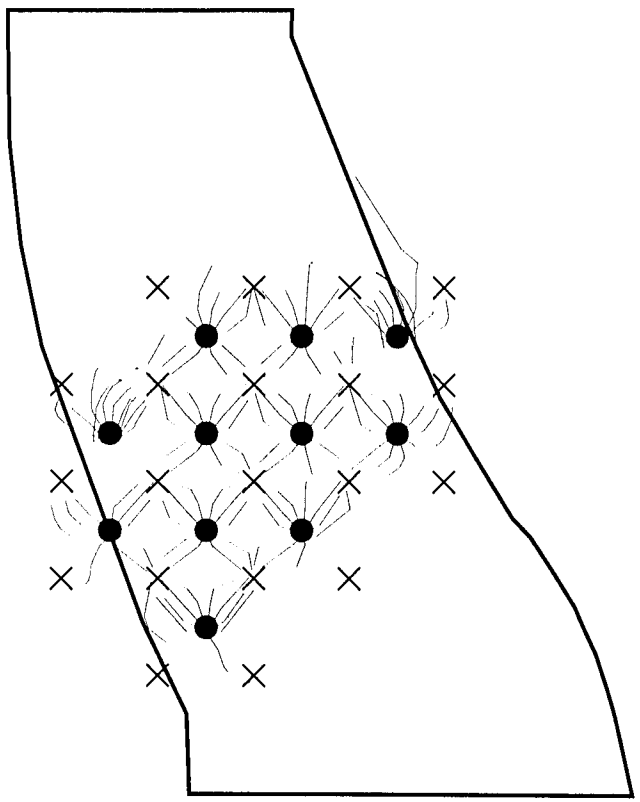

0 50 100 150 200
Scale in Feet

INJECTION WELL

RECOVERY WELL

PARTICLE TRACE FROM POINT OF INJECTION TO POINT OF CAPTURE

Particle trace output files show all particles not captured in this layer are captured in other layers

Figure 20 - Attachment 7 to Table 1
PARTICLE TRACKING SIMULATION SCENARIO 4a
PREFERENTIAL PATHWAY IN MODEL LAYER 5
MODEL LAYER 4

BROWN AND CALDWELL

BHP COPPER *Florence Project*

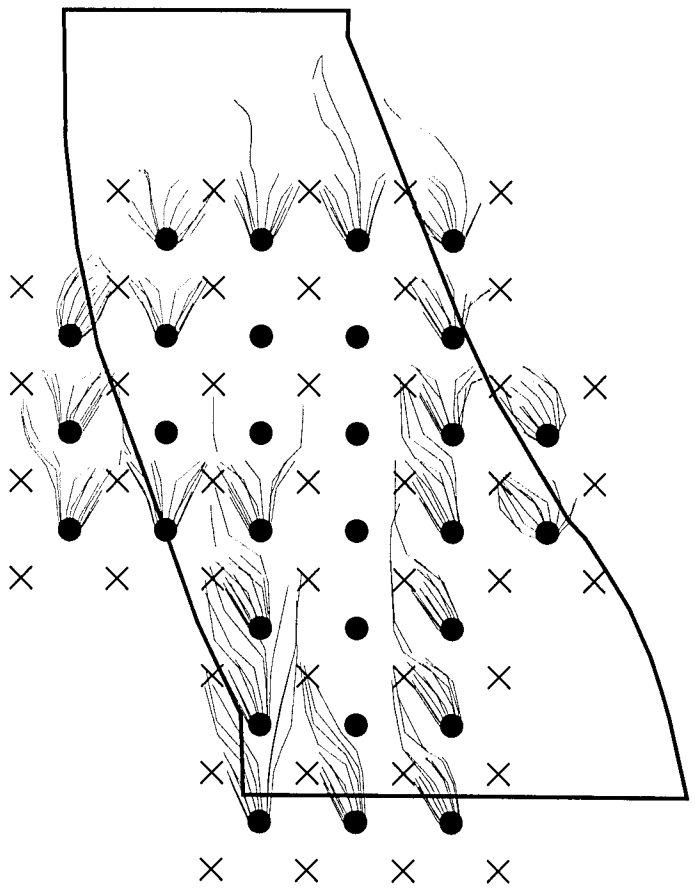

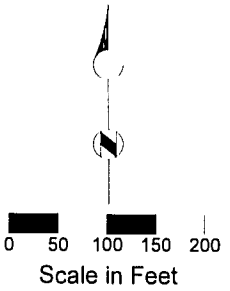

INJECTION WELL

RECOVERY WELL

PARTICLE TRACE FROM POINT OF INJECTION TO POINT OF CAPTURE

Particle trace output files show all particles not captured in this layer are captured in other layers

Figure 21 - Attachment 7 to Table 1
PARTICLE TRACKING SIMULATION SCENARIO 4a
PREFERENTIAL PATHWAY IN MODEL LAYER 5
MODEL LAYER 5

BROWN AND CALDWELL

BHP

BHP COPPER *Florence Project*

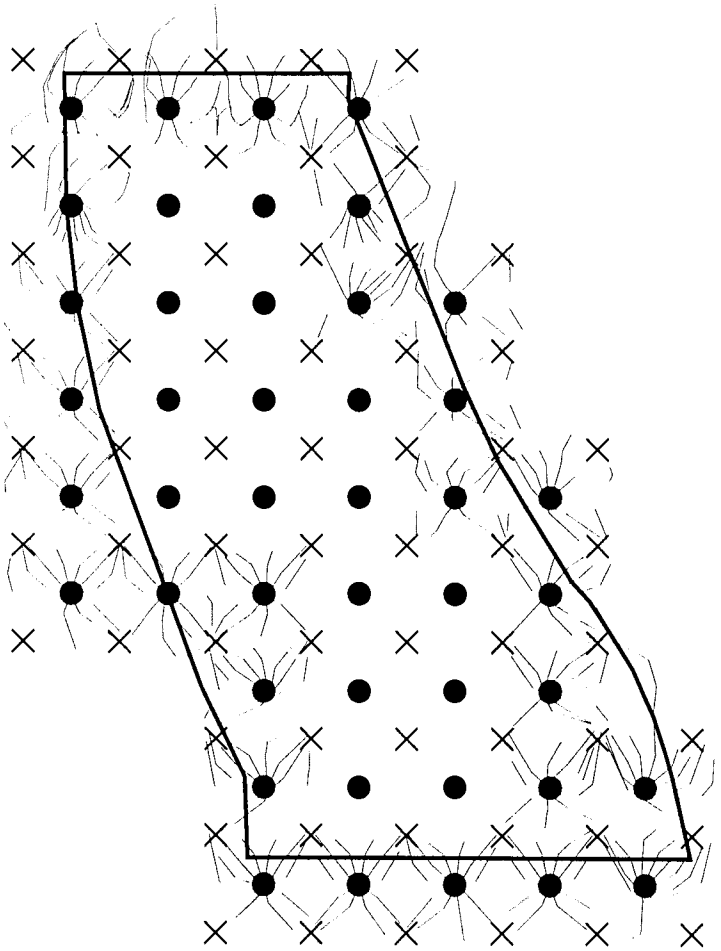

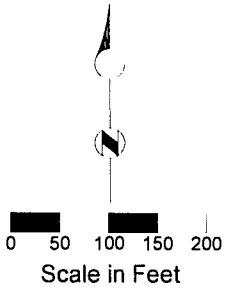

INJECTION WELL

RECOVERY WELL

PARTICLE TRACE FROM POINT OF INJECTION TO POINT OF CAPTURE

Particle trace output files show all particles not captured in this layer are captured in other layers

Figure 22 - Attachment 7 to Table 1
PARTICLE TRACKING SIMULATION SCENARIO 4a
PREFERENTIAL PATHWAY
IN MODEL LAYER 5
MODEL LAYER 6

BHP

BHP COPPER *Florence Project*

BROWN AND CALDWELL

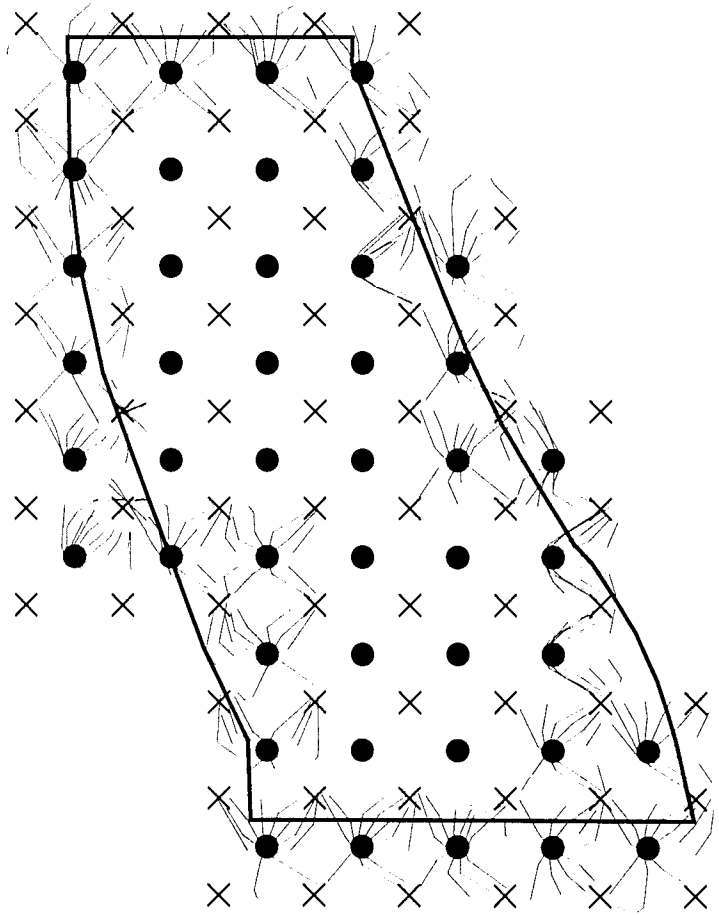

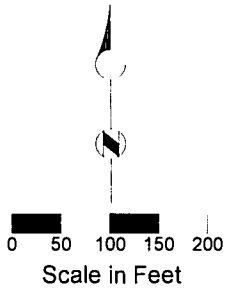

INJECTION WELL

RECOVERY WELL

PARTICLE TRACE FROM POINT OF INJECTION TO POINT OF CAPTURE

Particle trace output files show all particles not captured in this layer are captured in other layers

Figure 23 - Attachment 7 to Table 1
PARTICLE TRACKING SIMULATION SCENARIO 4a
PREFERENTIAL PATHWAY
IN MODEL LAYER 5
MODEL LAYER 7

BHP

BHP COPPER *Florence Project*

BROWN AND CALDWELL

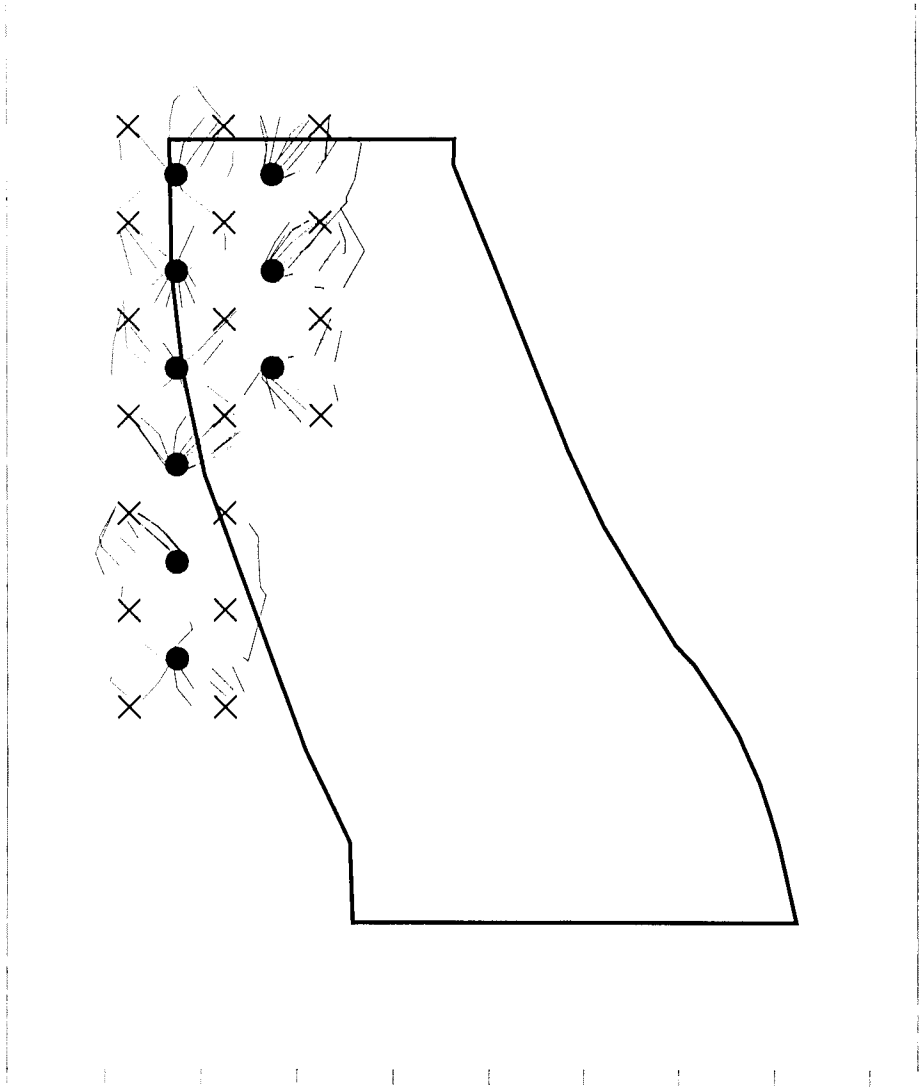

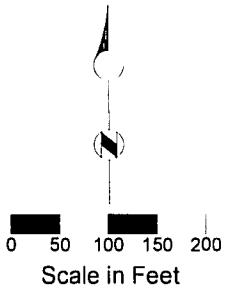

INJECTION WELL

RECOVERY WELL

PARTICLE TRACE FROM POINT OF INJECTION TO POINT OF CAPTURE

Particle trace output files show all particles not captured in this layer are captured in other layers

Figure 24 - Attachment 7 to Table 1
PARTICLE TRACKING SIMULATION SCENARIO 4a
PREFERENTIAL PATHWAY IN MODEL LAYER 5
MODEL LAYER 8

BHP

BHP COPPER *Florence Project*

BROWN AND CALDWELL

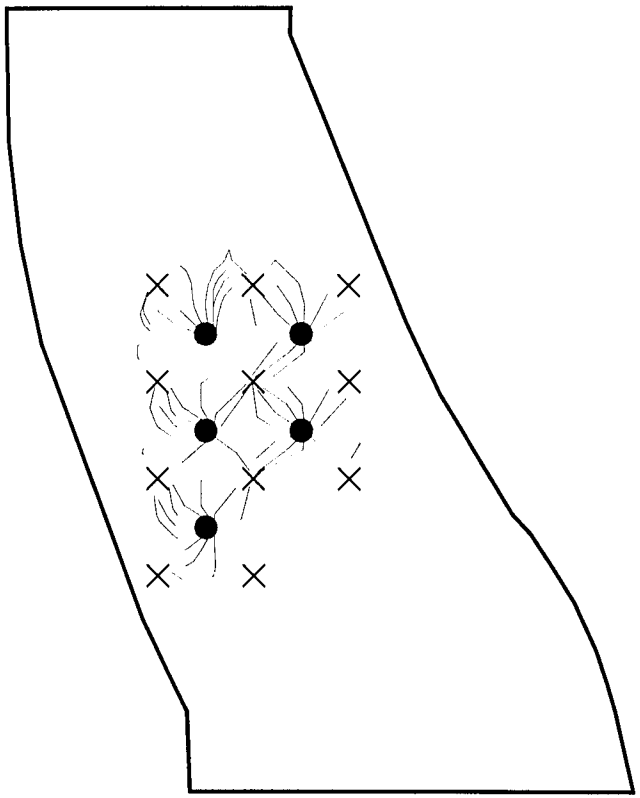

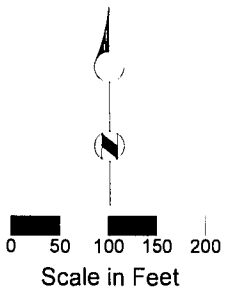

INJECTION WELL

RECOVERY WELL

PARTICLE TRACE FROM POINT OF INJECTION TO POINT OF CAPTURE

Particle trace output files show all particles not captured in this layer are captured in other layers

Figure25 - Attachment 7 to Table 1
PARTICLE TRACKING SIMULATION SCENARIO 4B NORTH-SOUTH ANISOTROPY IN MODEL LAYER 5 MODEL LAYER 3

BHP COPPER *Florence Project*

BROWN AND CALDWELL

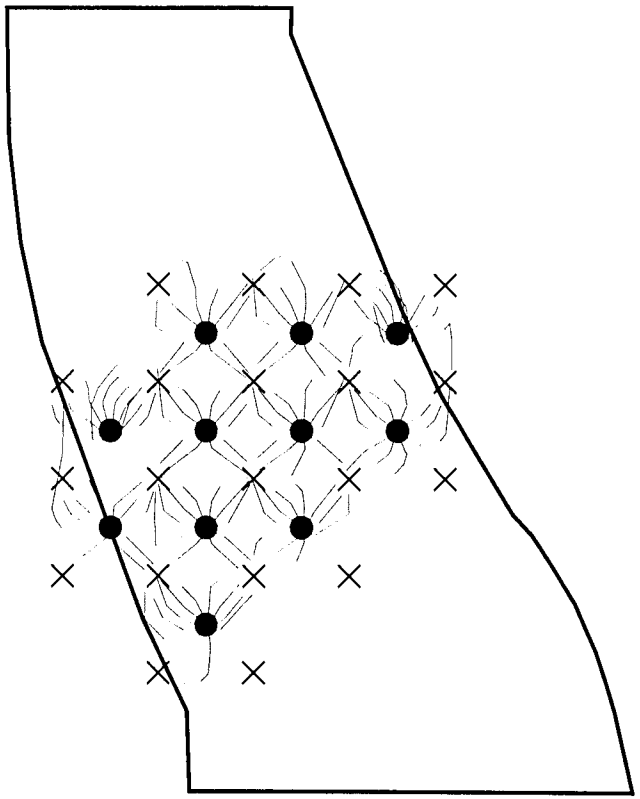

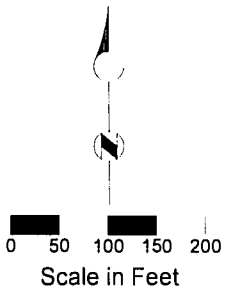

● INJECTION WELL

× RECOVERY WELL

PARTICLE TRACE FROM POINT OF INJECTION TO POINT OF CAPTURE

Particle trace output files show all particles not captured in this layer are captured in other layers

Figure 26 - Attachment 7 to Table 1
PARTICLE TRACKING SIMULATION SCENARIO 4B
NORTH-SOUTH ANISOTROPY IN MODEL LAYER 5
MODEL LAYER 4

BROWN AND CALDWELL

BHP

BHP COPPER *Florence Project*

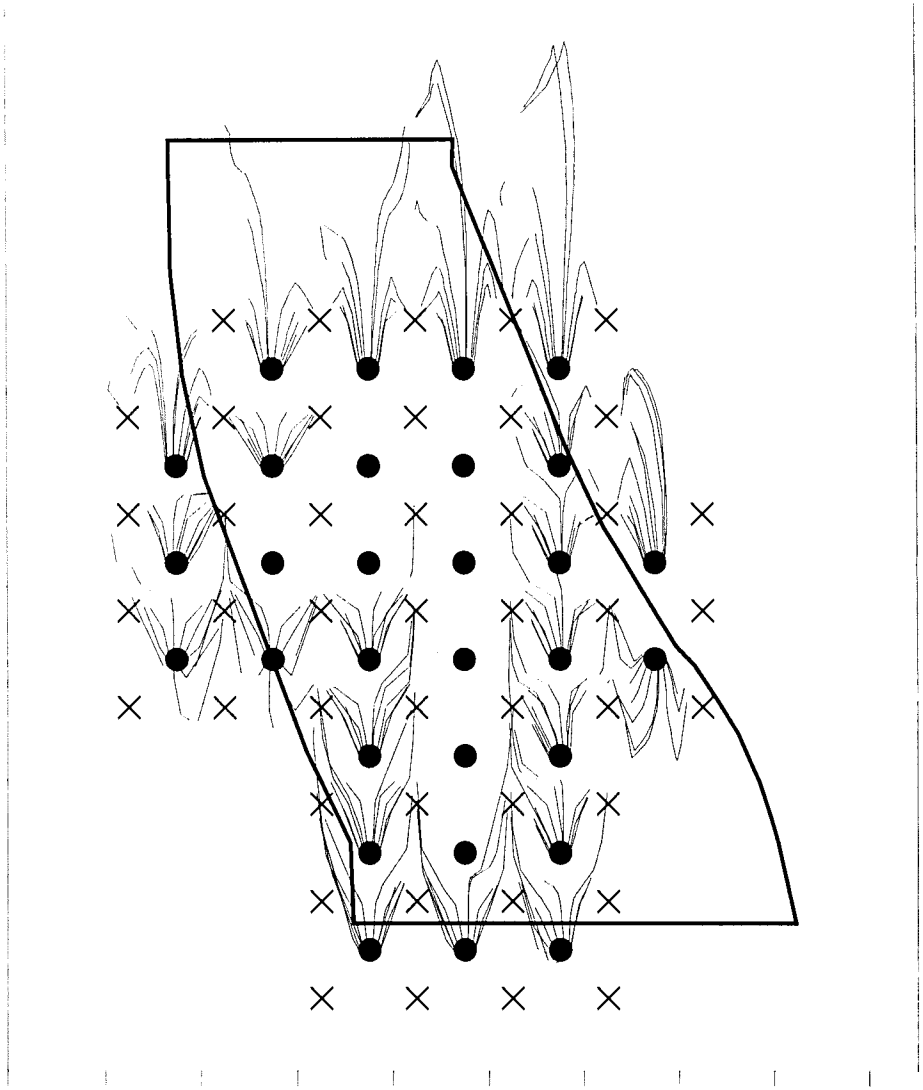

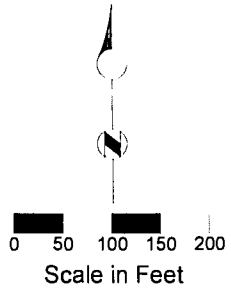

INJECTION WELL

RECOVERY WELL

PARTICLE TRACE FROM POINT OF INJECTION TO POINT OF CAPTURE

Particle trace output files show all particles not captured in this layer are captured in other layers

Figure 27 - Attachment 7 to Table 1
PARTICLE TRACKING
SIMULATION SCENARIO 4B
NORTH-SOUTH ANISOTROPY
IN MODEL LAYER 5
MODEL LAYER 5

BHP

BHP COPPER *Florence Project*

BROWN AND CALDWELL

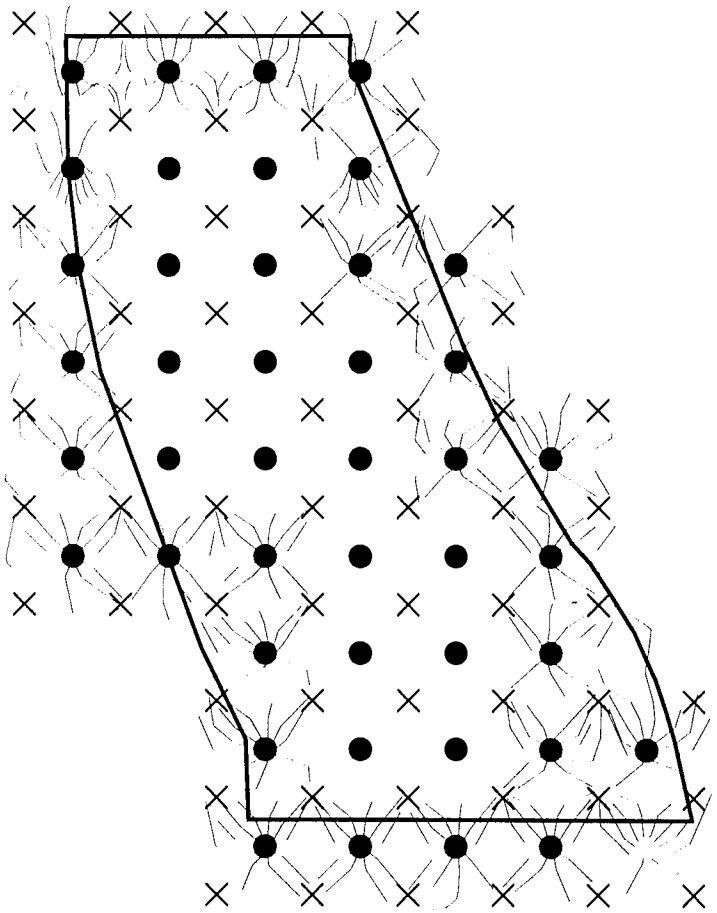

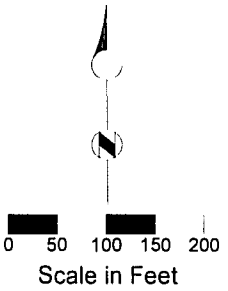

INJECTION WELL

RECOVERY WELL

PARTICLE TRACE FROM POINT OF INJECTION TO POINT OF CAPTURE

Particle trace output files show all particles not captured in this layer are captured in other layers

Figure 28 - Attachment 7 to Table 1
PARTICLE TRACKING SIMULATION SCENARIO 4B
NORTH-SOUTH ANISOTROPY IN MODEL LAYER 5
MODEL LAYER 6

BHP COPPER *Florence Project*

BROWN AND CALDWELL

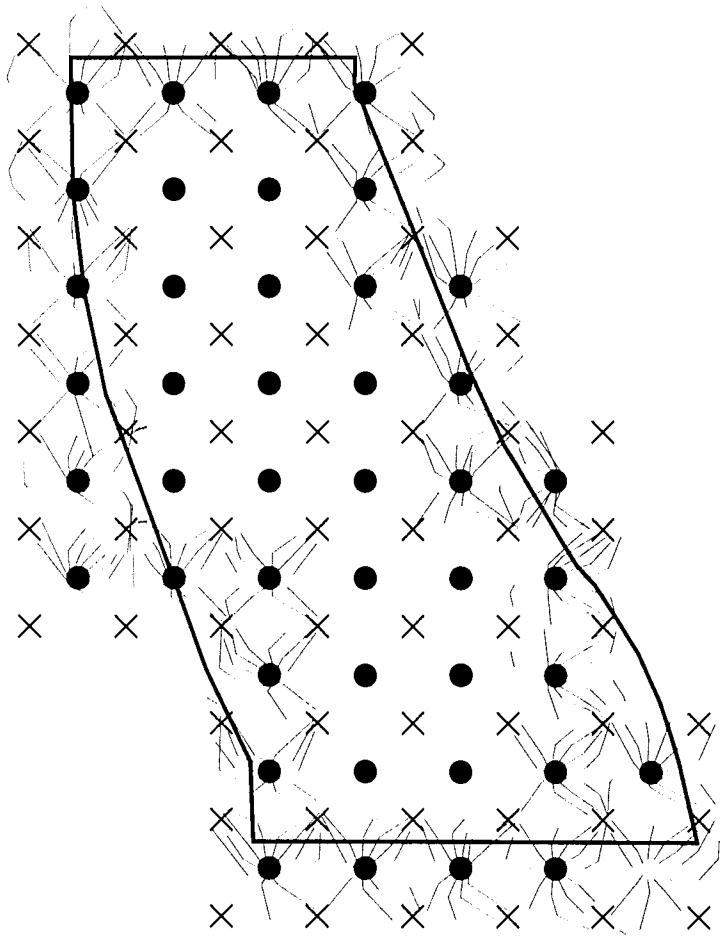

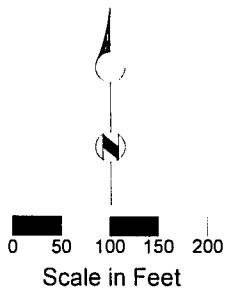

INJECTION WELL

RECOVERY WELL

PARTICLE TRACE FROM POINT OF INJECTION TO POINT OF CAPTURE

Particle trace output files show all particles not captured in this layer are captured in other layers

Figure 29 - Attachment 7 to Table 1
PARTICLE TRACKING SIMULATION SCENARIO 4B
NORTH-SOUTH ANISOTROPY IN MODEL LAYER 5
MODEL LAYER 7

BHP COPPER *Florence Project*

BROWN AND CALDWELL

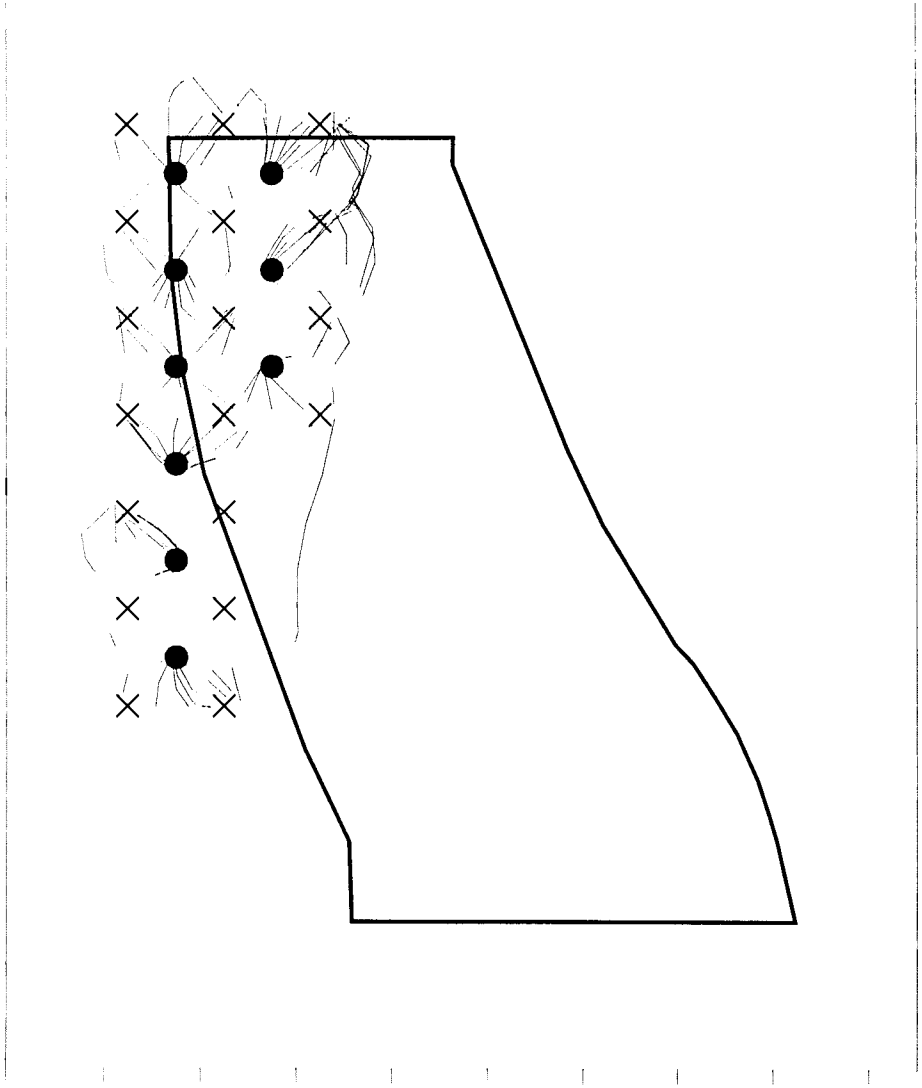

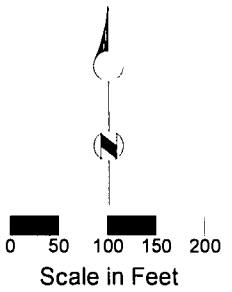

INJECTION WELL

RECOVERY WELL

PARTICLE TRACE FROM POINT OF INJECTION TO POINT OF CAPTURE

Particle trace output files show all particles not captured in this layer are captured in other layers

Figure 30 - Attachment 7 to Table 1
PARTICLE TRACKING SIMULATION SCENARIO 4B NORTH-SOUTH ANISOTROPY IN MODEL LAYER 5 MODEL LAYER 8

BHP COPPER *Florence Project*

BROWN AND CALDWELL

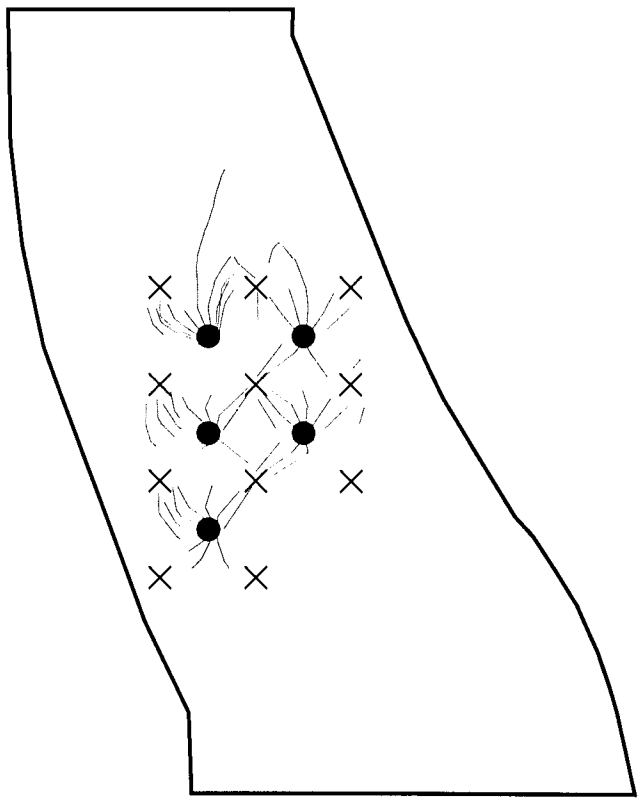

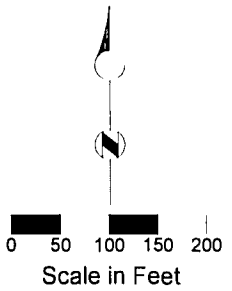

INJECTION WELL

RECOVERY WELL

PARTICLE TRACE FROM POINT OF INJECTION TO POINT OF CAPTURE

Particle trace output files show all particles not captured in this layer are captured in other layers

Figure 31 - Attachment 7 to Table 1
PARTICLE TRACKING SIMULATION SCENARIO 4C
EAST-WEST ANISOTROPY
IN MODEL LAYER 5
MODEL LAYER 3

BROWN AND CALDWELL

BHP COPPER *Florence Project*

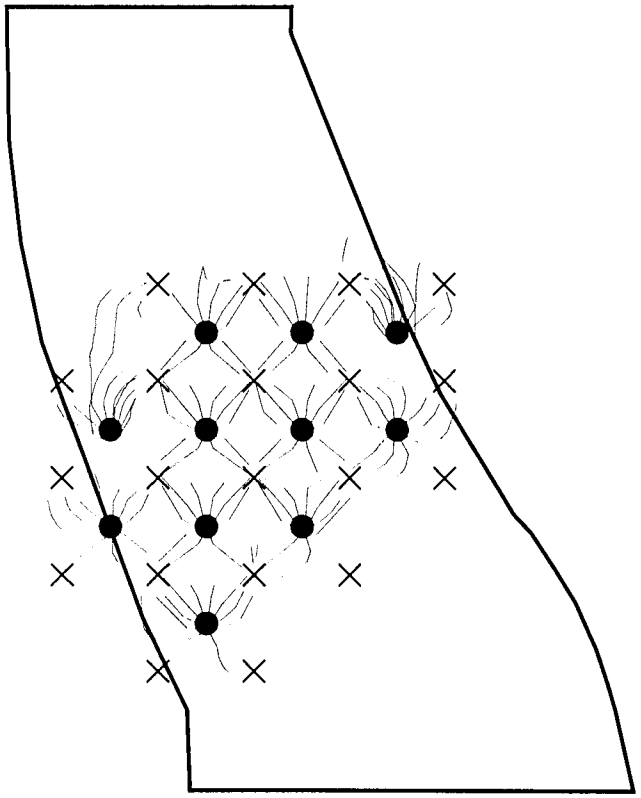

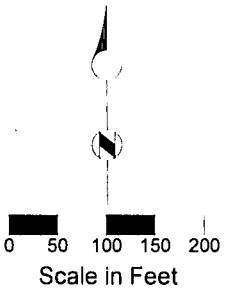

INJECTION WELL

RECOVERY WELL

PARTICLE TRACE FROM POINT OF INJECTION TO POINT OF CAPTURE

Particle trace output files show all particles not captured in this layer are captured in other layers

Figure 32 - Attachment 7 to Table 1
PARTICLE TRACKING SIMULATION SCENARIO 4C EAST-WEST ANISOTROPY IN MODEL LAYER 5 MODEL LAYER 4

BHP COPPER *Florence Project*

BROWN AND CALDWELL

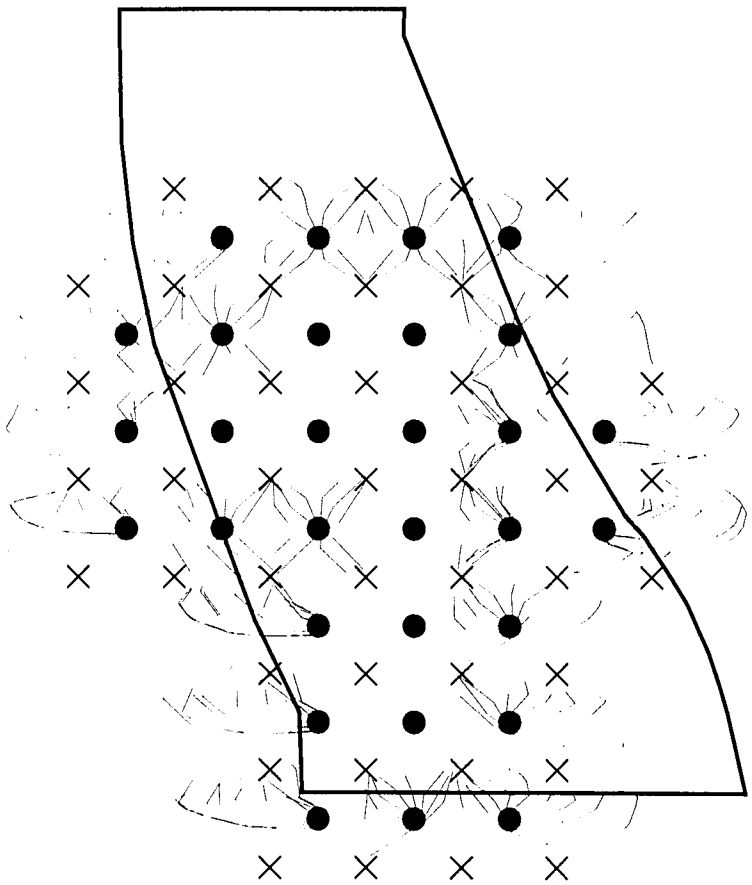

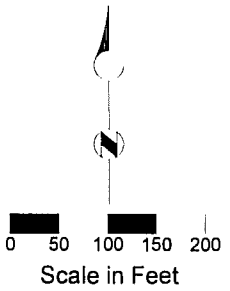

INJECTION WELL

RECOVERY WELL

PARTICLE TRACE FROM POINT OF INJECTION TO POINT OF CAPTURE

Particle trace output files show all particles not captured in this layer are captured in other layers

Figure 33 - Attachment 7 to Table 1
PARTICLE TRACKING SIMULATION SCENARIO 4C
EAST-WEST ANISOTROPY IN MODEL LAYER 5
MODEL LAYER 5

BHP

BHP COPPER *Florence Project*

BROWN AND CALDWELL

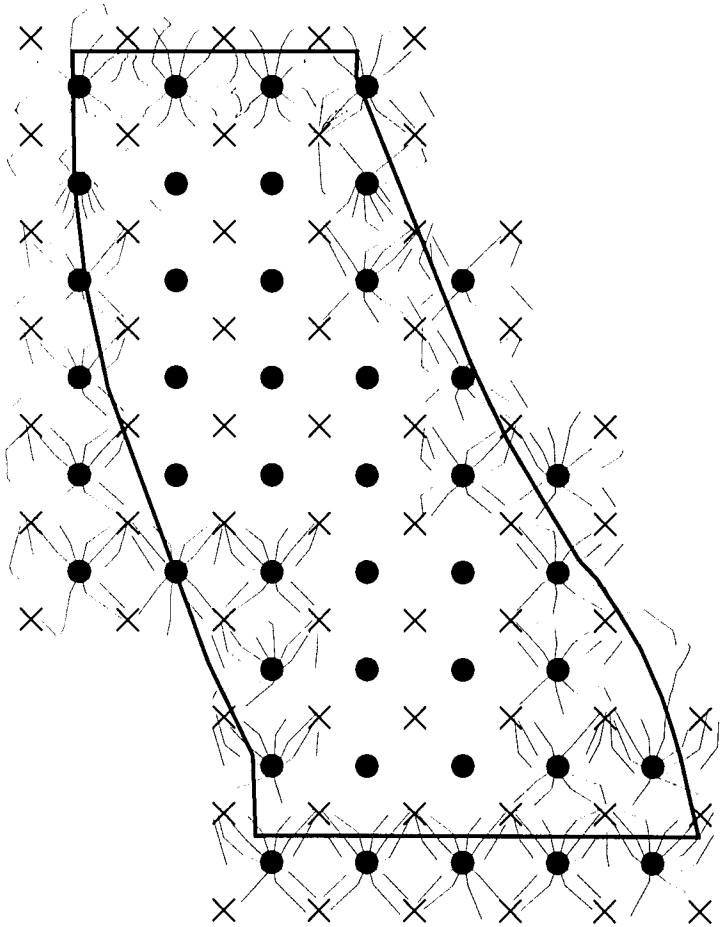

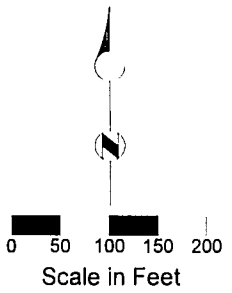

INJECTION WELL

RECOVERY WELL

PARTICLE TRACE FROM POINT OF INJECTION TO POINT OF CAPTURE

Particle trace output files show all particles not captured in this layer are captured in other layers

Figure 34 - Attachment 7 to Table 1
PARTICLE TRACKING SIMULATION SCENARIO 4C
EAST-WEST ANISOTROPY
IN MODEL LAYER 5
MODEL LAYER 6

BHP

BHP COPPER *Florence Project*

BROWN AND CALDWELL

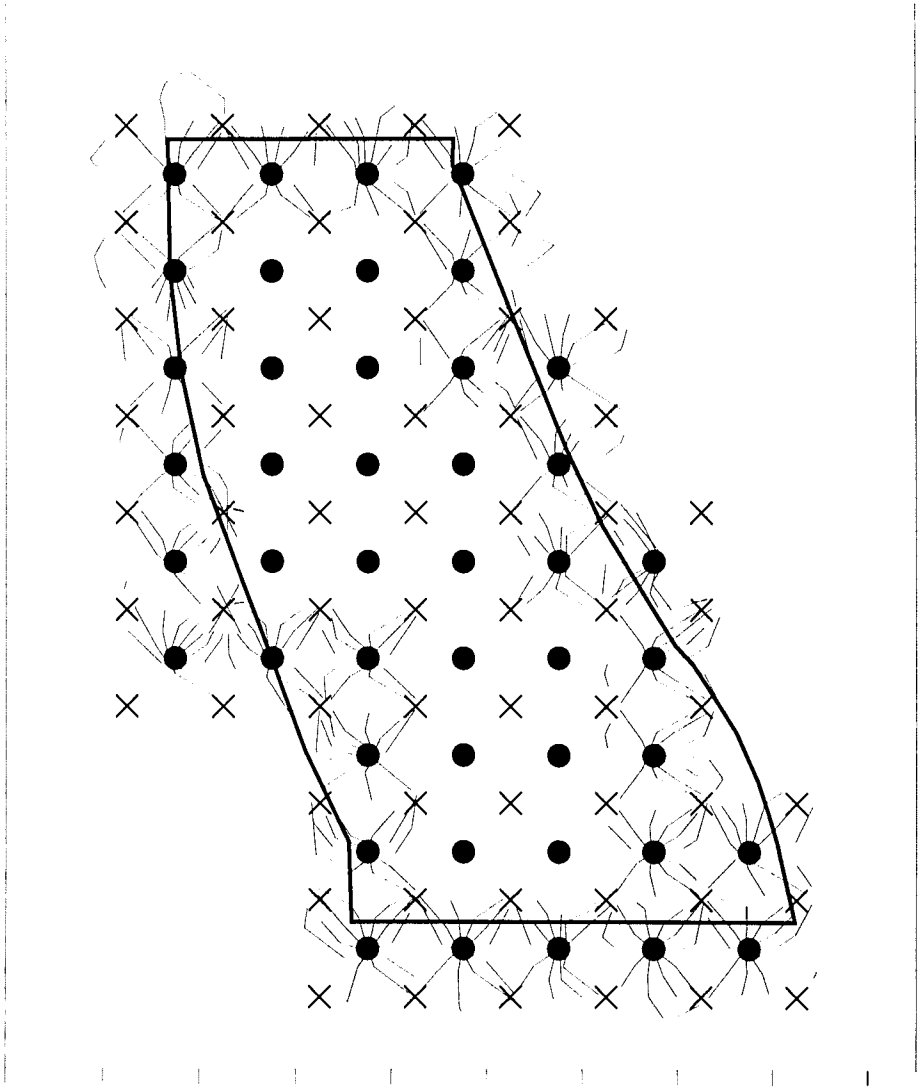

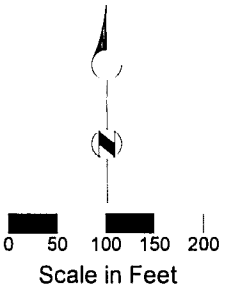

INJECTION WELL

RECOVERY WELL

PARTICLE TRACE FROM POINT OF INJECTION TO POINT OF CAPTURE

Particle trace output files show all particles not captured in this layer are captured in other layers

Figure 35 - Attachment 7 to Table 1
PARTICLE TRACKING SIMULATION SCENARIO 4C
EAST-WEST ANISOTROPY
IN MODEL LAYER 5
MODEL LAYER 7

BHP COPPER *Florence Project*

BROWN AND CALDWELL

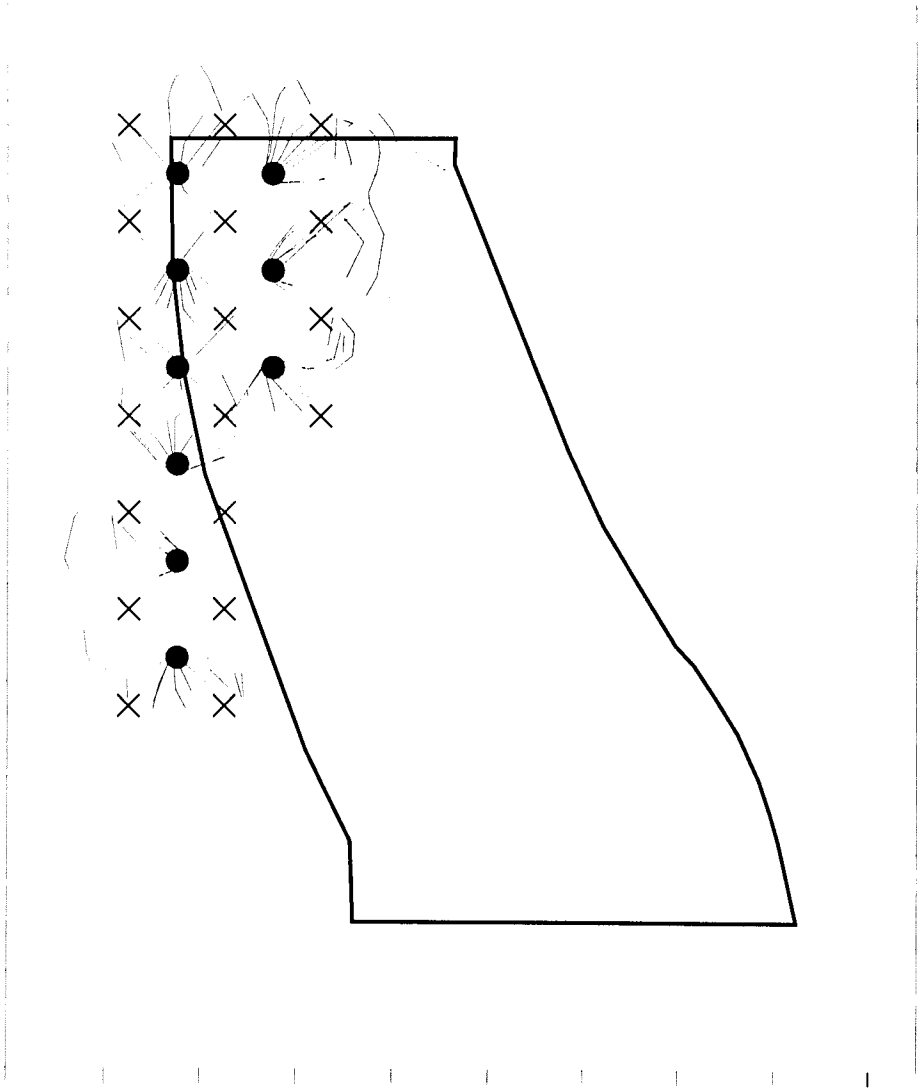

0 50 100 150 200
Scale in Feet

INJECTION WELL

RECOVERY WELL

PARTICLE TRACE FROM POINT OF INJECTION TO POINT OF CAPTURE

Particle trace output files show all particles not captured in this layer are captured in other layers

Figure 36 - Attachment 7 to Table 1
PARTICLE TRACKING
SIMULATION SCENARIO 4C
EAST-WEST ANISOTROPY
IN MODEL LAYER 5
MODEL LAYER 8

BHP
BHP COPPER *Florence Project*

BROWN AND CALDWELL

```
+++++++++++++++++++++++++++++++++++++++
+
+                    P A T H 3 D
+   A Ground-Water Path and Travel-Time
+                     (V. 3.20)
+
+++++++++++++++++++++++++++++++++++++++

Magma, Florence, NOV 95, Regional Domain, 8 layers:
UUU1 K=42,40,20,6; LCU 2,3 K=K1/10; OXIDE 4,5,6,7,8 K=0.3, 0.003
FLOW MODEL CONSISTS OF     8 LAYERS  176 ROWS  216 COLUMNS
NUMBER OF STRESS PERIOD(S) IN SIMULATION =         4
TIME UNIT USED IN THE MODEL IS DAYS
 PACKAGE:  BCF  WEL  DRN  RIV  EVT  GHB  RCH  STR
    UNIT:  11   12    0    0    0   17    0    0
FLOW FIELD IS TRANSIENT (ISS=0)
WETTING CAPABILITY IS NOT ACTIVE
HEAD AT CELLS THAT CONVERT TO DRY=  0.77778E+06
MAXIMUM NUMBER OF WELLS =       500
MAXIMUM NUMBER OF GHB CELLS =      6240
MAXIMUM NUMBER OF PARTICLES ALLOWED =      5000
FILE [P3DPLOT.DAT]  SAVED IN UNIT  4 FOR PLOTTING PATH LINES
FILE [P3DFRONT.DAT] SAVED IN UNIT  7 FOR PLOTTING FRONT POSITIONS
FILE [P3DCAPT.DAT]  SAVED IN UNIT  9 WITH FINAL & INITIAL POSITIONS OF CAPTU
INITIAL PARTICLE POSITIONS ARE ENTERED IN J, I, K CELL INDICES
PARTICLE REMOVAL OPTION [2] IS SELECTED
   3171961 ELEMENTS OF THE Y ARRAY USED OUT OF    9999999
NUMBER OF WELLS IN CURRENT STRESS PERIOD =  471

TIME STEP NO.    5
------------------
FROM TIME =   589.88     TO    730.00

HEADS FOR CURRENT TIME STEP READ UNFORMATTED ON UNIT   3

           ============================================================
           PARTICLE COORDINATES, TRAVEL TIMES AND VELOCITY COMPONENTS
           ============================================================

PARTICLE NO.         1
      X            Y            Z          TIME        Vx         Vy         Vz
PARTICLE HAS ALREADY BEEN REMOVED

PARTICLE NO.         2
      X            Y            Z          TIME        Vx         Vy         Vz
PARTICLE HAS ALREADY BEEN REMOVED

PARTICLE NO.         3
      X            Y            Z          TIME        Vx         Vy         Vz
PARTICLE HAS ALREADY BEEN REMOVED

PARTICLE NO.         4
      X            Y            Z          TIME        Vx         Vy         Vz
PARTICLE HAS ALREADY BEEN REMOVED
```

PARTICLE NO. 5

X	Y	Z	TIME	Vx	Vy	Vz

PARTICLE HAS ALREADY BEEN REMOVED

PARTICLE NO. 6

X	Y	Z	TIME	Vx	Vy	Vz

PARTICLE HAS ALREADY BEEN REMOVED

PARTICLE NO. 7

X	Y	Z	TIME	Vx	Vy	Vz

PARTICLE HAS ALREADY BEEN REMOVED

PARTICLE NO. 8

X	Y	Z	TIME	Vx	Vy	Vz

PARTICLE HAS ALREADY BEEN REMOVED

PARTICLE NO. 9

X	Y	Z	TIME	Vx	Vy	Vz

PARTICLE HAS ALREADY BEEN REMOVED

PARTICLE NO. 10

X	Y	Z	TIME	Vx	Vy	Vz

PARTICLE HAS ALREADY BEEN REMOVED

PARTICLE NO. 11

X	Y	Z	TIME	Vx	Vy	Vz

PARTICLE HAS ALREADY BEEN REMOVED

PARTICLE NO. 12

X	Y	Z	TIME	Vx	Vy	Vz

PARTICLE HAS ALREADY BEEN REMOVED

PARTICLE NO. 13

X	Y	Z	TIME	Vx	Vy	Vz

PARTICLE HAS ALREADY BEEN REMOVED

PARTICLE NO. 14

X	Y	Z	TIME	Vx	Vy	Vz

PARTICLE HAS ALREADY BEEN REMOVED

PARTICLE NO. 15

X	Y	Z	TIME	Vx	Vy	Vz

PARTICLE HAS ALREADY BEEN REMOVED

PARTICLE NO. 16

X	Y	Z	TIME	Vx	Vy	Vz

PARTICLE HAS ALREADY BEEN REMOVED

PARTICLE NO. 17

X	Y	Z	TIME	Vx	Vy	Vz

PARTICLE HAS ALREADY BEEN REMOVED

PARTICLE NO. 18

X	Y	Z	TIME	Vx	Vy	Vz

PARTICLE HAS ALREADY BEEN REMOVED

PARTICLE NO. 19

X	Y	Z	TIME	Vx	Vy	Vz

PARTICLE HAS ALREADY BEEN REMOVED

PARTICLE NO. 20

X	Y	Z	TIME	Vx	Vy	Vz

PARTICLE HAS ALREADY BEEN REMOVED

PARTICLE NO. 21

X	Y	Z	TIME	Vx	Vy	Vz

PARTICLE HAS ALREADY BEEN REMOVED

PARTICLE NO. 22

X	Y	Z	TIME	Vx	Vy	Vz

PARTICLE HAS ALREADY BEEN REMOVED

PARTICLE NO. 23

X	Y	Z	TIME	Vx	Vy	Vz

PARTICLE HAS ALREADY BEEN REMOVED

PARTICLE NO. 24

X	Y	Z	TIME	Vx	Vy	Vz

PARTICLE HAS ALREADY BEEN REMOVED

PARTICLE NO. 25

X	Y	Z	TIME	Vx	Vy	Vz

PARTICLE HAS ALREADY BEEN REMOVED

PARTICLE NO. 26

X	Y	Z	TIME	Vx	Vy	Vz

PARTICLE HAS ALREADY BEEN REMOVED

PARTICLE NO. 27

X	Y	Z	TIME	Vx	Vy	Vz

PARTICLE HAS ALREADY BEEN REMOVED

PARTICLE NO. 28

X	Y	Z	TIME	Vx	Vy	Vz

PARTICLE HAS ALREADY BEEN REMOVED

PARTICLE NO. 29

X	Y	Z	TIME	Vx	Vy	Vz

PARTICLE HAS ALREADY BEEN REMOVED

PARTICLE NO. 30

X	Y	Z	TIME	Vx	Vy	Vz

PARTICLE HAS ALREADY BEEN REMOVED

PARTICLE NO. 31

X	Y	Z	TIME	Vx	Vy	Vz

PARTICLE HAS ALREADY BEEN REMOVED

PARTICLE NO. 32

X	Y	Z	TIME	Vx	Vy	Vz

PARTICLE HAS ALREADY BEEN REMOVED

PARTICLE NO. 33

X	Y	Z	TIME	Vx	Vy	Vz

PARTICLE HAS ALREADY BEEN REMOVED

PARTICLE NO. 34

X	Y	Z	TIME	Vx	Vy	Vz

PARTICLE HAS ALREADY BEEN REMOVED

PARTICLE NO. 35

X	Y	Z	TIME	Vx	Vy	Vz

PARTICLE HAS ALREADY BEEN REMOVED

PARTICLE NO. 36

X	Y	Z	TIME	Vx	Vy	Vz

PARTICLE HAS ALREADY BEEN REMOVED

PARTICLE NO. 37

X	Y	Z	TIME	Vx	Vy	Vz

PARTICLE HAS ALREADY BEEN REMOVED

PARTICLE NO. 38

X	Y	Z	TIME	Vx	Vy	Vz

PARTICLE HAS ALREADY BEEN REMOVED

PARTICLE NO. 39

X	Y	Z	TIME	Vx	Vy	Vz

PARTICLE HAS ALREADY BEEN REMOVED

PARTICLE NO. 40

X	Y	Z	TIME	Vx	Vy	Vz

PARTICLE HAS ALREADY BEEN REMOVED

PARTICLE NO. 41

X	Y	Z	TIME	Vx	Vy	Vz

PARTICLE HAS ALREADY BEEN REMOVED

PARTICLE NO. 42

X	Y	Z	TIME	Vx	Vy	Vz

PARTICLE HAS ALREADY BEEN REMOVED

PARTICLE NO. 43

X	Y	Z	TIME	Vx	Vy	Vz

PARTICLE HAS ALREADY BEEN REMOVED

PARTICLE NO. 44

X	Y	Z	TIME	Vx	Vy	Vz

PARTICLE HAS ALREADY BEEN REMOVED

PARTICLE NO. 45

X	Y	Z	TIME	Vx	Vy	Vz

PARTICLE HAS ALREADY BEEN REMOVED

PARTICLE NO. 46
X Y Z TIME Vx Vy Vz
PARTICLE HAS ALREADY BEEN REMOVED

PARTICLE NO. 47
X Y Z TIME Vx Vy Vz
PARTICLE HAS ALREADY BEEN REMOVED

PARTICLE NO. 48
X Y Z TIME Vx Vy Vz
PARTICLE HAS ALREADY BEEN REMOVED

PARTICLE NO. 49
X Y Z TIME Vx Vy Vz
PARTICLE HAS ALREADY BEEN REMOVED

PARTICLE NO. 50
X Y Z TIME Vx Vy Vz
PARTICLE HAS ALREADY BEEN REMOVED

PARTICLE NO. 51
X Y Z TIME Vx Vy Vz
PARTICLE HAS ALREADY BEEN REMOVED

PARTICLE NO. 52
X Y Z TIME Vx Vy Vz
PARTICLE HAS ALREADY BEEN REMOVED

PARTICLE NO. 53
X Y Z TIME Vx Vy Vz
PARTICLE HAS ALREADY BEEN REMOVED

PARTICLE NO. 54
X Y Z TIME Vx Vy Vz
PARTICLE HAS ALREADY BEEN REMOVED

PARTICLE NO. 55
X Y Z TIME Vx Vy Vz
PARTICLE HAS ALREADY BEEN REMOVED

PARTICLE NO. 56
X Y Z TIME Vx Vy Vz
PARTICLE HAS ALREADY BEEN REMOVED

PARTICLE NO. 57
X Y Z TIME Vx Vy Vz
PARTICLE HAS ALREADY BEEN REMOVED

PARTICLE NO. 58
X Y Z TIME Vx Vy Vz
PARTICLE HAS ALREADY BEEN REMOVED

PARTICLE NO. 59
X Y Z TIME Vx Vy Vz
PARTICLE HAS ALREADY BEEN REMOVED

PARTICLE NO. 60
X Y Z TIME Vx Vy Vz
PARTICLE HAS ALREADY BEEN REMOVED

PARTICLE NO. 61
X Y Z TIME Vx Vy Vz
PARTICLE HAS ALREADY BEEN REMOVED

PARTICLE NO. 62
X Y Z TIME Vx Vy Vz
PARTICLE HAS ALREADY BEEN REMOVED

PARTICLE NO. 63
X Y Z TIME Vx Vy Vz
PARTICLE HAS ALREADY BEEN REMOVED

PARTICLE NO. 64
X Y Z TIME Vx Vy Vz
PARTICLE HAS ALREADY BEEN REMOVED

PARTICLE NO. 65
X Y Z TIME Vx Vy Vz
PARTICLE HAS ALREADY BEEN REMOVED

PARTICLE NO. 66
X Y Z TIME Vx Vy Vz
PARTICLE HAS ALREADY BEEN REMOVED

PARTICLE NO. 67
X Y Z TIME Vx Vy Vz
PARTICLE HAS ALREADY BEEN REMOVED

PARTICLE NO. 68
X Y Z TIME Vx Vy Vz
PARTICLE HAS ALREADY BEEN REMOVED

PARTICLE NO. 69
X Y Z TIME Vx Vy Vz
PARTICLE HAS ALREADY BEEN REMOVED

PARTICLE NO. 70
X Y Z TIME Vx Vy Vz
PARTICLE HAS ALREADY BEEN REMOVED

PARTICLE NO. 71
X Y Z TIME Vx Vy Vz
PARTICLE HAS ALREADY BEEN REMOVED

PARTICLE NO. 72
X Y Z TIME Vx Vy Vz
PARTICLE HAS ALREADY BEEN REMOVED

PARTICLE NO. 73
X Y Z TIME Vx Vy Vz

PARTICLE HAS ALREADY BEEN REMOVED

PARTICLE NO. 74

X	Y	Z	TIME	Vx	Vy	Vz

PARTICLE HAS ALREADY BEEN REMOVED

PARTICLE NO. 75

X	Y	Z	TIME	Vx	Vy	Vz

PARTICLE HAS ALREADY BEEN REMOVED

PARTICLE NO. 76

X	Y	Z	TIME	Vx	Vy	Vz

PARTICLE HAS ALREADY BEEN REMOVED

PARTICLE NO. 77

X	Y	Z	TIME	Vx	Vy	Vz

PARTICLE HAS ALREADY BEEN REMOVED

PARTICLE NO. 78

X	Y	Z	TIME	Vx	Vy	Vz

PARTICLE HAS ALREADY BEEN REMOVED

PARTICLE NO. 79

X	Y	Z	TIME	Vx	Vy	Vz

PARTICLE HAS ALREADY BEEN REMOVED

PARTICLE NO. 80

X	Y	Z	TIME	Vx	Vy	Vz

PARTICLE HAS ALREADY BEEN REMOVED

PARTICLE NO. 81

X	Y	Z	TIME	Vx	Vy	Vz

PARTICLE HAS ALREADY BEEN REMOVED

PARTICLE NO. 82

X	Y	Z	TIME	Vx	Vy	Vz

PARTICLE HAS ALREADY BEEN REMOVED

PARTICLE NO. 83

X	Y	Z	TIME	Vx	Vy	Vz

PARTICLE HAS ALREADY BEEN REMOVED

PARTICLE NO. 84

X	Y	Z	TIME	Vx	Vy	Vz

PARTICLE HAS ALREADY BEEN REMOVED

PARTICLE NO. 85

X	Y	Z	TIME	Vx	Vy	Vz

PARTICLE HAS ALREADY BEEN REMOVED

PARTICLE NO. 86

X	Y	Z	TIME	Vx	Vy	Vz

PARTICLE HAS ALREADY BEEN REMOVED

PARTICLE NO. 87

```
      X            Y            Z          TIME         Vx          Vy          Vz
 PARTICLE HAS ALREADY BEEN REMOVED

 PARTICLE NO.        88
      X            Y            Z          TIME         Vx          Vy          Vz
 PARTICLE HAS ALREADY BEEN REMOVED

 PARTICLE NO.        89
      X            Y            Z          TIME         Vx          Vy          Vz
 PARTICLE HAS ALREADY BEEN REMOVED

 PARTICLE NO.        90
      X            Y            Z          TIME         Vx          Vy          Vz
 PARTICLE HAS ALREADY BEEN REMOVED

 PARTICLE NO.        91
      X            Y            Z          TIME         Vx          Vy          Vz
 PARTICLE HAS ALREADY BEEN REMOVED

 PARTICLE NO.        92
      X            Y            Z          TIME         Vx          Vy          Vz
 PARTICLE HAS ALREADY BEEN REMOVED

 PARTICLE NO.        93
      X            Y            Z          TIME         Vx          Vy          Vz
 PARTICLE HAS ALREADY BEEN REMOVED

 PARTICLE NO.        94
      X            Y            Z          TIME         Vx          Vy          Vz
 PARTICLE HAS ALREADY BEEN REMOVED

 PARTICLE NO.        95
      X            Y            Z          TIME         Vx          Vy          Vz
 PARTICLE HAS ALREADY BEEN REMOVED

 PARTICLE NO.        96
      X            Y            Z          TIME         Vx          Vy          Vz
 PARTICLE HAS ALREADY BEEN REMOVED

 PARTICLE NO.        97
      X            Y            Z          TIME         Vx          Vy          Vz
 PARTICLE HAS ALREADY BEEN REMOVED

 PARTICLE NO.        98
      X            Y            Z          TIME         Vx          Vy          Vz
 PARTICLE HAS ALREADY BEEN REMOVED

 PARTICLE NO.        99
      X            Y            Z          TIME         Vx          Vy          Vz
   24082.       24588.       347.87        589.88    -0.168E+00-0.109E+00 0.921E-
   24082.       24588.       347.96        590.88    -0.169E+00-0.109E+00 0.919E-
   24082.       24587.       348.33        594.88    -0.171E+00-0.109E+00 0.913E-
   24079.       24585.       349.76        610.88    -0.178E+00-0.107E+00 0.887E-
   24031.       24510.       368.31        674.88    -0.367E+00-0.752E-01 0.309E+
 REMOVED: PARTICLE ENTERS WELL  K=     5,  I=    68,  J=    77
```

PARTICLE NO. 100
X Y Z TIME Vx Vy Vz
PARTICLE HAS ALREADY BEEN REMOVED

PARTICLE NO. 101
X Y Z TIME Vx Vy Vz
PARTICLE HAS ALREADY BEEN REMOVED

PARTICLE NO. 102
X Y Z TIME Vx Vy Vz
PARTICLE HAS ALREADY BEEN REMOVED

PARTICLE NO. 103
X Y Z TIME Vx Vy Vz
PARTICLE HAS ALREADY BEEN REMOVED

PARTICLE NO. 104
X Y Z TIME Vx Vy Vz
PARTICLE HAS ALREADY BEEN REMOVED

PARTICLE NO. 105
X Y Z TIME Vx Vy Vz
PARTICLE HAS ALREADY BEEN REMOVED

PARTICLE NO. 106
X Y Z TIME Vx Vy Vz
PARTICLE HAS ALREADY BEEN REMOVED

PARTICLE NO. 107
X Y Z TIME Vx Vy Vz
PARTICLE HAS ALREADY BEEN REMOVED

PARTICLE NO. 108
X Y Z TIME Vx Vy Vz
PARTICLE HAS ALREADY BEEN REMOVED

PARTICLE NO. 109
X Y Z TIME Vx Vy Vz
PARTICLE HAS ALREADY BEEN REMOVED

PARTICLE NO. 110
X Y Z TIME Vx Vy Vz
PARTICLE HAS ALREADY BEEN REMOVED

>>ALL PARTICLES HAVE ALREADY BEEN REMOVED

Attachment 8 to Table 1

Attachment 8 to Table 1

Response to ADEQ Comment-4.2.1-Mine Model

ADEQ-4.2.1-Injection Recovery Process-BHP proposes to leach in 100 to 400 foot vertical sections, "beginning from the top of the bedrock and at the base of the oxide ore zone." The Department insists that, because the hydraulic conductivity in the overlying sediments is greater than within the bedrock, fluids must not be injected at the bedrock/sediment interface. The Department is concerned that some injected fluids may preferentially flow into the sediments and not the recovery well. Some non-leached thickness of bedrock must remain at the top of the oxide zone.

The Department requests that BHP conduct another modeling exercise with particle tracking. This new model should be focused on, say, one injection well or one injection and one recovery well. The cell size, vertically as wells as horizontally, should be sufficiently fine to illustrate the hydrodynamics near the well bore and the bedrock/sediment interface. The purpose of this exercise is to determine the thickness of the oxide "buffer zone" that must exist above the leaching activities. The Department should then write this "buffer zone" thickness into the permit.

Summary and Recommendations

A model that included four injection wells and nine recovery wells was developed to evaluate the effects of injection near the bedrock/basin-fill interface (LBFU/oxide contact). The evaluation considered the need to: (1) maintain a level of hydraulic control that will protect groundwater quality outside the designated mine area; (2) minimize the use of groundwater in maintaining the required hydraulic control; and (3) recover copper at levels consistent with sound conservation principles.

Simulation of groundwater flow with particle tracking was used to evaluate injection/recovery scenarios simulating injections from 10 feet to 40 feet below the LBFU/oxide contact.

The modeling indicated that injection 40 feet below the LBFU/oxide contact results in the complete containment of the particles within the oxide zone and does not require excessive groundwater withdrawals. The model also indicated that capture efficiencies may be enhanced by setting screens in recovery wells within 10 feet of the LBFU/oxide contact. Further study, however, will be required to assess whether the higher screens will increase capture efficiency for larger well arrays.

BHP recommends, as an initial permit condition, that the top of the screened interval for injection wells be set no closer than 40 feet below the LBFU/oxide contact and that the top of the screened interval for recovery wells be set no closer than 10 feet below the LBFU/oxide contact.

The recommended restrictions will adequately protect the quality of groundwater outside the in-situ mine area without creating the need for excessive groundwater withdrawals.

Recognizing the conservative nature of the permit condition recommended above, BHP reserves the right to negotiate the permit condition in the event that operational monitoring shows that the condition is unnecessarily restrictive.

Model Design

The modeling was performed using the finite difference, block-centered groundwater flow code, MODFLOW, and the particle tracking program, Path3D.

Grid

The domain consists of a 1,000 feet by 1,000 feet square divided into a uniform grid of 100 columns and 100 rows resulting in a cell size of 10 feet by 10 feet (Figure 1). In the vertical dimension the model extends from ground surface to a depth of 400 feet (between 1,000 feet msl and 1,400 feet msl), consisting of 40 layers of 10 feet thickness each (Figure 2).

Aquifer Properties

Properties of the basin-fill units are assigned to the first 10 layers (100 feet) and the properties of the oxide zone are assigned to the remaining 30 layers (100 feet, Figure 2). This setup corresponds to a 300-foot thickness of the oxide zone overlain by the LBFU. The first layer is unconfined, the next nine layers can change from confined to unconfined, and the remaining layers are confined. The aquifer is assumed homogeneous and isotropic. The hydraulic conductivity of the 10 basin-fill layers is set to 20 feet/day and the hydraulic conductivity of the 30 oxide zone layers is set to 1 ft/day. Porosity in the basin-fill and the oxide zone is set to 10 percent and 2 percent, respectively.

Boundary and Initial Conditions

The simulations were conducted under transient state conditions with one stress period of 365 days. A hydraulic gradient of 0.005 feet per foot, similar to that observed in the field, was established across the domain. The initial condition water levels for this gradient are shown in Figure 3. The north-south boundaries are set to constant head, and the east-west boundaries are flow lines (no flow).

Pumping Scenarios

Nine extraction (recovery) wells and four injection wells are screened across layers 15 through 40 (the oxide zone). Figure 4 shows the model domain and the locations of the wells at the center of the domain. Injection and extraction begin in layer 15 at a base rate of 0.1 gpm/ft, resulting in 1 gpm per 10-foot layer for each injection well. The base extraction rate for the central well is equal to the injection rate, and the extraction rates at the corner wells are adjusted depending on

the number of injection wells they draw from in order to achieve an overall extraction rate equal to injection (net injection or extraction is zero). The base extraction rates were increased by 30 percent in order to achieve effective hydraulic control. The resulting injection and extraction rates are posted next to the wells on Figure 4.

Results

The hydraulic heads were calculated by MODFLOW and used by Path3D to simulate the paths of particles released at the injection wells under varying combinations of injection and extraction rates. The scenario described below shows successful containment (within the oxide zone), where the solution was injected in layers 15 to 40 (40 feet below the LBFU/oxide contact. The injection rates were kept at their base values and the extraction rate in the operating layers was increased by 30 percent. Figure 5 shows paths of particles released in layer 15. All particles are either captured within the same layer, or travel up to a higher layer before being captured. A vertical profile in the middle of the domain (Figure 6) indicates that all particles in all layers were either captured or are on a path towards an extraction well. Particle tracking simulations were performed with 20 particles randomly distributed in each cell, corresponding to the injection wells, and resulted in full capture of all particles. Figure 6 presents 5 particles per cell for clarity, but capture was achieved with 20 particles for this simulation too.

Two factors ensure that the amount of overpumping required for an actual mine block will be significantly less than the 30 percent indicated in the 13-well array used in the model. The first factor is that the amount of overpumping required to maintain hydraulic control is significantly less for interior wells than for exterior wells. The second is that percentage of overpumping decreases as the array size increases.

To evaluate the required buffer zone for interior wells, a simulation was run as shown in Figure 7. In this simulation, one cluster of interior wells were considered to be injecting and extracting at the same rate. The simulation was transient, under the following conditions: one stress period of 365 days, zero gradient, no flow across all the boundaries and variable head within the boundaries. There were 20 oxide layers used, each 20 feet thick. The thickness of the LBFU was 100 feet. The domain consisted of a uniform grid of 70 feet by 70 feet, divided into seven columns and seven rows. Hydraulic conductivity for the LBFU was set at 20 feet per day, and to 1 foot per day for the oxide zone. The particle tracking simulation shown in Figure 7 was performed with 10 particles, randomly distributed in each cell corresponding to the injection well from each layer. Note that all particles were captured and that none came closer than 9 feet to the LBFU/oxide contact.

Additional Comments

The simulations described above show that the particles are both confined and captured within the oxide zone. Simulations under different injection/recovery scenarios show that particles can enter into the LBFU and then be drawn back into the oxide zone where they are captured. In all such cases, the screens of the injection wells and the extraction wells were set below the LBFU/oxide contact.

Although BHP concurs that all injection and recovery wells should be set below the LBFU/oxide contact, BHP also believes it is important to note that full conservation of water and copper resources requires that some leach solutions enter the LBFU in order to leach all available copper. BHP is confident that this can be accomplished while maintaining hydraulic control, thereby fully protecting the quality of groundwater outside the pollutant management area.

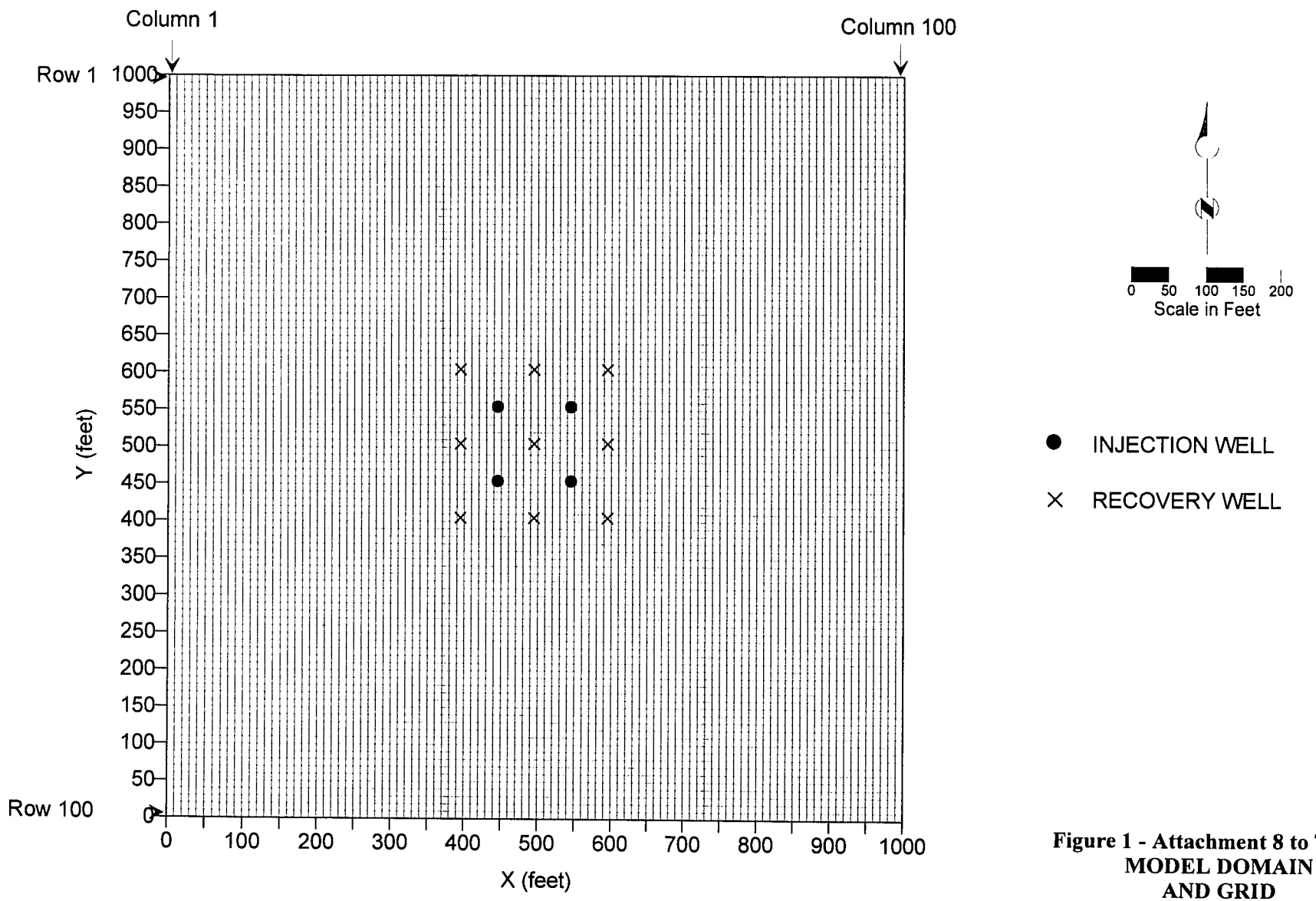

SFIG083 09/23/96 MikeS

BROWN AND CALDWELL

Figure 1 - Attachment 8 to Table 1
MODEL DOMAIN
AND GRID

BHP COPPER *Florence Project*

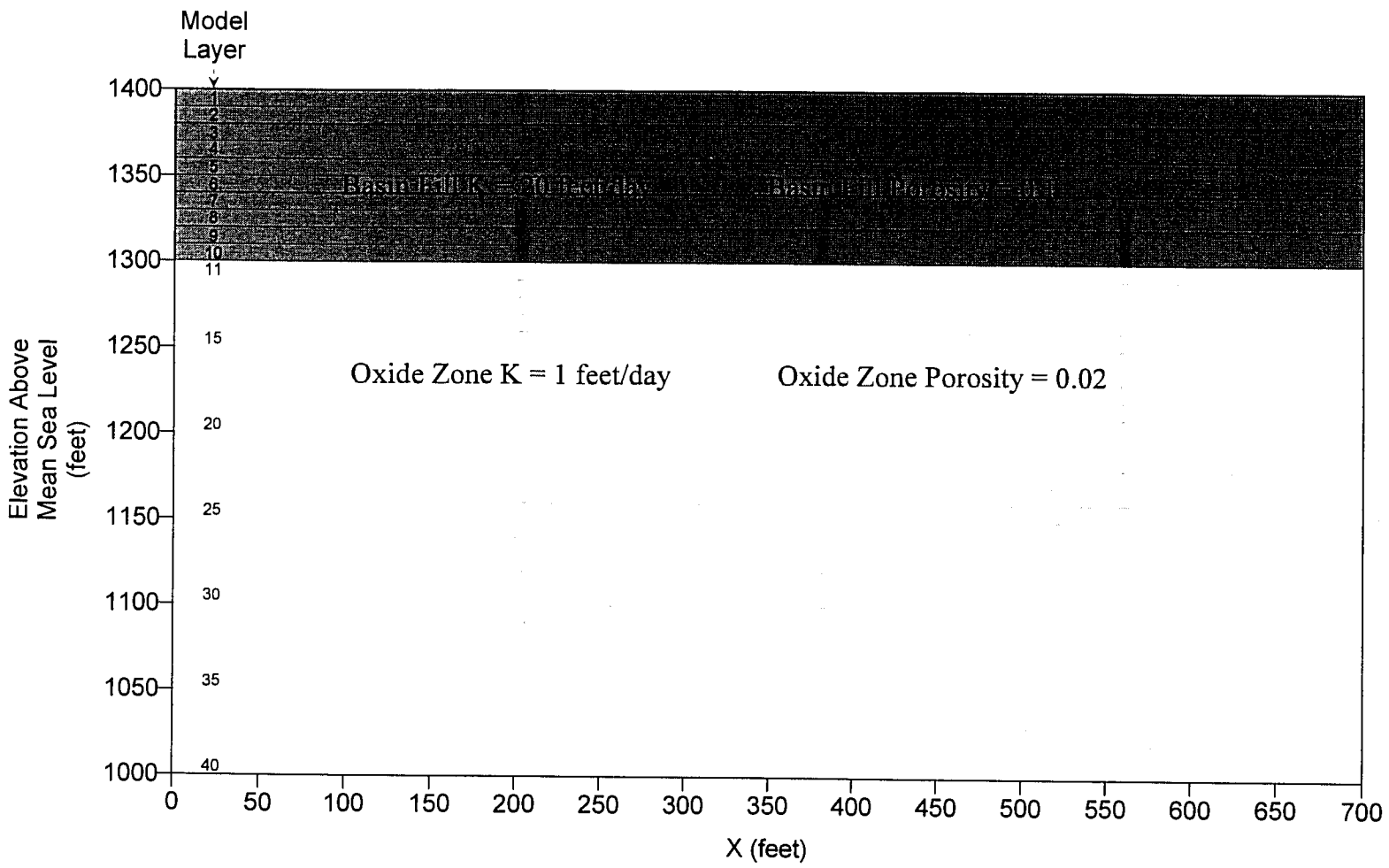

0 25 50 75 100
Scale in Feet

NOTE:
MODEL CONSISTS OF 40 LAYERS BETWEEN 1000 FEET AND 1400 FEET ABOVE MEAN SEA LEVEL. EACH LAYER IS 10 FEET THICK

Figure 2 - Attachment 8 to Table 1
VERTICAL VIEW
OF MODEL LAYERS

BROWN AND CALDWELL

BHP
BHP COPPER *Florence Project*

SFIG085 09/23/96 MikeS

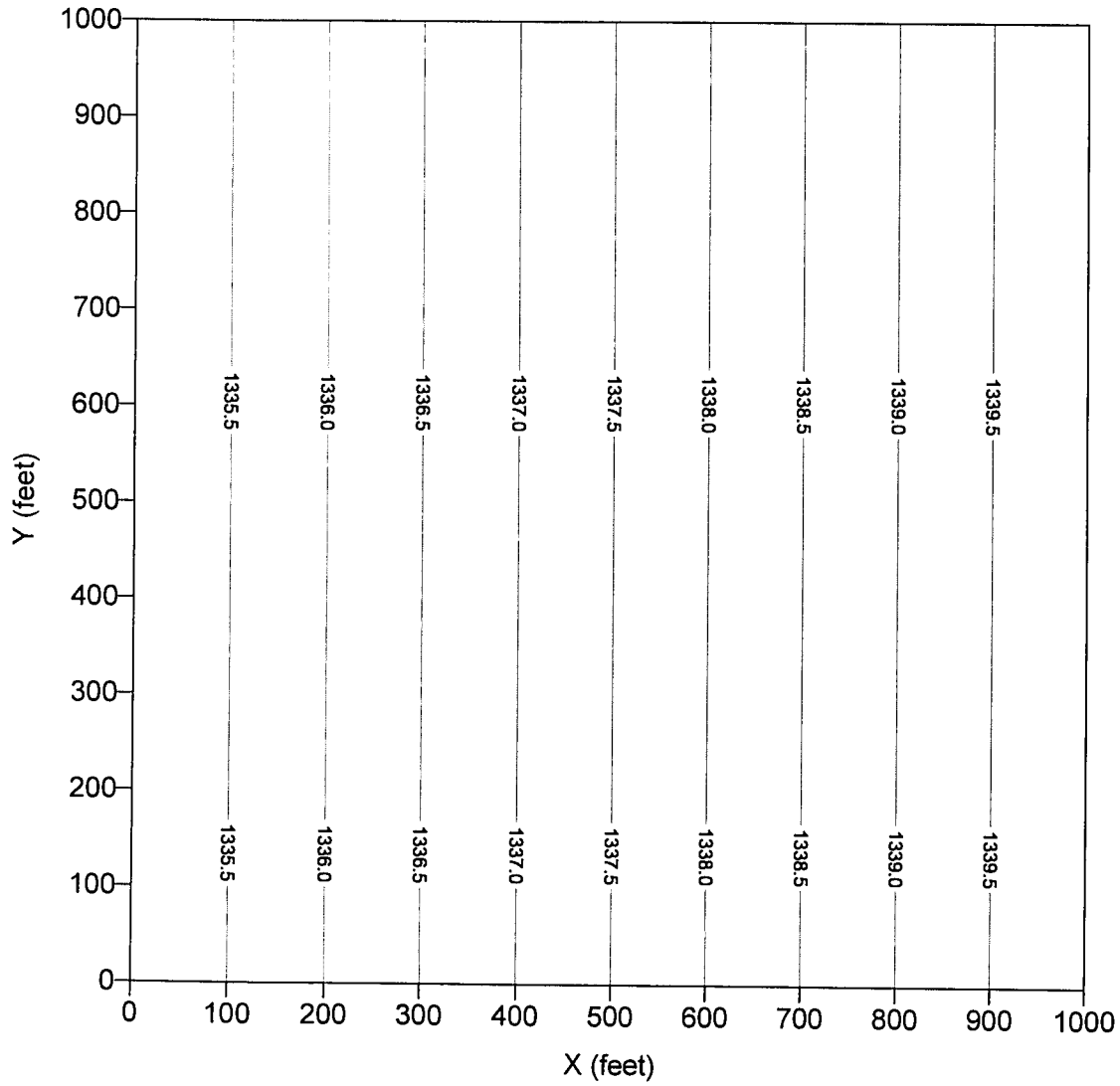

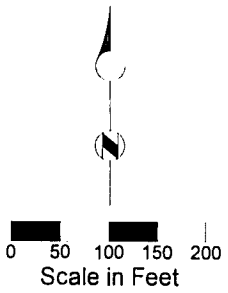

Figure 3 - Attachment 8 to Table 1
INITIAL GROUNDWATER LEVELS AT THE HYDRAULIC GRADIENT = 0.005

BROWN AND CALDWELL

BHP COPPER *Florence Project*

SFIG082 09/23/96 MikeS

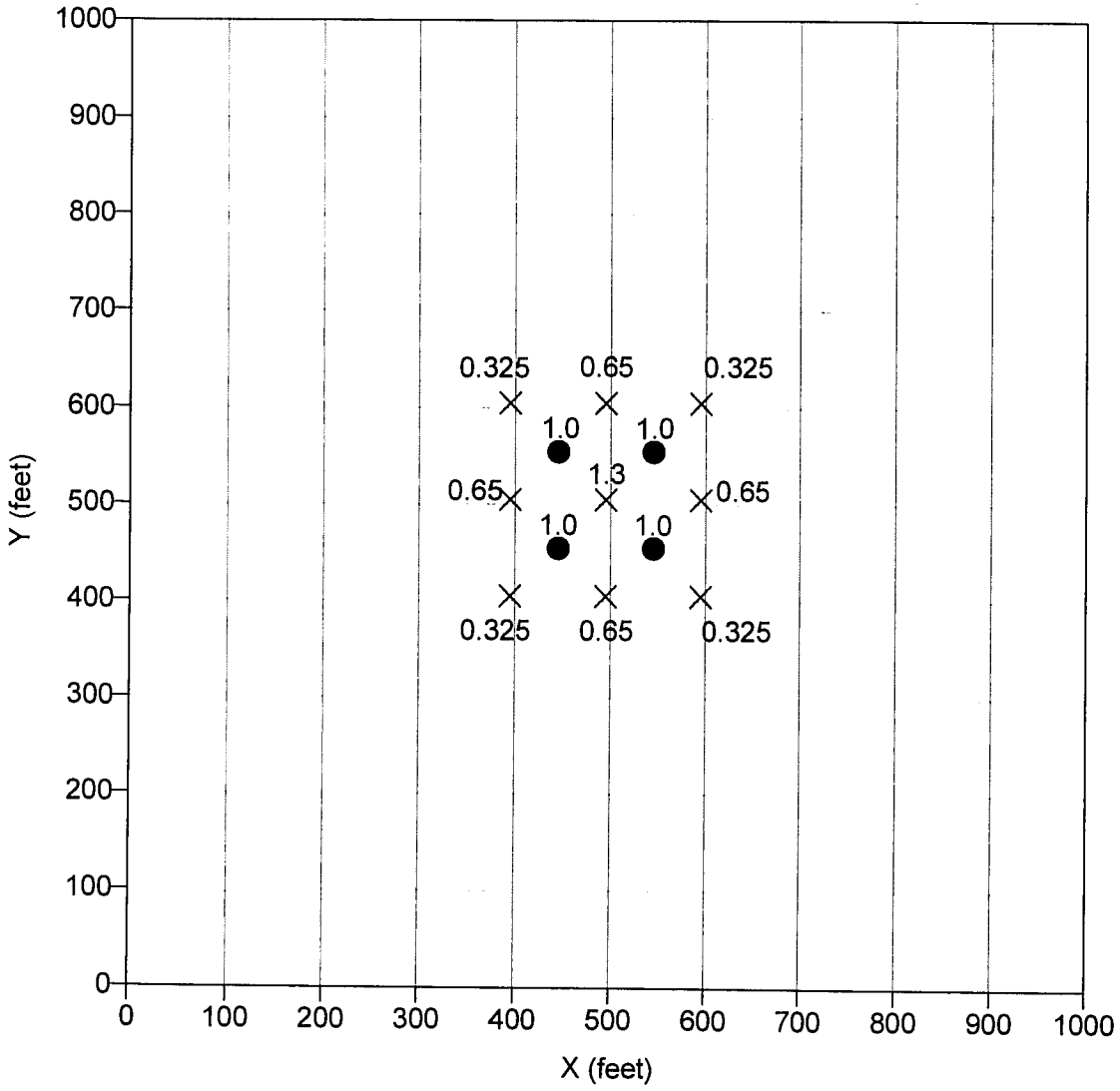

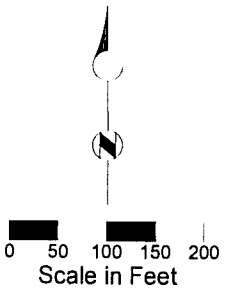

● INJECTION WELL

× RECOVERY WELL

1.0 PUMPING RATE IN GPM/LAYER

Figure 4 - Attachment 8 to Table 1
INJECTION AND RECOVERY WELL LOCATIONS AND PUMPING RATES

BHP COPPER *Florence Project*

BROWN AND CALDWELL

SFIG084 09/23/96 MikeS

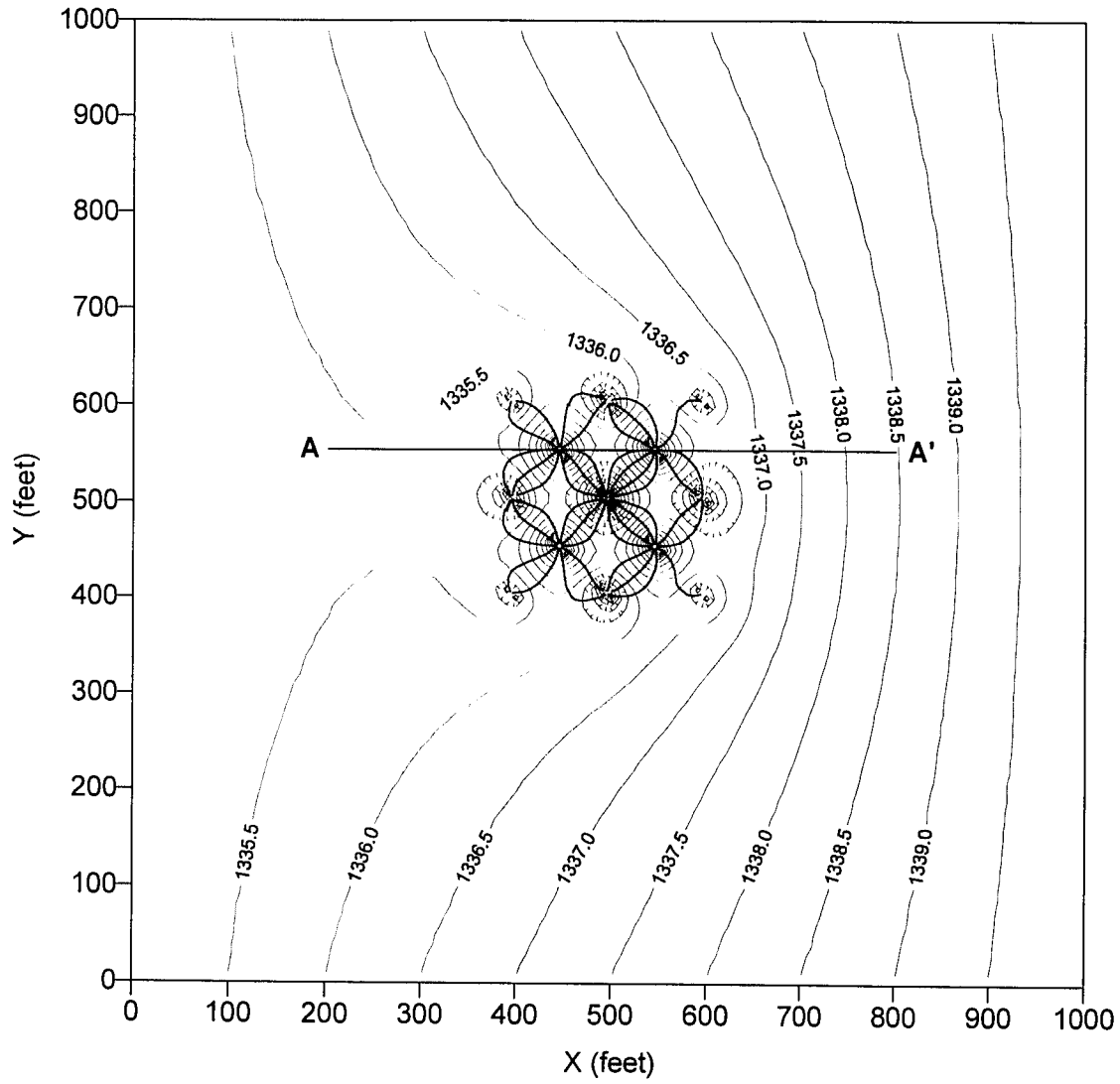

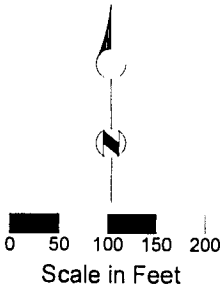

PARTICLE TRACE

1300 WATER LEVEL ELEVATION CONTOUR

CONTOUR INTERVAL = 0.5 FEET

Figure 5 - Attachment 8 to Table 1
WATER LEVEL ELEVATIONS AND PARTICLE PATHS AT LAYER 15

BROWN AND CALDWELL

BHP

BHP COPPER *Florence Project*

SFIG086 09/04/96 MikeS

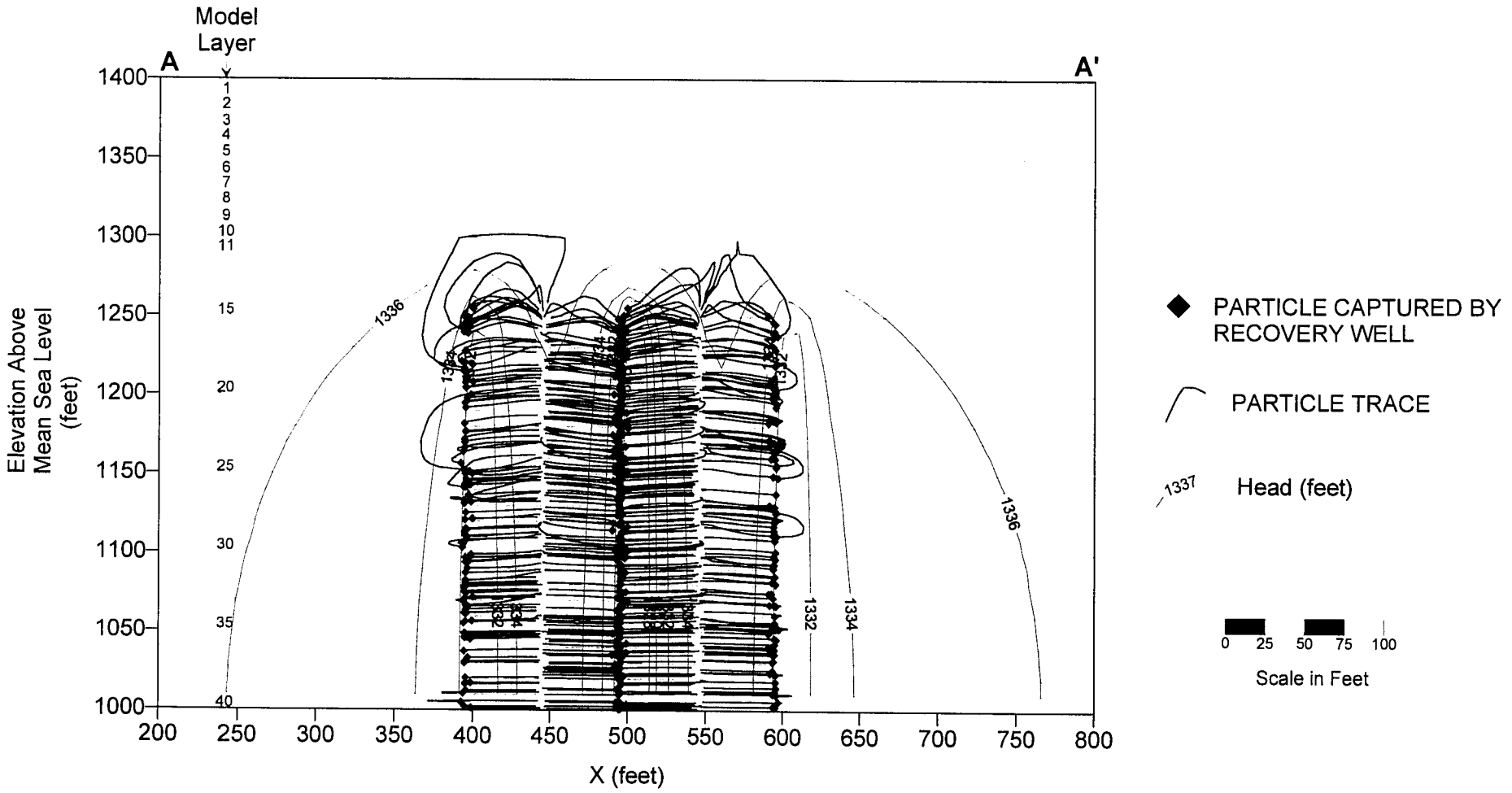

Figure 6 - Attachment 8 to Table 1
PARTICLE PATHS ALONG A VERTICAL PROFILE AT ROW 45

SFIG088 09/04/96 MikeS

BROWN AND CALDWELL

BHP COPPER *Florence Project*

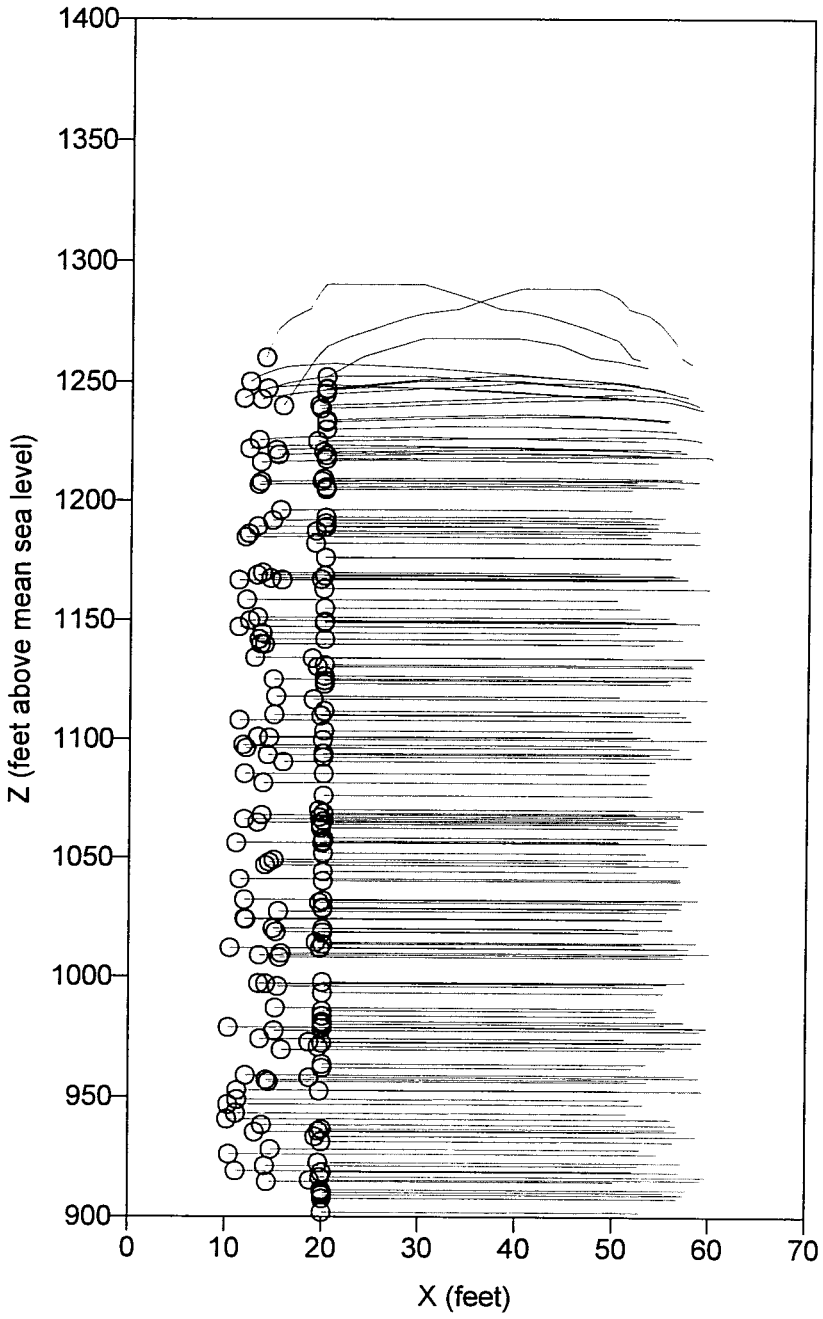

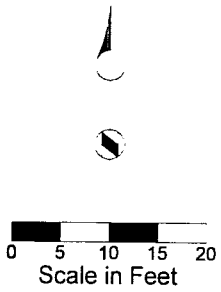

PATHLINE OF PARTICLES RELEASED FROM INJECTION WELL

PARTICLE CAPTURED AT RECOVERY WELL

Simulation Parameters

Two wells 40 feet below contact
Pumping Rate = 0.025 gpm/ft
Oxide Zone = 400 feet
LBFU = 100 feet
Oxide Zone K = 1 ft/day
LBFU K = 20 ft/day

NOTE:
Horizontal Exaggeration = 4:1

Figure 7 - Attachment 8 to Table 1
TWO WELL MODEL PARTICLE PATHS AND CAPTURE ZONES ALONG THE VERTICAL PROFILE FOR AN INTERIOR WELL SET

BROWN AND CALDWELL

BHP COPPER *Florence Project*

S3355001 09/04/96 MikeS

Attachment 9 to Table 1

Attachment 9 to Table 1

Responding to ADEQ-4.3.1.4-Capture Zones for the Town of Florence Municipal Wells

ADEQ-4.3.1.4-Results of Base Simulation-For clarification, BHP should depict the reference capture zones for the Town of Florence Municipal Wells.

Results of Base Simulations

Two Path3D runs were used to determine the capture zones for the Town of Florence Municipal Wells (Figure 1).The first run was used to identify the general area of each well's capture zone. This was accomplished by placing several particles around each municipal well and then noting which trajectories did or did not show capture. The trajectories showing capture thus indicated the general area of each capture zone. The areas were more precisely delineated during the second run, the results of which are shown on Figure 1. Several particles were placed in the general vicinity of the capture zone and the model was then run to see which particles would be captured. As shown on Figure 1, all but two particles were captured at each well. The trajectories of the particles that were captured at each well thus depicts each well's capture zone.

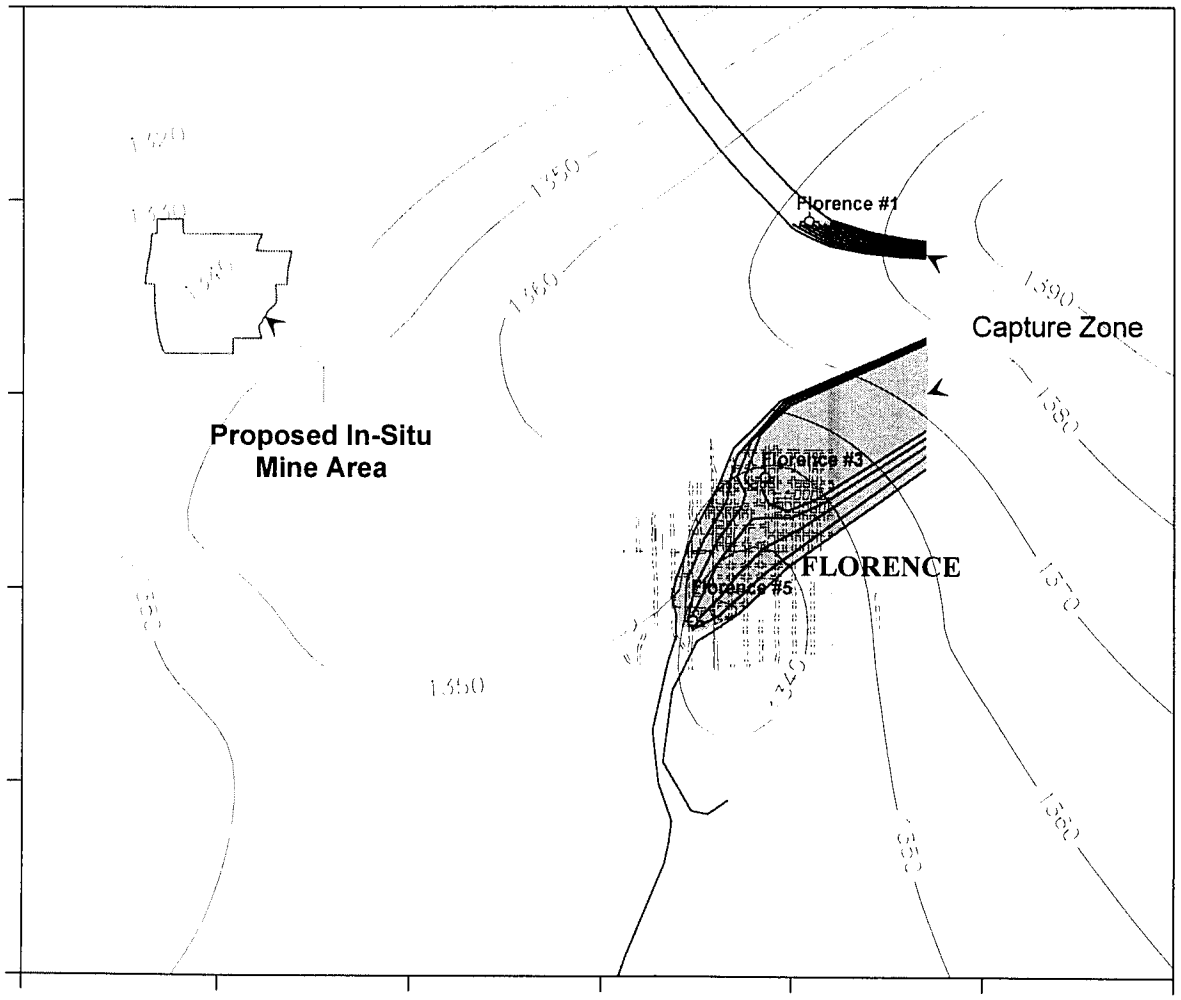

0 2500 5000
Scale in Feet

PARTICLE TRACE

1300 APRIL 1996 WATER LEVEL ELEVATION (FEET ABOVE MEAN SEA LEVEL)

Figure 1 - Attachment 9 to Table 1
CAPTURE ZONES FOR
THE TOWN OF FLORENCE
PUBLIC SUPPLY WELLS

BHP
BHP COPPER *Florence Project*

BROWN AND CALDWELL

SFIG067 08/13/96 MikeS

Attachment 10 to Table 1

Attachment 10 to Table 1

Response to ADEQ Comment-4.4.1-Well Tables and Modeling Scenarios

ADEQ-4.4.1-Rationale-BHP should clarify from which model layers the extraction wells are pumping.

Simulation Scenarios

Table 1 gives a description of the modeling scenarios and sensitivity analysis simulations presented in the APP application. This table references the appropriate section in which the scenario is presented and the figures depicting the results. Table 2 shows the pumping stresses in each scenario for each stress period.

Pumping Rates

The wells included in the base scenario, the closure scenario, and the increased withdrawal scenario are shown in Tables 3 through 5.

Table 1. Description of Modeling Simulations

Simulation Scenarios

	Name of Simulation	Section in APP Volume 4	Relevant Figures in Volume 4	Number of Stress Periods	Total Length of Simulation (days)	Length of Stress Period 1 (days)	Length of Stress Period 2 (days)	Length of Stress Period 3 (days)	Length of Stress Period 4 (days)
1	Base	4.3.1	4.3-8 thru 4.3-15	4	1460	365	365	365	365
2	Increased Withdrawal	4.3.2	4.3-16 thru 4.3-23	4	1460	365	365	365	365
3	Increased Recharge	4.3.3	4.3-24 thru 4.3-31	4	1460	365	365	365	90
4	Geologic Condition 1[(a)]	4.3.4	4.3-32 thru 4.3-39	4	1460	365	365	365	365
5	Geologic Condition 2[(b)]	4.3.4	4.3-40 thru 4.3-47	4	1460	365	365	365	365
6	Geologic Condition 3[(c)]	4.3.4	4.3-48 thru 4.3-55	4	1460	365	365	365	365
7	Block Closure	4.4	4.4-1 thru 4.4-8	4	1460	365	365	365	365
8	Post Closure[(d)]	4.5	4.5-1 thru 4.5-2	3	10950	3650	3650	3650	N/A

Sensitivity Analyses

	Name of Sensitivity Simulation	Section in APP Volume 4	Relevant Figures in Volume 4	Number of Stress Periods	Total Length of Simulation (days)	Length of Stress Period 1 (days)	Length of Stress Period 2 (days)	Length of Stress Period 3 (days)	Length of Stress Period 4 (days)
1	Decreased Storage	2.10.1	2.10-1	4	1460	365	365	365	365
2	Increased Storage	2.10.1	2.10-2	4	1460	365	365	365	365
3	Increase in Eastern General Head Boundaries	2.10.2	2.10-3	4	1460	365	365	365	365
4	Increase in All General Head Boundaries	2.10.2	2.10-4	4	1460	365	365	365	365
5	Increase in Hydraulic Conductivity	2.10.3	2.10-5	4	1460	365	365	365	365
6	Increase in Gila River Bed Conductance	2.10.4	2.10-6	4	1460	365	365	365	90

(a) Horizontal Preferential Pathway in Model Layer 5
(b) North-South Anisotropy in Model Layer 5
(c) East-West Anisotropy in Model Layer 5
(d) The only Simulation involving solute transport

Table 2. Pumping Scenarios Used in Modeling Simulations					
Name of Simulation	Section in APP Volume IV	Stress Period 1	Stress Period 2	Stress Period 3	Stress Period 4
Base	4.3-1	None	Regular	Regular	Regular
Increased Withdrawal	4.3-2	None	Regular	Regular	SCIDD Wells Doubled
Increased Recharge	4.3-3	None	Regular	Regular	Regular
Geologic Condition 1	4.3-4a	None	Regular	Regular	Regular
Geologic Condition 2	4.3-4b	None	Regular	Regular	Regular
Geologic Condition 3	4.3-4c	None	Regular	Regular	Regular
Block Closure	4.4	Closure Wells	Closure Wells	Closure Wells	Closure Wells
Post Closure	4.5	Regular	Regular	Regular	N/A

NOTES:

None: No Pumping Occurs During this Stress Period in the Simulation

Regular: SCIDD Wells, Riggins Wells, Public Supply Wells, and Mine Block 10 Wells Operating. Pumping Rates for SCIDD, Riggins, Public Supply and Block 10 Wells in the Florence Project Area Are Presented in Table 3.

Closure Wells: SCIDD Wells, Riggins Wells, Public Supply Wells and Control Wells Operating. See Table 4.

SCIDD Wells Doubled: Pumping Rates for SCIDD Wells Doubled. All Other Pumping Rates Remain Constant. See Table 5.

Table 3. Modflow Well Package Input Parameters, Base Scenario				
Well Name	Model Layer	Model Row	Model Column	Pumping Rate (ft^3/day)*
28cca	1	84	64	0.00
28cda	1	84	87	0.00
29ccb	1	83	18	-29401.86
29dad	1	79	215	-49281.93
31abb	1	109	208	-46756.33
32bad	1	124	213	-83479.55
32cbb	1	150	211	-100155.83
2aaa	1	156	7	0.00
13cdb	1	170	9	-63295.78
14cad2	1	170	5	-17632.95
23cbb3	1	174	3	-3952.97
24cda2	1	175	10	-6488.19
11cdc	1	166	196	-6716.02
12bbc	1	161	200	-97881.76
12bcb	1	162	200	-111761.65
14cbb	1	169	195	-27604.44
15dbc	1	169	189	-50911.77
19aab2	1	171	17	-62788.07
20dad	1	175	50	-29643.63
20dcc	1	176	24	-69075.64
21dbc	1	175	110	-58262.24
22cba	1	174	171	-7086.83
25bdc (#2) PS	1	40	202	0.00
25bdd (#1) PS	1	49	202	-23666.46
2ada (#5) PS	1	157	199	-39058.43
36cac1 (#4) PS	1	152	201	-858.45
36cac2 (#3) PS	1	152	201	-85046.15
31baa2 Riggins	1	109	15	-52367.76
32bda Riggins	1	136	22	-81884.33
32cbd1 Riggins	1	153	20	-92125.00
BIA9 New	1	94	193	-134428.53
Magma FC	1	87	195	-68744.92
BIA10B New	1	76	196	-110128.82
17bdd1	1	13	22	-148270.89
29dcac	1	17	25	-82383.24
28cca	2	84	64	0.00
28cda	2	84	87	0.00
29ccb	2	83	18	-2579.11
29dad	2	79	215	0.00
31abb	2	109	208	0.00
32bad	2	124	213	0.00
32cbb	2	150	211	0.00
2aaa	2	156	7	0.00
13cdb	2	170	9	-7275.38
14cad2	2	170	5	-2825.79
23cbb3	2	174	3	-4392.19
24cda2	2	175	10	-940.32
11cdc	2	166	196	-861.03
12bbc	2	161	200	-7155.10
12bcb	2	162	200	0.00
14cbb	2	169	195	-3566.46
15dbc	2	169	189	-4139.17
19aab2	2	171	17	-6380.90
20dad	2	175	50	-2470.30
20dcc	2	176	24	-14039.76
21dbc	2	175	110	-14073.01
22cba	2	174	171	-686.71
25bdc (#2) PS	2	40	202	0.00

Well Name	Model Layer	Model Row	Model Column	Pumping Rate (ft^3/day)*
25bdd (#1) PS	2	49	202	-2266.90
2ada (#5) PS	2	157	199	-3254.87
36cac1 (#4) PS	2	152	201	-77.34
36cac2 (#3) PS	2	152	201	-7661.82
31baa2 Riggins	2	109	15	0.00
32bda Riggins	2	136	22	-7182.84
32cbd1 Riggins	2	153	20	-4125.00
BIA9 New	2	94	193	0.00
Magma FC	2	87	195	-7116.45
BIA10B New	2	76	196	-11330.13
17bdd1	2	13	22	-35302.59
29dcac	2	17	25	-10095.98
28cca	3	84	64	0.00
28cda	3	84	87	0.00
29ccb	3	83	18	-1134.81
29dad	3	79	215	0.00
31abb	3	109	208	0.00
32bad	3	124	213	0.00
32cbb	3	150	211	0.00
2aaa	3	156	7	0.00
13cdb	3	170	9	-7275.38
14cad2	3	170	5	-2825.79
23cbb3	3	174	3	-4392.19
24cda2	3	175	10	-940.32
11cdc	3	166	196	-861.03
12bbc	3	161	200	-7155.10
12bcb	3	162	200	0.00
14cbb	3	169	195	-3566.46
15dbc	3	169	189	-2069.58
19aab2	3	171	17	-6380.90
20dad	3	175	50	-2470.30
20dcc	3	176	24	-14039.76
21dbc	3	175	110	-14073.01
22cba	3	174	171	-686.71
25bdc (#2) PS	3	40	202	0.00
25bdd (#1) PS	3	49	202	-2266.90
2ada (#5) PS	3	157	199	-3254.87
36cac1 (#4) PS	3	152	201	-77.34
36cac2 (#3) PS	3	152	201	-7661.82
31baa2 Riggins	3	109	15	-1629.22
32bda Riggins	3	136	22	-7182.84
32cbd1 Riggins	3	153	20	0.00
BIA9 New	3	94	193	0.00
Magma FC	3	87	195	-1138.63
BIA10B New	3	76	196	-11330.13
17bdd1	3	13	22	-35302.59
29dcac	3	17	25	-10095.98
Perimeter	3	70	73	-300.78125
Perimeter	3	72	73	-601.5625
Perimeter	3	74	73	-601.5625
Perimeter	3	76	73	-300.78125
Perimeter	3	70	75	-601.5625
Perimeter	3	74	75	-902.34375
Perimeter	3	76	75	-300.78125
Perimeter	3	70	77	-300.78125
Perimeter	3	72	77	-601.5625
Perimeter	3	74	77	-300.78125
Perimeter	4	72	71	-300.78125
Perimeter	4	74	71	-601.5625

Well Name	Model Layer	Model Row	Model Column	Pumping Rate (ft^3/day)*
Perimeter	4	76	71	-300.78125
Perimeter	4	70	73	-300.78125
Perimeter	4	72	73	-902.34375
Perimeter	4	76	73	-902.34375
Perimeter	4	78	73	-300.78125
Perimeter	4	70	75	-601.5625
Perimeter	4	76	75	-902.34375
Perimeter	4	78	75	-300.78125
Perimeter	4	70	77	-601.5625
Perimeter	4	74	77	-902.34375
Perimeter	4	76	77	-300.78125
Perimeter	4	70	79	-300.78125
Perimeter	4	72	79	-601.5625
Perimeter	4	74	79	-300.78125
Perimeter	5	70	69	-902.34375
Perimeter	5	72	69	-1804.6875
Perimeter	5	74	69	-1804.6875
Perimeter	5	76	69	-902.34375
Perimeter	5	68	71	-902.34375
Perimeter	5	70	71	-2707.03125
Perimeter	5	76	71	-1804.6875
Perimeter	5	68	73	-1804.6875
Perimeter	5	76	73	-2707.03125
Perimeter	5	78	73	-1804.6875
Perimeter	5	80	73	-1804.6875
Perimeter	5	82	73	-902.34375
Perimeter	5	68	75	-1804.6875
Perimeter	5	82	75	-1804.6875
Perimeter	5	68	77	-1804.6875
Perimeter	5	82	77	-1804.6875
Perimeter	5	68	79	-902.34375
Perimeter	5	70	79	-1804.6875
Perimeter	5	72	79	-2707.03125
Perimeter	5	76	79	-902.34375
Perimeter	5	78	79	-1804.6875
Perimeter	5	80	79	-1804.6875
Perimeter	5	82	79	-902.34375
Perimeter	5	72	81	-902.34375
Perimeter	5	74	81	-1804.6875
Perimeter	5	76	81	-902.34375
Perimeter	6	64	69	-1203.125
Perimeter	6	66	69	-2406.25
Perimeter	6	68	69	-2406.25
Perimeter	6	70	69	-2406.25
Perimeter	6	72	69	-2406.25
Perimeter	6	74	69	-2406.25
Perimeter	6	76	69	-1203.125
Perimeter	6	64	71	-2406.25
Perimeter	6	76	71	-2406.25
Perimeter	6	64	73	-2406.25
Perimeter	6	76	73	-3609.375
Perimeter	6	78	73	-2406.25
Perimeter	6	80	73	-2406.25
Perimeter	6	82	73	-1203.125
Perimeter	6	64	75	-2406.25
Perimeter	6	82	75	-2406.25
Perimeter	6	64	77	-1203.125
Perimeter	6	66	77	-2406.25
Perimeter	6	68	77	-3609.375

Well Name	Model Layer	Model Row	Model Column	Pumping Rate (ft^3/day)*
Perimeter	6	82	77	-2406.25
Perimeter	6	68	79	-1203.125
Perimeter	6	70	79	-2406.25
Perimeter	6	72	79	-3609.375
Perimeter	6	82	79	-2406.25
Perimeter	6	72	81	-1203.125
Perimeter	6	74	81	-2406.25
Perimeter	6	76	81	-2406.25
Perimeter	6	78	81	-3609.375
Perimeter	6	82	81	-2406.25
Perimeter	6	78	83	-1203.125
Perimeter	6	80	83	-2406.25
Perimeter	6	82	83	-1203.125
Perimeter	7	64	69	-2406.25
Perimeter	7	66	69	-4812.5
Perimeter	7	68	69	-4812.5
Perimeter	7	70	69	-4812.5
Perimeter	7	72	69	-4812.5
Perimeter	7	74	69	-4812.5
Perimeter	7	76	69	-2406.25
Perimeter	7	64	71	-4812.5
Perimeter	7	76	71	-4812.5
Perimeter	7	64	73	-4812.5
Perimeter	7	76	73	-7218.75
Perimeter	7	78	73	-4812.5
Perimeter	7	80	73	-4812.5
Perimeter	7	82	73	-2406.25
Perimeter	7	64	75	-4812.5
Perimeter	7	82	75	-4812.5
Perimeter	7	64	77	-2406.25
Perimeter	7	66	77	-4812.5
Perimeter	7	68	77	-7218.75
Perimeter	7	82	77	-4812.5
Perimeter	7	68	79	-2406.25
Perimeter	7	70	79	-4812.5
Perimeter	7	72	79	-7218.75
Perimeter	7	82	79	-4812.5
Perimeter	7	72	81	-2406.25
Perimeter	7	74	81	-4812.5
Perimeter	7	76	81	-4812.5
Perimeter	7	78	81	-7218.75
Perimeter	7	82	81	-4812.5
Perimeter	7	78	83	-2406.25
Perimeter	7	80	83	-4812.5
Perimeter	7	82	83	-2406.25
Perimeter	8	64	69	-1804.6875
Perimeter	8	66	69	-3609.375
Perimeter	8	68	69	-3609.375
Perimeter	8	70	69	-3609.375
Perimeter	8	72	69	-3609.375
Perimeter	8	74	69	-3609.375
Perimeter	8	76	69	-1804.6875
Perimeter	8	64	71	-3609.375
Perimeter	8	76	71	-3609.375
Perimeter	8	64	73	-3609.375
Recovery	3	72	75	-962.5
Injection	3	71	74	962.5
Injection	3	73	74	962.5
Injection	3	75	74	962.5

Well Name	Model Layer	Model Row	Model Column	Pumping Rate (ft^3/day)*
Injection	3	71	76	962.5
Injection	3	73	76	962.5
Recovery	4	74	73	-962.5
Recovery	4	72	75	-962.5
Recovery	4	74	75	-962.5
Recovery	4	72	77	-962.5
Injection	4	73	72	962.5
Injection	4	75	72	962.5
Injection	4	71	74	962.5
Injection	4	73	74	962.5
Injection	4	75	74	962.5
Injection	4	77	74	962.5
Injection	4	71	76	962.5
Injection	4	73	76	962.5
Injection	4	75	76	962.5
Injection	4	71	78	962.5
Injection	4	73	78	962.5
Recovery	5	72	71	-2887.5
Recovery	5	74	71	-2887.5
Recovery	5	70	73	-2887.5
Recovery	5	72	73	-2887.5
Recovery	5	74	73	-2887.5
Recovery	5	70	75	-2887.5
Recovery	5	72	75	-2887.5
Recovery	5	74	75	-2887.5
Recovery	5	76	75	-2887.5
Recovery	5	78	75	-2887.5
Recovery	5	80	75	-2887.5
Recovery	5	70	77	-2887.5
Recovery	5	72	77	-2887.5
Recovery	5	74	77	-2887.5
Recovery	5	76	77	-2887.5
Recovery	5	78	77	-2887.5
Recovery	5	80	77	-2887.5
Recovery	5	74	79	-2887.5
Injection	5	71	70	2887.5
Injection	5	73	70	2887.5
Injection	5	75	70	2887.5
Injection	5	69	72	2887.5
Injection	5	71	72	2887.5
Injection	5	73	72	2887.5
Injection	5	75	72	2887.5
Injection	5	69	74	2887.5
Injection	5	71	74	2887.5
Injection	5	73	74	2887.5
Injection	5	75	74	2887.5
Injection	5	77	74	2887.5
Injection	5	79	74	2887.5
Injection	5	81	74	2887.5
Injection	5	69	76	2887.5
Injection	5	71	76	2887.5
Injection	5	73	76	2887.5
Injection	5	75	76	2887.5
Injection	5	77	76	2887.5
Injection	5	79	76	2887.5
Injection	5	81	76	2887.5
Injection	5	69	78	2887.5
Injection	5	71	78	2887.5
Injection	5	73	78	2887.5

Well Name	Model Layer	Model Row	Model Column	Pumping Rate (ft^3/day)*
Injection	5	75	78	2887.5
Injection	5	77	78	2887.5
Injection	5	79	78	2887.5
Injection	5	81	78	2887.5
Injection	5	73	80	2887.5
Injection	5	75	80	2887.5
Recovery	6	66	71	-3850
Recovery	6	68	71	-3850
Recovery	6	70	71	-3850
Recovery	6	72	71	-3850
Recovery	6	74	71	-3850
Recovery	6	66	73	-3850
Recovery	6	68	73	-3850
Recovery	6	70	73	-3850
Recovery	6	72	73	-3850
Recovery	6	74	73	-3850
Recovery	6	66	75	-3850
Recovery	6	68	75	-3850
Recovery	6	70	75	-3850
Recovery	6	72	75	-3850
Recovery	6	74	75	-3850
Recovery	6	76	75	-3850
Recovery	6	78	75	-3850
Recovery	6	80	75	-3850
Recovery	6	70	77	-3850
Recovery	6	72	77	-3850
Recovery	6	74	77	-3850
Recovery	6	76	77	-3850
Recovery	6	78	77	-3850
Recovery	6	80	77	-3850
Recovery	6	74	79	-3850
Recovery	6	76	79	-3850
Recovery	6	78	79	-3850
Recovery	6	80	79	-3850
Recovery	6	80	81	-3850
Injection	6	65	70	3850
Injection	6	67	70	3850
Injection	6	69	70	3850
Injection	6	71	70	3850
Injection	6	73	70	3850
Injection	6	75	70	3850
Injection	6	65	72	3850
Injection	6	67	72	3850
Injection	6	69	72	3850
Injection	6	71	72	3850
Injection	6	73	72	3850
Injection	6	75	72	3850
Injection	6	65	74	3850
Injection	6	67	74	3850
Injection	6	69	74	3850
Injection	6	71	74	3850
Injection	6	73	74	3850
Injection	6	75	74	3850
Injection	6	77	74	3850
Injection	6	79	74	3850
Injection	6	81	74	3850
Injection	6	65	76	3850
Injection	6	67	76	3850
Injection	6	69	76	3850

Well Name	Model Layer	Model Row	Model Column	Pumping Rate (ft^3/day)*
Injection	6	71	76	3850
Injection	6	73	76	3850
Injection	6	75	76	3850
Injection	6	77	76	3850
Injection	6	79	76	3850
Injection	6	81	76	3850
Injection	6	69	78	3850
Injection	6	71	78	3850
Injection	6	73	78	3850
Injection	6	75	78	3850
Injection	6	77	78	3850
Injection	6	79	78	3850
Injection	6	81	78	3850
Injection	6	73	80	3850
Injection	6	75	80	3850
Injection	6	77	80	3850
Injection	6	79	80	3850
Injection	6	81	80	3850
Injection	6	79	82	3850
Injection	6	81	82	3850
Recovery	7	66	71	-7700
Recovery	7	68	71	-7700
Recovery	7	70	71	-7700
Recovery	7	72	71	-7700
Recovery	7	74	71	-7700
Recovery	7	66	73	-7700
Recovery	7	68	73	-7700
Recovery	7	70	73	-7700
Recovery	7	72	73	-7700
Recovery	7	74	73	-7700
Recovery	7	66	75	-7700
Recovery	7	68	75	-7700
Recovery	7	70	75	-7700
Recovery	7	72	75	-7700
Recovery	7	74	75	-7700
Recovery	7	76	75	-7700
Recovery	7	78	75	-7700
Recovery	7	80	75	-7700
Recovery	7	70	77	-7700
Recovery	7	72	77	-7700
Recovery	7	74	77	-7700
Recovery	7	76	77	-7700
Recovery	7	78	77	-7700
Recovery	7	80	77	-7700
Recovery	7	74	79	-7700
Recovery	7	76	79	-7700
Recovery	7	78	79	-7700
Recovery	7	80	79	-7700
Recovery	7	80	81	-7700
Injection	7	65	70	7700
Injection	7	67	70	7700
Injection	7	69	70	7700
Injection	7	71	70	7700
Injection	7	73	70	7700
Injection	7	75	70	7700
Injection	7	65	72	7700
Injection	7	67	72	7700
Injection	7	69	72	7700
Injection	7	71	72	7700

Well Name	Model Layer	Model Row	Model Column	Pumping Rate (ft^3/day)*
Injection	7	73	72	7700
Injection	7	75	72	7700
Injection	7	65	74	7700
Injection	7	67	74	7700
Injection	7	69	74	7700
Injection	7	71	74	7700
Injection	7	73	74	7700
Injection	7	75	74	7700
Injection	7	77	74	7700
Injection	7	79	74	7700
Injection	7	81	74	7700
Injection	7	65	76	7700
Injection	7	67	76	7700
Injection	7	69	76	7700
Injection	7	71	76	7700
Injection	7	73	76	7700
Injection	7	75	76	7700
Injection	7	77	76	7700
Injection	7	79	76	7700
Injection	7	81	76	7700
Injection	7	69	78	7700
Injection	7	71	78	7700
Injection	7	73	78	7700
Injection	7	75	78	7700
Injection	7	77	78	7700
Injection	7	79	78	7700
Injection	7	81	78	7700
Injection	7	73	80	7700
Injection	7	75	80	7700
Injection	7	77	80	7700
Injection	7	79	80	7700
Injection	7	81	80	7700
Injection	7	79	82	7700
Injection	7	81	82	7700
Recovery	8	66	71	-3850
Recovery	8	68	71	-3850
Recovery	8	70	71	-3850
Recovery	8	72	71	-3850
Recovery	8	74	71	-3850
Recovery	8	66	73	-3850
Recovery	8	68	73	-3850
Recovery	8	70	73	-3850
Injection	8	65	70	5775
Injection	8	67	70	5775
Injection	8	69	70	5775
Injection	8	71	70	5775
Injection	8	73	70	5775
Injection	8	75	70	5775
Injection	8	65	72	5775
Injection	8	67	72	5775
Injection	8	69	72	5775

* Negative Values Indicate Extraction

Table 4. Modflow Well Package Input Parameters, Closure Scenario				
Well Name	Model Layer	Model Row	Model Column	Pumping Rate (ft^3/day)*
28cca	1	84	64	0.00
28cda	1	84	87	0.00
29ccb	1	83	18	-29401.26
29dad	1	79	215	-49299.10
31abb	1	109	208	-46755.50
32bad	1	124	213	-83479.40
32cbb	1	150	211	-100156.20
2aaa	1	156	7	0.00
13cdb	1	170	9	-63295.63
14cad2	1	170	5	-17632.42
23cbb3	1	174	3	-3953.11
24cda2	1	175	10	-6488.15
11cdc	1	166	196	-6716.55
12bbc	1	161	200	-97882.60
12bcb	1	162	200	-111761.60
14cbb	1	169	195	-27604.15
15dbc	1	169	189	-50912.02
19aab2	1	171	17	-62788.50
20dad	1	175	50	-29644.00
20dcc	1	176	24	-69075.54
21dbc	1	175	110	-58262.23
22cba	1	174	171	-7087.07
25bdc (#2) PS	1	40	202	0.00
25bdd (#1) PS	1	49	202	-23666.46
2ada (#5) PS	1	157	199	-39058.43
36cac1 (#4) PS	1	152	201	-858.45
36cac2 (#3) PS	1	152	201	-85046.15
31baa2 Riggins	1	109	15	-52367.76
32bda Riggins	1	136	22	-81884.33
32cbd1 Riggins	1	153	20	-92125.00
BIA9 New	1	94	193	-134429.17
Magma FC	1	87	195	-68744.92
BIA10B New	1	76	196	-110128.33
17bdd1	1	13	22	-148270.89
29dcac	1	17	25	-82383.24
28cca	2	84	64	0.00
28cda	2	84	87	0.00
29ccb	2	83	18	-2579.06
29dad	2	79	215	0.00
31abb	2	109	208	0.00
32bad	2	124	213	0.00
32cbb	2	150	211	0.00
2aaa	2	156	7	0.00
13cdb	2	170	9	-7275.36
14cad2	2	170	5	-2825.71
23cbb3	2	174	3	-4392.35
24cda2	2	175	10	-940.31
11cdc	2	166	196	-861.10
12bbc	2	161	200	-7155.16
12bcb	2	162	200	0.00
14cbb	2	169	195	-3566.43
15dbc	2	169	189	-4139.19
19aab2	2	171	17	-6380.95
20dad	2	175	50	-2470.33
20dcc	2	176	24	-14039.74
21dbc	2	175	110	-14073.00
22cba	2	174	171	-686.73
25bdc (#2) PS	2	40	202	0.00

Well Name	Model Layer	Model Row	Model Column	Pumping Rate (ft^3/day)*
25bdd (#1) PS	2	49	202	-2266.90
2ada (#5) PS	2	157	199	-3254.87
36cac1 (#4) PS	2	152	201	-77.34
36cac2 (#3) PS	2	152	201	-7661.82
31baa2 Riggins	2	109	15	0.00
32bda Riggins	2	136	22	-7182.84
32cbd1 Riggins	2	153	20	-4125.00
BIA9 New	2	94	193	0.00
Magma FC	2	87	195	-7116.45
BIA10B New	2	76	196	-11330.07
17bdd1	2	13	22	-35302.59
29dcac	2	17	25	-10095.98
28cca	3	84	64	0.00
28cda	3	84	87	0.00
29ccb	3	83	18	-1134.79
29dad	3	79	215	0.00
31abb	3	109	208	0.00
32bad	3	124	213	0.00
32cbb	3	150	211	0.00
2aaa	3	156	7	0.00
13cdb	3	170	9	-7275.36
14cad2	3	170	5	-2825.71
23cbb3	3	174	3	-4392.35
24cda2	3	175	10	-940.31
11cdc	3	166	196	-861.10
12bbc	3	161	200	-7155.16
12bcb	3	162	200	0.00
14cbb	3	169	195	-3566.43
15dbc	3	169	189	-2069.59
19aab2	3	171	17	-6380.95
20dad	3	175	50	-2470.33
20dcc	3	176	24	-14039.74
21dbc	3	175	110	-14073.00
22cba	3	174	171	-686.73
25bdc (#2) PS	3	40	202	0.00
25bdd (#1) PS	3	49	202	-2266.90
2ada (#5) PS	3	157	199	-3254.87
36cac1 (#4) PS	3	152	201	-77.34
36cac2 (#3) PS	3	152	201	-7661.82
31baa2 Riggins	3	109	15	-1629.22
32bda Riggins	3	136	22	-7182.84
32cbd1 Riggins	3	153	20	0.00
BIA9 New	3	94	193	0.00
Magma FC	3	87	195	-1138.63
BIA10B New	3	76	196	-11330.07
17bdd1	3	13	22	-35302.59
29dcac	3	17	25	-10095.98
control well 1	3	57	116	-6737.5
control well 1	4	57	116	-6737.5
control well 2	6	57	82	-2695
control well 3	7	47	72	-5390
control well 4	4	71	74	-8927.19
control well 4	5	71	74	-26781.56
control well 4	6	71	74	-35708.75
control well 5	3	57	94	-693
control well 5	4	57	94	-693
control well 5	5	57	94	-2079

* Negative Values Indicate Extraction

Table 5. Modflow Well Package Input Parameters, SCIDD Wells Doubled				
Well Name	Model Layer	Model Row	Model Column	Pumping Rate (ft^3/day)*
28cca	1	84	64	0.00
28cda	1	84	87	0.00
29ccb	1	83	18	-58803.71
29dad	1	79	215	-98563.85
31abb	1	109	208	-93512.65
32bad	1	124	213	-166959.10
32cbb	1	150	211	-200311.65
2aaa	1	156	7	0.00
13cdb	1	170	9	-126591.57
14cad2	1	170	5	-35265.90
23cbb3	1	174	3	-7905.94
24cda2	1	175	10	-12976.38
11cdc	1	166	196	-13432.04
12bbc	1	161	200	-195763.52
12bcb	1	162	200	-223523.30
14cbb	1	169	195	-55208.87
15dbc	1	169	189	-101823.54
19aab2	1	171	17	-125576.14
20dad	1	175	50	-59287.26
20dcc	1	176	24	-138151.28
21dbc	1	175	110	-116524.48
22cba	1	174	171	-14173.65
25bdc (#2) PS	1	40	202	0.00
25bdd (#1) PS	1	49	202	-47332.92
2ada (#5) PS	1	157	199	-78116.85
36cac1 (#4) PS	1	152	201	-1716.89
36cac2 (#3) PS	1	152	201	-170092.30
31baa2 Riggins	1	109	15	-104735.52
32bda Riggins	1	136	22	-163768.66
32cbd1 Riggins	1	153	20	-184250.00
BIA9 New	1	94	193	-268857.05
Magma FC	1	87	195	-137489.83
BIA10B New	1	76	196	-220257.64
17bdd1	1	13	22	-296541.79
29dcac	1	17	25	-164766.47
28cca	2	84	64	0.00
28cda	2	84	87	0.00
29ccb	2	83	18	-5158.22
29dad	2	79	215	0.00
31abb	2	109	208	0.00
32bad	2	124	213	0.00
32cbb	2	150	211	0.00
2aaa	2	156	7	0.00
13cdb	2	170	9	-14550.75
14cad2	2	170	5	-5651.59
23cbb3	2	174	3	-8784.37
24cda2	2	175	10	-1880.63
11cdc	2	166	196	-1722.06
12bbc	2	161	200	-14310.20
12bcb	2	162	200	0.00
14cbb	2	169	195	-7132.93
15dbc	2	169	189	-8278.34
19aab2	2	171	17	-12761.80
20dad	2	175	50	-4940.60
20dcc	2	176	24	-28079.53
21dbc	2	175	110	-28146.01
22cba	2	174	171	-1373.42
25bdc (#2) PS	2	40	202	0.00

Well Name	Model Layer	Model Row	Model Column	Pumping Rate (ft^3/day)*
25bdd (#1) PS	2	49	202	-4533.80
2ada (#5) PS	2	157	199	-6509.74
36cac1 (#4) PS	2	152	201	-154.68
36cac2 (#3) PS	2	152	201	-15323.63
31baa2 Riggins	2	109	15	0.00
32bda Riggins	2	136	22	-14365.67
32cbd1 Riggins	2	153	20	-8250.00
BIA9 New	2	94	193	0.00
Magma FC	2	87	195	-14232.90
BIA10B New	2	76	196	-22660.25
17bdd1	2	13	22	-70605.19
29dcac	2	17	25	-20191.97
28cca	3	84	64	0.00
28cda	3	84	87	0.00
29ccb	3	83	18	-2269.62
29dad	3	79	215	0.00
31abb	3	109	208	0.00
32bad	3	124	213	0.00
32cbb	3	150	211	0.00
2aaa	3	156	7	0.00
13cdb	3	170	9	-14550.75
14cad2	3	170	5	-5651.59
23cbb3	3	174	3	-8784.37
24cda2	3	175	10	-1880.63
11cdc	3	166	196	-1722.06
12bbc	3	161	200	-14310.20
12bcb	3	162	200	0.00
14cbb	3	169	195	-7132.93
15dbc	3	169	189	-4139.17
19aab2	3	171	17	-12761.80
20dad	3	175	50	-4940.60
20dcc	3	176	24	-28079.53
21dbc	3	175	110	-28146.01
22cba	3	174	171	-1373.42
25bdc (#2) PS	3	40	202	0.00
25bdd (#1) PS	3	49	202	-4533.80
2ada (#5) PS	3	157	199	-6509.74
36cac1 (#4) PS	3	152	201	-154.68
36cac2 (#3) PS	3	152	201	-15323.63
31baa2 Riggins	3	109	15	-3258.44
32bda Riggins	3	136	22	-14365.67
32cbd1 Riggins	3	153	20	0.00
BIA9 New	3	94	193	0.00
Magma FC	3	87	195	-2277.26
BIA10B New	3	76	196	-22660.25
17bdd1	3	13	22	-70605.19
29dcac	3	17	25	-20191.97
Perimeter	3	70	73	-300.78125
Perimeter	3	72	73	-601.5625
Perimeter	3	74	73	-601.5625
Perimeter	3	76	73	-300.78125
Perimeter	3	70	75	-601.5625
Perimeter	3	74	75	-902.34375
Perimeter	3	76	75	-300.78125
Perimeter	3	70	77	-300.78125
Perimeter	3	72	77	-601.5625
Perimeter	3	74	77	-300.78125
Perimeter	4	72	71	-300.78125
Perimeter	4	74	71	-601.5625

Well Name	Model Layer	Model Row	Model Column	Pumping Rate (ft^3/day)*
Perimeter	4	76	71	-300.78125
Perimeter	4	70	73	-300.78125
Perimeter	4	72	73	-902.34375
Perimeter	4	76	73	-902.34375
Perimeter	4	78	73	-300.78125
Perimeter	4	70	75	-601.5625
Perimeter	4	76	75	-902.34375
Perimeter	4	78	75	-300.78125
Perimeter	4	70	77	-601.5625
Perimeter	4	74	77	-902.34375
Perimeter	4	76	77	-300.78125
Perimeter	4	70	79	-300.78125
Perimeter	4	72	79	-601.5625
Perimeter	4	74	79	-300.78125
Perimeter	5	70	69	-902.34375
Perimeter	5	72	69	-1804.6875
Perimeter	5	74	69	-1804.6875
Perimeter	5	76	69	-902.34375
Perimeter	5	68	71	-902.34375
Perimeter	5	70	71	-2707.0313
Perimeter	5	76	71	-1804.6875
Perimeter	5	68	73	-1804.6875
Perimeter	5	76	73	-2707.0313
Perimeter	5	78	73	-1804.6875
Perimeter	5	80	73	-1804.6875
Perimeter	5	82	73	-902.34375
Perimeter	5	68	75	-1804.6875
Perimeter	5	82	75	-1804.6875
Perimeter	5	68	77	-1804.6875
Perimeter	5	82	77	-1804.6875
Perimeter	5	68	79	-902.34375
Perimeter	5	70	79	-1804.6875
Perimeter	5	72	79	-2707.0313
Perimeter	5	76	79	-2707.0313
Perimeter	5	78	79	-1804.6875
Perimeter	5	80	79	-1804.6875
Perimeter	5	82	79	-902.34375
Perimeter	5	72	81	-902.34375
Perimeter	5	74	81	-1804.6875
Perimeter	5	76	81	-902.34375
Perimeter	6	64	69	-1203.125
Perimeter	6	66	69	-2406.25
Perimeter	6	68	69	-2406.25
Perimeter	6	70	69	-2406.25
Perimeter	6	72	69	-2406.25
Perimeter	6	74	69	-2406.25
Perimeter	6	76	69	-1203.125
Perimeter	6	64	71	-2406.25
Perimeter	6	76	71	-2406.25
Perimeter	6	64	73	-2406.25
Perimeter	6	76	73	-3609.375
Perimeter	6	78	73	-2406.25
Perimeter	6	80	73	-2406.25
Perimeter	6	82	73	-1203.125
Perimeter	6	64	75	-2406.25
Perimeter	6	82	75	-2406.25
Perimeter	6	64	77	-1203.125
Perimeter	6	66	77	-2406.25
Perimeter	6	68	77	-3609.375

Well Name	Model Layer	Model Row	Model Column	Pumping Rate (ft^3/day)*
Perimeter	6	82	77	-2406.25
Perimeter	6	68	79	-1203.125
Perimeter	6	70	79	-2406.25
Perimeter	6	72	79	-3609.375
Perimeter	6	82	79	-2406.25
Perimeter	6	72	81	-1203.125
Perimeter	6	74	81	-2406.25
Perimeter	6	76	81	-2406.25
Perimeter	6	78	81	-3609.375
Perimeter	6	82	81	-2406.25
Perimeter	6	78	83	-1203.125
Perimeter	6	80	83	-2406.25
Perimeter	6	82	83	-1203.125
Perimeter	7	64	69	-2406.25
Perimeter	7	66	69	-4812.5
Perimeter	7	68	69	-4812.5
Perimeter	7	70	69	-4812.5
Perimeter	7	72	69	-4812.5
Perimeter	7	74	69	-4812.5
Perimeter	7	76	69	-2406.25
Perimeter	7	64	71	-4812.5
Perimeter	7	76	71	-4812.5
Perimeter	7	64	73	-4812.5
Perimeter	7	76	73	-7218.75
Perimeter	7	78	73	-4812.5
Perimeter	7	80	73	-4812.5
Perimeter	7	82	73	-2406.25
Perimeter	7	64	75	-4812.5
Perimeter	7	82	75	-4812.5
Perimeter	7	64	77	-2406.25
Perimeter	7	66	77	-4812.5
Perimeter	7	68	77	-7218.75
Perimeter	7	82	77	-4812.5
Perimeter	7	68	79	-2406.25
Perimeter	7	70	79	-4812.5
Perimeter	7	72	79	-7218.75
Perimeter	7	82	79	-4812.5
Perimeter	7	72	81	-2406.25
Perimeter	7	74	81	-4812.5
Perimeter	7	76	81	-4812.5
Perimeter	7	78	81	-7218.75
Perimeter	7	82	81	-4812.5
Perimeter	7	78	83	-2406.25
Perimeter	7	80	83	-4812.5
Perimeter	7	82	83	-2406.25
Perimeter	8	64	69	-1804.6875
Perimeter	8	66	69	-3609.375
Perimeter	8	68	69	-3609.375
Perimeter	8	70	69	-3609.375
Perimeter	8	72	69	-3609.375
Perimeter	8	74	69	-3609.375
Perimeter	8	76	69	-1804.6875
Perimeter	8	64	71	-3609.375
Perimeter	8	76	71	-3609.375
Perimeter	8	64	73	-3609.375
Recovery	3	72	75	-962.5
Injection	3	71	74	962.5
Injection	3	73	74	962.5
Injection	3	75	74	962.5

Well Name	Model Layer	Model Row	Model Column	Pumping Rate (ft^3/day)*
Injection	3	71	76	962.5
Injection	3	73	76	962.5
Recovery	4	74	73	-962.5
Recovery	4	72	75	-962.5
Recovery	4	74	75	-962.5
Recovery	4	72	77	-962.5
Injection	4	73	72	962.5
Injection	4	75	72	962.5
Injection	4	71	74	962.5
Injection	4	73	74	962.5
Injection	4	75	74	962.5
Injection	4	77	74	962.5
Injection	4	71	76	962.5
Injection	4	73	76	962.5
Injection	4	75	76	962.5
Injection	4	71	78	962.5
Injection	4	73	78	962.5
Recovery	5	72	71	-2887.5
Recovery	5	74	71	-2887.5
Recovery	5	70	73	-2887.5
Recovery	5	72	73	-2887.5
Recovery	5	74	73	-2887.5
Recovery	5	70	75	-2887.5
Recovery	5	72	75	-2887.5
Recovery	5	74	75	-2887.5
Recovery	5	76	75	-2887.5
Recovery	5	78	75	-2887.5
Recovery	5	80	75	-2887.5
Recovery	5	70	77	-2887.5
Recovery	5	72	77	-2887.5
Recovery	5	74	77	-2887.5
Recovery	5	76	77	-2887.5
Recovery	5	78	77	-2887.5
Recovery	5	80	77	-2887.5
Recovery	5	74	79	-2887.5
Injection	5	71	70	2887.5
Injection	5	73	70	2887.5
Injection	5	75	70	2887.5
Injection	5	69	72	2887.5
Injection	5	71	72	2887.5
Injection	5	73	72	2887.5
Injection	5	75	72	2887.5
Injection	5	69	74	2887.5
Injection	5	71	74	2887.5
Injection	5	73	74	2887.5
Injection	5	75	74	2887.5
Injection	5	77	74	2887.5
Injection	5	79	74	2887.5
Injection	5	81	74	2887.5
Injection	5	69	76	2887.5
Injection	5	71	76	2887.5
Injection	5	73	76	2887.5
Injection	5	75	76	2887.5
Injection	5	77	76	2887.5
Injection	5	79	76	2887.5
Injection	5	81	76	2887.5
Injection	5	69	78	2887.5
Injection	5	71	78	2887.5
Injection	5	73	78	2887.5

Well Name	Model Layer	Model Row	Model Column	Pumping Rate (ft^3/day)*
Injection	5	75	78	2887.5
Injection	5	77	78	2887.5
Injection	5	79	78	2887.5
Injection	5	81	78	2887.5
Injection	5	73	80	2887.5
Injection	5	75	80	2887.5
Recovery	6	66	71	-3850
Recovery	6	68	71	-3850
Recovery	6	70	71	-3850
Recovery	6	72	71	-3850
Recovery	6	74	71	-3850
Recovery	6	66	73	-3850
Recovery	6	68	73	-3850
Recovery	6	70	73	-3850
Recovery	6	72	73	-3850
Recovery	6	74	73	-3850
Recovery	6	66	75	-3850
Recovery	6	68	75	-3850
Recovery	6	70	75	-3850
Recovery	6	72	75	-3850
Recovery	6	74	75	-3850
Recovery	6	76	75	-3850
Recovery	6	78	75	-3850
Recovery	6	80	75	-3850
Recovery	6	70	77	-3850
Recovery	6	72	77	-3850
Recovery	6	74	77	-3850
Recovery	6	76	77	-3850
Recovery	6	78	77	-3850
Recovery	6	80	77	-3850
Recovery	6	74	79	-3850
Recovery	6	76	79	-3850
Recovery	6	78	79	-3850
Recovery	6	80	79	-3850
Recovery	6	80	81	-3850
Injection	6	65	70	3850
Injection	6	67	70	3850
Injection	6	69	70	3850
Injection	6	71	70	3850
Injection	6	73	70	3850
Injection	6	75	70	3850
Injection	6	65	72	3850
Injection	6	67	72	3850
Injection	6	69	72	3850
Injection	6	71	72	3850
Injection	6	73	72	3850
Injection	6	75	72	3850
Injection	6	65	74	3850
Injection	6	67	74	3850
Injection	6	69	74	3850
Injection	6	71	74	3850
Injection	6	73	74	3850
Injection	6	75	74	3850
Injection	6	77	74	3850
Injection	6	79	74	3850
Injection	6	81	74	3850
Injection	6	65	76	3850
Injection	6	67	76	3850
Injection	6	69	76	3850

Well Name	Model Layer	Model Row	Model Column	Pumping Rate (ft^3/day)*
Injection	6	71	76	3850
Injection	6	73	76	3850
Injection	6	75	76	3850
Injection	6	77	76	3850
Injection	6	79	76	3850
Injection	6	81	76	3850
Injection	6	69	78	3850
Injection	6	71	78	3850
Injection	6	73	78	3850
Injection	6	75	78	3850
Injection	6	77	78	3850
Injection	6	79	78	3850
Injection	6	81	78	3850
Injection	6	73	80	3850
Injection	6	75	80	3850
Injection	6	77	80	3850
Injection	6	79	80	3850
Injection	6	81	80	3850
Injection	6	79	82	3850
Injection	6	81	82	3850
Recovery	7	66	71	-7700
Recovery	7	68	71	-7700
Recovery	7	70	71	-7700
Recovery	7	72	71	-7700
Recovery	7	74	71	-7700
Recovery	7	66	73	-7700
Recovery	7	68	73	-7700
Recovery	7	70	73	-7700
Recovery	7	72	73	-7700
Recovery	7	74	73	-7700
Recovery	7	66	75	-7700
Recovery	7	68	75	-7700
Recovery	7	70	75	-7700
Recovery	7	72	75	-7700
Recovery	7	74	75	-7700
Recovery	7	76	75	-7700
Recovery	7	78	75	-7700
Recovery	7	80	75	-7700
Recovery	7	70	77	-7700
Recovery	7	72	77	-7700
Recovery	7	74	77	-7700
Recovery	7	76	77	-7700
Recovery	7	78	77	-7700
Recovery	7	80	77	-7700
Recovery	7	74	79	-7700
Recovery	7	76	79	-7700
Recovery	7	78	79	-7700
Recovery	7	80	79	-7700
Recovery	7	80	81	-7700
Injection	7	65	70	7700
Injection	7	67	70	7700
Injection	7	69	70	7700
Injection	7	71	70	7700
Injection	7	73	70	7700
Injection	7	75	70	7700
Injection	7	65	72	7700
Injection	7	67	72	7700
Injection	7	69	72	7700
Injection	7	71	72	7700

Well Name	Model Layer	Model Row	Model Column	Pumping Rate (ft^3/day)*
Injection	7	73	72	7700
Injection	7	75	72	7700
Injection	7	65	74	7700
Injection	7	67	74	7700
Injection	7	69	74	7700
Injection	7	71	74	7700
Injection	7	73	74	7700
Injection	7	75	74	7700
Injection	7	77	74	7700
Injection	7	79	74	7700
Injection	7	81	74	7700
Injection	7	65	76	7700
Injection	7	67	76	7700
Injection	7	69	76	7700
Injection	7	71	76	7700
Injection	7	73	76	7700
Injection	7	75	76	7700
Injection	7	77	76	7700
Injection	7	79	76	7700
Injection	7	81	76	7700
Injection	7	69	78	7700
Injection	7	71	78	7700
Injection	7	73	78	7700
Injection	7	75	78	7700
Injection	7	77	78	7700
Injection	7	79	78	7700
Injection	7	81	78	7700
Injection	7	73	80	7700
Injection	7	75	80	7700
Injection	7	77	80	7700
Injection	7	79	80	7700
Injection	7	81	80	7700
Injection	7	79	82	7700
Injection	7	81	82	7700
Recovery	8	66	71	-3850
Recovery	8	68	71	-3850
Recovery	8	70	71	-3850
Recovery	8	72	71	-3850
Recovery	8	74	71	-3850
Recovery	8	66	73	-3850
Recovery	8	68	73	-3850
Recovery	8	70	73	-3850
Injection	8	65	70	5775
Injection	8	67	70	5775
Injection	8	69	70	5775
Injection	8	71	70	5775
Injection	8	73	70	5775
Injection	8	75	70	5775
Injection	8	65	72	5775
Injection	8	67	72	5775
Injection	8	69	72	5775

* Negative Values Indicate Extraction

Attachment 11 to Table 1

Attachment 11 to Table 1

Response to ADEQ Comment 4.5.3-Geochemical Transport Parameters

ADEQ-4.5.3-Geochemical Transport Parameters-Distribution coefficient (K_d) values for sulfate and other parameters were calculated and compared with published results.

Section 3.0 of Volume IV ("Geochemical Evaluation") did not contain a discussion of the derivation of K_d values. BHP should provide this discussion of the derivation of K_d values. BHP should also indicate the source of the bulk density parameters listed in Table 4.5-1.

The Department is not familiar with the cited methods of estimating dispersivity. BHP should provide the pertinent parts of Gelhar and others (1992) and Zheng and Bennett (1995) that describe these methods.

The distribution coefficient (K_d) values for sulfate and other parameters are provided in Table A to this table. The K_d values were determined from the column attenuation tests by using the concentrations of the various constituents in the initial feed solution and the final solution.

$$K_d = (C_i - C_f)/ C_f * V/M$$

Where:

C_i = concentration of a parameter in the initial feed solution (mg/L)

C_f = concentration of a parameter in the final solution after the attenuation test is completed (mg/L)

V = volume of feed solution passed through a known mass of rock (ml)

M = mass of rock or soil material exposed to a known volume of solution (gram)

Bulk density values for the oxide and sulfide were derived based on the density of granite (2.65 g/cm^3) presented in: *Handbook of Physical Constants; Sydney P. Clark, Jr., 1966.* The bulk density value for the LBFU was estimated based on using a slightly higher protolith density than granite and subtracting the porosity estimate of 10 percent. A very conservative value of bulk density was estimated for the UBFU. The estimated bulk density represents the lower estimated range of unconsolidated sands and gravels. Bulk density is represented in the calculation of the retardation factor (R) for sulfide migration. The retardation factor relates the relationship between the average groundwater flow velocity (V_w) and the sulfate velocity (V_c). The equation is:

$$V_c=V_w/R$$

R is calculated form the following relationship:

$$R=1+\rho_b/\eta Kd$$

Therefore; the effect of having a low-bulk density is to lower R and increase the velocity of the sulfate with respect to the average groundwater velocity.

P_b = bulk density (g/cm^3)
N = porosity

Table A. Attenuation Coefficients Derived From Column Tests									
	Alluvial Materials		Basin-fill Deposits		QMO[a]	GDO[b]	Diabase	QMS[C]	GDS[d]
pH	3.30	5.35	4.00	7.20	1.53	1.77	2.20	1.75	2.55
Aluminum	2.13	2,933.7	14.44	1,509	0.86	0.64	0.06	0.76	0.47
Antimony	18.0	200.89	16.53	49.0	1.09	5.65	0.37	40.56	932.89
Arsenic	ND	-2.44	-2.48	0.66	ND	ND	ND	ND	ND
Barium	1,495	ND	741.52	ND	744.51	738.53	744.51	726.57	729.56
Cadmium	ND	ND	ND	ND	ND	ND	ND	ND	ND
Calcium	-0.86	0.09	-0.62	-0.08	-0.07	-1.26	-0.29	-0.73	-0.59
Chromium	13.82	827.16	267.92	ND	0.00	0.00	-0.05	-0.17	0.25
Cobalt	1.40	13.77	0.25	10.88	0.53	0.44	-0.16	0.27	0.46
Copper	1.87	198.59	7.53	395.25	0.23	0.30	-0.55	-0.07	0.98
Iron	8.05	3.65	12.51	828	0.58	0.59	0.42	0.58	1.18
Lead	14.75	383.08	20.97	0.10	1.12	0.43	-0.23	0.08	14.86
Magnesium	1.71	-0.03	1.13	0.50	1.00	1.01	0.75	0.98	1.00
Manganese	0.39	-0.32	0.45	-0.08	0.80	0.76	0.35	0.51	0.64
Mercury	17.67	1,046.76	158.72	29.00	7.12	4,814.03	321.21	471.42	25.55
Nickel	2.89	35.14	3.05	217.00	0.49	0.47	-0.21	0.29	0.63
Potassium	8.91	-0.23	2.11	1.08	0.23	0.45	0.53	0.24	1.57
Selenium	5.00	14.64	9.09	2.00	29.20	0.41	0.00	0.19	1.83
Silver	ND	ND	ND	ND	ND	ND	ND	ND	ND
Sodium	1.45	0.03	0.56	-0.39	0.84	0.79	-0.06	0.67	0.69
Sulfate	0.88	1.51	1.72	0.24	-0.06	0.03	-0.01	0.02	0.17
Zinc	2.87	25.87	1.80	52.45	1.08	1.05	0.97	0.85	1.04

[a] QMO: Quartz monzonite oxide
[b] GDO: Granodiorite oxide
[c] QMS: Quartz monzonite sulfide
[d] GDS: Granodiorite sulfide

Attachment 11-A to Table 1

APPLIED CONTAMINANT TRANSPORT MODELING

Theory and Practice

Chunmiao Zheng

Department of Geology
University of Alabama
Tuscaloosa, Alabama

Gordon D. Bennett

S.S. Papadopulos & Associates, Inc.
Bethesda, Maryland

VAN NOSTRAND REINHOLD
I(T)P™ A Division of International Thomson Publishing Inc.

New York • Albany • Bonn • Boston • Detroit • London • Madrid • Melbourne
Mexico City • Paris • San Francisco • Singapore • Tokyo • Toronto

TABLE 9-3 Values of Porosity for Various Geologic Materials

Material	Porosity (%)
Sedimentary	
Gravel, coarse	24–36
Gravel, fine	25–38
Sand, coarse	31–46
Sand, fine	26–53
Silt	34–61
Clay	34–60
Sedimentary rocks	
Sandstone	5–30
Siltstone	21–41
Limestone, dolomite	0–20
Karst limestone	5–50
Shale	0–10
Crystalline rocks	
Fractured crystalline rocks	0–10
Dense crystalline rocks	0–5
Basalt	3–35
Weathered granite	34–57
Weathered gabbro	42–45

Source: Davis (1969); Johnson and Morris (1962).

regimes, representing for example the fracture network and the unfractured rock matrix, are assumed to be distributed throughout the same space, and are characterized by separate porosity values. In theory, flow and solute transport may be calculated in each regime, although more commonly flow and advection are considered dominant in one, while processes such as diffusion and reaction are considered dominant in the other. In either case relations must be specified governing the transfer of water and solute between the two regimes. Some transport codes, including SWIFT/386 (Ward, 1991), provide options for simulating flow and transport using the dual-porosity concept.

Fractured rock regimes can also be addressed through conventional single-porosity transport calculation, provided the fracture spacing is much smaller than the spacing used in model discretization. However, the user should recognize that the porosities required in transport calculation are often much smaller for fractured rock than for problems characterized only by primary porosity.

9.3.2 Dispersivity

Definition of dispersivity values for use in field-scale transport simulation is inherently difficult and has been the subject of some controversy. Numerous studies have been undertaken to characterize field-scale dispersivity values; summaries are provided by Anderson (1979, 1984) and by Gelhar et al. (1985, 1992). The figures and tables presented in this section are adapted from Gelhar et al. (1992), who provide the most recent review and discuss many practical implications for transport modeling.

Values of dispersivity generally appear to be dependent on the scale of testing or observation, as one would expect on the basis of the factors discussed in Chapter 2; however, the form of this dependence is far from certain (e.g., Pickens and Grisak, 1981; Molz et al., 1983; Neuman, 1990). Figure 9-3, based on 59 field-scale tests, clearly indicates a trend of increasing longitudinal dispersivity with the scale of observation, which is defined as the distance between the observation points and the source. Dispersivity values derived from tracer tests, which are usually performed on a relatively local scale, tend to be smaller than those developed from modeling contaminant events or from observation of environmental tracers, which usually involve larger scales. Figure 9-3 also suggests that there is little significant difference between data obtained in porous media and in fractured rock.

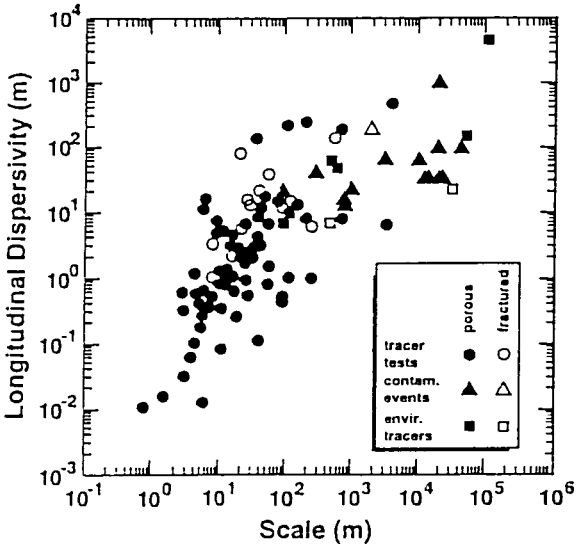

FIGURE 9-3. Longitudinal dispersivity versus scale of observation, identified by type of observation and type of aquifer. The data are from 59 field sites characterized by widely differing geologic materials (after Gelhar et al., 1992).

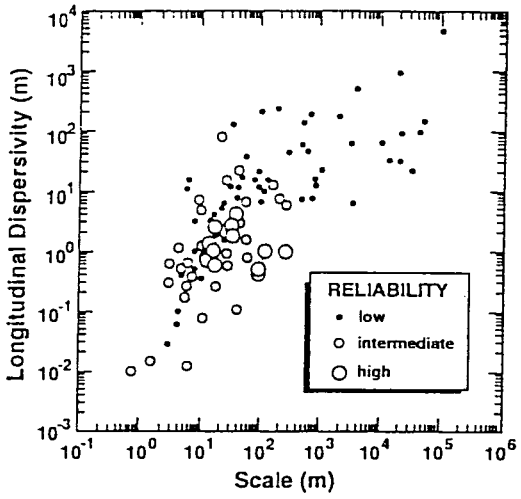

FIGURE 9-4. Longitudinal disparity versus scale of observation; data classified by reliability (after Gelhar et al., 1992).

Figure 9-3, which first appeared in a similar form in Gelhar et al. (1985), has been routinely cited as the reference for assigning longitudinal dispersivity in transport simulation. However, Gelhar et al. (1992) suggest that it is not appropriate to use the data in Figure 9-3 without considering the data reliability. The basis of their reasoning is that there is a wide range in the characteristics of the aquifers in which the tests were conducted, and in the methods of interpretation by which the results were obtained. Using a set of predefined criteria, they classify the data into categories of low, intermediate, and high reliability. Figure 9-4 shows longitudinal dispersivity versus observation scale for data classified in this way. The trend of increasing longitudinal dispersivity with observation scale is less apparent when data reliability is taken into consideration. Gelhar et al. (1992) note that some stochastic theories predict an asymptotic approach to a constant dispersivity value with increasing scale of observation. The more reliable data in Figures 9-4 and 9-5 appear to be more compatible with that prediction than are the unclassified data of Figure 9-3. However, it should also be noted that the more reliable data represent measurements at local to intermediate scale: Gelhar et al. (1992) point out the need to develop reliable measurements at larger scales. At a given scale, the values of longitudinal dispersivity range over two to three orders of magnitude, but the more reliable values tend to fall in the lower portion of this range.

Transverse dispersivity is generally observed to be smaller than longi-

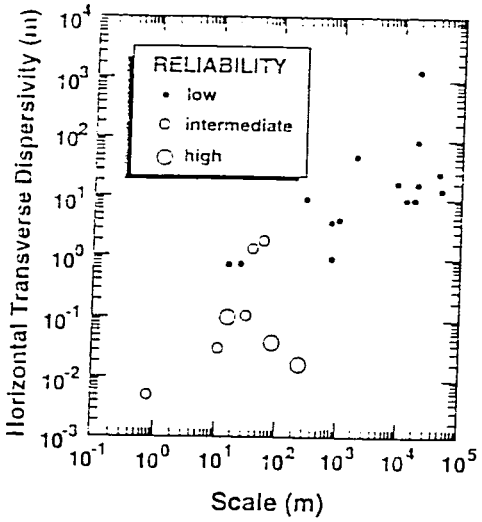

FIGURE 9-5. Horizontal transverse dispersivity as a function of observation scale; data classified by reliability (after Gelhar et al., 1992).

tudinal dispersivity and appears also to be influenced by the scale of observation. The transverse dispersivity in the vertical direction has been shown to be smaller than the transverse dispersivity in the horizontal direction. A limited number of horizontal and vertical transverse dispersivities are plotted in Figures 9-5 and 9-6. As in the case of longitudinal dispersivity, transverse dispersivities show a clear increasing trend with the observation scale if data reliability is not considered. However, when data reliability is taken into account, the trend is again less clear. The ratio of longitudinal dispersivity to horizontal transverse dispersivity and the ratio of longitudinal dispersivity to vertical transverse dispersivity are plotted in Figure 9-7. While data of lower reliability suggest a horizontal transverse dispersivity roughly one third of the longitudinal dispersivity, the data of high reliability indicate a horizontal transverse dispersivity at least one order of magnitude smaller than the longitudinal dispersivity. In all cases where dispersivities in all three principal directions are estimated (indicated by dashed vertical lines in Figure 9-7), the vertical transverse dispersivity is one to two orders smaller than the horizontal transverse dispersivity.

Because of the difficulty and expense of obtaining dispersivity values in the field, it is likely that most practical modeling studies will continue to rely on sources like Figures 9-3 through 9-7, at least for initial approximation. Gelhar et al. (1992) favor the use of dispersivity values in the lower half of

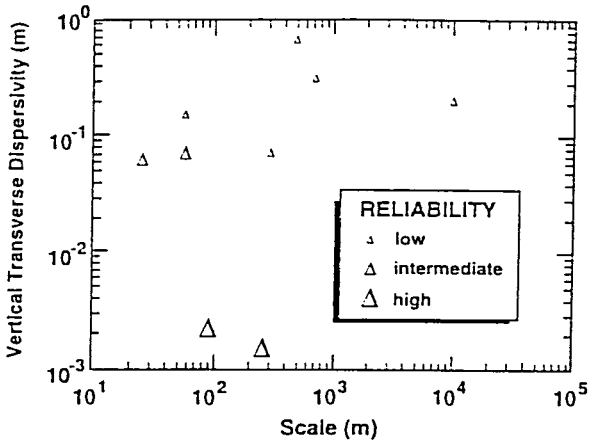

FIGURE 9-6. Vertical transverse dispersivity as a function of observation scale; data classified by reliability (after Gelhar et al., 1992).

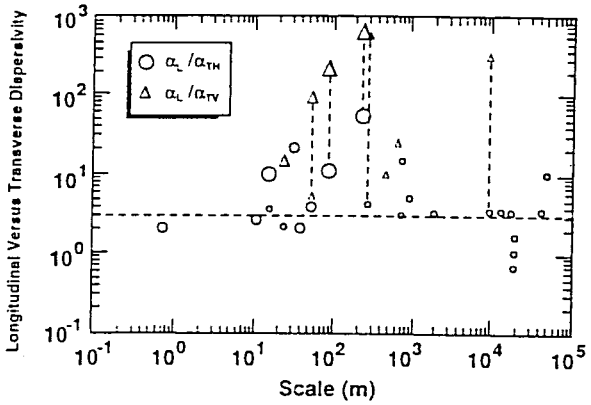

FIGURE 9-7. Ratio of longitudinal (α_L) to horizontal and vertical transverse (α_{TH} and α_{TV}) dispersivities; largest symbols are high reliability and smallest symbols are low reliability. Vertical dashed lines connecting two points indicate sites where all three principal components of the dispersivity tensor have been measured. Horizontal dashed line indicates a ratio of $\alpha_L / \alpha_{TH} = 3:1$, which has been widely used in numerical simulations (modified from Gelhar et al., 1992).

the range at any scale. In the case of transverse dispersivity, they point out that it is particularly important to recognize the very low vertical transverse dispersivity at two well-controlled field sites: the Borden site (see Chapter 12) and the Cape Cod site (e.g., LeBlanc et al., 1991). The implication of low vertical transverse dispersivity is that vertical mixing may be limited, resulting in strongly nonuniform vertical concentration profiles; this in turn

implies that three-dimensional simulation and three-dimensional monitoring networks are often necessary.

As a rule of thumb, and in the absence of site specific data, horizontal transverse dispersivity can be taken about one order of magnitude smaller than longitudinal dispersivity, while vertical transverse dispersivity can be taken about two orders of magnitude smaller. As discussed in Chapter 2, aquifer heterogeneity and the degree to which heterogeneity is represented in the flow simulation exert a strong influence on the required dispersivity values in a solute transport simulation. Gelhar et al. (1992) provide detailed information on each field test, and a general summary of information on field-scale dispersivity values.

9.4 CHEMICAL PARAMETERS

9.4.1 Sorption Constants

As noted in Chapter 3, representation of complex solute-solid relations in transport simulation using equilibrium-controlled reversible sorption isotherms is adequate only in idealized situations (e.g., Reardon, 1981; Cherry et al., 1984). However, there are still few practical alternatives. While many forms of kinetically controlled sorption isotherms have been proposed, aimed at providing more realistic simulation of sorption processes (e.g., Travis and Etnier, 1981; Harmon et al., 1989), they generally require additional empirical parameters that are often poorly defined and cannot be estimated independently. Until the data issue is resolved, the use of more sophisticated sorption isotherms in practical applications is likely to remain very limited.

As noted in Chapter 3, the linear, Freundlich, and Langmuir isotherms are the most commonly used relations for describing equilibrium-controlled reversible sorption. The definition of these sorption isotherms and the coefficients used in each of them are discussed in Chapter 3. The linear isotherm has to date been applied far more widely than the other two, largely because it is simpler and more convenient to use in practice. The linear isotherm uses a single distribution coefficient, K_d, to define the relation between the concentration in the dissolved phase and the concentration of sorbed material in the porous matrix.

Values of K_d are typically estimated from batch experiments. Dissolved concentrations are plotted versus sorbed concentrations at different sampling intervals, and the slope of a best-fit line through the data points is measured, yielding the value of K_d. Table 9-4 is a list of distribution coefficients for selected radionuclides migrating in several rock types (Moody, 1982). The real difficulty in estimating consistent K_d values is that the distribution

WATER RESOURCES RESEARCH, VOL. 28, NO. 7, PAGES 1955–1974, JULY 1992

A Critical Review of Data on Field-Scale Dispersion in Aquifers

LYNN W. GELHAR

Department of Civil Engineering, Massachusetts Institute of Technology, Cambridge

CLAIRE WELTY

Department of Civil and Architectural Engineering, Drexel University, Philadelphia, Pennsylvania

KENNETH R. REHFELDT

Illinois State Water Survey, Champaign

A critical review of dispersivity observations from 59 different field sites was developed by compiling extensive tabulations of information on aquifer type, hydraulic properties, flow configuration, type of monitoring network, tracer, method of data interpretation, overall scale of observation and longitudinal, horizontal transverse and vertical transverse dispersivities from original sources. This information was then used to classify the dispersivity data into three reliability classes. Overall, the data indicate a trend of systematic increase of the longitudinal dispersivity with observation scale but the trend is much less clear when the reliability of the data is considered. The longitudinal dispersivities ranged from 10^{-2} to 10^{4} m for scales ranging from 10^{-1} to 10^{5} m, but the largest scale for high reliability data was only 250 m. When the data are classified according to porous versus fractured media there does not appear to be any significant difference between these aquifer types. At a given scale, the longitudinal dispersivity values are found to range over 2–3 orders of magnitude and the higher reliability data tend to fall in the lower portion of this range. It is not appropriate to represent the longitudinal dispersivity data by a single universal line. The variations in dispersivity reflect the influence of differing degrees of aquifer heterogeneity at different sites. The data on transverse dispersivities are more limited but clearly indicate that vertical transverse dispersivities are typically an order of magnitude smaller than horizontal transverse dispersivities. Reanalyses of data from several of the field sites show that improved interpretations most often lead to smaller dispersivities. Overall, it is concluded that longitudinal dispersivities in the lower part of the indicated range are more likely to be realistic for field applications.

INTRODUCTION

The phenomenon of dispersive mixing of solutes in aquifers has been the subject of considerable research interest over the past 10 years. Characterizing the dispersivity at a particular field site is essential to any effort in predicting the subsurface movement and spreading of a contaminant plume at that location. Both theoretical and experimental investigations have found that field-scale dispersivities are several orders of magnitude greater than lab-scale values for the same material; it is generally agreed that this difference is a reflection of the influence of natural heterogeneities which produce irregular flow patterns at the field scale. Consequently, laboratory measurements of dispersivity cannot be used to predict field values of dispersivity. Instead field-scale tracer tests are sometimes conducted to estimate dispersivity at a particular site.

Early efforts to document the scale dependence of dispersivity [*Lallemand-Barres and Peaudecerf*, 1978; *Anderson*, 1979; *Pickens and Grisak*, 1981; *Beims*, 1983; *Neretnieks*, 1985] were based on field values of dispersivity reported in the literature and the test scales associated with those values. These studies were useful in that they indeed documented field evidence of the scale effect, but they were lacking in that they did not assess the reliability of the data presented. Because we felt that the data would be more meaningful if their variable quality was recognized, we assembled the dispersivity data along with related information from the original sources and evaluated the reliability or quality of these data [*Gelhar et al.*, 1985]. The graphical results of that work have been widely used by both practitioners and theoreticians, often without appropriate consideration of the reliability of the data. For example, recent theoretical developments based on fractal concepts [*Philip*, 1986; *Wheatcraft and Tyler*, 1988; *Neuman*, 1990] have relied on information similar to that in the work by *Gelhar et al.* [1985] but those studies disregarded the issue of the reliability of the data. We feel that it is important to update the dispersivity information including results from recent comprehensive field experiments and at the same time focus on the interpretations of the reliability of the data. With these goals in mind, this work develops the following: (1) an outline of the theoretical description of dispersive mixing in porous media; (2) a tabular summary of existing data on values of field-scale dispersivity and related site information reported in the literature; (3) an evaluation of the reliability or quality of these values based on clearly delineated criteria; and (4) discussion and interpretation of the applied and theoretical implications of the data.

Paper number 92WR00607.
0043-1397/92/92WR-00607$05.00

THEORETICAL CONCEPTS OF FIELD-SCALE DISPERSIVE MIXING

The mass balance equation governing the transport of an ideal chemically nonreactive conservative solute by a homo-

geneous fluid (constant density and viscosity) that flows through a rigid saturated porous medium is commonly expressed as [e.g., *Bear*, 1972; *de Marsily*, 1986]

$$\frac{\partial c}{\partial t} + v_i \frac{\partial c}{\partial x_i} = \frac{\partial}{\partial x_i}\left(D_{ij} \frac{\partial c}{\partial x_j}\right) \qquad i, j = 1, 2, 3 \qquad (1)$$

where c is the solute concentration, v_i is the seepage velocity component in the x_i direction, and D_{ij} are the components of the dispersion coefficient tensor. The right-hand side of (1) represents the net dispersive transport which is presumed to be Fickian, i.e., the dispersive mass flux is proportional to the concentration gradient. Some investigators [e.g., *Robertson and Barraclough*, 1973; *Bredehoeft and Pinder*, 1973] alternatively define the dispersion coefficient tensor including the porosity n as $D^*_{ij} = nD_{ij}$. When it was clear that D^*_{ij} was used in a study, we converted to the more common form used in (1). The mean flow direction is taken to be x_1, with $v_1 = v$, $v_2 = v_3 = 0$. Assuming that x_1, x_2, and x_3 are principal directions, the dispersivity is simply the ratio of the appropriate component of the dispersive coefficient tensor divided by the magnitude of the seepage velocity, v. To distinguish the field-scale dispersivities from laboratory values, the field-scale values are designated by the uppercase letter A [see *Gelhar and Axness*, 1983] and, to allow for anisotropy of transverse dispersion, a third dispersivity coefficient is used as follows:

$$D_{11} = A_L v \qquad D_{22} = A_T v \qquad D_{33} = A_V v \qquad (2)$$

where A_L is the longitudinal macrodispersivity (field scale), and A_T is the horizontal transverse macrodispersivity, and A_V is the vertical transverse macrodispersivity.

The classical equation (1) with macrodispersivities (2) is standardly used for applied modeling of field-scale solute transport. The macrodispersivities are considered to be a property of some region of the aquifer. Although the macrodispersivity may be a function of space, in most applications it is assumed constant over a region of the aquifer that encompasses the entire plume both horizontally and vertically. Real solute plumes are observed to be three-dimensional [*LeBlanc*, 1982; *Perlmutter and Lieber*, 1970; *MacFarlane et al.*, 1983] and often of limited vertical extent. Although the classical equation is three-dimensional, the two-dimensional form is most commonly applied. Reasons for the use of the two-dimensional form of the equation include lack of three-dimensional data and in the case of numerical models, restrictions on the size of data arrays in the model. Seldom is the two-dimensional form justified on the basis of site conditions or plume observations.

A number of theoretical studies have proposed methods of describing field-scale dispersive mixing. All of the theories view field-scale dispersion as being produced by some kind of small-scale heterogeneity or variability of the aquifer. At present there is considerable debate concerning how to parameterize the variability and model field-scale solute transport. Assuming a perfectly layered aquifer, one group [*Molz et al.*, 1983, 1986] suggests measuring the variability in detail and modeling the transport in each layer with local-scale dispersivities, thus eliminating the need for a field-scale dispersivity. Again assuming a layered aquifer, a second group suggests the use of a scale-dependent or time-dependent field-scale dispersivity [e.g., *Pickens and Grisak*, 1981; *Dieulin*, 1980]. A third group [e.g., *Gelhar and Axness*, 1983; *Dagan*, 1982; *Neuman et al.*, 1987] has examined more general three-dimensional heterogeneity with stochastic methods and concluded the classical equation with constant field-scale dispersivities is applicable to describe transport over large distances. These stochastic approaches incorporate the effects of practically unknowable small-scale variations in flow by means of macrodispersivities which are used in a deterministic transport model describing the large-scale variations in flow by means of the convection terms. Nonetheless, under what circumstances a field-scale dispersivity can be used to describe field-scale solute transport is still an open question. Until the issue is resolved, the field-scale dispersivity concept can be regarded as a working hypothesis which has a sound theoretical basis and finds wide application.

FIELD DATA ON DISPERSIVITY

Summary of Observations

A literature review was conducted to collect reported values of dispersivity from published analyses of field-scale tracer tests and contaminant transport modeling efforts. The literature sources and pertinent data characterizing each reviewed study are summarized in Table 1 which includes information on 59 different field sites. The information compiled from each study includes site location, description of aquifer material, average aquifer saturated thickness, hydraulic conductivity or transmissivity, effective porosity, mean pore velocity, flow configuration, dimensionality of monitoring network, tracer type and input conditions, length scale of the test or problem, reported values of longitudinal and horizontal and vertical transverse dispersivities, and classification of the reliability of the reported data. Blank entries indicate that the information was not provided in the cited documents. This table summarizes information for purposes of comparison only. More detail regarding a particular study may be found in the original sources.

Aquifer characteristics. As indicated by the second through sixth columns from the left, the study sites represent a wide variety of aquifer conditions and settings. Summarized in these columns is information on aquifer material, saturated thickness, hydraulic conductivity or transmissivity, and velocity. The aquifer thickness for each site is the arithmetic average of the range at that site. Hydraulic conductivity and transmissivity values show the range reported at the site. Reported values for effective porosity vary from 0.5% (for fractured media) to 60% (for porous media). When a value was reported as "porosity," we interpreted this as the effective porosity (interconnected pore space), the value used in analysis of the advection-dispersion equation. Where porosity was reported as "total porosity," we have indicated this in the table. The velocity column indicates the mean pore or seepage velocity at a site. In some cases the values were calculated from information provided on average specific discharge, q, and effective porosity, n, as $v = q/n$. Velocities ranged from 0.0003 to 200 m/d.

Methods of determining dispersivity. The seventh through tenth columns from the left summarize the method used to determine the dispersivity for each site. The seventh, eighth, and ninth columns from the left describe experimental conditions: flow configuration, monitoring, tracer and

input; the tenth column from the left summarizes methods of data interpretation. Dispersivity values were calculated or inferred from one of two types of subsurface solute transport events: large-scale, uncontrolled contamination (naturally occurring or human-induced) events, or controlled tracer tests.

Uncontrolled events are characterized by a source input history that is unknown, transport of contaminants by the ambient flow of groundwater, and solute plumes that often extend over regional scales (hundreds of meters). We describe naturally occurring events as "environmental" tracers, implying chemical constituents associated with uncontrolled natural changes occurring in groundwater before the start of a study. Examples of naturally occurring events include tritium in groundwater from recharge containing atmospheric bomb tritium, seawater intrusion, and mineral dissolution. These events are indicated in the "tracer and input" column by the notation "environmental" along with the type of chemical species reported. Examples of human-induced contamination events include leaks and spills to groundwater from landfills, storage tanks, surface impoundments, and infiltration basins. These types of events are indicated by the notation "contamination" in the tracer and input column. Values of dispersivity for uncontrolled events are commonly determined by fitting a one-, two-, or three-dimensional solute transport model to historical data; i.e., values of dispersivity are altered until model output matches historical solute concentration measurements.

The main features distinguishing controlled tracer tests from uncontrolled ones is that in the former, both the quantity and duration of solute input are known. This is indicated by "step" (continuous input of mass) or "pulse" ("instantaneous" or slug input) in the "tracer and input" column. Controlled tracer tests may be conducted under ambient groundwater flow conditions (also referred to as natural gradient tests), or under conditions where the flow configuration is induced by pumping or recharge. The type of test is reported in the "flow configuration" column. Induced flow configurations include radial, two-well, and forced uniform flow. In radial flow tracer tests, a pulse or step input of tracer is injected at a recharge well and the time distribution of tracer is recorded at an observation well (diverging radial flow test), or the tracer is injected at an observation well and the time distribution is recorded at a distant pumping well (converging radial flow test). In a two-well test, both a recharge well and pumping well are operating; tracer is injected at the recharge well and tracer breakthrough is observed at the pumping well. Recirculation of the water (containing tracer) from the pumping well to the recharge well is often employed. "Forced uniform flow" refers to the flow regime at the Bonnaud site in France, where a uniform flow field was generated between two lines of equally spaced wells, one line recharging and one line pumping, with both screened to the full depth of the aquifer. A discussion of the advantages and disadvantages of different types of tracer tests is presented by *Welty and Gelhar* [1989].

A number of methods have been used to evaluate the data from controlled tracer tests, as indicated by column headed "method of data interpretation." These include fitting of one-, or two- or three-dimensional solute transport analytical solutions, and the method of spatial moments. It should be noted that since the velocity is nonuniform for both radial and two-well tracer tests, analysis of the data must account for this effect to determine dispersivity properly for such cases. Nonuniform velocity effects have also been observed in ambient flow tracer tests.

The types of tracers used to determine dispersivity at each site are summarized in the "tracer and input" column along with the input conditions. A variety of chemical and microbiological tracers have been employed for controlled tracer tests. Discussions of the suitability of different chemical and microbial species for tracer tests are presented by *Davis et al.* [1980, 1985] and *Betson et al.* [1985]. A primary consideration in designing a controlled tracer test is whether the species is conservative or nonconservative. A conservative tracer is one that moves with the same velocity as the groundwater and does not undergo radioactive decay, adsorption, degradation, chemical reaction (or in the case of microorganisms, death). If any of these effects are present, they must be accounted for in evaluation of the dispersivity. Another factor important in the choice of a tracer is that it is not present in naturally occurring groundwater, or that it is injected at concentrations much higher than natural background levels.

The "monitoring" column indicates whether two- or three-dimensional monitoring was employed at a site. By two-dimensional monitoring we mean depth-averaged (vertically mixed). Three-dimensional monitoring implies point samples with depth. This information is noted because vertical mixing in an observation well influences the concentration of tracer in a water sample. Several studies [*Meyer et al.*, 1981; *Pickens and Grisak*, 1981] have shown that when a tracer is not injected over the full aquifer depth, vertically mixed samples underestimate the tracer concentration and as a result the longitudinal dispersivity is overestimated. This occurs because the tracer occupies only a portion of the vertical thickness. When a sample from the entire thickness is taken, the true tracer concentration is diluted in the well with tracer-free water. If an attempt is made to interpret the diluted ("measured") concentration, the dispersivity will be overestimated. At many sites there was no indication whether point or fully mixed sampling was performed. From examination of the cases where three-dimensional measurements of solute concentrations were made, it is clear that vertical mixing of the tracer as it travels through the aquifer is often very small [*Sudicky et al.*, 1983; *LeBlanc*, 1982; *Freyberg*, 1986; *Garabedian et al.*, 1988, 1991].

Field dispersivities and scale. The "scale of test" column represents the distance traveled from the source for ambient conditions, or the distance between injection and observation wells for the case of an induced flow configuration. The values of dispersivity reported at the indicated scale are given in the second column from the right. Data from the 59 sites yielded 106 values of longitudinal dispersivity, since often multiple investigations or multiple experiments by one investigator were performed at one site. A plot of the longitudinal dispersivity values as a function of scale is presented in Figure 1. The arithmetic average was plotted in cases where a range was reported either for the scale or dispersivity in Table 1. In some cases, values of dispersivity for individual layers were reported as well as an average "aquifer" value. In these cases the latter value was plotted for the given scale. The symbols on Figure 1 indicate whether the dispersivity value is for fractured media (open symbols, 18 values) or porous media (solid symbols, 88

TABLE 1. Summary of

Reference and Site Name	Aquifer Material	Average Aquifer Thickness, m	Hydraulic Conductivity (m/s) or Transmissivity (m^2/s)	Effective Porosity, %	Velocity, m/d	Flow Configuration
Adams and Gelhar [1991],§ Columbus, Mississippi	very heterogeneous sand and gravel	8	10^{-5} to 10^{-3} m/s	35	0.03–0.5	ambient
Ahlstrom et al. [1977], Hanford, Washington	glaciofluviatile sands and gravels	64	5.7×10^{-4} to 3.0×10^{-2} m/s			ambient
Bentley and Walter [1983], WIPP	fractured dolomite	5.5		18	0.3	two-well recirculating
Bierschenk [1959] and *Cole* [1972], Hanford, Washington	glaciofluviatile sands and gravels	64	1.7×10^{-1} m^2/s	10	26 31	ambinet
Bredehoeft and Pinder [1973], Brunswick, Georgia	limestone	50	6.5×10^{-7} to 8.6×10^{-7} m^2/s	35		radial converging
Claasen and Cordes [1975], Amargosa, Nevada	fractured dolomite and limestone	15	5×10^{-2} to 11×10^{-2} m^2/s	6–60	0.14–3.4	two-well recirculating
Daniels [1981, 1982], Nevada Test Site	alluvium derived from tuff	500	1.7×10^{-5} m/s		0.04	radial converging
Dieulin [1981], Le Cellier (Lozere, France)	fractured granite	20	3×10^{-4} to 9×10^{-4} m/s	2–8	3	radial converging
Dieulin [1980], Torcy, France	alluvial deposits	6	3×10^{-4} m/s		0.5	ambient
Egboka et al. [1983], Borden	glaciofluvial sand	7–27	10^{-5} to 10^{-7} m/s	38	0.01–0.04	ambient
Fenske [1973], Tatum Salt Dome, Mississippi	limestone	53	4.7×10^{-6} m/s	23	1.2	radial diverging
Freyberg [1986], Borden	glaciofluvial sand	9	7.2×10^{-5} m/s	33 (total)	0.09	ambient
Fried and Ungemach [1971], Rhine aquifer	sand, gravel, and cobbles	12			9.6	radial diverging
Fried [1975], Rhine aquifer (salt mines) southern Alsace, France	alluvial; mixture of sand, gravel, and pebbles with clay lenses	125	10^{-3} m/s			ambient
Fried [1975], Lyons, France (sanitary landfill)	alluvial, with sand and gravel and slightly stratified clay lenses	20			5.0	ambient
Garabedian et al. [1988] Cape Cod, Massachusetts	medium to coarse sand with some gravel overlying silty sand and till	70	1.3×10^{-3} m/s	39	0.43	ambient
Gelhar [1982], Hanford, Washington	brecciated basalt interflow zone					two-well without recirculation
Goblet [1982], site B, France	fractured granite	50	10^{-5} to 10^{-7} m/s		84	radial converging
Grove [1977], NRTS, Idaho	basaltic lava and sediments	76	1.4×10^{-1} to 1.4×10^{1} m^2/s	10		ambient
Grove and Beetem [1971], Eddy County (near Carlsbad), New Mexico	fractured dolomite	12		12	3.5	two-well recirculating
Gupta et al. [1975], Sutter Basin, California	sandstone, shale, sand, and alluvial sediments					ambient
Halevy and Nir [1962] and *Lenda and Zuber* [1970], Nahal Oren, Israel	dolomite	100		3.4	4.0	radial converging
Harpaz [1965], southern coastal plain, Israel	sandstone with silt and clay layers	90			14	radial diverging
Helweg and Labadie [1977], Bonsall subbasin, California						ambient
Hoehn [1983], lower Glatt Valley, Switzerland	layered gravel and silty sand	25	9.2×10^{-4} to 6.6×10^{-3} m/s		3.4 1.8 1.2 8.6 4.1 1.7	ambient

Field Observations

Monitoring	Tracer and Input*	Method of Data Interpretation	Scale of Test, m	Dispersivity $A_L/A_T/A_V$,† m	Classification of Reliability of $A_L/A_T/A_V$ (I, II, III)‡
three-dimensional	Br^- (pulse)	spatial moments	200	7.5	II
two-dimensional	^3H (contamination)	two-dimensional numerical model	20,000	30.5/18.3	III
two-dimensional	PFB, SCN (step)	one-dimensional quasi-uniform flow solution [*Grove and Beetem*, 1971]	23	5.2	III
two-dimensional	fluorescein (pulse)	one-dimensional uniform flow solution	3,500 4,000	6 460	III III
two-dimensional	Cl^- (contamination)	two-dimensional numerical model	2,000	170/52‖	III
two-dimensional	^3H (pulse)	one-dimensional quasi-uniform flow solution [*Grove and Beetem*, 1971]	122	15	III
two-dimensional	^3H (contamination)	radial flow type curve [*Sauty*, 1980]	91	10–30	III
two-dimensional	Cl^-, I^- (pulse)	radial flow type curve [*Sauty*, 1980]	5	0.5	II
two-dimensional (resistivity)	Cl^- (pulse)	one-dimensional uniform flow solution	15	3	III
three-dimensional	^3H (environmental)	one-dimensional uniform flow solution	600	30–60	III
	^3H (pulse)	one-dimensional uniform flow solution	91	11.6	III
three-dimensional	Br^-, Cl^- (pulse)	spatial moments	90	0.43/0.039	I
	Cl^- (pulse)	one-dimensional radial flow numerical model	6	11	III
three-dimensional	Cl^- (contamination)	two-dimensional numerical model	800	15/1	III
two-dimensional	EC (contamination)	two-dimensional numerical model	600–1000	12/4	III
three-dimensional	Br^- (pulse)	spatial moments	250	0.96/0.018/ 0.0015	I
two-dimensional	^{131}I (pulse)	one-dimensional nonuniform flow solution along streamlines [*Gelhar*, 1982]	17.1	0.60	I
two-dimensional	RhWt, SrCl (pulse)	one-dimensional uniform flow solution including borehole flushing effects	17	2	III
two-dimensional	Cl^- (contamination)	two-dimensional numerical model	20,000	91/91	III
two-dimensional	^3H (step)	one-dimensional quasi-uniform flow solution [*Grove and Beetem*, 1971]	55	38.1	III
	Cl^- (environmental)	three-dimensional numerical model	50,000	80–200/ 8–20	III
two-dimensional	^{60}Co (pulse)	one-dimensional uniform flow solution	250	6	II
two-dimensional	Cl^- (step)	one-dimensional radial flow solution	28	0.1–1.0	II
	TDS (contamination)	two-dimensional numerical model	14,000	30.5/9.1	III
two-dimensional	uranine (pulse)	one-dimensional uniform flow solution for layers	4.4 4.4 4.4 10.4 10.4 10.4	0.1 0.01 0.2 0.3 0.04 0.7	III III

TABLE 1.

Reference and Site Name	Aquifer Material	Average Aquifer Thickness, m	Hydraulic Conductivity (m/s) or Transmissivity (m^2/s)	Effective Porosity, %	Velocity, m/d	Flow Configuration
Hoehn and Santschi [1987], lower Glatt Valley, Switzerland	layered gravel and silty sand	27.5	8.1×10^{-5} to 6.6×10^{-3} m/s		1.5 3.2	ambient
					5.6 3.9 3.2	ambient
Huyakorn et al. [1986], Mobile, Alabama	layered medium sand	21.6		0.35		two-well without recirculation
Iris [1980], Campuget (Gard), France	alluvial deposits	9	3.6×10^{-3} m^2/s		0.05	radial diverging
Ivanovitch and Smith [1978], Dorset, England	fractured chalk		2.2×10^{-3} m/s (fast pulse)	0.5	57.6	radial converging
	chalk		3.6×10^{-4} m/s (slow pulse)	2.3	9.6	radial converging
Kies [1981], New Mexico State University, Las Cruces	fluvial sands		9.55×10^{-5} m/s	42 (total)		ambient
Klotz et al. [1980], Dormach, Germany	fluvioglacial gravels	14			20	radial converging
Konikow [1976], Rocky Mountain Arsenal	alluvium			30		ambient
Konikow and Bredehoeft [1974], Arkansas River valley (at La Junta, Colorado)	alluvium, inhomogeneous clay, silt, sand and gravel		2.4×10^{-4} to 4.2×10^{-3} m/s	20		ambient
Kreft et al. [1974], Poland	sand	2.5	3.1×10^{-5} to 1.5×10^{-4} m/s; 1.2×10^{-4} m^2/s	24	29	radial converging
Kreft et al. [1974], Zn-Pb deposits, Poland	fractured dolomite	57	2.5×10^{-4} to 4.7×10^{-4} m/s	2.4	7.5 100	radial converging
	fractured dolomite	48	2.5×10^{-4} to 4.7×10^{-4} m/s	2.4	60.1 22.7	radial converging
Kreft et al. [1974], sulfur deposits, Poland	limestone	7	1.1×10^{-4} m/s	12.3	10 10.8	radial converging
	limestone	7	1.1×10^{-4} m/s	12.3	8.6	radial converging
Lau et al. [1957], University of California, Berkeley	sand and gravel with clay lenses	1.5	9×10^{-4} m/s	30	7	radial diverging
Lee et al. [1980], Perch Lake, Ontario, (lake bed)	sand		3.2×10^{-5} m/s		0.14	ambient
Leland and Hillel [1981], Amherst, Massachusetts	fine sand and glacial till	0.75	2.4 to 3×10^{-5} m/s	40	0.3–0.6	ambient
Mercado [1966], Yavne region, Israel	sand and sandstone with some silt and clay	80	2.1×10^{-8} to 2.4×10^{-8} m^2/s	23.3	0.84–3.4	radial diverging/converging
Meyer et al. [1981]; Koeberg Nuclear Power Station, South Africa	sand	20			0.12	ambient
Molinari and Peaudecerf [1977] and *Sauty* [1977], Bonnaud, France	sand	3	8.3×10^{-4} to 1.1×10^{-3} m^2/s		2.7 1.0 2.4 1.0 2.0 2.0	forced uniform
Moltyaner and Killey [1988*a*, *b*], Twin Lake aquifer (Chalk River)	fluvial sand			40.8 (total)	1.2	ambient
Naymik and Barcelona [1981], Meredosia, Illinois (Morgan County)	unconsolidated sand and gravel	27	2.2×10^{-2} to 4.3×10^{-2} m^2/s			ambient

(continued)

Monitoring	Tracer and Input*	Method of Data Interpretation	Scale of Test, m	Dispersivity $A_L/A_T/A_V$,† m	Classification of Reliability of $A_L/A_T/A_V$ (I, II, III)‡
two-dimensional	uranine (pulse)	temporal moments	4.4	1.1	II
			10.4	1.2	II
two-dimensional	^3H (environmental)	temporal moments	100	6.7	III
			110	10.0	III
			500	58.0	III
two-dimensional	Br^- (pulse)	two-dimensional numerical model	38.3	4.0	I
three-dimensional	heat (pulse)	two-dimensional radial numerical model	40	3/1.5	II
	^{82}Br (pulse)	one-dimensional uniform flow solution	8	3.1	III
	^{82}Br (pulse)	one-dimensional uniform flow solution	8	1.0	III
two-dimensional	NO_3^- (pulse)	two-dimensional uniform flow solution	25	1.6/0.76	III
two-dimensional	^{82}Br, uranine (pulse)	one-dimensional uniform flow solution	10	5, 1.9	II
	Cl^- (contamination)	two-dimensional numerical model	13,000	30.5	III
two-dimensional	dissolved solids (contamination)	two-dimensional numerical model	18,000	30.5/9.1	III
two-dimensional	^{131}I (pulse)	one-dimensional uniform flow solution	5–6	0.18	II
	^{131}I (pulse)	one-dimensional uniform flow solution	22	44–110	II
	^{131}I (pulse)	one-dimensional uniform flow solution	21.3	2.1	II
	^{58}Co (pulse)	one-dimensional uniform flow solution	27	2.7–27	II
	^{58}Co (pulse)	one-dimensional uniform flow solution	41.5	20.8	II
	Cl^- (step)	one-dimensional radial numerical model	19	2–3	I
three-dimensional	Cl^- (pulse)	one-dimensional uniform flow solution	≤6	0.012	II
three-dimensional	Cl^- (pulse)	two-dimensional uniform flow solution	4	0.05–0.07	III
three-dimensional	^{60}Co, Cl^- (step)	one-dimensional radial flow solution	≤115 (observation wells)	0.5–1.5 (injection phase)	I
three-dimensional	^{131}I (pulse)	one-dimensional uniform flow solution for layers	2–8	0.01, 0.03, 0.01, 0.05 for layers; 0.42 for depth average	III
two-dimensional	I^-	two-dimensional uniform flow solution	13	0.79	I
	^3H		13	1.27	I
	^{131}I		13	0.72	I
	^{131}I		26	2.23	I
	^{131}I		33.2	1.94/0.11	I
	^{131}I (pulse)		32.5	2.73/0.11	I
three-dimensional	^{131}I (pulse)	two-dimensional uniform flow solution	40	0.06–0.16/· · ·/ 0.0006–0.002	II
two-dimensional	NH_3 (contamination)	two-dimensional numerical model	16.4	2.13–3.35/ 0.61–0.915	III

TABLE 1.

Reference and Site Name	Aquifer Material	Average Aquifer Thickness, m	Hydraulic Conductivity (m/s) or Transmissivity (m^2/s)	Effective Porosity, %	Velocity, m/d	Flow Configuration
New Zealand Ministry of Works and Development [1977] Heretaunga aquifer, New Zealand: Roys Hill site	gravel with cobbles	100	0.29 m^2/s	22	150–200	ambient
Flaxmere site 2	alluvium (gravels)	120	0.37 m^2/s	22	20–25	ambient
Hastings City rubbish dump	alluvium (gravels)		0.14, 0.35 m^2/s		20	ambient
Oakes and Edworthy [1977], Clipstone, United Kingdom	sandstone	44	2.4×10^{-6} to 1.4×10^{-4} m/s	32–48	5.6, 4.0 9.6	radial diverging
					2.4, 3.6	radial converging
Papadopulos and Larson [1978], Mobile, Alabama	medium to fine sand interspersed with clay and silt	21	5×10^{-4} m/s (horizontal) and 5.1×10^{-5} m/s (vertical)	25	0.05	radial diverging
Pickens and Grisak [1981], Chalk River	sand	8.5	2×10^{-5} to 2×10^{-4} m/s	38	0.15	two-well recirculating
	sand	8.5	2×10^{-5} to 2×10^{-4} m/s	38	0.15	radial diverging/converging
Pinder [1973], Long Island	glacial outwash	43	7.5×10^{-4} m/s	35	0.43	regional
Rabinowitz and Gross [1972], Roswell Basin, New Mexico	fractured limestone	61	1.1×10^{-2} to 2.9×10^{-1} m^2/s	1	11–21	regional
Rajaram and Gelhar [1991], Borden	glaciofluvial sand	9	7.2×10^{-5} m/s	33 (total)	0.09	ambient
Roberts et al. [1981], Palo Alto bay lands	sand, gravel, and silt	2	1.25×10^{-3} m^2/s (lower aquifer); 5.0×10^{-4} m^2/s (upper aquifer)	25	15.5 12.0 3.5 25.6 7.9	radial diverging
Robertson [1974] and *Robertson and Barraclough* [1973], NRTS, Idaho	basaltic lava and sediments	76	1.4×10^{-1} to 1.4×10^{1} m^2/s	10	1.5–8	regional
Robson [1974, 1978], Barstow, California	alluvial sediments	27	2.1×10^{-4} to 1×10^{-2} m^2/s	40		two-well recirculating
				40	3	regional
Robson [1978], Barstow, California	alluvial sediments	30.5	5×10^{-4} m/s	40		regional
Rousselot et al. [1977], Byles–Saint Vulbas near Lyon, France	clay, sand, and gravel	12	6.5×10^{-3} to 1.5×10^{-2} m/s	14 2.1–18 1.8–5.9 11–24	18 11.5, 3.8 46.7, 16 24	radial converging
Saury [1977], Corbas, France	sand and gravel	12			125, 100 15.5, 78 6.9	radial converging
Saury et al. [1978], Bonnaud, France	sand	3	8.3×10^{-4} to 1.1×10^{-3} m^2/s			radial diverging
Segol and Pinder [1976], Cutler area, Biscayne Bay aquifer, Florida	fractured limestone and calcareous sandstone	30.5	0.45×10^{-2} m/s (horizontal) and 0.09×10^{-4} m/s (vertical)	25	20	ambient
Sudicky et al. [1983], Borden	glaciofluvial sand	7–27	4.8×10^{-5} to 7.6×10^{-5} m/s	38	0.07–0.25	ambient
Sykes et al. [1982, 1983], Borden	sand		5.8 to 7.2×10^{-5} m/s	35		ambient
Sykes et al.[1983], Mobile, Alabama	sand, silt, and clay	21	5×10^{-4} m/s (horizontal) and 2.5×10^{-5} m/s (vertical)	25	0.05	radial diverging

(continued)

Monitoring	Tracer and Input*	Method of Data Interpretation	Scale of Test, m	Dispersivity $A_L/A_T/A_V$,† m	Classification of Reliability of $A_L/A_T/A_V$ (I, II, III)‡
three-dimensional	^{131}I, RhWt, ^{82}Br, Cl^-, *E. Coli* (pulse)	three-dimensional uniform flow solution	54–59	1.4–11.5/ 0.1–3.3/ 0.04–0.10	II
three-dimensional	RhWt, ^{82}Br (pulse)	three-dimensional uniform flow solution	25	0.3–1.5/ · · ·/0.06	II
three-dimensional	Cl^- (contamination)	three-dimensional uniform flow solution	290	41/10/0.07	III
two-dimensional	^{82}Br (pulse)	radial flow numerical model	6	0.16, 0.38	II
			3	0.31	II
two-dimensional	Cl^-, I^- (pulse)		6	0.6	II
			3	0.6	II
two-dimensional	heat (step)	two-dimensional numerical model	57.3	1.5	II
three-dimensional	^{51}Cr (step)	one-dimensional quasi-uniform flow solution	8	0.5	III
three-dimensional	^{131}I (step)	one-dimensional radial flow solution	3	0.03	III
three-dimensional	Cr^{+6} (contamination)	two-dimensional numerical model	1,000	21.3/4.2	III
two-dimensional	^3H (environmental)	one-dimensional uniform flow solution	32,000	20–23	III
three-dimensional	Br^-, Cl^- (pulse)	spatial moments	90	0.50/0.05/ 0.0022	I
two-dimensional	Cl^- (step)	one-dimensional uniform flow solution	11	5	III
			20	2	III
			40	8	III
			16	4	III
			43	11	III
two-dimensional	Cl^- (contamination)	two-dimensional numerical model	20,000	910/1370‖	III
two-dimensional	Cl^- (step)	one-dimensional quasi-uniform flow solution	6.4	15.2	III
two-dimensional	TDS (contamination)	two-dimensional numerical model	10,000	61/18	III
three-dimensional	TDS (contamination)	two-dimensional numerical model (vertical section)	3,200	61/· · ·/0.2	III
two-dimensional	I^- (pulse)	one-dimensional uniform flow solution for layers	9.3	6.9	II
			5.3	0.3, 0.7	III
			10.7	0.46, 1.1	III
			7.1	0.37	II
two-dimensional	I^- (pulse)	one-dimensional uniform flow solution for layers	25	11, 1.25	III
			50	25, 6.25	III
			150	12.5	II
two-dimensional	heat (step)	one-dimensional radial flow solution	13	1.0	II
three-dimensional	Cl^- (environmental)	two-dimensional numerical model	490	6.7/· · ·/0.67	III
three-dimensional	Cl^- (pulse)	three-dimensional uniform flow solution	11	0.08/0.03	II
			0.75	0.01/0.005	II
three-dimensional	Cl^- (pulse)	two-dimensional numerical model	700	7.6/· · ·/0.31	III
three-dimensional	heat (step)	three-dimensional numerical model	57.3	0.76/· · ·/0.15	II

TABLE 1.

Reference and Site Name	Aquifer Material	Average Aquifer Thickness, m	Hydraulic Conductivity (m/s) or Transmissivity (m^2/s)	Effective Porosity, %	Velocity, m/d	Flow Configuration
Vaccaro and Bolke [1983], Spokane aquifer, Washington and Idaho	glaciofluvial sand and gravel	152	9×10^{-5} m^2/s to 6.5 m^2/s	7–40	0.003–2.8	ambient
Valocchi et al. [1981], Palo Alto bay lands	sand, gravel, and silt	2	1.25×10^{-3} m^2/s (lower aquifer); 5.0×10^{-4} m^2/s (upper aquifer)	25	27	radial diverging
Walter [1983], WIPP	fractured dolomite	7	8.0×10^{-5} m^2/s	0.7 and 11 (along separate paths)	4.7, 2.4	radial converging
Webster et al. [1970], Savannah River Plant, South Carolina	crystalline, fractured schist and gneiss	76	3.6×10^{-7} m/s		1.3 21.4	two-well recirculating
Werner et al. [1983], Hydrothermal Test Site, Aefligen, Switzerland	gravel	20	6×10^{-3} m/s	17	9.1	ambient
Wiebenga et al. [1967] and *Lenda and Zuber* [1970], Burdekin Delta, Australia	sand and gravel	6.1	5.5×10^{-3} m/s	32	29	radial converging
Wilson [1971] and *Robson* [1974], Tucson, Arizona	unconsolidated gravel, sand, and silt		5.75×10^{-3} m^2/s	38		two-well without recirculation radial diverging
Wood [1981], Aquia Formation, southern Maryland	sand	1,000	2.9×10^{-4} to 8.7×10^{-4} m^2/s	35	0.0003–0.0007	ambient
Wood and Ehrlich [1978] and *Bassett et al.* [1980], Lubbock, Texas	sand and gravel	17	3.2×10^{-3} to 4.4×10^{-3} m^2/s		78	radial converging

*TDS denotes total dissolved solids; EC, electrical conductivity; PFB, pentafluorobenzoate; MTFMB, metatrifluoromethylbenzoate; MFB, metafluorobenzoate; Para-FB, parafluorobenzoate; RhWT, rhodamine-WT dye; and SCN, thiocyanate.

†A_L denotes longitudinal dispersivity; A_T, horizontal transverse dispersivity; and A_V, vertical transverse dispersivity. Reported values for A_L, A_T, and A_V are separated by slashes. Absence of slashes means that values were reported for A_L only. A comma or a dash separating entries means that multiple values or a range of values, respectively, were reported for a particular dispersivity component.

‡For description of classification criteria, see text.

§E. E. Adams and L. W. Gelhar, Field study of dispersion in a heterogeneous aquifer: Spatial moments analysis (submitted to *Water Resources Research*, 1991).

‖Porosity-corrected dispersivity value.

values). The type of event evaluated is indicated by a circle (tracer test, 83 values), triangle (contamination event, 15 values), or square (environmental tracer, eight values). The total numbers of values of dispersivity for each type of medium and test are shown in Table 2. Any reported values of horizontal transverse dispersivity or vertical transverse dispersivity are also listed in the dispersivity column of Table 1. For the cases examined, 24 values of horizontal transverse dispersivity and nine values of vertical transverse dispersivity were reported. In nearly all cases, the horizontal values were found to be 1–2 orders of magnitude less than the longitudinal values, and the vertical values smaller by another order of magnitude.

Evaluation of Dispersivity Data

From Figure 1, it appears that longitudinal dispersivity increases with scale. Field observations of dispersivity ranged from 0.01 m to approximately 5500 m at scales of 0.75 m to 100 km. The longitudinal dispersivity for the two types of aquifer material (porous versus fractured media) tends to scatter over a similar range, although at a smaller scale fractured media seem to show higher values. At each scale there is at least a two-order-of-magnitude range in dispersivity. Because we noted a number of problems with data and their interpretation as we gathered them for Table 1, we would regard any conclusions about Figure 1 with skepticism until further qualifying statements can be made about the data points. Typical problems that we found with the studies reported in Table 1 include the following: data analysis not matched to flow configuration; mass input history unknown; nonconservative effects of tracer not accounted for; dimensionality of the monitoring not matched to the dimensionality of the analysis; and assumption of distinct geologic layers in analysis when their actual presence was not documented. Based on these problems, we decided to rate the data as high (I), medium (II), or low (III) reliability according to the criteria set forth below. Table 3 lists the criteria used to designate either high- or low-reliability data. No specific criteria were defined for the intermediate classification; it encompasses the dispersivity

(continued)

Monitoring	Tracer and Input*	Method of Data Interpretation	Scale of Test, m	Dispersivity $A_L/A_T/A_V$,† m	Classification of Reliability of $A_L/A_T/A_V$ (I, II, III)‡
	Cl^- (contamination)	two-dimensional numerical model	43,400	91.4/27.4	III
	Cl^- (step)	two-dimensional numerical model	16	1.0/0.1	I
two-dimensional	MTFMB, PFB, MFB, para-FB (pulse)	one-dimensional uniform flow solution	30	10–15	III
two-dimensional	^{85}Sr ^{85}Br (pulse)	one-dimensional quasi-uniform flow solution	538	134	III
three-dimensional	heat (step)	one-dimensional numerical model	700	130–234	III
			37	131	III
			105	208	III
			200	234	III
	^{131}I, ^{3}H (pulse)	one-dimensional uniform flow solution	18.3	0.26	II
three-dimensional	Cl^- (step)	one-dimensional quasi-uniform flow solution	79.2	15.2	III
two-dimensional	Cl^- (step)	one-dimensional radial flow solution	4.6	0.55	III
	Na^+ (environmental)	one-dimensional uniform flow solution	10^5	5,600–40,000	III
two-dimensional	I^- (pulse)	one-dimensional radial flow solution	1.52	0.015	II

values that do not fall into the high or low groups. These classifications do not place strict numerical confidence limits on reported dispersivities, but rather are intended to provide an order-of-magnitude estimate of the confidence we place on a given value. In general, we consider high-reliability dispersivity values to be accurate within a factor of 2. Low-reliability values are considered to be no more accurate than within 1 or 2 orders of magnitude. Intermediate reliability falls somewhere between the extremes. We wish to make a distinction between the judgment of the reliability of the reported dispersivity and the worth of a study. Often, the purpose of a study was for something other than the determination of dispersivity. Our classification of dispersivity is not intended as a judgment on the quality of a study as a whole, but rather to provide us with some criteria with which to screen the large number of data values obtained. By then examining the more reliable data, conclusions which evolve from the data will be more soundly based and alternative interpretations may become apparent.

High-reliability dispersivity data. For a reported dispersivity value to be classified as high reliability, each of the following criteria must have been met.

1. The tracer test was either ambient flow with known input, diverging radial flow, or a two-well pulse test (without recirculation). These three test configurations produce breakthrough curves which are sensitive to the dispersion coefficient and appear to work well in field applications [*Welty and Gelhar*, 1989]. The radial converging flow test is generally considered less satisfactory than the diverging test because breakthrough curves at the pumping well for the converging test frequently exhibit tailing, which complicates the interpretation of these tests. Some researchers attribute this behavior to two or more discrete geologic layers and try to reproduce the observed breakthrough curve by superposition of breakthrough curves in each layer, where the properties of each layer may differ [e.g., *Ivanovitch and Smith*, 1978; *Sauty*, 1977]. The problem with this interpretation is that there are typically numerous heterogeneities on a small scale that cannot be attributed solely to identifiable layers. One possible explanation of the tailing in radial convergent tests is sometimes termed "borehole flushing," where the tail of the breakthrough curve is attributed to the slow flushing of the input slug of tracer out of the injection borehole by the ambient groundwater flow. *Goblet* [1982] measured the slow flushing of tracer out of the

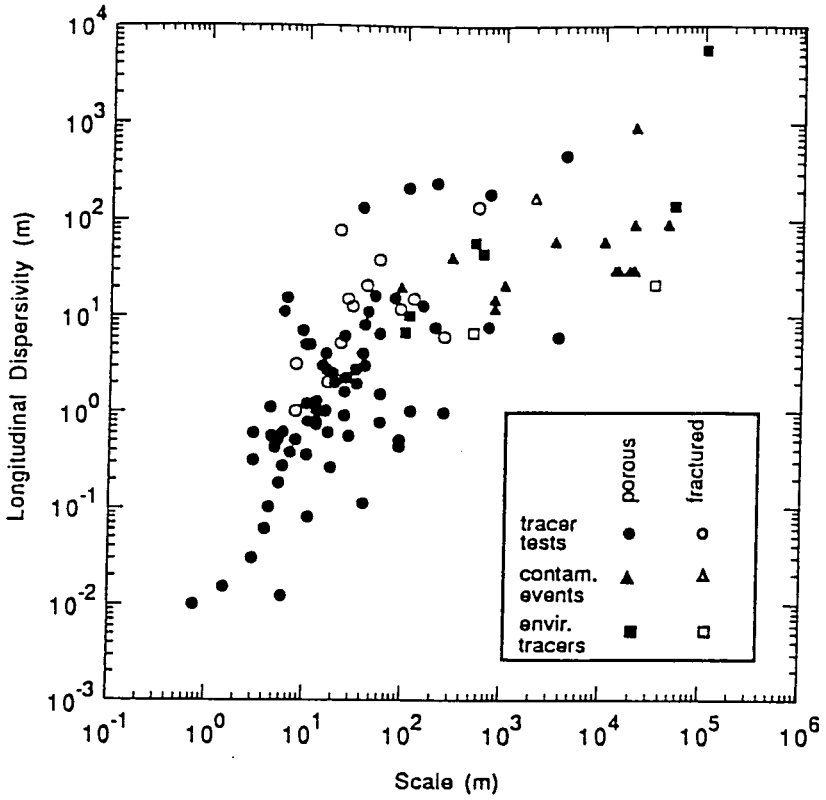

Fig. 1. Longitudinal dispersivity versus scale of observation identified by type of observation and type of aquifer. The data are from 59 field sites characterized by widely differing geologic materials.

borehole and modeled the effect as an exponentially decreasing input. His solution reproduced the tailing observed at the pumping well. In cases where borehole flushing was observed and accounted for, dispersivities obtained from a radial convergent flow test were not excluded from the high-reliability category.

2. The tracer input must be well defined. Both the input concentration and the temporal distribution of the input concentrations must be known (measured). If not, the input is another unknown in the solution of the advection-dispersion equation, and we are less confident in the resulting value of dispersivity.

3. The tracer must be conservative. A reactive or nonconservative tracer complicates the governing equations and resulted in additional parameters that must be estimated. Consequently, we are less confident in the resulting dispersivity. Tracers such as Cl^-, I^-, Br^-, and tritium were considered to be conservative.

4. The dimensionality of the tracer concentration measurements was appropriate. A tracer introduced into an aquifer will spread in three spatial dimensions. High-reliability dispersivities were judged to be those where three-dimensional monitoring was used in all cases except where the aquifer tracer had been injected and measured over the full depth of the aquifer; in this case two-dimensional monitoring was acceptable. In all other cases, where the dimension of the measurement was either not reported or where two-dimensional measurements were used where three-dimensional measurements should have been used, the dispersivity values were judged to be of lower reliability.

5. The analysis of the concentration data was appropriate. Since the interpretation of the tracer data is necessarily linked to the type of tracer test to which the interpretation method is applied, these two features of the field studies were evaluated together. The three general categories of data interpretation can be grouped as follows: (1) breakthrough curve analysis, usually applied to uniform ambient flow tests and radial flow tests [e.g., *Sauty*, 1980]; (2) method of spatial moments, applied to uniform ambient flow tests [*Freyberg*, 1986]; and (3) numerical methods, applied to contamination events [e.g., *Pinder*, 1973; *Konikow and Bredehoeft*, 1974].

A common difficulty with the interpretation of concentration data using breakthrough curve matching to determine dispersivity is the assumption that the dispersivity is constant. The field data assembled in this review suggest that this assumption is not valid, at least for small-scale tests (tens of meters). At larger scales (hundreds of meters) an asymptotic constant value of dispersivity is predicted by some theories. However, at most sites the displacement distance after which the dispersivity is constant is not

TABLE 2. Numbers of Dispersivities for Different Types of Tests and Media

	Tracer Type			
Media Type	Artificial	Contamination	Environmental	Total
Porous	68	14	6	88
Fractured	15	1	2	18
Total	83	15	8	106

TABLE 3. Criteria Used to Classify the Reliability of the Reported Dispersivity Values

Classification	Criteria
High reliability	Tracer test was either ambient flow, radial diverging flow, or two-well instantaneous pulse test (without recirculation). Tracer input was well defined. Tracer was conservative. Spatial dimensionality of the tracer concentration measurements was appropriate. Analysis of the tracer concentration data was appropriate.
Low reliability	Two-well recirculating test with step input was used. Single-well injection-withdrawal test with tracer monitoring at the single well was used. Tracer input was not clearly defined. Tracer breakthrough curve was assumed to be the superposition of breakthrough curves in separate layers. Measurement of tracer concentration in space was inadequate. Equation used to obtain dispersivity was not appropriate for the data collected.

known. Data for which no a priori assumptions were made regarding the dispersivity were considered to be highly reliable.

A second major problem with many of the analyses reviewed was that a one- or two-dimensional solution to the advection-dispersion equation was used when the spreading of the plume under consideration was three-dimensional in nature. High-reliability dispersivities were those for which the dimensionality of the solute plume, the solute measurements, and the data analyses were consistent.

Low-reliability dispersivity data. A reported dispersivity was classified as being of low reliability if one of the following criteria was met.

1. The two-well recirculating test with a step input was used. The problem with this configuration is that, except for very early time where concentrations are low, the breakthrough curve is not strongly influenced by dispersion, but rather is determined by the different travel times along the flow paths established by injection and pumping wells [*Welty and Gelhar*, 1989]. As a result, the two-well test with a step input is generally insensitive to dispersion. For this reason all tests of this type were considered to produce data of low reliability.

2. The single-well injection-withdrawal test was used with tracer monitoring at the pumping well. A difficulty encountered in the small-scale, single-well, injection-withdrawal test (where water is pumped into and out of one well) is that if observations are made at the production well, the dispersion process observed is different from one of unidirectional flow. The problem stems from the fact that macrodispersion near the injection well is due to velocity differences associated with layered heterogeneity of the hydraulic conductivity. In the single-well test with observations made at the production well, the effect observed is that of reversing the velocity of the water. If the tracer travels at different velocities in layers as it radiates outward, it will also travel with the same velocity pattern as it is drawn back to the production well. As a result, the mixing process is partially reversible and the dispersivity would be underestimated relative to the value for unidirectional flow. *Heller* [1972] has carried out experiments which demonstrate the reversibility effect on a laboratory scale.

3. The tracer input was not clearly defined. When a contamination event or environmental tracer is modeled, the tracer input (both quantity and temporal distribution) is not well defined and becomes another unknown in solving the advection-dispersion equation.

4. The tracer breakthrough curve was assumed to be the superposition of breakthrough curves in separate layers when there was little or no evidence of such layers at the field site. These studies generally assume that the porous medium is perfectly stratified, which, especially at the field scale, may not be a valid assumption. At a small scale (a few meters) where the existence of continuous layers may be a reasonable assumption, the dispersivity of each layer does not represent the field-scale parameter. The field-scale dispersivity is a result of the spreading due to the different velocities in each layer.

5. The measurement of tracer concentration in space was inadequate. Under ambient flow conditions the tracer is usually distributed in three-dimensional space, but if the measurements are two-dimensional then the actual tracer cloud cannot be analyzed lacking the appropriate data. If the tracer is introduced over the entire saturated thickness, then two-dimensional measurements would be adequate.

6. The equation used to obtain dispersivity was not appropriate for the data collected. Various assumptions regarding flow and solute characteristics are made in obtaining a solution to the advection-dispersion equation. To apply a particular solution to the data from a field experiment, the assumptions in that solution must be consistent with the experimental conditions. One common example is the case of applying a one-dimensional (uniform velocity) flow solution to a radial flow test in which the converging (or diverging) flow field around the pumping or injection well is clearly nonuniform.

Results of classification. From the classification process, 14 dispersivity values were judged to be of high reliability. The sites where these values were determined include Borden, Ontario, Canada; Otis Air Force Base, Cape Cod, Massachusetts; Hanford, Washington; Mobile, Alabama; University of California, Berkeley; Yavne region, Israel; Bonnaud, France (six tests); and Palo Alto bay lands. There were 61 values judged to be of low reliability for one or more of the reasons discussed above; 31 sites provided data judged to be of intermediate value. Figure 2 depicts the longitudinal dispersivity data replotted with symbols reflecting the reliability classification; the largest symbols indicate data judged to be of highest reliability.

The general compilation of all dispersivity data in Figure 1 indicates that dispersivity might increase indefinitely with scale, but after critically evaluating the data in terms of reliability as shown in Figure 2, it is evident that this trend cannot be extrapolated with confidence to all scales. The largest high-reliability dispersivity value is 4 m (Mobile, Alabama) and the largest scale of high-reliability values is 250 m (Cape Cod, Massachusetts). It is not clear from these data whether dispersivity increases indefinitely with scale or whether the relationship becomes constant for very large scales, as would be predicted by some theories. This points

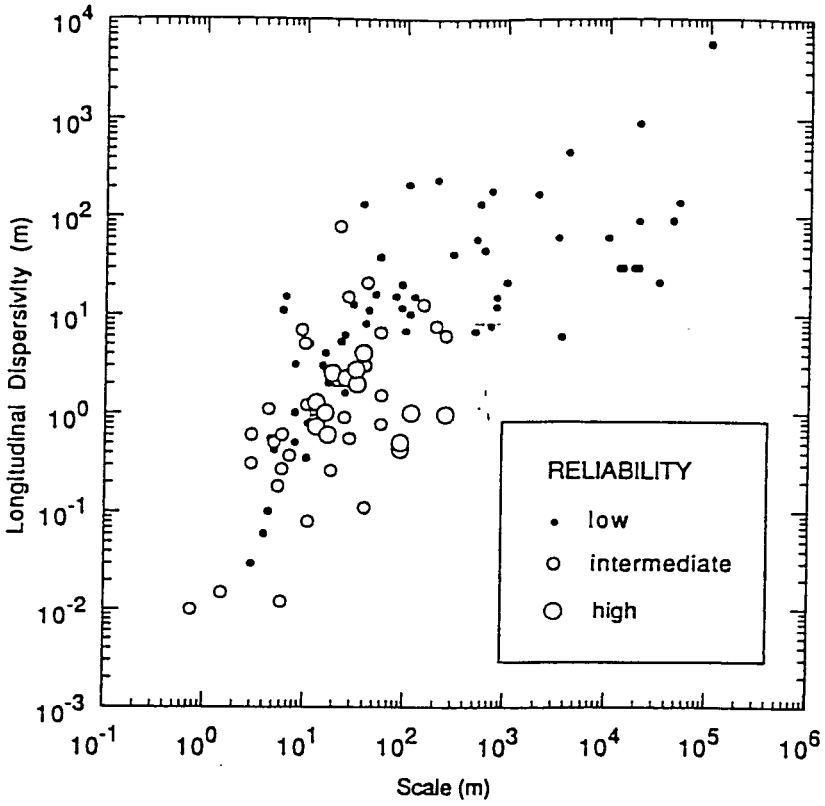

Fig. 2. Longitudinal dispersivity versus scale with data classified by reliability.

to a need for reliable data at scales larger than 250 m. Whether conducting controlled tracer tests at these very large scales is feasible is open to question.

When the reliability of the data is considered, the apparent difference between fractured and porous media at small scales (Figure 1) is regarded to be less significant because none of the fractured media data are of high reliability.

Reanalyses of Selected Dispersivity Data

In cases where the concentration data collected were of high reliability but the method of analysis could be improved, we reevaluated the data to determine a dispersivity value which we judged to be of higher reliability. The details of these analyses are reported by *Welty and Gelhar* [1989]. The results are summarized here.

Corbas, France. The data from this converging radial flow tracer test are reported by *Sauty* [1977]. These data are of particular interest because tests were conducted at three different scales in the same aquifer material; tracer was injected at 25, 50, and 150 m from a pumping well. *Sauty* [1977] evaluated these data using uniform flow solutions to the one-dimensional advection-dispersion equation. At the two smaller-scale tests, he assumed a two-layer scheme, although this assumption was not supported by geologic evidence. For this reason the data at the smaller scales were rated to be of lower reliability than the data at 150 m. We reevaluated these data using a solution that accounts for nonuniform, convergent radial flow effects and that makes no assumptions about geologic layers [*Welty and Gelhar*, 1989]. The values of dispersivity reported by Sauty at 25 m are 11 m and 1.25 m for the two hypothesized layers; we calculated a value of 2.4 m without the assumption of layers. At 50 m, Sauty calculated dispersivity values of 25 m and 6.25 m for the two layers; we calculate an overall value of 4.6 m. At a scale of 150 m, Sauty calculated a dispersivity value of 12.5 m without the assumption of layers; our calculation of 10.5 m is in close agreement. Our calculations indicate that dispersivity increases with scale, accounting for nonuniform flow effects and without the arbitrary assumption of geologic layers.

Savannah River Plant, Georgia. *Webster et al.* [1970] evaluated data from a two-well recirculating test using the methodology of *Grove and Beetem* [1971]. This analysis assumes uniform flow along stream tubes and sums individual breakthrough curves along the stream tubes to obtain a composite breakthrough curve. A dispersivity value of 134 m at a scale of 538 m was obtained using this method. We reevaluated the data using the methodology of *Gelhar* [1982] which accounts for nonuniform flow effects. We obtained a dispersivity value of 47 m from our analysis. We have more confidence in this value because the analysis more accurately represents the actual flow configuration.

Tucson, Arizona. The data reported by *Wilson* [1971] for a two-well test were also evaluated by *Robson* [1974] using a Grove and Beetem–type analysis. Wilson reported a value of longitudinal dispersivity of 15.2 m at a scale of 79.2 m. Using a nonuniform flow solution based on that of *Gelhar* [1982], we calculated a value of longitudinal dispersivity of 1.2 m, an order of magnitude smaller than that of Robson. Again, we have more confidence in this value because the analysis more accurately reflects the actual flow situation.

Columbus, Mississippi. The natural gradient tracer test at the Columbus site (E. E. Adams and L. W. Gelhar, Field

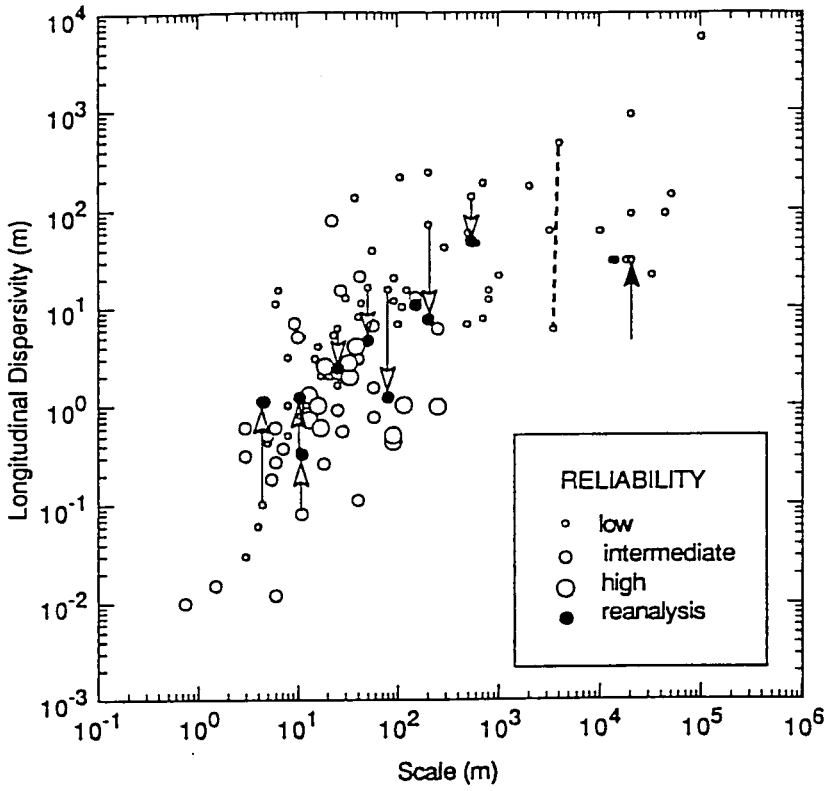

Fig. 3. Longitudinal dispersivity versus scale of observation with adjustments resulting from reanalyses. Arrows indicate reported values at tails and corresponding values from reanalyses at heads. Dashed line connects two dispersivity values determined at the Hanford site.

study of dispersion in a heterogeneous aquifer: Spatial moments analysis, submitted to *Water Resources Research*, 1991; hereinafter Adams and Gelhar, submitted manuscript, 1991) is unique in that the large-scale ambient flow field exhibits strong nonuniformity and the aquifer is very heterogeneous. A superficial spatial moments interpretation, ignoring the flow nonuniformity, indicated a longitudinal dispersivity of around 70 m, whereas a more refined analysis that explicitly includes the influence of flow nonuniformity yields a dispersivity of around 7 m (Adams and Gelhar, submitted manuscript, 1991). This refined estimate is regarded to be of intermediate reliability because of the uncertainty regarding the mass balance at the Columbus site.

From the above reanalyses, all values of dispersivity calculated were smaller than the original values. We have higher confidence in these values because they are associated with solutions to the advection-dispersion equation with more realistic assumptions. In all cases we would rate the new values to be of intermediate reliability instead of low reliability. The reevaluated data are shown as solid symbols on Figure 3 connected to their original values by vertical arrows.

Based on the above reanalyses, we suspect that it is most likely that improved analyses would reduce many of the lower-reliability dispersivities in Figure 2. However, there are a few cases for which more appropriate observations and/or interpretations would most likely lead to larger dispersivities. For example, the Twin Lake natural gradient tracer test [*Moltyaner and Killey*, 1988*a*, *b*] was interpreted by using breakthrough curves at individual boreholes constructed as the average of breakthrough curves in three somewhat arbitrarily defined layers. We suspect that this kind of localized observation will produce a significantly lower dispersivity than would result from a spatial moments analysis which considers the overall spreading of the plume. The magnitude of the possible increase in the dispersivity cannot be assessed because the sampling network did not completely encompass the plume at the Twin Lake site.

Another example is that of the first Borden site natural gradient experiment [*Sudicky et al.*, 1983] which was analyzed using an analytical solution with spatially constant dispersivities. In the near-source region where dispersivities are actually increasing with displacement, this approach will tend to underestimate the magnitude of the dispersivity. *Gelhar et al.* [1985] reanalyzed the first Borden experiment using the method of spatial moments and found that the longitudinal dispersivity at 11 m was 2–4 times that found by *Sudicky et al.* [1983]. The resulting increase in the dispersivity is illustrated in Figure 3 connected to the original point by a vertical line. Because of the incomplete plume sampling and plume bifurcation in this test (only the "slow zone" was analyzed), this point is still regarded to be of intermediate reliability.

Dispersivities at small displacements will also be underestimated if based on breakthrough curves measured in localized samplers in individual layers. Such effects are likely, for example, in the Perch Lake [*Lee et al.*, 1980] and Lower Glatt Valley [*Hoehn*, 1983] interpretations. Later interpretation of the Lower Glatt Valley data using temporal moments [*Hoehn and Santschi*, 1987] shows values an order of

magnitude larger; these are connected with the original values by vertical lines in Figure 3.

As a further illustration of the uncertainty in the longitudinal dispersivity values in Figure 2, consider the data for the Hanford site. The tracer test [*Bierschenk*, 1959; *Cole*, 1972] interpreted from breakthrough curves at two different wells at roughly the same distance (around 4000 m) from the injection point produced values differing by 2 orders of magnitude (see dashed line in Figure 3). This difference illustrates the difficulty in interpreting point breakthrough curves in heterogeneous aquifers, even at this large displacement. The numerical simulations of the contamination plume [*Ahlstrom et al.*, 1977] extending to 20,000 m used a dispersivity of 30.5 m (100 feet) as identified by the bold arrow in Figure 3. Evidently this round number (100 feet) was popular in several different simulations of contaminant plumes.

In none of the cases of simulations of contamination events is there any explicit information on how the dispersivity values were selected or in what sense the values may be optimal. Consequently it is not possible to quantify the uncertainty in dispersivity values based on contamination event simulations. However, experience suggests that, because of the possible tendency to select large dispersivities which avoid the numerical difficulties associated with large grid Peclet numbers, some of the dispersivity values based on contaminant plumes are likely to be biased toward higher values. Such overestimates would occur mainly at larger scales.

The results of these reanalyses provide an explicit indication of the uncertainty in the dispersivity values in Figure 2 and suggest that for large displacements the low-reliability dispersivities are likely to decrease whereas for small displacements some increases can be expected.

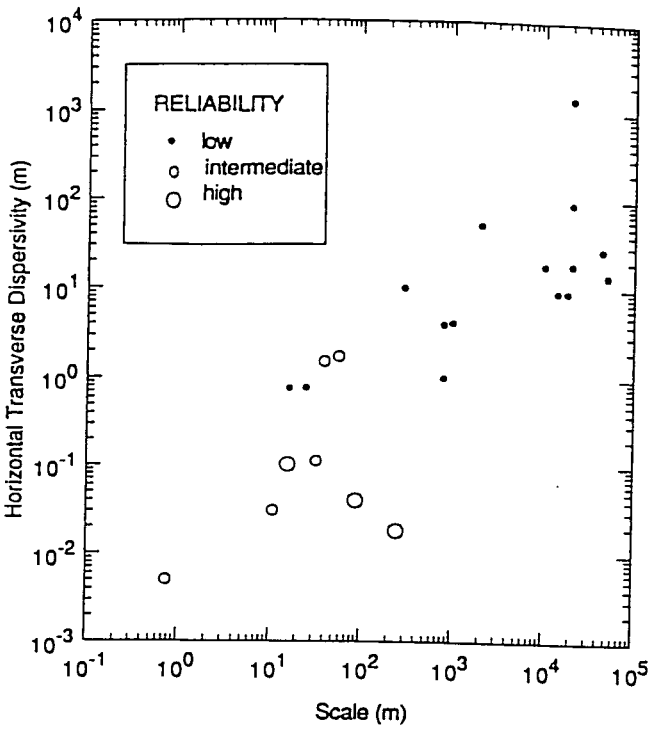

Fig. 4. Horizontal transverse dispersivity as a function of observation scale.

Transverse Dispersivities

Although the data on transverse dispersivity are much more limited, they reveal some features which are important in applications. The data on horizontal and vertical transverse dispersivities are summarized in Figures 4 and 5, which show these parameters as a function of scale of observation. The data are portrayed in terms of reliability classification with the largest symbols identifying the high-reliability points.

In the case of the horizontal dispersivity, there appears to be some trend of increasing dispersivity with scale but this appearance results from low-reliability data which finds their origin largely in contaminant event simulations using two-dimensional depth-averaged descriptions. In these contamination situations the sources are often ill-defined; if the actual source area is larger than that represented in the model there will be greater transverse spreading which would incorrectly be attributed to transverse dispersion.

In the case of vertical transverse dispersion (Figure 5), the data are even more limited and certainly do not imply any significant trend with overall scale. Note that there are only two points of high reliability, those corresponding to the Borden [*Freyberg*, 1986] and Cape Cod [*Garabedian et al.*, 1988, 1991] sites. The estimate of the vertical transverse dispersivity for the Borden site is from the recent three-dimensional analysis of *Rajaram and Gelhar* [1991]. The vertical transverse dispersivity is seen to be much smaller than the horizontal transverse dispersivity, apparently reflecting the roughly horizontal stratification of hydraulic conductivity encountered in permeable sedimentary materials. All of the vertical dispersivities are less than 1 m and high-reliability values are only a few millimeters, this being the same order of magnitude as the local transverse dispersivity for sandy materials.

The ratio of longitudinal dispersivity to the horizontal and vertical transverse dispersivities is shown in Figure 6. This form of presentation is used because it is common practice to select constant values for the ratio of longitudinal to transverse dispersivities. For one thing, this plot illustrates the popularity of using, in numerical simulations, a horizontal transverse dispersivity which is about one third of the longitudinal dispersivity (the horizontal dashed line in Figure 6). There does not appear to be any real justification for using this ratio. We are not aware of any simulation work which systematically demonstrates the appropriateness of this value for the horizontal transverse dispersivity. The two high-reliability points show an order of magnitude higher ratio of longitudinal to horizontal transverse dispersivities. The vertical dashed lines in Figure 6 are used to identify three-dimensionally monitored sites for which all three principal components of the dispersivity tensor have been estimated. In all of these cases, the vertical transverse dispersivity is 1–2 orders of magnitude smaller than the horizontal transverse dispersivity. This behavior further emphasizes the small degree of vertical mixing which is frequently encountered in naturally stratified sediments. This small degree of vertical mixing is clearly an important consideration in many applications, such as the design of observation networks to monitor contamination plumes and the development of remediation schemes. Consequently, in order to model many field situations realistically, it will be necessary to use three-dimensional transport models which adequately represent the small but finite vertical mixing.

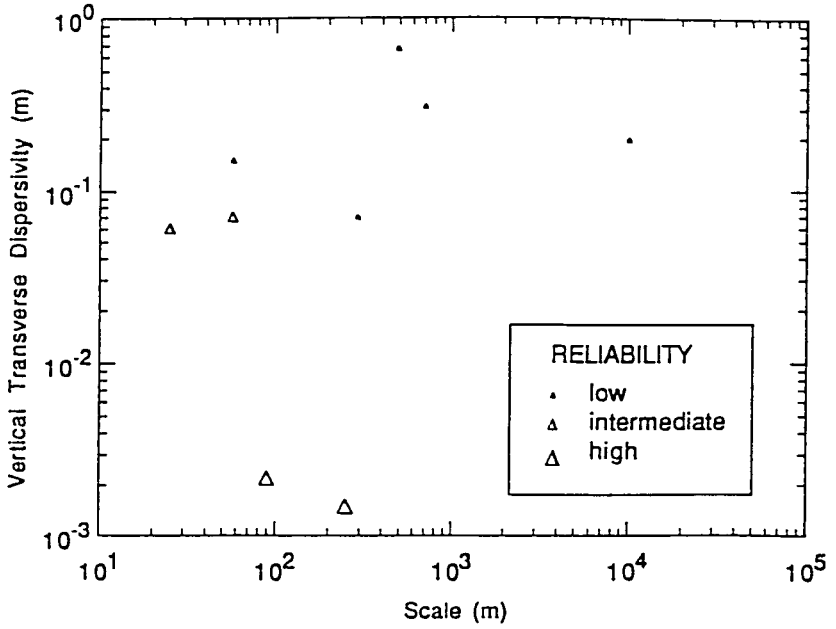

Fig. 5. Vertical transverse dispersivity as a function of observation scale.

INTERPRETATIONS

This review of field observations of dispersive mixing in aquifers demonstrates several overall features which are evident from the graphical and tabular information developed here. Taken in aggregate, without regard for reliability, the data indicate a clear trend of systematic increase of longitudinal dispersivity with scale. In terms of aquifer type (porous versus fractured media) the data at smaller scale may seem to be higher for fractured media but, in view of the lower reliability of the fractured media data, this difference is of minimal significance.

When the data on longitudinal dispersivity are classified according to reliability, the pattern regarding scale dependence of dispersivity is less clear (see Figure 2). There are no high-reliability points at scales greater than 300 m and the high-reliability points are systematically in the lower portion of the scattering of data. The lack of high-reliability data at scales greater than 300 m reflects the fact that the data beyond that scale are almost exclusively from contamination simulations or environmental tracer studies for which the solute input is typically ill-defined. Because of the very long period of time required to carry out controlled input tracer experiments at these larger scales, such experiments have not been undertaken.

Although the data shown in Figure 2 suggest that some overall trend of increasing dispersivity with scale is plausible, it does not seem reasonable to conclude that a single universal line [*Neuman*, 1990] can be meaningfully identified

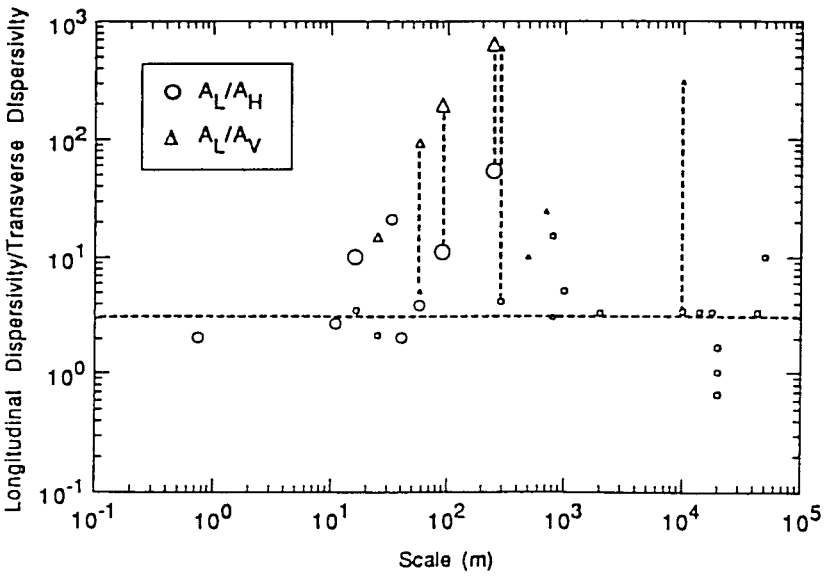

Fig. 6. Ratio of longitudinal to horizontal and vertical transverse dispersivities; largest symbols are high reliability and smallest symbols are low reliability. Vertical dashed lines connecting two points indicate sites where all three principal components of the dispersivity tensor have been measured. Horizontal dashed line indicates a ratio of A_L/A_T = 1/3, which has been widely used in numerical simulations.

by applying standard linear regression to all of the data. Rather we would expect a family of curves reflecting different dispersivities in aquifers with different degrees of heterogeneity. At a given scale, the longitudinal dispersivity typically ranges over 2–3 orders of magnitude. This degree of variation can be explained in terms of the established stochastic theory [e.g., *Gelhar and Axness*, 1983; *Dagan*, 1984] which shows that the longitudinal dispersivity is proportional to the product of the variance and the correlation scale of the natural logarithm of hydraulic conductivity. A compilation of data on these parameters [*Gelhar*, 1986] shows that they vary over a range that can easily explain the range of variation in Figure 2. The theoretical results for the developing dispersion process [*Gelhar et al.*, 1979; *Dagan*, 1984; *Gelhar*, 1987; *Naff et al.*, 1988] show that the longitudinal dispersivity initially increases linearly with displacement distance and gradually approaches a constant asymptotic value [see *Gelhar*, 1987, Figure 9]. One could visualize the behavior of Figure 2 as being the result of superimposing several such theoretical curves with different parameters characterizing aquifer heterogeneity.

The results of reanalyses for several of the individual sites serve to illustrate explicitly the uncertainty involved in the estimates of longitudinal dispersivity. The reanalyses indicate that, for the most part, improved analysis will lead to decreases in the longitudinal dispersivity except possibly for very small displacements where limited localized sampling can produce underestimates of the bulk spreading and mixing. In cases where the dispersivity estimates were based on numerical simulations of contamination events, the degree of uncertainty is likely large and ill-determined, but bias in some of the estimates toward the high side seems most likely.

From an applications perspective, the information assembled here should serve as a strong cautionary note about routinely adopting dispersivities from Figure 2 or a linear regression representation through the data. We feel that the preponderance of evidence favors the use of dispersivity values in the lower half of the range at any given scale. If values in the upper part of the range are adopted, excessively large dilution may be predicted and the environmental consequences misrepresented. In the case of transverse dispersivities, it is particularly important to recognize the very low vertical transverse dispersivities that have been observed at several sites. As a result, many contamination plumes will exhibit very limited vertical mixing with high concentrations at a given horizon. The recognition of such features is of obvious importance in designing monitoring schemes and implementing aquifer remediation. Horizontal transverse dispersivities are typically an order of magnitude smaller than the longitudinal dispersivity whereas vertical transverse dispersivities are another order of magnitude lower.

From a research perspective, the data reviewed here suggest a need for some skepticism regarding "universal" models which represent the scattered data of varying reliability by a single straight line. The presumption of such a universal model ignores the fact that different aquifers will have different degrees of heterogeneity at a given scale. The data suggest that there is a scale dependence of longitudinal dispersivity but reliable data must be developed at larger scales in order to establish the nature of the dependence. Clearly, there is a need for very large scale, long-term, carefully planned experiments extending to several kilometers.

Acknowledgments. The work was supported in part by the Electric Power Research Institute (EPRI), project 2485-5, which was a joint effort of the Massachusetts Institute of Technology (MIT) and the Tennessee Valley Authority (TVA). This portion of the work was done at MIT under contract TV-61664A with TVA. The work was also supported by the National Science Foundation, grant CES-8814615.

REFERENCES

Ahlstrom, S. W., H. P. Foote, R. C. Arnett, C. P. Cole, and R. J. Serne, Multicomponent mass transport model: Theory and numerical implementation (discrete-particle-random-walk-version), *Rep. BNWL-2127*, Battelle Pac. Northwest Lab., Richland, Wash., 1977.

Anderson, M. P., Using models to simulate the movement of contaminants through groundwater flow systems, *CRC Crit. Rev. Environ. Control*, *9*, 97–156, 1979.

Bassett, R. L., et al., Preliminary data from a series of artificial recharge experiments at Stanton, Texas, *U.S. Geol. Surv. Open File Rep.*, *81-0149*, 1980.

Bear, J., *Dynamics of Fluids in Porous Media*, Elsevier Scientific, New York, 1972. (Reprinted by Dover, New York, 1988.)

Beims, U., Planung, Durchführung und Auswertung von Gütepumpversuchen, *Z. Angew. Geol.*, *29*(10), 482–490, 1983.

Bentley, H. W., and G. R. Walter, Two-well recirculating tracer tests at H-2: Waste Isolation Pilot Plant (WIPP), southwest New Mexico, draft paper, Hydro Geochem., Inc., Tucson, Ariz., 1983.

Betson, R. P., J. M. Boggs, S. C. Young, W. R. Waldrop, and L. W. Gelhar, Macrodispersion experiment (MADE): Design of a field experiment to investigate transport processes in a saturated groundwater zone, *Rep. EPRI EA-4082*, Elec. Power Res. Inst., Palo Alto, Calif., June 1985.

Bierschenk, W. H., Aquifer characteristics and ground-water movement at Hanford, *Rep. HW-60601*, Hanford At. Products Oper., Richland, Wash., 1959.

Bredehoeft, J. D., and G. F. Pinder, Mass transport in flowing groundwater, *Water Resour. Res.*, *9*(1), 144–210, 1973.

Claasen, H. C., and E. H. Cordes, Two-well recirculating tracer test in fractured carbonate rock, Nevada, *Hydrol. Sci. Bull.*, *20*(3), 367–382, 1975.

Cole, J. A., Some interpretations of dispersion measurements in aquifers, *Groundwater Pollution in Europe*, edited by J. A. Cole, pp. 86–95, Water Research Association, Reading, England, 1972.

Dagan, G., Stochastic modeling of groundwater flow by unconditional and conditional probabilities, 2, The solute transport, *Water Resour. Res.*, *18*(4), 835–848, 1982.

Dagan, G., Solute transport in heterogeneous porous formations, *J. Fluid Mech.*, *145*, 151–177, 1984.

Daniels, W. R. (Ed.), Laboratory field studies related to the radionuclide migration project, *Progress Rep. LA-8670-PR*, Los Alamos Sci. Lab., Los Alamos, N. M., 1981.

Daniels, W. R. (Ed.), Laboratory field studies related to the radionuclide migration project (draft), *Progress Rep. LA-9192-PR*, Los Alamos Sci. Lab., Los Alamos, N. M., 1982.

Davis, S. N., G. M. Thompson, H. W. Bentley, and G. Stiles, Groundwater tracers—A short review, *Ground Water*, *18*(1), 14–23, 1980.

Davis, S. N., D. J. Campbell, H. W. Bentley, and T. J. Flynn, An introduction to groundwater tracers, *Rep. EPA/600/2-85/022*, Environ. Prot. Agency, Washington, D. C., 1985. (Available as *NTIS PB86-100591* from Natl. Tech. Inf. Serv., Springfield, Va.)

de Marsily, G., *Quantitative Hydrogeology*, Academic, San Diego, Calif., 1986.

Dieulin, A., Propagation de pollution dans un aquifere alluvial: L'effet de parcours, doctoral dissertation, Univ. Pierre et Marie Curie-Paris VI and l'Ecole Natl. Super. des Mines de Paris, Fontainebleau, France, 1980.

Dieulin, A., Lixiviation in situ d'un gisement d'uranium en milieu granitique, *Draft Rep. LHM/RD/81/63*, Ecole Natl. Super. des Mines de Paris, Fontainebleau, France, 1981.

Egboka, B. C. E., J. A. Cherry, R. N. Farvolden, and E. O. Frind, Migration of contaminants in groundwater at a landfill: A case study, 3, Tritium as an indicator of dispersion and recharge, *J. Hydrol.*, *63*, 51–80, 1983.

Fenske, P. R., Hydrology and radionuclide transport, monitoring well HT-2m, Tatum Dome, Mississippi, *Proj. Rep. 25, Tech. Rep.*

NVD-1253-6, Cent. for Water Resour. Res., Desert Res. Inst., Univ. of Nev. Syst., Reno, 1973.

Freyberg, D. L., A natural gradient experiment on solute transport in a sand aquifer, 2, Spatial moments and the advection and dispersion of nonreactive tracers, *Water Resour. Res.*, *22*(13), 2031–2046, 1986.

Fried, J. J., *Groundwater Pollution*, Elsevier, New York, 1975.

Fried, J. J., and P. Ungemach, Determination in situ du coefficient de dispersion longitudinale d'un milieu poreux naturel, *C. R. Acad. Sci., Ser. 2*, *272*, 1327–1329, 1971.

Garabedian, S. P., L. W. Gelhar, and M. A. Celia, Large-scale dispersive transport in aquifers: Field experiments and reactive transport theory, *Rep. 315*, Ralph M. Parsons Lab. for Water Resour. and Hydrodyn., Mass. Inst. of Technol., Cambridge, 1988.

Garabedian, S. P., D. R. LeBlanc, L. W. Gelhar, and M. A. Celia, Large-scale natural gradient tracer test in sand and gravel, Cape Cod, Massachusetts, 2, Analysis of tracer moments for a nonreactive tracer, *Water Resour. Res.*, *27*(5), 911–924, 1991.

Gelhar, L. W., Analysis of two-well tracer tests with a pulse input, *Rep. RHO-BW-CR-131 P*, Rockwell Intl., Richland, Wash., 1982.

Gelhar, L. W., Stochastic subsurface hydrology from theory to applications, *Water Resour. Res.*, *22*, 135S–145S, 1986.

Gelhar, L. W., Stochastic analysis of solute transport in saturated and unsaturated porous media, *NATO ASI Ser., Ser. E*, *128*, 657–700, 1987.

Gelhar, L. W., and C. L. Axness, Three dimensional stochastic analysis of macrodispersion in aquifers, *Water Resour. Res.*, *19*(1), 161–180, 1983.

Gelhar, L. W., A. L. Gutjahr, and R. L. Naff, Stochastic analysis of macrodispersion in a stratified aquifer, *Water Resour. Res.*, *15*(6), 1387–1397, 1979.

Gelhar, L. W., A. Mantaglou, C. Welty, and K. R. Rehfeldt, A review of field-scale physical solute transport processes in saturated and unsaturated porous media, *EPRI Rep. EA-4190*, Elec. Power Res. Inst., Palo Alto, Calif., Aug. 1985.

Goblet, P., Interpretation d'experiences de tracage en milieu granitique (site B), *Rep. LHM/RD/82/11*, Cent. d'Inf. Geol., Ecole Natl. Super. des Mines de Paris, Fontainebleau, France, 1982.

Grove, D. B., The use of Galerkin finite-element methods to solve mass transport equations, *Rep. USGS/WRD/WRI-78/011*, U.S. Geol. Surv., Denver, Colo., 1977. (Available as *NTIS PB 277-532* from Natl. Tech. Inf. Serv., Springfield, Va.)

Grove, D. B., and W. A. Beetem, Porosity and dispersion constant calculations for a fractured carbonate aquifer using the two-well tracer method, *Water Resour. Res.*, *7*(1), 128–134, 1971.

Gupta, S. K., K. K. Tanji, and J. N. Luthin, A three-dimensional finite element ground water model, *Rep. UCAL-WRC-C-152*, Calif. Water Resour. Cent., Univ. of Calif., Davis, 1975. (Available as *NTIS PB 248-925* from Natl. Tech. Inf. Serv., Springfield, Va.)

Halevy, E., and A. Nir, Determination of aquifer parameters with the aid of radioactive tracers, *J. Geophys. Res.*, *67*(5), 2403–2409, 1962.

Harpaz, Y., Field experiments in recharge and mixing through wells, *Underground Water Storage Study Tech. Rep. 17, Publ. 483*, Tahal–Water Plann. for Isr., Tel Aviv, 1965.

Heller, J. P., Observations of mixing and diffusion in porous media, *Proc. Symp. Fundam. Transp. Phenom. Porous Media, 2nd*, 1–26, 1972.

Helweg, O. J., and J. W. Labadie, Linked models for managing river basin salt balance, *Water Resour. Res.*, *13*(2), 329–336, 1977.

Hoehn, E., Geological interpretation of local-scale tracer observations in a river-ground water infiltration system, draft report, Swiss Fed. Inst. Reactor Res. (EIR), Würenlingen, Switzerland, 1983.

Hoehn, E., and P. H. Santschi, Interpretation of tracer displacement during infiltration of river water to groundwater, *Water Resour. Res.*, *23*(4), 633–640, 1987.

Huyakorn, P. S., P. F. Anderson, F. J. Motz, O. Güven, and J. G. Melville, Simulations of two-well tracer tests in stratified aquifers at the Chalk River and the Mobile sites, *Water Resour. Res.*, *22*(7), 1016–1030, 1986.

Iris, P., Contribution à l'étude de la valorisation energetique des aquifères peu profonds, thèse de docteur-ingenieur, Ecole des Mines de Paris, Fontainebleau, France, 1980.

Ivanovitch, M., and D. B. Smith, Determination of aquifer parameters by a two-well pulsed method using radioactive tracers, *J. Hydrol.*, *36*(1/2), 35–45, 1978.

Kies, B., Solute transport in unsaturated field soil and in groundwater, Ph.D. dissertation, Dep. of Agron., N. M., State Univ., Las Cruces, 1981.

Klotz, D., K. P. Seiler, H. Moser, and F. Neumaier, Dispersivity and velocity relationship from laboratory and field experiments, *J. Hydrol.*, *45*(3/4), 169–184, 1980.

Konikow, L. F., Modeling solute transport in ground water, in *Environmental Sensing and Assessment: Proceedings of the International Conference*, article 20-3, Institute for Electrical and Electronic Engineers, Piscataway, N. J., 1976.

Konikow, L. F., and J. D. Bredehoeft, Modeling flow and chemical quality changes in an irrigated stream-aquifer system, *Water Resour. Res.*, *10*(3), 546–562, 1974.

Kreft, A., A. Lenda, B. Turek, A. Zuber, and K. Czauderna, Determination of effective porosities by the two-well pulse method, *Isot. Tech. Groundwater Hydrol., Proc. Symp.*, *2*, 295–312, 1974.

Lallemande-Barres, A., and P. Peaudecerf, Recherche des relations entre la valeur de la dispersivité macroscopique d'un milieu aquifère, ses autres caractéristiques et les conditions de mesure, *Bull. Bur. Rech. Geol. Min., Sect. 3, Ser. 2*, *4*, 1978.

Lau, L. K., W. J. Kaufman, and D. K. Todd, Studies of dispersion in a radial flow system, Canal Seepage Research: Dispersion Phenomena in Flow Through Porous Media, *Progress Rep. 3, I.E.R. Ser. 93, Issue 3*, Sanit. Eng. Res. Lab., Dep. of Eng. and School of Public Health, Univ. of Calif., Berkeley, 1957.

LeBlanc, D. R., Sewage plume in a sand and gravel aquifer, Cape Cod, Massachusetts, *U.S. Geol. Surv. Open File Rep.*, *82-274*, 35 pp., 1982.

Lee, D. R., J. A. Cherry, and J. F. Pickens, Groundwater transport of a salt tracer through a sandy lakebed, *Limnol. Oceanogr.*, *25*(1), 46–61, 1980.

Leland, D. F., and D. Hillel, Scale effects on measurement of dispersivity in a shallow, unconfined aquifer, paper presented at Chapman Conference on Spatial Variability in Hydrologic Modeling, AGU, Fort Collins, Colo., July 21–23, 1981.

Lenda, A., and A. Zuber, Tracer dispersion in groundwater experiments, in *Isot. Hydrol. Proc. Symp. 1970*, 619–641, 1970.

MacFarlane, D. S., J. A. Cherry, R. W. Gilham, and E. A. Sudicky, Migration of contaminants at a landfill: A case study, 1, Groundwater flow and plume delineation, *J. Hydrol.*, *63*, 1–29, 1983.

Mercado, A., Recharge and mixing tests at Yavne 20 well field, *Underground Water Storage Study Tech. Rep. 12, Publ. 611*, Tahal–Water Plann. for Isr., Tel Aviv, 1966.

Meyer, B. R., C. A. R. Bain, A. S. M. DeJesus, and D. Stephenson, Radiotracer evaluation of groundwater dispersion in a multilayered aquifer, *J. Hydrol.*, *50*(1/3), 259–271, 1981.

Molinari, J., and P. Peaudecerf, Essais conjoints en laboratoire et sur le terrain en vue d'une approach simplefiée de la prévision des propagations de substances miscibles dans les aquifères réels, paper presented at Symposium on Hydrodynamic Diffusion and Dispersion in Porous Media, Int. Assoc. for Hydraul. Res., Pavis, Italy, 1977.

Moltyaner, G. L., and R. W. D. Killey, Twin Lake tracer tests: Longitudinal dispersion, *Water Resour. Res.*, *24*(10), 1613–1627, 1988*a*.

Moltyaner, G. L., and R. W. D. Killey, Twin Lake tracer tests: Transverse dispersion, *Water Resour. Res.*, *24*(10), 1628–1637, 1988*b*.

Molz, F. J., O. Güven, and J. G. Melville, An examination of scale-dependent dispersion coefficients, *Ground Water*, *21*, 715–725, 1983.

Molz, F. J., O. Güven, J. G. Melville, R. D. Crocker, and K. T. Matteson, Performance, analysis, and simulation of a two-well tracer test at the Mobile site, *Water Resour. Res.*, *22*(7), 1031–1037, 1986.

Naff, R. L., T.-C. J. Yeh, and M. W. Kemblowski, A note on the recent natural gradient tracer test at the Borden site, *Water Resour. Res.*, *24*(12), 2099–2103, 1988.

Naymik, T. G., and M. J. Barcelona, Characterization of a contaminant plume in ground water, Meredosia, Illinois, *Ground Water*, *19*(5), 517–526, 1981.

Neretnieks, I., Transport in fractured rocks, paper presented at the

17th International Congress on the Hydrology of Rock of Low Permeability, Intl. Assoc. of Hydrogeol., Tucson, Ariz., Jan. 7–12, 1985.

Neuman, S. P., Universal scaling of hydraulic conductivities in geologic media, *Water Resour. Res.*, *26*(8), 1749–1758, 1990.

Neuman, S. P., C. L. Winter, and C. M. Newman, Stochastic theory of field-scale dispersion in anisotropic porous media, *Water Resour. Res.*, *23*(3), 453–466, 1987.

New Zealand Ministry of Works and Development, Water and Soil Division, Movement of contaminants into and through the Heretaunga Plains aquifer, report, Wellington, 1977.

Oakes, D. B., and D. J. Edworthy, Field measurement of dispersion coefficients in the United Kingdom, in *Ground Water Quality, Measurement, Prediction, and Protection*, pp. 327–340, Water Research Centre, Reading, England, 1977.

Papadopulos, S. S., and S. P. Larson, Aquifer storage of heated water: II, Numerical simulation of field results, *Ground Water*, *16*(4), 242–248, 1978.

Perlmutter, N. M., and M. Lieber, Dispersal of plating wastes and sewage contaminants in the groundwater and surface water: South Farmingdale–Massapequid area, Nassau County, New York, *U.S. Geol. Surv. Water Supply Pap.*, *1879-G*, 1970.

Philip, J. R., Issues in flow and transport in heterogeneous porous media, *Transp. Porous Media*, *1*, 319–338, 1986.

Pickens, J. F., and G. E. Grisak, Scale dependent dispersion in a stratified granular aquifer, *Water Resour. Res.*, *17*(4), 1191–1211, 1981.

Pinder, G. F., A Galerkin–finite element simulation of groundwater contamination on Long Island, *Water Resour. Res.*, *9*(6), 1657–1669, 1973.

Rabinowitz, D. D., and G. W. Gross, Environmental tritium as a hydrometeorologic tool in the Roswell Basin, New Mexico, *Tech. Completion Rep. OWRR:A-037-NMEX*, N. M. Water Resour. Res. Inst., Las Cruces, 1972.

Rajaram, H., and L. W. Gelhar, Three-dimensional spatial moments analysis of the Borden tracer test, *Water Resour. Res.*, *27*(6), 1239–1251, 1991.

Roberts, P. V., M. Reinhard, G. D. Hopkins, and R. S. Summers, Advection-dispersion-sorption models for simulating the transport of organic contaminants, paper presented at *International Conference on Ground Water Quality Research*, Rice Univ., Houston, Tex., 1981.

Robertson, J. B., Digital modeling of radioactive and chemical waste transport in the Snake River Plain aquifer of the National Reactor Testing Station, Idaho, *U.S. Geol. Surv. Open File Rep.*, *IDO-22054*, 1974.

Robertson, J. B., and J. T. Barraclough, Radioactive and chemical waste transport in groundwater of National Reactor Testing Station: 20-year case history and digital model, *Underground Waste Manage. Artif. Recharge Prepr. Pap. Int. Symp. 2nd*, *1*, 291–322, 1973.

Robson, S. G., Feasibility of digital water quality modeling illustrated by application at Barstow, California, *U.S. Geol. Surv. Water Resourc. Invest.*, *46-73*, 1974.

Robson, S. G., Application of digital profile modeling techniques to ground-water solute transport at Barstow, California, *U.S. Geol. Surv. Water Supply Pap.*, *2050*, 1978.

Rousselot, D., J. P. Sauty, and B. Gaillard, Etude hydrogéologique de la zone industrielle de Blyes-Saint-Vulbas, rapport préliminaire no. 5: Caracteristiques hydrodynamiques du système aquifère, *Rep. Jal 77/33*, Bur. de Rech. Geol. et Min., Orleans, France, 1977.

Sauty, J. P., Contribution à l'identification des paramèters de dispersion dans les aquifères par interprétation des expériences de tracage, dissertation, Univ. Sci. et Med. et Inst. Natl. Polytech. de Grenoble, Grenoble, France, 1977.

Sauty, J. P., An analysis of hydrodispersive transfer in aquifers, *Water Resour. Res.*, *16*(1), 145–158, 1980.

Sauty, J. P., A. C. Gringarten, and P. A. Landel, The effects of thermal dispersion on injection of hot water in aquifers, paper presented at Invitational Well-Testing Symposium, Lawrence Berkeley Lab., Berkeley, Calif., 1978.

Segol, G., and G. F. Pinder, Transient simulation of saltwater intrusion in southeastern Florida, *Water Resour. Res.*, *12*(1), 65–70, 1976.

Sudicky, E. A., J. A. Cherry, and E. O. Frind, Migration of contaminants in groundwater at a landfill: A case study, 4, A natural-gradient dispersion test, *J. Hydrol.*, *63*, 81–108, 1983.

Sykes, J. F., S. B. Pahwa, R. B. Lantz, and D. S. Ward, Numerical simulation of flow and contaminant migration at an extensively monitored landfill, *Water Resour. Res.*, *18*(6), 1687–1704, 1982.

Sykes, J. F., S. B. Pahwa, D. S. Ward, and D. S. Lantz, The validation of SWENT, a geosphere transport model, in *Scientific Computing*, edited by R. Stapleman et al., pp. 351–361, IMAES/North-Holland, Amsterdam, 1983.

Vaccaro, J. J., and E. L. Bolke, Evaluation of water quality characteristics of part of the Spokane aquifer, Washington and Idaho, using a solute transport digital model, *U.S. Geol. Surv. Open File Rep.*, *82-769*, 1983.

Valocchi, A. J., P. V. Roberts, G. A. Parks, and R. L. Street, Simulation of the transport of ion-exchanging solutes using laboratory-determined chemical parameter values, *Ground Water*, *19*(6), 600–607, 1981.

Walter, G. B., Convergent flow tracer test at H-6: Waste isolation pilot plant (WIPP), southeast New Mexico (draft), Hydro Geochem, Inc., Tucson, Ariz., 1983.

Webster, D. S., J. F. Procter, and J. W. Marine, Two-well tracer test in fractured crystalline rock, *U.S. Geol. Surv., Water Supply Pap.*, *1544-I*, 1970.

Welty, C., and L. W. Gelhar, Evaluation of longitudinal dispersivity from tracer test data, *Rep. 320*, Ralph M. Parsons Lab. for Water Resour. and Hydrodyn., Mass. Inst. of Technol., Cambridge, 1989.

Werner, A., et al., Nutzung von Grundwasser fur Warmepumpen, Versickerrungstest Aefligen, Versuch 2, 1982/83, Water and Energy Manage. Agency of the State of Bern, Switzerland, 1983.

Wheatcraft, S. W., and S. W. Tyler, An explanation of scale-dependent dispersivity in heterogeneous aquifers using concepts of fractal geometry, *Water Resour. Res.*, *24*(4), 566–578, 1988.

Wiebenga, W. A., et al., Radioisotopes as groundwater tracers, *J. Geophys. Res.*, *72*(16), 4081–4091, 1967.

Wilson, L. G., Investigations on the subsurface disposal of waste effluents at inland sites, *Res. Develop. Progress Rep. 650*, U.S. Dep. of Interior, Washington, D. C., 1971.

Wood, W., A geochemical method of determining dispersivity in regional groundwater systems, *J. Hydrol.*, *54*(1/3), 209–224, 1981.

Wood, W. W., and G. G. Ehrlich, Use of baker's yeast to trace microbial movement in ground water, *Ground Water*, *16*(6), 398–403, 1978.

L. W. Gelhar, Ralph M. Parsons Laboratory, Department of Civil Engineering, Massachusetts Institute of Technology, Cambridge, MA 02139.

K. R. Rehfeldt, Illinois State Water Survey, 2204 Griffith Drive, Champaign, IL 61820.

C. Welty, Department of Civil and Architectural Engineering, Drexel University, Philadelphia, PA 19104.

(Received April 8, 1991;
revised March 4, 1992;
accepted March 12, 1992.)

Attachment 12 to Table 1

Attachment 12 to Table 1

Response to ADEQ Comment-4.5.5, Results of Post Closure Simulations

ADEQ-4.5.5-Results of Post Closure Simulations-BHP should provide the rationale for the 30-year duration of the post-closure transport simulation and the rationale for not using a longer duration. BHP should also clarify whether the maximum extent of sulfate concentration is 0.5 ppm above background, the background value used, and its determination.

Rationale

A 30-year post-closure period was selected because of the precedent established in the U.S. EPA rulemaking for post-closure plans required under 40 CFR 264 and 265. Additionally, problems that might occur as a result of inadequate closure would be detected in less than 30 years through the operation of the post-closure monitoring program. In the event a problem is detected, the 30-year post-closure period will be automatically extended, by virtue of the provisions of the post-closure plan, until such time that the problem has been properly resolved.

The 0.5 ppm sulfate contour was shown as an above-background value. The simulated contour represents the outermost detectable limit of sulfate migration that could occur during the 30-year post-closure period, assuming that the initial sulfate concentration in the Oxide Zone was 750 ppm.

The 750 ppm sulfate value was chosen because BHP's closure plan requires the mined area to be cleaned to 750 ppm sulfates, or lower, if necessary, to reduce contaminant concentrations to below their respective MCLs for metals.

Attachment 13 to Table 1

Attachment 13 to Table 1

Response to ADEQ Comment-4.5.6-Porosity Sensitivity Analysis

ADEQ-4.5.6-Chemical transport Sensitivity Analysis-As stated in section 2.7.4 of Volume IV, BHP did not determine the site-specific porosity values. Because assumed values were used in the modeling efforts, BHP should determine the sensitivity of the calculations as porosity to assess whether site-specific porosity measurements should be conducted.

Porosity Sensitivity Analysis

As demonstrated below, lower porosity values used in the models result in increased migration of the plume and are thus more conservative. In the sensitivity analysis presented here, a lower limit of 2 percent was assumed for the porosity of the oxide zone. In contrast, field data indicating porosities averaging 7.5 percent have been documented for a similar buried copper oxide deposit near Casa Grande, Arizona (USGS Open File Report 91-357, 1991).

The new version of MT3D96, released in June 1996, improved treatment of heterogeneous porosity, and expanded mass accounting, was used to rerun the post-closure scenario and associated sensitivity analysis simulation. The resulting simulated concentration values discussed here represent sulfate concentrations in excess of the background concentrations (Figures 1 through 8).

Measured K_d values from column tests conducted for the Florence project varied between 0.15 and 1.5 with a mode of 1 for the basin-fill deposits. For the post-closure scenario, simulation with K_d of 0.15 ml/g (the most conservative of the column test derived values) and dispersivity of 10 feet, the resulting 0.5 ppm contour in layer 1 extends 3,100 feet north of the mine area boundary (500 feet north of the 1/2 boundary) and the 10.0 ppm contour extends 1,400 feet north of the mine area boundary.

Because the chemical transport simulations were not calibrated against a field data set, the four types of sensitivity presented in the ASTM D 5611-94 are not applicable to these simulations. Instead, the range of possible outcomes corresponding to the range of possible input parameter values are presented and discussed below.

Two sensitivity analysis simulations were conducted where porosities were increased and then decreased by 50 percent from the base values for each layer. The porosity for the oxide zone was assumed to be 2 percent. In the sensitivity analysis this value was increased by 50 percent to 3 percent and decreased by 50 percent to 1 percent. Increasing the porosity results in a smaller seepage velocity and a plume of more limited extent. Decreasing the porosity increases the seepage velocity and thus the extent of the plume. In the decreased porosity simulation, the 0.5 ppm contour in Model Layer 1 extends to 4,500 feet north of the mine area boundary (1,300 feet further than the simulation with base porosity values). Figures 9 through 16 show the effects of

deceased porosity in each of the model layers. In the increased porosity simulation, the 0.5 ppm contour extends to 2,400 feet north of the mine area boundary in Model Layer 1 (500 feet closer than the simulation with base porosity values). Figures 17 through 24 show the effect of increased porosity in each of the model layers.

Additional on-site porosity testing will not likely increase the lateral extent of the simulated plume because (1) a plume conservative value of porosity was selected and (2) measured values of similar materials have been considerably higher than the estimated porosity values at the Florence site.

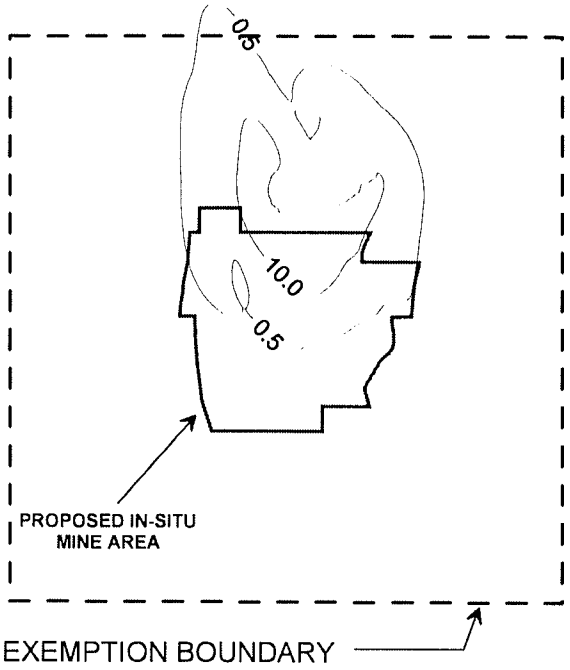

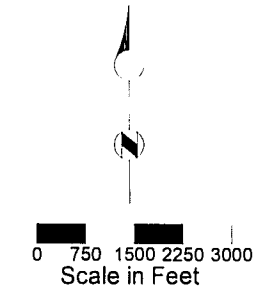

SIMULATED 0.5 PPM (PART PER MILLION)
SULFATE CONCENTRATION CONTOUR

SIMULATION PARAMETERS

INITIAL CONCENTRATION = 750 PPM

SIMULATION TIME = 30 YEARS

$K_d = 0.15\ cm^3/g$

LONGITUDINAL DISPERSIVITY = 10 FEET

HORIZONTAL DISPERSIVITY = 1 FEET

Figure 1 - Attachment 13 to Table 1
SIMULATED EXTENT
OF SULFATE 30 YEARS
AFTER CLOSURE
MODEL LAYER 1

BHP
BHP COPPER *Florence Project*

BROWN AND CALDWELL

SFIG098 08/13/96 MikeS

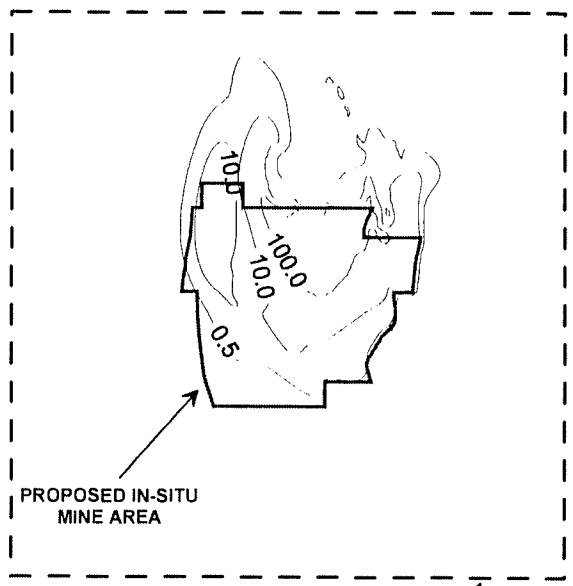

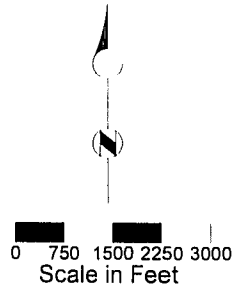

SIMULATED 0.5 PPM (PART PER MILLION)
SULFATE CONCENTRATION CONTOUR

SIMULATION PARAMETERS

INITIAL CONCENTRATION = 750 PPM

SIMULATION TIME = 30 YEARS

K_d = 0.15 cm^3/g

LONGITUDINAL DISPERSIVITY = 10 FEET

HORIZONTAL DISPERSIVITY = 1 FEET

Figure 2 - Attachment 13 to Table 1
SIMULATED EXTENT
OF SULFATE 30 YEARS
AFTER CLOSURE
MODEL LAYER 2

BHP COPPER *Florence Project*

BROWN AND CALDWELL

SFIG099 08/13/96 MikeS

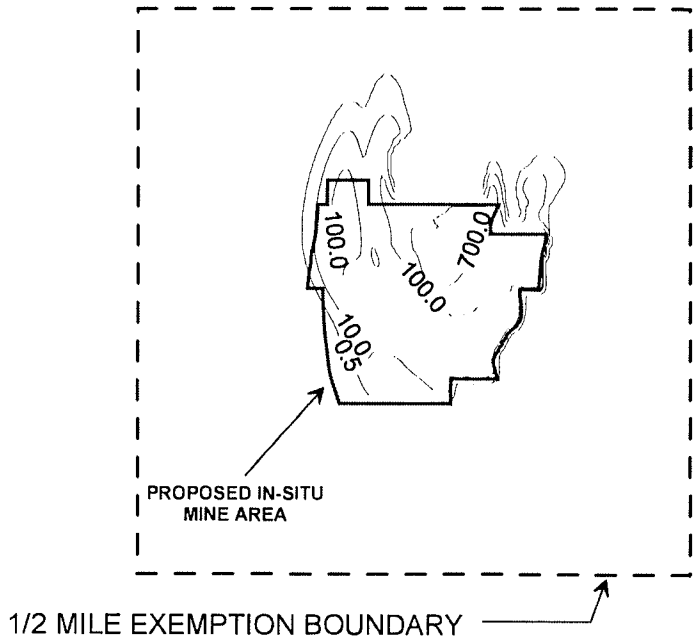

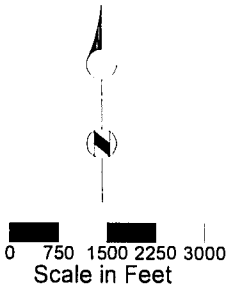

SIMULATED 0.5 PPM (PART PER MILLION)
SULFATE CONCENTRATION CONTOUR

SIMULATION PARAMETERS

INITIAL CONCENTRATION = 750 PPM

SIMULATION TIME = 30 YEARS

K_d = 0.15 cm^3/g

LONGITUDINAL DISPERSIVITY = 10 FEET

HORIZONTAL DISPERSIVITY = 1 FEET

Figure 3 - Attachment 13 to Table 1
SIMULATED EXTENT
OF SULFATE 30 YEARS
AFTER CLOSURE
MODEL LAYER 3

BHP
BHP COPPER *Florence Project*

BROWN AND CALDWELL

SFIG100 08/13/96 MikeS

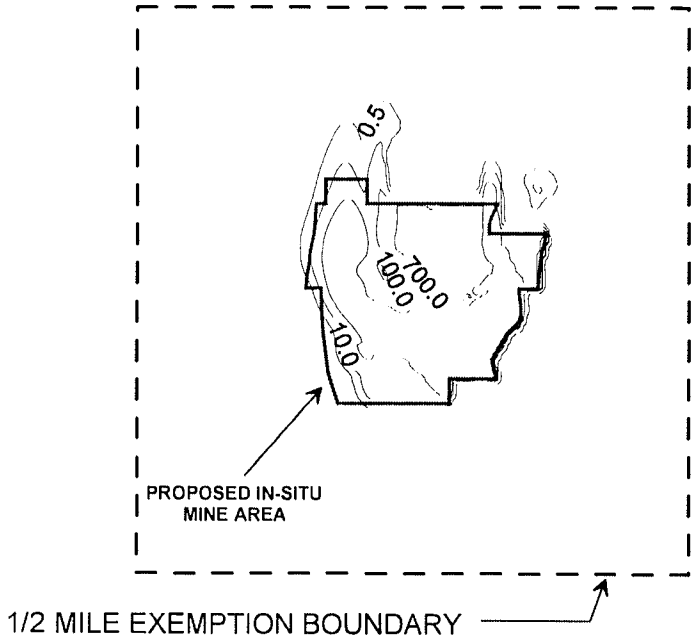

SIMULATED 0.5 PPM (PART PER MILLION)
SULFATE CONCENTRATION CONTOUR

SIMULATION PARAMETERS

INITIAL CONCENTRATION = 750 PPM

SIMULATION TIME = 30 YEARS

$K_d = 0.15\ cm^3/g$

LONGITUDINAL DISPERSIVITY = 10 FEET

HORIZONTAL DISPERSIVITY = 1 FEET

Figure 4 - Attachment 13 to Table 1
SIMULATED EXTENT
OF SULFATE 30 YEARS
AFTER CLOSURE
MODEL LAYER 4

BHP
BHP COPPER *Florence Project*

BROWN AND CALDWELL

SFIG101 08/13/96 MikeS

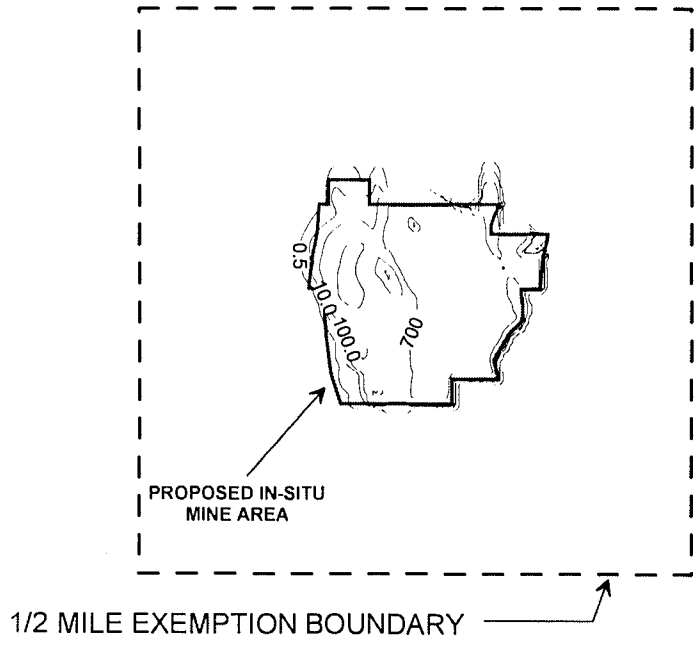

SIMULATED 0.5 PPM (PART PER MILLION)
SULFATE CONCENTRATION CONTOUR

SIMULATION PARAMETERS

INITIAL CONCENTRATION = 750 PPM

SIMULATION TIME = 30 YEARS

$K_d = 0.15\ cm^3/g$

LONGITUDINAL DISPERSIVITY = 10 FEET

HORIZONTAL DISPERSIVITY = 1 FEET

Figure 5 - Attachment 13 to Table 1
SIMULATED EXTENT
OF SULFATE 30 YEARS
AFTER CLOSURE
MODEL LAYER 5

BHP
BHP COPPER *Florence Project*

BROWN AND CALDWELL

SFIG102 08/13/96 MikeS

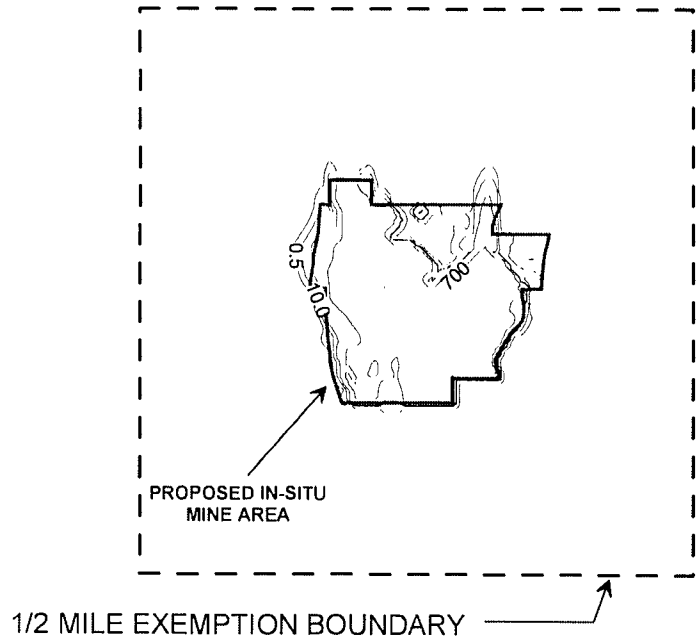

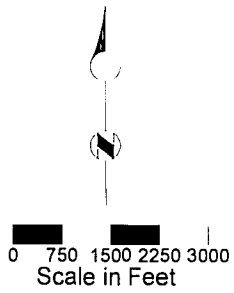

SIMULATED 0.5 PPM (PART PER MILLION)
SULFATE CONCENTRATION CONTOUR

SIMULATION PARAMETERS

INITIAL CONCENTRATION = 750 PPM

SIMULATION TIME = 30 YEARS

K_d = 0.15 cm^3/g

LONGITUDINAL DISPERSIVITY = 10 FEET

HORIZONTAL DISPERSIVITY = 1 FEET

Figure 6 - Attachment 13 to Table 1
SIMULATED EXTENT
OF SULFATE 30 YEARS
AFTER CLOSURE
MODEL LAYER 6

BHP
BHP COPPER *Florence Project*

BROWN AND CALDWELL

SFIG103 08/13/96 MikeS

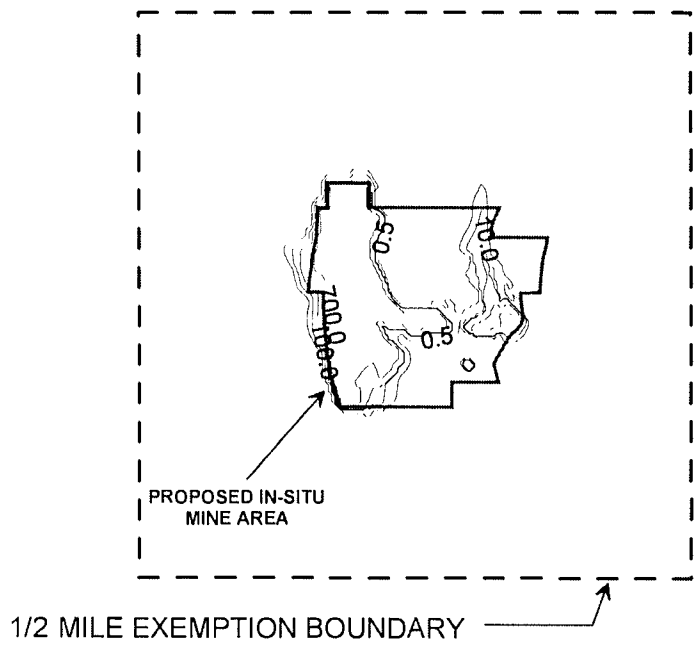

0 750 1500 2250 3000
Scale in Feet

SIMULATED 0.5 PPM (PART PER MILLION)
SULFATE CONCENTRATION CONTOUR

SIMULATION PARAMETERS

INITIAL CONCENTRATION = 750 PPM

SIMULATION TIME = 30 YEARS

K_d = 0.15 cm^3/g

LONGITUDINAL DISPERSIVITY = 10 FEET

HORIZONTAL DISPERSIVITY = 1 FEET

Figure 7 - Attachment 13 to Table 1
SIMULATED EXTENT
OF SULFATE 30 YEARS
AFTER CLOSURE
MODEL LAYER 7

BHP COPPER *Florence Project*

BROWN AND CALDWELL

SFIG104 08/13/96 MikeS

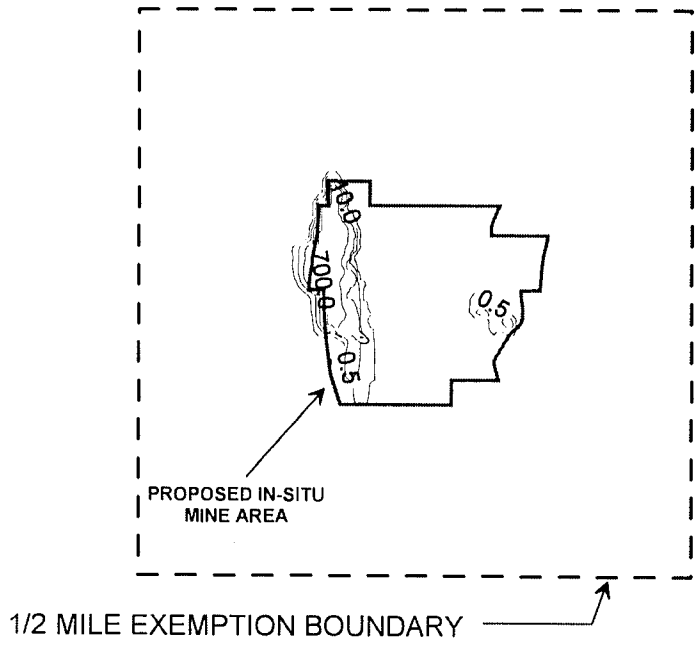

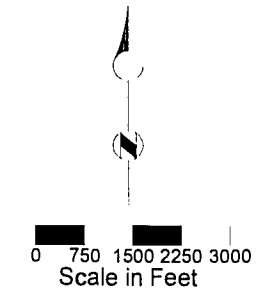

SIMULATED 0.5 PPM (PART PER MILLION)
SULFATE CONCENTRATION CONTOUR

SIMULATION PARAMETERS

INITIAL CONCENTRATION = 750 PPM

SIMULATION TIME = 30 YEARS

K_d = 0.15 cm^3/g

LONGITUDINAL DISPERSIVITY = 10 FEET

HORIZONTAL DISPERSIVITY = 1 FEET

Figure 8 - Attachment 13 to Table 1
SIMULATED EXTENT
OF SULFATE 30 YEARS
AFTER CLOSURE
MODEL LAYER 8

BHP
BHP COPPER *Florence Project*

BROWN AND CALDWELL

SFIG105 08/13/96 MikeS

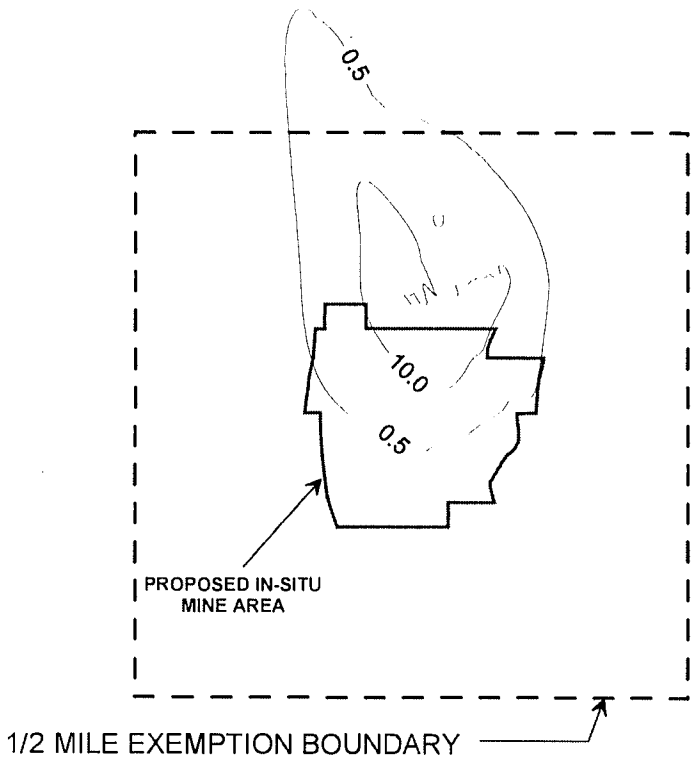

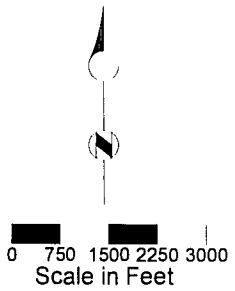

SIMULATED 0.5 PPM (PART PER MILLION)
SULFATE CONCENTRATION CONTOUR

SIMULATION PARAMETERS

INITIAL CONCENTRATION = 750 PPM

SIMULATION TIME = 30 YEARS

$K_d = 0.15\ cm^3/g$

LONGITUDINAL DISPERSIVITY = 10 FEET

HORIZONTAL DISPERSIVITY = 1 FEET

Figure 9 - Attachment 13 to Table 1
SIMULATED EXTENT
OF SULFATE 30 YEARS
AFTER CLOSURE
POROSITY DECREASED 50%
MODEL LAYER 1

BHP
BHP COPPER *Florence Project*

BROWN AND CALDWELL

SFIG106 08/13/96 MikeS

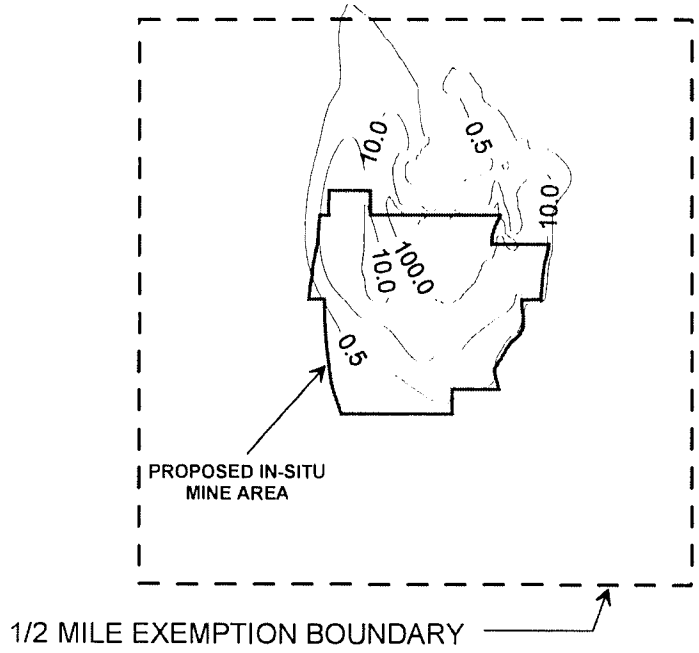

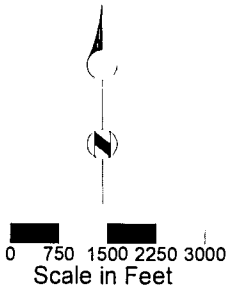

SIMULATED 0.5 PPM (PART PER MILLION)
SULFATE CONCENTRATION CONTOUR

SIMULATION PARAMETERS

INITIAL CONCENTRATION = 750 PPM

SIMULATION TIME = 30 YEARS

$K_d = 0.15\ cm^3/g$

LONGITUDINAL DISPERSIVITY = 10 FEET

HORIZONTAL DISPERSIVITY = 1 FEET

Figure 10 - Attachment 13 to Table 1
SIMULATED EXTENT
OF SULFATE 30 YEARS
AFTER CLOSURE
POROSITY DECREASED 50%
MODEL LAYER 2

BHP
BHP COPPER *Florence Project*

BROWN AND CALDWELL

SFIG107 08/13/96 MikeS

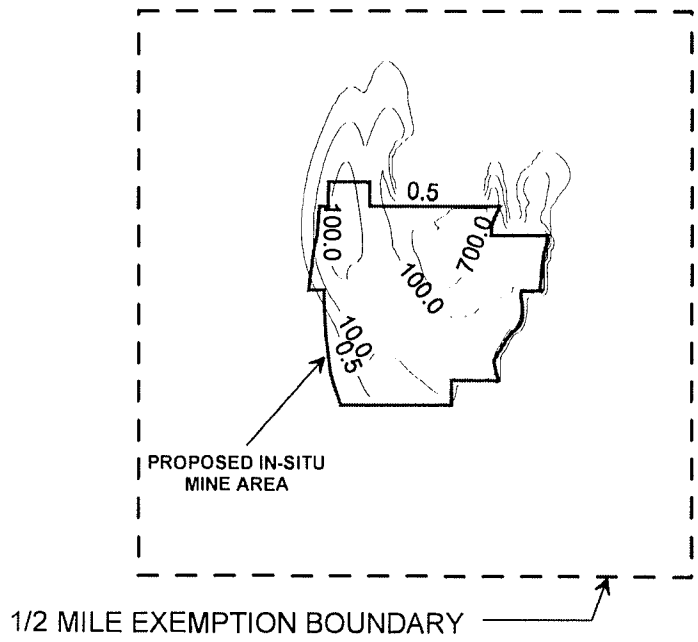

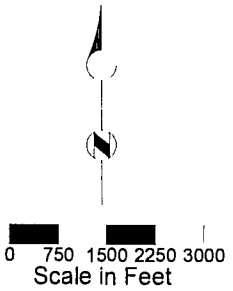

SIMULATED 0.5 PPM (PART PER MILLION)
SULFATE CONCENTRATION CONTOUR

SIMULATION PARAMETERS

INITIAL CONCENTRATION = 750 PPM

SIMULATION TIME = 30 YEARS

K_d = 0.15 cm^3/g

LONGITUDINAL DISPERSIVITY = 10 FEET

HORIZONTAL DISPERSIVITY = 1 FEET

Figure 11 - Attachment 13 to Table 1
SIMULATED EXTENT
OF SULFATE 30 YEARS
AFTER CLOSURE
POROSITY DECREASED 50%
MODEL LAYER 3

BHP COPPER *Florence Project*

BROWN AND CALDWELL

SFIG108 08/13/96 MikeS

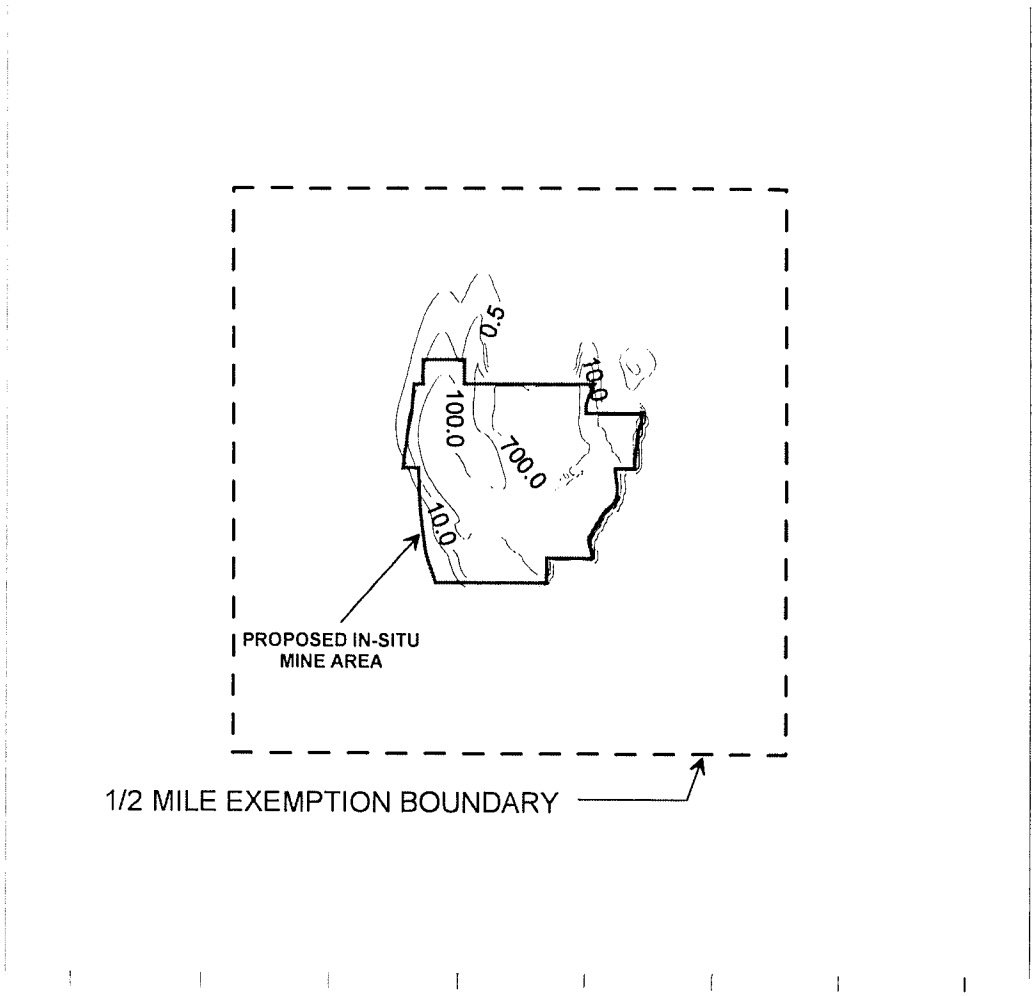

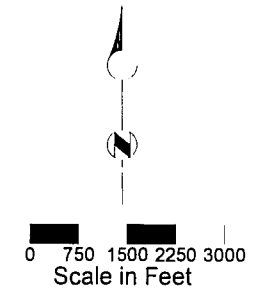

SIMULATED 0.5 PPM (PART PER MILLION)
SULFATE CONCENTRATION CONTOUR

SIMULATION PARAMETERS

INITIAL CONCENTRATION = 750 PPM

SIMULATION TIME = 30 YEARS

$K_d = 0.15\ cm^3/g$

LONGITUDINAL DISPERSIVITY = 10 FEET

HORIZONTAL DISPERSIVITY = 1 FEET

Figure 12 - Attachment 13 to Table 1
SIMULATED EXTENT
OF SULFATE 30 YEARS
AFTER CLOSURE
POROSITY DECREASED 50%
MODEL LAYER 4

BHP
BHP COPPER *Florence Project*

BROWN AND CALDWELL

SFIG109 08/13/96 MikeS

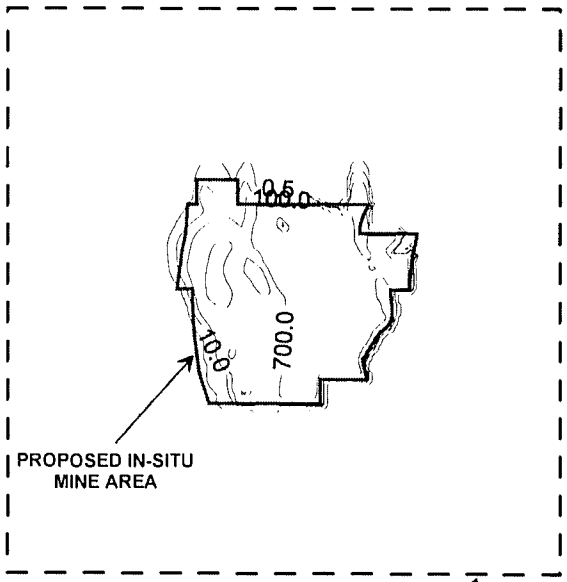

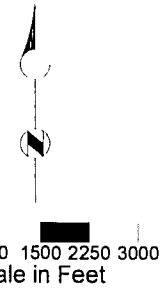

SIMULATED 0.5 PPM (PART PER MILLION)
SULFATE CONCENTRATION CONTOUR

SIMULATION PARAMETERS

INITIAL CONCENTRATION = 750 PPM

SIMULATION TIME = 30 YEARS

$K_d = 0.15\ cm^3/g$

LONGITUDINAL DISPERSIVITY = 10 FEET

HORIZONTAL DISPERSIVITY = 1 FEET

Figure 13 - Attachment 13 to Table 1
SIMULATED EXTENT
OF SULFATE 30 YEARS
AFTER CLOSURE
POROSITY DECREASED 50%
MODEL LAYER 5

BHP
BHP COPPER *Florence Project*

BROWN AND CALDWELL

SFIG110 08/13/96 MikeS

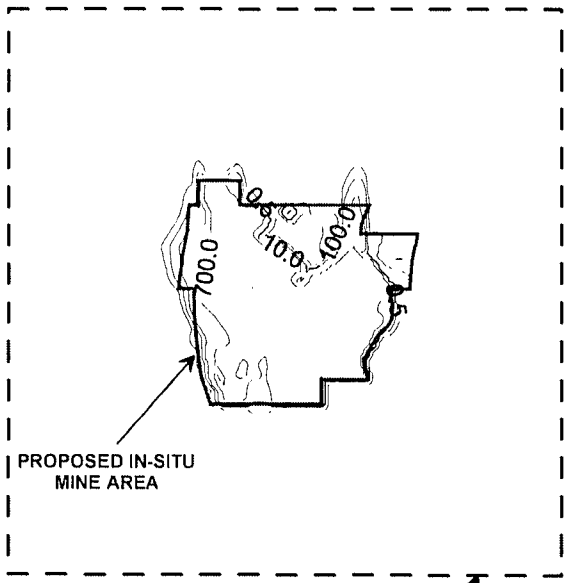

0 750 1500 2250 3000
Scale in Feet

SIMULATED 0.5 PPM (PART PER MILLION)
SULFATE CONCENTRATION CONTOUR

SIMULATION PARAMETERS

INITIAL CONCENTRATION = 750 PPM

SIMULATION TIME = 30 YEARS

$K_d = 0.15\ cm^3/g$

LONGITUDINAL DISPERSIVITY = 10 FEET

HORIZONTAL DISPERSIVITY = 1 FEET

Figure 14 - Attachment 13 to Table 1
SIMULATED EXTENT
OF SULFATE 30 YEARS
AFTER CLOSURE
POROSITY DECREASED 50%
MODEL LAYER 6

BHP
BHP COPPER *Florence Project*

BROWN AND CALDWELL

SFIG111 08/13/96 MikeS

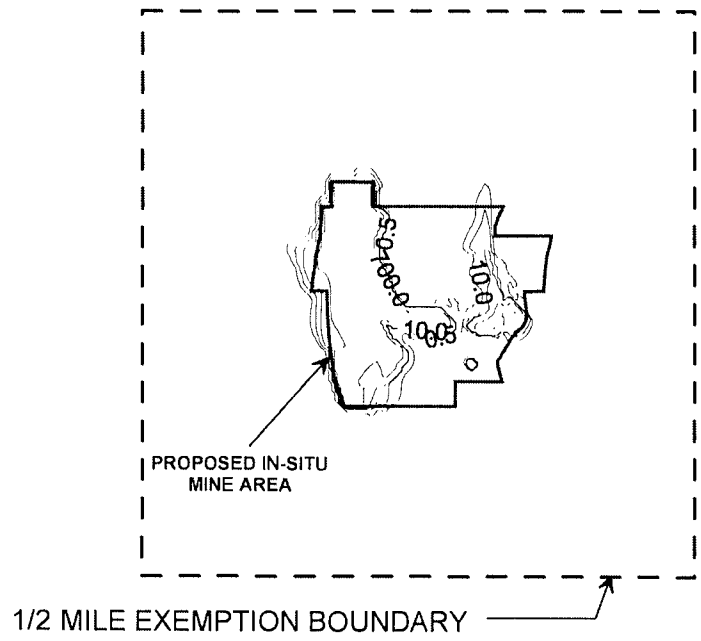

SIMULATED 0.5 PPM (PART PER MILLION)
SULFATE CONCENTRATION CONTOUR

SIMULATION PARAMETERS

INITIAL CONCENTRATION = 750 PPM

SIMULATION TIME = 30 YEARS

K_d = 0.15 cm^3/g

LONGITUDINAL DISPERSIVITY = 10 FEET

HORIZONTAL DISPERSIVITY = 1 FEET

Figure 15 - Attachment 13 to Table 1
SIMULATED EXTENT
OF SULFATE 30 YEARS
AFTER CLOSURE
POROSITY DECREASED 50%
MODEL LAYER 7

BHP
BHP COPPER *Florence Project*

BROWN AND CALDWELL

SFIG112 08/13/96 MikeS

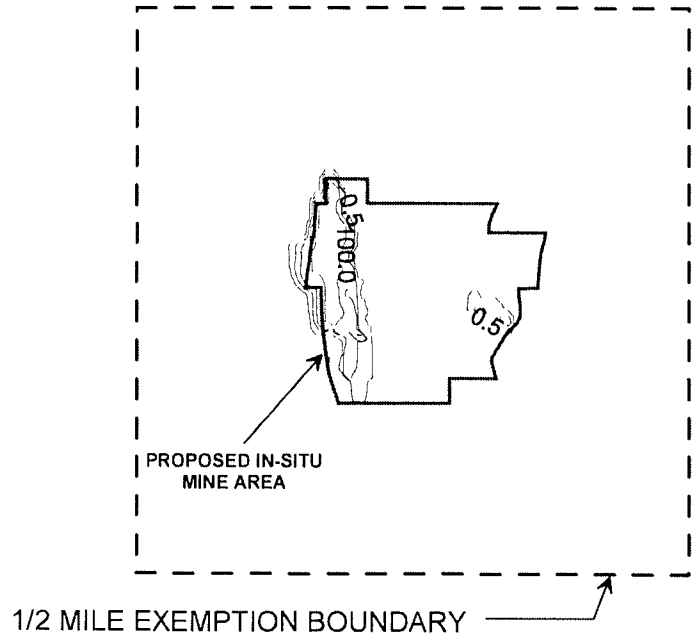

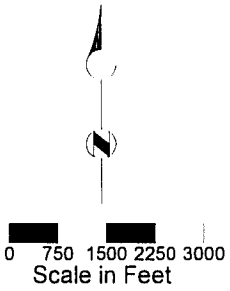

SIMULATED 0.5 PPM (PART PER MILLION)
SULFATE CONCENTRATION CONTOUR

SIMULATION PARAMETERS

INITIAL CONCENTRATION = 750 PPM

SIMULATION TIME = 30 YEARS

K_d = 0.15 cm^3/g

LONGITUDINAL DISPERSIVITY = 10 FEET

HORIZONTAL DISPERSIVITY = 1 FEET

Figure 16 - Attachment 13 to Table 1
SIMULATED EXTENT
OF SULFATE 30 YEARS
AFTER CLOSURE
POROSITY DECREASED 50%
MODEL LAYER 8

BHP
BHP COPPER *Florence Project*

BROWN AND CALDWELL

SFIG113 08/13/96 MikeS

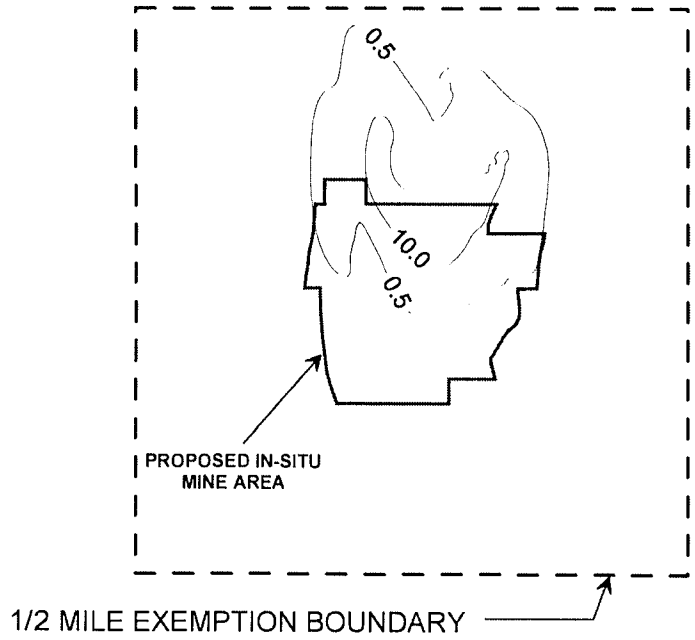

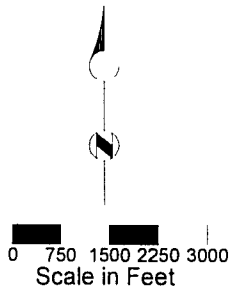

SIMULATED 0.5 PPM (PART PER MILLION)
SULFATE CONCENTRATION CONTOUR

SIMULATION PARAMETERS

INITIAL CONCENTRATION = 750 PPM

SIMULATION TIME = 30 YEARS

K_d = 0.15 cm^3/g

LONGITUDINAL DISPERSIVITY = 10 FEET

HORIZONTAL DISPERSIVITY = 1 FEET

Figure 17 - Attachment 13 to Table 1
SIMULATED EXTENT
OF SULFATE 30 YEARS
AFTER CLOSURE
POROSITY INCREASED 50%
MODEL LAYER 1

BHP
BHP COPPER *Florence Project*

BROWN AND CALDWELL

SFIG114 08/13/96 MikeS

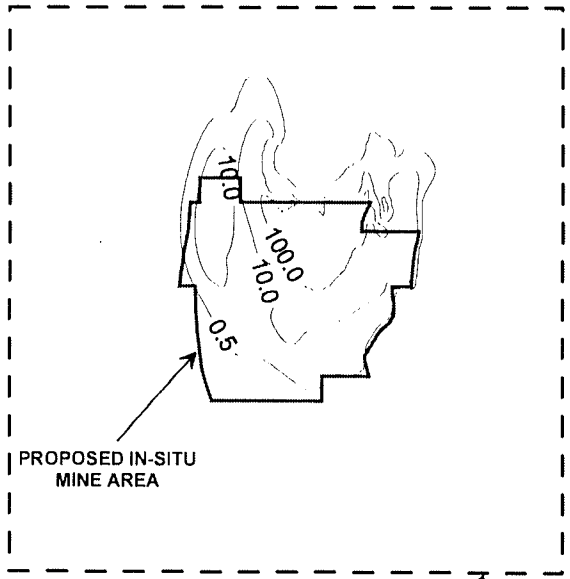

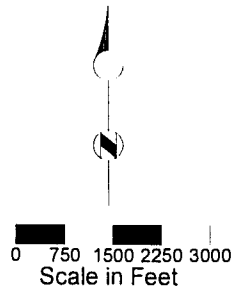

SIMULATED 0.5 PPM (PART PER MILLION)
SULFATE CONCENTRATION CONTOUR

SIMULATION PARAMETERS

INITIAL CONCENTRATION = 750 PPM

SIMULATION TIME = 30 YEARS

K_d = 0.15 cm^3/g

LONGITUDINAL DISPERSIVITY = 10 FEET

HORIZONTAL DISPERSIVITY = 1 FEET

Figure 18 - Attachment 13 to Table 1
SIMULATED EXTENT
OF SULFATE 30 YEARS
AFTER CLOSURE
POROSITY INCREASED 50%
MODEL LAYER 2

BHP COPPER *Florence Project*

BROWN AND CALDWELL

SFIG115 08/13/96 MikeS

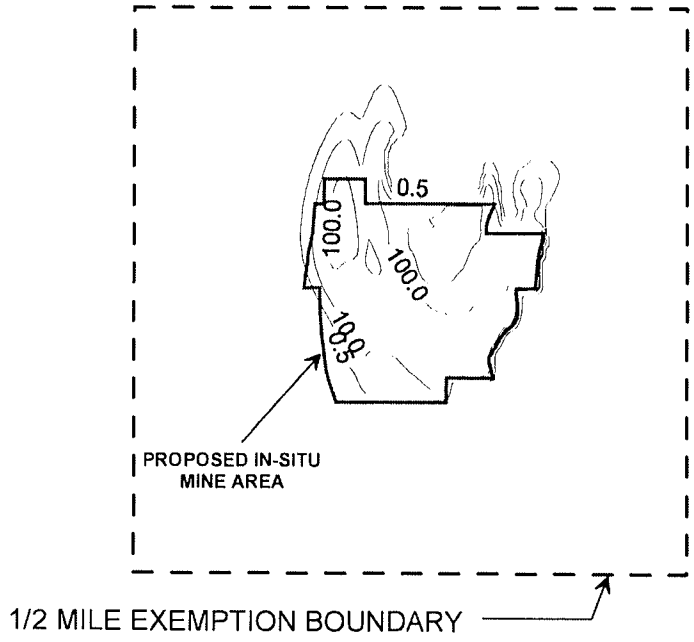

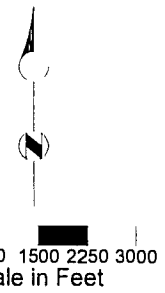

SIMULATED 0.5 PPM (PART PER MILLION)
SULFATE CONCENTRATION CONTOUR

SIMULATION PARAMETERS

INITIAL CONCENTRATION = 750 PPM

SIMULATION TIME = 30 YEARS

$K_d = 0.15\ cm^3/g$

LONGITUDINAL DISPERSIVITY = 10 FEET

HORIZONTAL DISPERSIVITY = 1 FEET

Figure 19 - Attachment 13 to Table 1
SIMULATED EXTENT
OF SULFATE 30 YEARS
AFTER CLOSURE
POROSITY INCREASED 50%
MODEL LAYER 3

BHP
BHP COPPER *Florence Project*

BROWN AND CALDWELL

SFIG116 08/13/96 MikeS

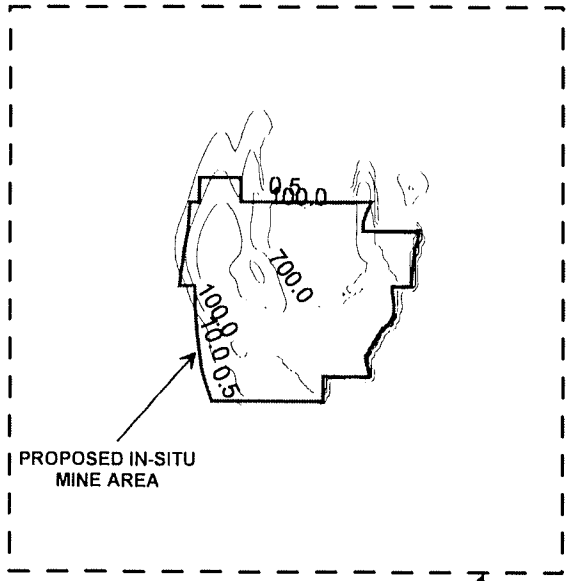

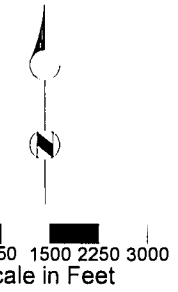

SIMULATED 0.5 PPM (PART PER MILLION)
SULFATE CONCENTRATION CONTOUR

SIMULATION PARAMETERS

INITIAL CONCENTRATION = 750 PPM

SIMULATION TIME = 30 YEARS

K_d = 0.15 cm^3/g

LONGITUDINAL DISPERSIVITY = 10 FEET

HORIZONTAL DISPERSIVITY = 1 FEET

Figure 20 - Attachment 13 to Table 1
SIMULATED EXTENT
OF SULFATE 30 YEARS
AFTER CLOSURE
POROSITY INCREASED 50%
MODEL LAYER 4

BHP
BHP COPPER *Florence Project*

BROWN AND CALDWELL

SFIG117 08/13/96 MikeS

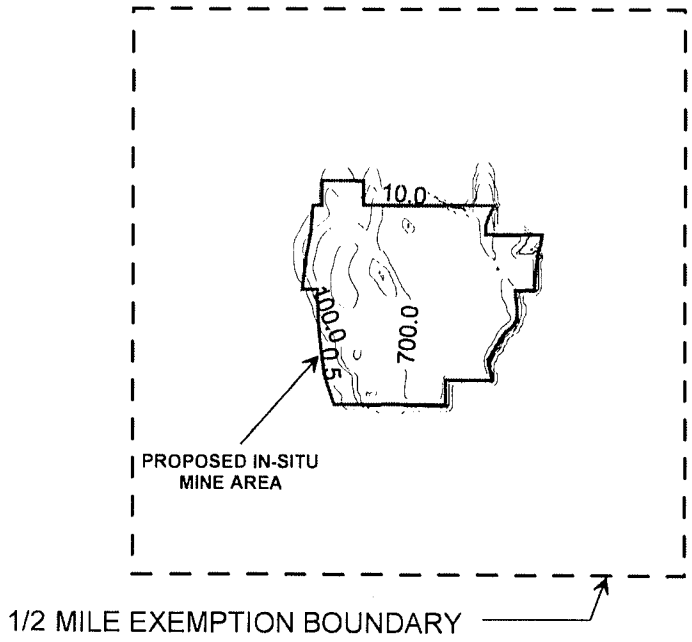

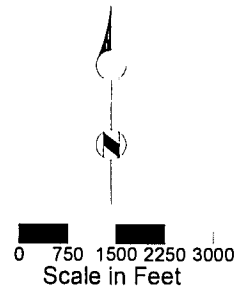

SIMULATED 0.5 PPM (PART PER MILLION)
SULFATE CONCENTRATION CONTOUR

SIMULATION PARAMETERS

INITIAL CONCENTRATION = 750 PPM

SIMULATION TIME = 30 YEARS

K_d = 0.15 cm^3/g

LONGITUDINAL DISPERSIVITY = 10 FEET

HORIZONTAL DISPERSIVITY = 1 FEET

Figure 21 - Attachment 13 to Table 1
SIMULATED EXTENT
OF SULFATE 30 YEARS
AFTER CLOSURE
POROSITY INCREASED 50%
MODEL LAYER 5

BHP COPPER *Florence Project*

BROWN AND CALDWELL

SFIG121 08/13/96 MikeS

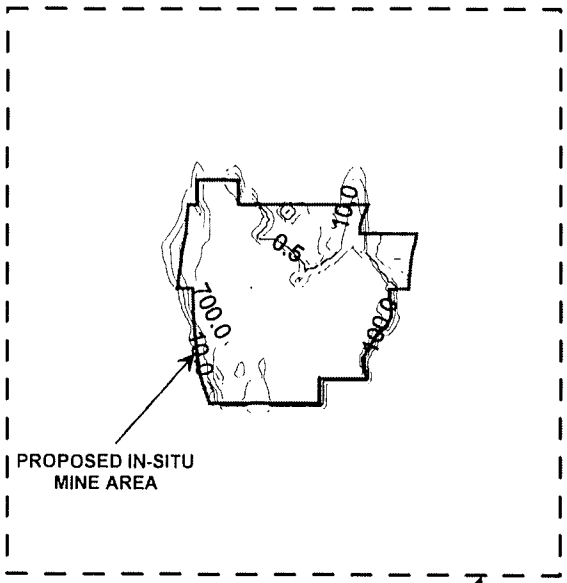

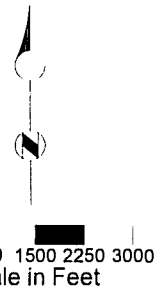

SIMULATED 0.5 PPM (PART PER MILLION)
SULFATE CONCENTRATION CONTOUR

SIMULATION PARAMETERS

INITIAL CONCENTRATION = 750 PPM

SIMULATION TIME = 30 YEARS

K_d = 0.15 cm^3/g

LONGITUDINAL DISPERSIVITY = 10 FEET

HORIZONTAL DISPERSIVITY = 1 FEET

Figure 22 - Attachment 13 to Table 1
SIMULATED EXTENT
OF SULFATE 30 YEARS
AFTER CLOSURE
POROSITY INCREASED 50%
MODEL LAYER 6

BHP
BHP COPPER *Florence Project*

BROWN AND CALDWELL

SFIG118 08/13/96 MikeS

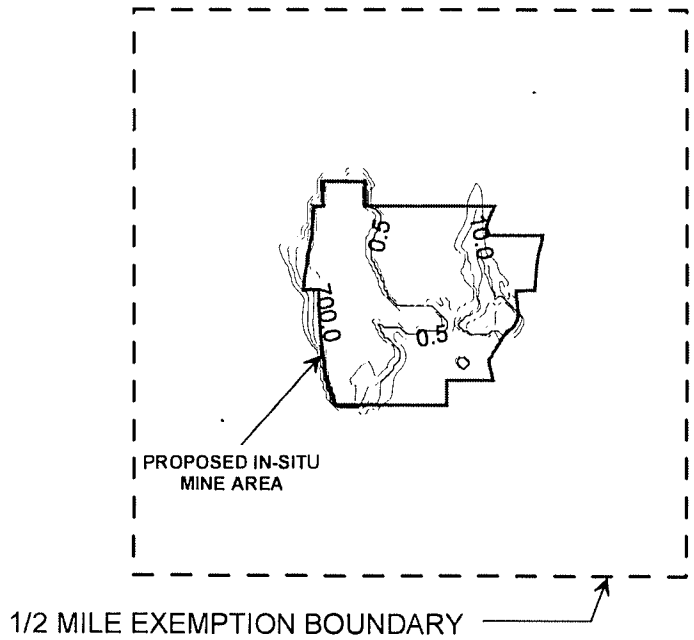

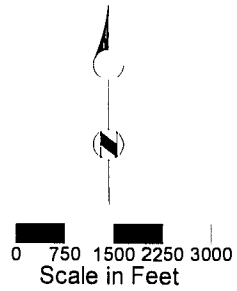

SIMULATED 0.5 PPM (PART PER MILLION)
SULFATE CONCENTRATION CONTOUR

SIMULATION PARAMETERS

INITIAL CONCENTRATION = 750 PPM

SIMULATION TIME = 30 YEARS

K_d = 0.15 cm^3/g

LONGITUDINAL DISPERSIVITY = 10 FEET

HORIZONTAL DISPERSIVITY = 1 FEET

Figure 23 - Attachment 13 to Table 1
SIMULATED EXTENT
OF SULFATE 30 YEARS
AFTER CLOSURE
POROSITY INCREASED 50%
MODEL LAYER 7

BHP COPPER *Florence Project*

BROWN AND CALDWELL

SFIG119 08/13/96 MikeS

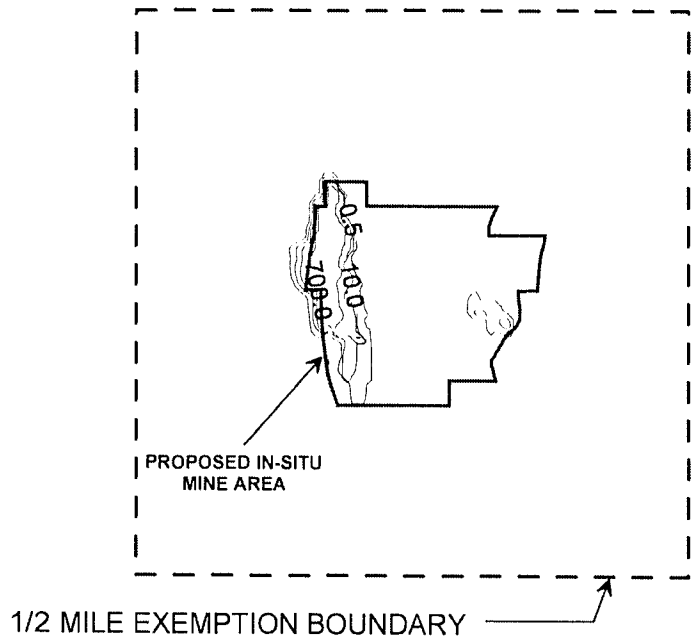

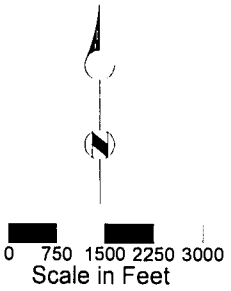

SIMULATED 0.5 PPM (PART PER MILLION)
SULFATE CONCENTRATION CONTOUR

SIMULATION PARAMETERS

INITIAL CONCENTRATION = 750 PPM

SIMULATION TIME = 30 YEARS

$K_d = 0.15\ cm^3/g$

LONGITUDINAL DISPERSIVITY = 10 FEET

HORIZONTAL DISPERSIVITY = 1 FEET

Figure 24 - Attachment 13 to Table 1
SIMULATED EXTENT
OF SULFATE 30 YEARS
AFTER CLOSURE
POROSITY INCREASED 50%
MODEL LAYER 8

BHP COPPER *Florence Project*

BROWN AND CALDWELL

SFIG120 08/13/96 MikeS